Introducing A Model Emulsion Replicating SAGD Reservoir Emulsion Features

by

Arian Velayati

A thesis submitted in partial fulfillment of the requirements for the degree of

Doctor of Philosophy

In

Petroleum Engineering

Department of Civil and Environmental Engineering
University of Alberta

Abstract

This thesis introduces a model emulsion that replicates the physical features of steam-assisted gravity drainage (SAGD) reservoir emulsion. Moreover, a framework was presented which enables adjusting the emulsion properties such as dynamic viscosity, size of the droplets, kinetic stability, and asphaltene precipitation to reach the target features accurately. For this purpose, the research followed two primary phases.

In the first phase, a base recipe containing water, the external oil phase, and a non-ionic surfactant (Span 83) was selected and screening and comparative tests were carried out to determine the proper homogenization settings, assess the surfactant performance, add/introduce other surfactants/components such as gilsonite and hexane to the recipe and evaluate the effect of electrolyte, phase ratio, and additives concentrations on the features of the emulsions.

The second phase of the research started once the decision on the final components of the model emulsion recipe was made. In this stage, BoxBehnken experimental design was adopted to run the experiments and establish correlations for the target features with the concentration of the additives/components. These correlations were used as objective functions in the optimization to attain the goals, which were SAGD emulsion features.

This research employs different techniques to evaluate the emulsion properties. The kinetic stability of emulsions was monitored by optical microscopy, water phase separation in the bottle tests, and interfacial tension measurements. The viscosity of emulsions was measured by a cone and plate viscometer, and the size of the droplets and asphaltene aggregates were determined by optical microscopy.

In addition to the primary objective of the research several other marginal objectives were followed. This research presents a comprehensive characterization of w/o macro-emulsions

stabilized by a non-ionic surfactant (Span 83), where the effect of phase ratio, oil composition, electrolyte, and surfactant concentration on the emulsion features was investigated. Moreover, gilsonite is introduced as a new additive that can be used to mimic asphaltene precipitation in oil.

Asphaltene precipitation in different oil blends was monitored and characterized, and the effect of gilsonite concentration, oil composition, electrolyte, and phase ratio on emulsions properties was studied. Molecular dynamic simulation coupled with experimental results in terms of water phase separation, interfacial tension measurements, viscosity measurements, and micrography reveal some important aspects of the asphaltene aggregation role in the stability of w/o emulsions.

The application of the model emulsion is quite extensive. It can be used in sand pack and core flooding tests that currently neglect the emulsion flow. Utilizing model emulsion eliminates the need to run similar tests at high-pressure high-temperature conditions with bitumen, which is risky and hazardous, and can replace the difficult procedure of asphaltene extraction from bitumen. Additionally, the results presented in this research around asphaltene precipitation behavior and stability of w/o emulsions by asphaltene aggregates have important implications for solvent-SAGD operations.

Acknowledgments
I praise the almighty, the creator, and the bringer of light and wisdom to whom I seek resort and guidance.

I wish to express my sincere gratitude and appreciation to my supervisor, Prof. Nouri, for selecting me from the many applicants who wanted to work under his supervision, guiding and supporting me from the very start of my studies, and helping me overcome all the difficulties in the way. Also, I would like to thank the supervisory committee, Dr. Zeng and Dr. Dehghanpour, for the mentorship.

I dedicate this thesis to my lovely and forgiving wife, Nazanin, for her patience and support during this period. Thanks for everything.

I feel very humbled and grateful for everything my parents provided for me over the years. This work would not have been possible without their support. So, I also dedicate this work to the best parents in the world, Fariba and Behzad.

I would like to thank my friends, especially Hossein Izadi, who helped and encouraged me to keep going strong.

Last but not least, in the dark times where backwardness seems to be the trend and meritocracy is fading away fast, the words and thoughts of Dr. J.R. Jorjani and his Promethean philosophy were the intellectual inspiration to me.

Table of Contents

List of Tables

List of Figures

Chapter 1: Introduction

1.1 Overview and Problem Statement

Steam-assisted gravity drainage (SAGD) is a popular method used to extract bitumen from the reservoir through injection of steam, transfer of steam latent heat to cold bitumen facilitating the flow of oil, and production of oil and condensate by the assistance of gravity [1]. The production of emulsion has been detected from the very beginning of SAGD deployment [2]. Field samples, micromodel experiments, and high-pressure high-temperature experiments verify the production of w/o emulsion and a free water phase during production [3-6]. However, emulsification and emulsion flow have been neglected for the most part in the SAGD modelling, lab testing, and production analysis. Currently, core flooding and sand pack testing such as Sand Retention Testing (SRT), Full-scale Completion Testing (FCT), and Scaled Completion Testing (SCT) facilities, that are used to evaluate the productivity issues in SAGD operations overlook emulsion flow altogether [7].

The properties of emulsions are different from their constituent phases [8]. Dynamic viscosity of w/o emulsions is typically higher than the base oil phase and increases rapidly with higher water content in emulsion [9]. This could affect the flow of oil toward the producer well and hinder production. Formation damage from emulsion blockage and droplet pore restrainment could also be detrimental to production [7]. The interparticle forces between emulsion and the porous media in the microscopic scale are different from the single-phase oil flow due to the polarity of the water in the emulsion. This might affect the fine mobilization in the reservoir. Moreover, crude sales and downstream facilities requirements dictate the separation of phases and demulsification of the produced fluids [10].

Model emulsions can be utilized to obtain more realistic results in the SAGD lab testing such as the sand pack and flowline testing. Using bitumen in experiments requires high-pressure high-temperature facilities equipped with steam generators. Moreover, there are safety concerns in this type of testing that motivated us to introduce model fluids that can replicate the SAGD reservoir emulsion features. In this way, experiments can be conducted with much lower costs and minimal safety issues while the results will be more representative of the field conditions compared to the single-phase and multi-phase separated flow scenarios currently embedded in SAGD testing standard operating procedures (SOPs) [11].

This research introduces a model emulsion with features similar to that of SAGD reservoir emulsions in terms of the type of emulsion, dynamic viscosity, kinetic stability, size of the droplets, emulsified water content, and asphaltene precipitation. The emulsion mimics these properties in atmospheric pressure and room temperature conditions. Extensive experiments were carried out in the process of preparing this reference fluid which led to the comprehensive characterization of w/o emulsions stabilized by a non-ionic surfactant, introducing gilsonite as an additive that may be used to mimic the asphaltene precipitation behavior in SAGD operation, and investigating the role of asphaltene aggregates in stabilizing w/o emulsions.

1.2 Research Objectives

- Introducing a model emulsion replicating SAGD reservoir emulsions features in terms of the type of emulsion, dynamic viscosity, kinetic stability, size of the droplets, emulsified water content, and asphaltene precipitation.
- Developing a framework that may be utilized to mimic the bulk properties of any w/o in-situ emulsion.
- Characterization of w/o macro emulsions stabilized by a non-ionic surfactant (Span 83) and investigating the effect of electrolyte, phase ratio, and homogenization settings on emulsion features.
- Determining the onset of asphaltene precipitation (gilsonite).
- Investigating the asphaltene precipitation and aggregation profile in different oil blends.
- Investigating the performance of surfactant blends (Span 83+Gilsonite) in stabilizing w/o emulsion, and evaluating the effect of oil composition, electrolyte, and phase ratio.
- Investigating the underlying physics behind the stability of w/o emulsions by asphaltene aggregates.

1.3 Research Hypothesis

- The model emulsion shows similar properties (viscosity, kinetic stability, and mean droplet size) as the SAGD in-situ emulsions.
- Gilsonite, which contains asphaltene in large portions can be used to mimic the asphaltene precipitation phenomenon in oil.
- A blend of surfactants yields better kinetic stability in emulsions.
- The presence of salt affects emulsion stability and may change water droplet diameter.
- An increase in salinity results in an increase in the surfactant activity difference, decreasing the hydrophilicity of the emulsifier in the system.
- There is an interactive effect between viscosity, droplet size, and kinetic stability in emulsions.
- Asphaltene precipitation and aggregation promote the stability of emulsions.

1.4 Research Methodology

The research was conducted in two primary phases. The first phase involves the characterization of the emulsion base recipe and determining the homogenization settings, the performance of the surfactant, and investigating the feasibility of reaching the targets for the current recipe. New components and additives are introduced when required to adjust the emulsion features. The experimental designs used in this stage were mainly of screening types, with more points added when it was intended to do more investigations or establish correlations.

Once the decision on the components of the model emulsion was finalized, second phase of the research starts. In this part of the research, BoxBehnken's experimental design was employed to conduct tests and establish correlations for the emulsion properties based on the concentration of the additives. These correlations are the objective functions used in the multi-objective multivariate optimization to find the optimal recipe which yields the target SAGD emulsion

features. The optimal recipe was prepared in the lab and validation tests were performed to assess the accuracy of the model predictions. The overall scheme of the research followed is demonstrated in **Figure 1.1.**

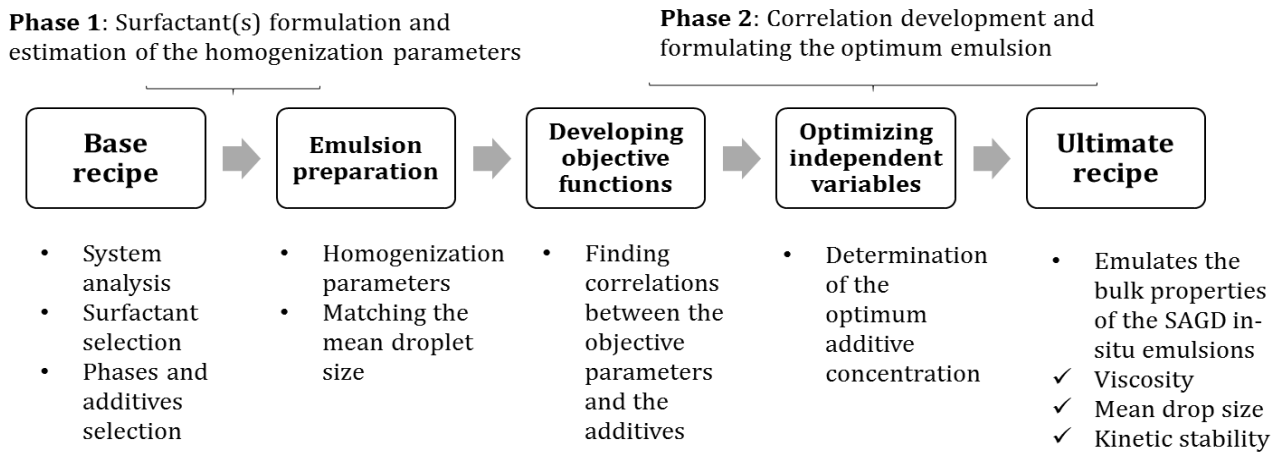

Figure 1.1: Scheme of the research workflow

Different techniques and approaches were employed to characterize the emulsion properties. Optical microscopy was used to determine the size of the droplets and qualitatively evaluate the instability mechanisms such as flocculation and coalescence in emulsions. An optical microscope was equipped with a camera to capture images of the fresh and aged sample emulsions. After image processing, various representative sizes were computed using a Matlab in-house code to monitor the size evolution of droplets in emulsions. Dynamic viscosity of emulsions was measured using a cone and plate type viscometer. This type of viscometer has the advantage of requiring small sample volumes for the measurements.

Water phase separation was selected as the ultimate indication of instability in emulsions and bottle tests were performed to record the separated water level with time for the emulsion samples. Moreover, interfacial tension measurements, optical microscopy, and monitoring the size of the droplets with time were used to further describe the stability of emulsions. In the analysis of the stability results, molecular dynamic simulation and incorporated thermodynamics-colloidal approach were employed to reveal the underlying mechanism of stability in emulsions, particularly in the case of emulsions stabilized by gilsonite.

1.5 Thesis Outline

This is a paper-based formatted thesis containing five chapters. The first chapter comprises an overview of the problem and a brief background, research objectives, research hypotheses, and research methodology.

The second chapter presents an investigation on emulsification and emulsion flow in thermal recovery operations with a focus on SAGD operations. In this chapter, a comprehensive literature review of the thesis topic is presented where the mechanisms of emulsification, emulsion flow characteristics, and emulsion viscosity models in SAGD operations are discussed extensively.

The third chapter contains the characterization results of the w/o emulsion stabilized by a non-ionic surfactant. These are the results obtained in the first phase of the research where comprehensive testing was performed on the base emulsion recipe to investigate the effect of homogenization settings, surfactant concentration, phase ratio, and electrolyte on the emulsion features.

The fourth chapter still represents the results from the first phase of the research. However, in this chapter, the effect of gilsonite on emulsion properties is investigated. Moreover, this chapter contains results and discussions on asphaltene precipitation and aggregation behavior in different oil blends, and the role of gilsonite and the blend of surfactants on emulsion stability.

The fifth chapter contains some information from the first phase of the research such as the effect of hexane on emulsions features, the onset of asphaltene precipitation, interfacial tension measurements of the base emulsion samples with different surfactants, and molecular dynamics study of the asphaltene aggregates in the emulsion system. Additionally, this chapter presents the results from the second phase of the research where the correlations were developed for the emulsion features of interest, optimization was performed, and the optimal recipe of the model emulsion was introduced. The final chapter (chapter six) contains the conclusions, general discussions, and contributions of the research.

Nomenclature

FCT: Full-scale Completion Testing

SAGD: Steam Assisted Gravity Drainage

SCT: Scaled Completion Testing

SRT: Sand Retention Testing

References

[1] Butler, R.M., McNab, G.S. and Lo, H.Y., 1981. Theoretical studies on the gravity drainage of heavy oil during in-situ steam heating. *The Canadian journal of chemical engineering*, *59*(4), pp.455-460.

[2] Butler, R.M. and Stephens, D.J., 1981. The gravity drainage of steam-heated heavy oil to parallel horizontal wells. *Journal of Canadian Petroleum Technology*, *20*(02).

[3] Sasaki, K., Akibayashi, S., Yazawa, N., Doan, Q. and Ali, S.M., 1999, January. Experimental Modelling of the SAGD Process 3/4 Enhancing SAGD Performance with Periodic Stimulation of the Horizontal Producer. In *SPE Annual Technical Conference and Exhibition*. Society of Petroleum Engineers.

[4] Jamaluddin, A.K.M. and Butler, R.M., 1988. Factors Affecting the Formation of Water-in-Oil Emulsions During Thermal Recovery. *AOSTRA J. Research*, *4*(2), pp.109-116.

[5] Mohammadzadeh, O. and Chatzis, I., 2010. Pore-level investigation of heavy oil recovery using steam assisted gravity drainage (SAGD). *Oil & Gas Science and Technology–Revue d'IFP Energies nouvelles*, *65*(6), pp.839-857.

[6] Kumasaka, J., Sasaki, K., Sugai, Y., Alade, O.S. and Nakano, M., 2016. Measurement of Viscosity Alteration for Emulsion and Numerical Simulation on Bitumen Production by SAGD Considering In-situ Emulsification. *Journal of Earth Science and Engineering*, *6*, pp.10-17.

[7] Velayati, A. and Nouri, A., 2020. Emulsification and emulsion flow in thermal recovery operations with a focus on SAGD operations: A critical review. *Fuel*, *267*, p.117141.

[8] Schramm, L.L., 1992. Fundamentals and applications in the petroleum Industry. *Adv. Chem*, *231*, pp.3-24.

[9] Leal-Calderon, F., Schmitt, V. and Bibette, J., 2007. *Emulsion science: basic principles*. Springer Science & Business Media.

[10] Kokal, S.L., 2005. Crude oil emulsions: A state-of-the-art review. *SPE Production & facilities*, *20*(01), pp.5-13.

[11] Haftani, M., Wang, C., Montero Pallares, J.D., Mahmoudi, M., Fattahpour, V. and Nouri, A., 2019, April. An Investigation into the Effect of Brine Salinity on Fines Migration in SAGD Operations. In *SPE Western Regional Meeting*. Society of Petroleum Engineers.

Chapter 2: Emulsification and Emulsion Flow in Thermal Recovery Operations with a Focus on SAGD Operations: A Critical Review

This paper was published in the Journal of Fuel.

Velayati, A. and Nouri, A., 2020. Emulsification and emulsion flow in thermal recovery operations with a focus on SAGD operations: A critical review. Fuel, 267, p.117141.

2.1 Preface

Steam-assisted gravity drainage (SAGD) is a thermal hydrocarbon recovery method by which extra-heavy oil is produced through steam injection and bitumen heating. The presence of emulsions in the produced fluid has been detected from the very beginning of SAGD deployment. However, this phenomenon is still not fully understood. This paper reviews some significant aspects of emulsification and emulsion flow in SAGD operations. Such includes downhole emulsification mechanisms, the effect of natural emulsifiers in the emulsion stability, different types of emulsions, emulsion characteristics in terms of viscosity, droplet size distribution, stability, features of continuous and dispersed phases, interactive effects of downhole conditions (e.g., pressure, temperature, and rock properties) and other relevant parameters. Additionally, the paper reviews currently available emulsion modelling techniques. A better understanding of emulsion flow is essential to designing more accurate models for SAGD production, testing sand control devices, and explaining the physics involved in SAGD operations. The focus of this paper is emulsification in thermal recovery methods, particularly in-situ emulsification in the reservoir for SAGD operations.

2.2 Introduction

An emulsion is a system of mixture fluid in which one liquid phase is dispersed within a continuous liquid phase. Emulsions are a part of a more general system of a two-phase matter referred to as colloids. However, in emulsions, both dispersed and continuous phases are liquids [1-3].

Produced oil from the reservoir is almost always commingled with water in the form of emulsion when produced [4]. The upstream and downstream oil industry deals with many issues associated with emulsion production from oil wells. Flow deficiencies in the reservoir (emulsion blockage), high-pressure drops in flow lines, upsets in downstream wet crude facilities, crude sales requirements including basic sediment and water (BS&W), and salt are a few examples of the considerations which need to be accounted for when the emulsion is produced [4-6]. A regular type of emulsion observed in the oilfield is "Water-in-Oil" emulsion, with the most common range of emulsified water in light crudes (>20 API) of 5-20 vol% and 10-35 vol% in heavier crudes (< 20 API) [4]. This shows that emulsification is more severe in hydrocarbon recovery from the heavy crude reservoirs.

Steam-assisted gravity drainage (SAGD) is a thermal enhanced oil recovery (EOR) technology used for producing bitumen and heavy oil from the reservoir. This method was first introduced and further developed by Butler et al. [7-10]. This technology is an advanced form of steam stimulation in which a pair of wells, one (injector) located approximately 5 m above the other (producer), is used to upgrade the bitumen through a continuous steam injection and heat transfer. The heated oil loses viscosity and is mobilized towards the producer. SAGD is associated with high recovery rates (over 50%) with steam-to-oil ratios 2-5 and is superior to the other commercially applied steamflooding techniques, including cyclic steam stimulation in terms of recovery rate, energy efficiency, number of wells, and operational pressure requirements [11,12]. **Figure 2.1** demonstrates the SAGD concept, schematically.

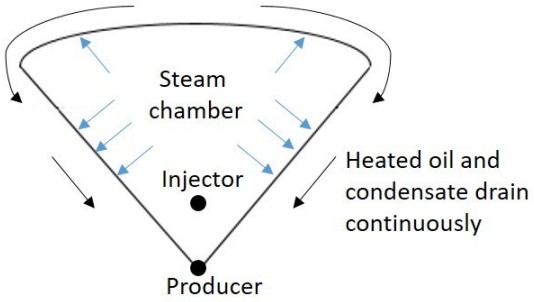

Figure 2.1: SAGD concept schematic (modified after Butler [10])

The produced fluids in the SAGD recovery method have been reported to be in emulsion form [13]. Characterization of the produced SAGD emulsion shows variable emulsion properties. This is particularly the case for the emulsion type, droplet size distribution, rheological behavior, emulsified water content, free water phase content, and so on. To the knowledge of the authors, there has been no comprehensive review of the SAGD produced fluid emulsion characterization. Additionally, emulsion flow has been neglected in the SAGD production models presented in the literature.

It is important to understand the emulsification mechanism, emulsion properties, and the complexities associated with this phenomenon in SAGD operations. Such complexities include different emulsion flow behavior that is a result of the change in the viscosity of the emulsion compared to the base oil phase, alteration in the relative permeability of the phases, droplets restrainment in the pore throat, and emulsion blockage among other factors [4-6,13]. These phenomena occur in the reservoir and may affect productivity and productivity issues such as sand production and fines migration.

This review paper attempts to gather, categorize and analyze the SAGD emulsion flow characterization results and identify the type of produced emulsions, downhole emulsification mechanisms, and effective parameters. Also, ranges are identified to bind the emulsion properties, including droplet size. Moreover, numerical and analytical models presented to address the emulsion flow in SAGD have been reviewed, including the effect of emulsification on the relative permeability curves and the residual fluids saturations. Emulsification in the flow lines and downstream is out of the scope of this article. The focus is on reservoir emulsification.

2.3 Theory

Colloids are dispersed systems that have at least one dimension between 1 and 1000 nm [5]. Emulsions are special types of colloids that contain immiscible liquids, one dispersed (internal phase) into another (external phase). However, the size of the droplets often exceeds 1000 nm and is in the order of micrometers [1-2]. Some emulsions form spontaneously and are characterized as thermodynamically stable. In contrast, other emulsions are metastable as they require a certain amount of energy to form and need specific properties to remain stable [2]. Petroleum crude emulsion cannot form spontaneously as the phases are most stable when separated (except for microemulsion). There are other mechanisms involved in the in-situ emulsification of the crude oil and water in the reservoir.

2.3.1 Emulsions Categorization

Emulsions are often categorized based on their type, droplets' size range, and stability. It is common to divide emulsions into microemulsions and macroemulsion based on the droplets (internal phase) size being smaller or larger than 10 nm [1,4]. Although, this classification of emulsions is somewhat arbitrary. Most of the crude emulsions are categorized as macroemulsions and are inherently unstable, ignoring the natural emulsifiers and their role in emulsion stability. The emulsions are classified based on the continuous phase into three major groups [14]:

- Water-in-Oil Emulsion (W/O): Oil is the continuous phase and water droplets are dispersed,
- Oil-in-Water Emulsion (O/W): Water is the continuous phase and oil droplets are dispersed,
- Multiple Emulsions (Complex Emulsion): i.e. Water-in-Oil-in-Water (W/O/W) emulsion, which denotes a multiple emulsion that contains water drops dispersed in the oil phase which in turn is dispersed in the continuous water phase.

2.3.2 Emulsions Stability

Crude oil emulsions are thermodynamically unstable and mainly observed in the W/O emulsion form [4,15-16]. However, the emulsified water content of the emulsion varies significantly from one case to another. The type of emulsion formed relies on several factors. There is a rule of thumb that states the volume fraction of the phases dictates the continuous and dispersed phases [17]. Though this is not always the case, particularly for the crude oil emulsions and other factors are involved, such as the type of the emulsifier. Bancroft rule states that the phase in which an emulsifier is more soluble constitutes the continuous phase [18]. This explains why most of the crude emulsions are of W/O emulsion-type as natural emulsifiers which exist in the formations (asphaltenes, resins, organic acids, and bases) are more soluble in oil rather than water. **Figure 2.2** displays a basic illustration of different types of emulsions.

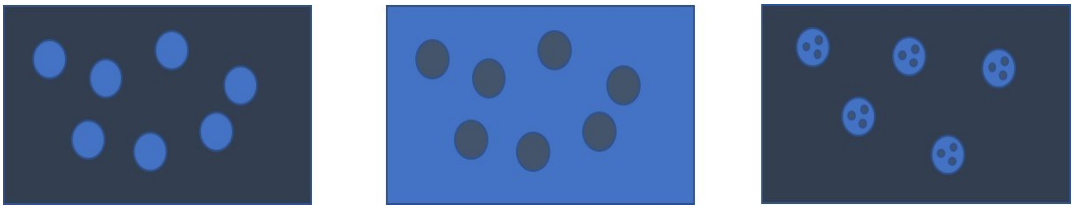

(a) (b) (c)

Figure 2.2: Basic schematic of the different types of emulsions; (a) W/O emulsion, (b) O/W emulsion, (c) complex emulsion

The stability of an emulsion is defined as the emulsion ability in resisting changes in its properties over time [19]. Emulsions tend to be thermodynamically unstable. The reason is emulsification requires a significant amount of energy and the system tends to go back to its former thermodynamic state with lower energy level by phase separation and interfacial area and energy reduction. Gibbs free energy equation can be used to describe this process [1].

$$\Delta G = (\gamma \Delta A) - (T \Delta S) \quad (1)$$

where γ is interfacial tension, A is the interfacial area, T is temperature, and ΔS is Entropy.

If ΔG is positive, spontaneous emulsification is unlikely to occur. This is often the case since often $\gamma \Delta A >> T\Delta S$ and the emulsions typically tend to be thermodynamically unstable. When the droplets are dispersed within the continuous fluid interfacial area increases largely and ΔG increases consequently and results in added instability to the system. The only way to resist phase separation then is through the reduction of the interfacial tension. Emulsifiers are used in the emulsions for the specific purpose of stabilizing the fluid mixture. However, this stability is referred to as "kinetic stability," meaning that the emulsion's properties will remain fairly unchanged for a certain period. Oil field emulsions are categorized based on their kinetic stability to loose (rapid phase separation), medium, and tight emulsions that can remain stable for days [4]. There are other detailed classifications of the water-in-crude oil emulsions, where emulsions stability is clustered based on their appearance, oil chemical composition, and measured rheology into unstable, metastable, and stable emulsions [20-22].

The mechanisms of emulsion instability are characterized by flocculation, creaming/sedimentation, coalescence, Ostwald ripening, and phase inversion phenomena. Flocculation is a result of attractive forces between the droplets, while coalescence is the process of droplets collisions and fusion into larger droplets. Creaming is the rise of the droplets to the top as a result of the buoyancy force. In contrast, sedimentation is the settling of the droplets due to the gravity force and the weight of the droplets. Ostwald ripening is a thermodynamic driven spontaneous phenomenon, where smaller droplets shrink in size due to their higher solubility compared with the larger droplets. Over time, smaller droplets are deposited on the larger droplets, shifting the droplet size distribution to larger values. Finally, phase inversion is the alteration of the continuous phase as a result of several factors that lead to a drastic change in emulsion properties and structure [1-3,23]. **Figure 2.3** displays the instability mechanisms schematically.

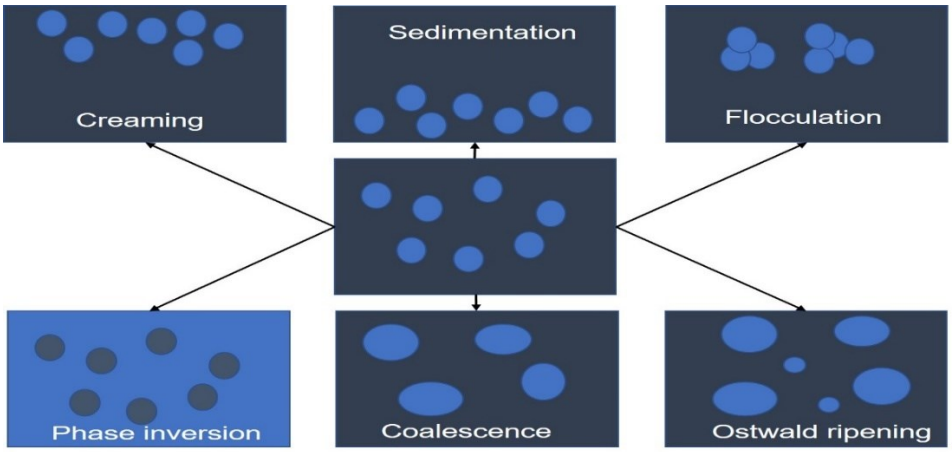

Figure 2.3: Different breakdown processes in emulsions (modified and reproduced with permission after [23])

Stokes law relates the settling velocity of the spherical particles (v_s) at terminal velocities to the density of the particle (ρ_p) and fluid (ρ_f), the radius of the particle (R), and viscosity of the fluid (μ) [24]. According to the Stokes equation (**Equation** 2), the density difference between the particle and the fluid dictates the sedimentation or the creaming of the dispersed phase system inside the fluid mixture system. For heavy oil systems such as in SAGD, where the density difference is minimal between the oil and water, phase separation due to this factor is low.

$$v_s = \frac{2}{9}\frac{(\rho_p - \rho_f)}{\mu} gR^2 \quad (2)$$

2.3.3 Emulsifiers

Emulsifiers are substances that promote the dispersion and stability of the emulsions by reducing the interfacial tension, and steric hindrance [1-5]. Surfactants or surface-active agents are a class of emulsifiers. Emulsifiers have two polar (hydrophilic) and non-polar (hydrophobic) components. This molecular structure enables the emulsifier to be soluble in both oil and water phases.

Surfactants are classified based on their polarity to anionic, cationic, non-ionic, and zwitterionic [1]. According to this classification, anionic surfactants carry a negative charge, cationic surfactants positive charge, zwitterionic surfactants both positive and negative charges, and non-ionic surfactants are not electrically charged. Surfactants are either synthetically derived such as fatty acid esters of sorbitol, or natural such as the asphaltenes and resins in the heavy fraction of the crude oil [2-4].

Emulsifiers have an important role in forming the type of emulsion. Bancroft rule is an empirical observation with some exceptions but describes this role clearly. According to Bancroft's rule, emulsifiers with more solubility in oil will form W/O emulsion. In contrast, emulsifiers that are more soluble in water create O/W emulsions. This is explained by the fact that if the surfactant is in the droplets, the interfacial tension gradient cannot form and drops are prone to coalescence upon collision [18]. Therefore, hydrophilic-lipophilic balance (HLB) of a surfactant which is a measure of surfactant solubility in a phase may determine the type of the formed emulsion [3]. **Figure 2.4** shows the emulsifier structure and how it is oriented in different types of emulsion.

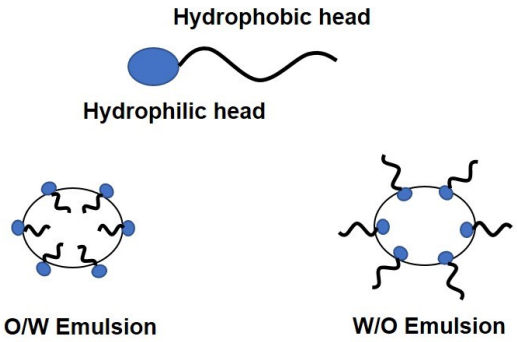

Figure 2.4: Schematic representation of the emulsifiers and their orientation in different types of the emulsions

2.4 SAGD In-situ Emulsion

Thermal methods such as SAGD are special types of steamflooding enhanced oil recovery techniques, which are widely used for bitumen and heavy oil production. The viscosity of oil in these reserves is so high that the fluids need heating to be mobilized. In SAGD, steam is continuously injected by a horizontal injector well located approximately five meters above a horizontal producer well. Consequently, a steam chamber is developed, and the latent heat of steam is transferred to the bitumen, causing a reduction in the viscosity of the oil. Therefore, mobilized oil and condensate flow towards the producer well. However, the produced oil is in emulsion form.

The type of the produced fluids has been observed to be, in most cases, a free water phase and W/O emulsion [13,25-27].

2.4.1 Observations Based on Scaled Laboratory Tests

One of the early studies on emulsification in SAGD was carried out by Chung and Butler [25]. In their research, they scaled down the physical field parameters to conduct the SAGD test in the lab such that one hour of the lab experiment in the lab model was equivalent to 1.57 years at the field conditions. They designed a reservoir model with pre-set well configurations and installed thermocouples to measure the temperature as a result of steam chamber growth. Cold lake bitumen was used in their experiments and steam was injected at 109 ° C. They detected a free water phase and W/O emulsion in their experiments regardless of the operating conditions. However, they recorded a significant change in the Emulsified Water to Oil Ratio (EWOR), which is the volume fraction of water dispersed in the volume of oil based on the geometry of the injector relative to the producer well. In the case where the injector was vertical, EWOR was relatively constant, with a value of 0.19 in the entire experiment. In contrast, an EWOR value of 0.7 was measured for the case in which the injector was horizontal in the early production stage. This value declined to 0.3 in the late production stage. They concluded that the state of the steam chamber highly influences emulsification.

Jamaluddin and Butler conducted similar experiments to investigate the emulsification in SAGD operations [27]. They also used a lab model with Cold lake bitumen. However, they employed packing material with different types of wettability. Moreover, they assessed the effect of steam injection pressure and steam quality on emulsification. They reported that the produced fluids in their experiments included W/O emulsion and a continuous water phase, which contains very little suspended bitumen. EWOR varied considerably for different wetting systems. **Table 2.1** shows the EWOR for different wetting systems in the early and late production stages at 10 psig steam injection pressure. They observed that EWOR decreases for higher steam injection pressures, which will be discussed in detail in Section 4.

Table 2.1: EWOR values for different wetting systems (after [27])

Wetting system	Early production EWOR	Late production EWOR
Oil wet	0.76	0.52
Water wet	0.46	0.32
Neutral wet	0.61	0.34

Sasaki et al. monitored the initial stages of the SAGD operation by the employment of a 2-D scaled reservoir model [28]. A camera was installed to capture thermal-video pictures and record the steam chamber expansion. Synthetic oil (Motor oil) was utilized instead of bitumen with a roughly 1/5 viscosity of the Athabasca bitumen. Nevertheless, viscosity trends as a function of temperature are similar between the synthetic oil and the bitumen. Glass beads were used as the packing material representing the porous media. Dry steam was injected at the saturated steam temperature into the reservoir model. Produced fluid in their experiments consisted of single-phase condensate and a W/O emulsion phase after breakthrough. Single-phase oil was produced for a short period before the steam breakthrough. EWOR was reported to be less than one before the rise of the steam

chamber but increased to 1.2 and remained fairly constant after the steam breakthrough. The oil volume fraction of emulsion produced after a steam breakthrough was 45%. An important observation in these experiments was the change in the free water phase volume fraction. Results showed that the free water phase was about 66 % in the early production stage but increased to 90% in the late production stages. However, these values decreased with the installation of thermal insulators to minimize heat loss.

Several other studies can be found in the literature, confirming the W/O type for the produced emulsion [29-31]. These findings are either based on scaled reservoir high-pressure high-temperature experiments or actual field samples. There are also some reports on the inverse and complex emulsions such as W/O/W or O/W/O emulsions [32-35]. It should be noted that the sampling point matters in the case of field emulsion characterization. Emulsification and change in the emulsion properties may occur in-situ and by flow through the reservoir rock, in the flow lines and production valves, fittings and chokes, and the surface equipment. So, if it is intended to address the emulsion flow characteristics in the reservoir, surface emulsion samples are not representative and scaled reservoir modelling experiments are more reliable to understand what happens in the reservoir.

To summarize, produced fluids in SAGD operations consist of a single-phase condensate (water), W/O emulsion, and single-phase oil only in a short period before the steam chamber rising to the top. EWOR varies mostly with the wettability of the system and steam chamber growth. The free water phase is relatively pure with a minimal amount of bitumen particles, and the studies show the amount of free water phase changes with time. This is a result of steam chamber growth in the reservoir, and it is shown that when the steam chamber is developed, more condensates are produced. Therefore, emulsification is more severe in the early stages of production and declines in the late production stages.

2.4.2 SAGD Emulsion Characterization Techniques

Emulsions are physically characterized by their color and appearance, droplet size distribution, rheology, emulsion type, dispersed phase volume fraction (emulsion quality), interfacial properties, and stability [1-4]. Various techniques have been proposed to determine emulsion properties. However, emulsions are thermodynamically unstable and prone to change in the properties and phase separation. Hence, it is critical to characterize the emulsion expeditiously. Phase inversion and alteration in the emulsion characteristics should be expected during the sampling and characterization, and one needs to follow the protocols to determine the emulsion properties accurately. Some of the emulsion characterization parameters and techniques are described herein.

Solids Concentration in Emulsion: Produced fluids in the reservoir almost always transport detached fine solids. The particle detachment has been reported to be influenced by several parameters, particularly brine composition and concentration [36-39]. So, the emulsion characterization needs to account for solids concentrations inside the fluid mixture as well. The effect of fine solids on the emulsion properties is described in Section 5.1.

Determination of Continuous Phase: The first step is the identification of the continuous phase. The most basic method to do so is the dilution method, in which a few drops are added to the water

[40]. If the emulsion is of the type W/O, it will remain in the form of a drop, otherwise (O/W) drops will spread. Another basic method is dyeing in which the continuous phase can be detected with oil/water-soluble dyes. This method is most efficient when done under a microscope. If a water-soluble dye is mixed with the emulsion and no change in color occurs, it means the continuous phase has to be oil. However, coloring methods are not useful in crude emulsions as these types of emulsions are opaque. Electrical conductivity can also be employed to determine the continuous phase since water as a polar substance has more conductivity compared with oil. Hence, an O/W emulsion potentially has more electrical conductivity. The limitation of this method is the vague results generated when there is a considerable amount of solids in the phases [1].

Emulsion Phase Weight Ratios: The content of the emulsified water, oil, and solids within an emulsion is often measured by the modified Dean-Stark procedure. In this method, the emulsion is placed inside a porous thimble above a refluxing solvent [41]. The components are distinguished through a distillation process.

Another existing method is diluting the emulsion with solvent and then centrifuging it for a certain period [42]. This method is fast and reliable and very common for field evaluations. In the SAGD experimental models, practical solutions have been offered before the centrifuge test. Chung and Butler proposed cooling down the samples at 5° C for 24 hours and then removing the separated water phase by a needle syringe [25]. The centrifuge method presented in the ASTM D4007-B1 was then followed to identify the emulsified water content [43]. Other methods are available to determine the dispersed phase contents such as Karl Fischer Titration, and Gamma-ray attenuation, however, these methods have limitations when it comes to the presence of the fine solids in the system or water content [1,44-45].

Emulsions Rheology: Bulk rheology of emulsions can be measured by several methods. Researchers have used different viscometers to determine the viscosity of emulsions at desirable temperatures. Bennion et al. [46] used pressure differential measurements inside a capillary tube to find the dynamic viscosity of the bitumen emulsion using Poiseuille's law. Kumasaka et al. [31] and Olalekan et al. [47] used plumbing type viscosity sensors for the measurement of emulsion viscosity at elevated temperatures. Rotational viscometers have been used in some studies to characterize SAGD emulsions [29,31]. Such measurement techniques can be erroneous as a result of the emulsion instability and phase separation during the measurements. For instance, there is a possibility of the bitumen separation from the fluid system at the rotor-plate interface of a rotational viscometer. It can be useful to try different techniques to determine the emulsion viscosity to minimize measurement errors.

Emulsion Stability: Various techniques can be used to determine emulsion stability, including simple bottle tests, centrifugation, microscopic techniques, light scattering, and electrokinetics methods. The bottle test is the most basic method for emulsion stability determination, where phase separation in the emulsion is monitored with time. The method is vastly popular due to its simplicity. However, when the separation is not distinct, the results are biased and depend on the operator readings. More advanced methods, including centrifugation, light scattering, and optical

microscopy, are employed to eliminate the errors associated with the complexities in distincting phase interfaces.

Stability in the emulsion system comes from both a steric hindrance and electrostatic stability. The methods described above measure general stability that includes all the parameters involved in the demulsification process. It is also possible to assess the electrostatic stability of the emulsions directly by electrokinetic measurements. This is achievable through measurement of the zeta potential, which is the potential difference between the mobile dispersed medium and the stationary layer of the dispersion medium attached to the dispersed particle [1-4,48].

The most relevant study in which emulsion stability is addressed as a result of the measured zeta potential is the criteria presented by Riddick and presented in **Table 2.2** [49]. However, he was looking into blood cells of typically 7-10 micrometer in size, and SAGD emulsions are somewhat within the size range, but not necessarily with the size distribution. One also needs to consider the fact that electrostatic repulsion is not the only source of stability. Steric hindrance, emulsifier concentration, density differences, droplet size, and many other important contributing mechanisms are involved in the process. There are several studies on the SAGD crude emulsion stability in which zeta potential measurements were used along with other means of the emulsion stability tests [33, 35].

Table 2.2: Relation between the suspension stability and the measured zeta potential (after [49])

Stability characteristics	Avg. ZP (mv)
Maximum agglomeration and precipitation	0 to +3
Range of strong agglomeration and precipitation	+5 to -5
Threshold of agglomeration	-10 to -15
Threshold of delicate dispersion	-16 to -30
Moderate stability	-31 to -40
Fairly good stability	-41 to -60
Very good stability	-61 to -80
Extremely good stability	-81 to -100

Size Distribution of Dispersed Phase: The size distribution of the droplets within an emulsion influences many emulsion characteristics. This includes the stability and bulk viscosity of the emulsions. Several methods exist for the dispersed phase size distribution characterization, such as optical microscopy, laser diffraction, scanning electron microscopy, and Near-Infrared Spectroscopy [1-4,50-51]. Microscopic methods are preferred as they provide visual means by which the dispersed phase size range can be identified. However, results obtained from these techniques are highly sensitive to the sampling method. In the laser diffraction method, the deviation of a light source (laser) from the particle is measured, and the final patterns are analyzed

to give the particle size distribution [51]. This method is prone to errors caused by the particle shape since the analysis theory is based on spherical particles.

Interface Properties: It is well documented in the literature that the emulsion characteristics, especially the stability, are severely affected by the droplets' film properties [52-54]. Surface rheology and elasticity, interfacial tension, and electrical double layer (EDL) can change the stability state of the emulsion. Tensiometers and surface rheometers of different types are used to determine the interfacial tension and dynamic interfacial rigidity modulus (surface elasticity, G'), respectively.

Non-conventional techniques: Non-conventional advanced techniques such as Differential Scanning Calorimetry (DSC) have gained popularity recently in the characterization of the thermal EOR and SAGD emulsions [29,33,55]. DSC is a thermoanalytical method in which the amount of heat or cooling required to increase or decrease the sample temperature is monitored as a function of time or temperature [29]. This method is very useful in SAGD emulsion characterization since the supercooling behaviors of the free phase water and emulsified water are very different. Therefore it is possible to distinguish between the free water phase and emulsified water in this method. However, finer solids in the SAGD emulsions can influence the latent heat and freezing temperature by providing nucleation sites.

Summary: Simple and basic methods like bottle tests, as well as unconventional advanced techniques such as Differential Scanning Calorimetry (DSC), are available for the characterization of emulsion properties. Interpretation of the results from one test seems to be insufficient as each one of these methods has its limitations and sources of errors. Additionally, sampling can be a significant cause of inaccuracy in some of the presented methods. Incorporating several techniques can be useful in the identification and reduction of potential errors and also providing insights on the time and mechanisms of alterations in the emulsion properties.

2.5 SAGD Emulsification Mechanisms

Emulsions are not present in the reservoir before recovery procedures, and their formation is attributed to the mixing (Dispersivity)/or changes in pressure, temperature, and presence of natural emulsifiers [15]. Researchers have theorized the existence of a mobile oil phase following this process and as a result of the thermal gradient in the steam bitumen contact region. It is explained that the water droplets are engulfed by this mobile oil phase and "W/O" emulsion is formed in this way [25,27, 30]. Moreover, the presence of emulsions was verified in micromodels visually in SAGD-Solvent injections as well [56,57]. **Figure 2.5** shows this phenomenon schematically and visually in a SAGD micro model.

Higher temperature decreases the Gibbs free energy, hence, facilitates emulsification. Moreover, studies have shown that increasing the temperature leads to a reduction in the interfacial tension of the fluid system, reducing the system energy and magnifying the potential of emulsification [46,58]. Perhaps this is one of the reasons why emulsification is reported to be more severe in thermal EOR operations.

In SAGD, it seems that the emulsification and the amount of water emulsification in the mobile oil phase are closely linked to the steam chamber growth [13,25,27]. In the very early production stage where the steam chamber is not developed, bitumen is mainly heated by conduction, resulting

in the mobilization of single-phase heated oil towards the producer well [59]. This stage of single-phase oil production is short as the steam chamber begins its rise and lateral growth. Lab modelling of SAGD process shows that as the steam chamber is rising (early stages in SAGD production), a counter-current flow of steam and mobile oil (mobilized downward by gravity force) is developing within the steam chamber, magnifying the emulsification. However, when the steam chamber spreads laterally, a stratified two-phase steam-oil flow is formed, where the steam flow takes place at the interface, and oil flow occurs below the interface toward the producer well. A lower EWOR is observed under such steam chamber growth profile [25-27]. Additionally, it has been shown that if the process of the steam chamber growth speeds up through higher steam injection pressure, lower EWOR values are obtained [27].

When the steam comes in contact with the cold bitumen, heat is transferred from the steam to the bitumen, reducing the oil viscosity. Jamaluddin and Butler explained that steam needs to be undercooled to form spontaneous nucleation in such a process to result in condensation. If there is a relatively flat steam-water interface, steam most likely condenses at this interface before achieving the degree of supercooling required for nucleation on the oil surface. They concluded that microscopic droplets on the oil surface cannot form under such conditions [27]. However, this logic seems to be incomplete as "spontaneous nucleation," and "supercooling" phenomena are unlikely to occur in porous media.

Spontaneous nucleation (homogeneous nucleation) occurs when there are no foreign materials or wall surfaces. Under these circumstances, the phase change is blocked by an activation free energy barrier [60]. This barrier is a result of surface free energy increase, which is caused by the embryos of the more condensed phase. Hence, in the case that no impurities exist, steam may supercool below the dew point until the occurrence of the homogeneous nucleation. However, the prerequisites for such a thermodynamic process are not met in SAGD and in porous media. The reasons are the water in the reservoir is saline and polarized, different types of sand and clay fines are packed, and steam is in contact with an impure bitumen interface that contains hetero atoms (ionic). These factors most likely cause heterogeneous condensation.

On the other hand, the amount of work required to form a water droplet in different wetting systems in a capillary tube has been investigated. It was shown that the work required to have a single drop of water in an oil-wet system is less than in water-wet and neutral-wet systems, as shown by **Equation 4** [27].

$$P_{emuls} = \frac{W_n}{V_w} = \frac{3\sigma}{R}\ (1 + \frac{2}{3}\ Cos\theta) \qquad (4)$$

where P_{emuls} is the pressure required to disperse water drop in the oil phase (Nm^{-2}), W_n is the net work required to disperse water droplets in the oil phase (N.m), V_w is the water drop volume (m^3), σ is the interfacial energy ($J\ m^{-2}$), R is the radius of curvature (m) and θ is the contact angle of the water phase and capillary wall.

For strongly water-wet systems, the work required to form W/O emulsion can be much more than for strongly oil-wet systems. In stable waterfronts and water films, the condensation will likely take place at the water phase, and this theory can support the reports of less emulsification in the late SAGD production stage. It has been shown that temperature can decrease the interfacial forces

and increase the water wetness and relative permeability of the oil over time [61,62]. The resulting condensate drops must be tiny at the beginning [27]. As the steam condenses, the excess energy contained is released to the surroundings in the form of latent heat, causing a reduction in the bitumen viscosity at contact with the steam.

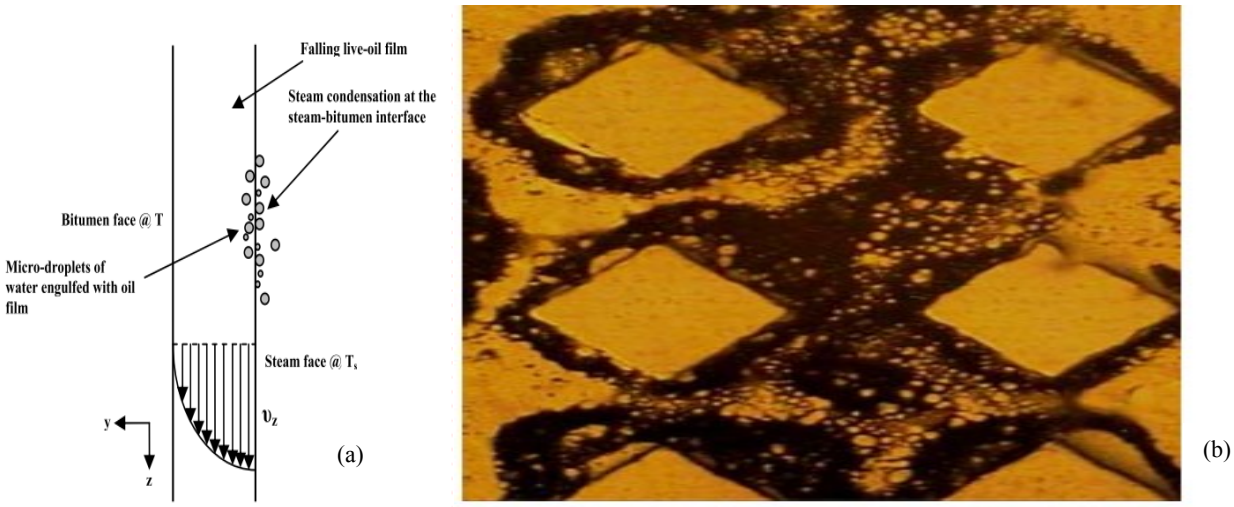

Figure 2.5: Emulsification at the steam-bitumen interface, (a) schematic (Adapted with permission from source [30]), (b) W/O Emulsion formed in a SAGD micromodel, Adapted with permission from source [30]

To summarize, the high steam temperature in SAGD facilitates the emulsification through a reduction of interfacial forces and magnification of the system entropy. These factors decrease the required work for emulsification. Condensation of the steam within the heated (mobilized) oil results in the engulfment of water droplets by the oil phase carrier fluid; hence, the formation of a "W/O" emulsion. EWOR is highly sensitive to the steam chamber profile. More emulsification is anticipated due to the extra direct condensation in the counter-current flow of steam-oil while the steam chamber is rising. Lower EWOR is expected when the steam chamber is spreading laterally.

2.6 SAGD Emulsion Features

In this Section, some of the most prominent features of SAGD emulsions are described. These include the effect of physio-chemical factors on the emulsion properties. Such factors mainly influence the stability, viscosity, droplet size, and droplet size distribution of the emulsion. Additionally, conventional emulsion flow models presented in the literature are critically reviewed in this Section.

2.6.1 Primary Stability Factors

Emulsions are generally thermodynamically unstable (except for the micro-emulsion) and may exhibit kinetic stability in the presence of emulsifiers. Emulsifiers promote the stability of emulsions through steric hindrance, electrostatic repulsion, viscosification, promotion of rigidity of the droplet film, and the reduction of the interfacial tension between phases [1-4].

SAGD "W/O" emulsions have been reported to display kinetic stability [25,35,46,63]. Reasonable kinetic stability of the emulsions has been detected visually [28,30], and through produced fluid sampling from the SAGD lab models [25,27]. However, there is mention of the possible instability mechanisms such as coalescence [30] and the indirect effect of temperature in destabilizing the

emulsion through a reduction in the emulsion viscosity [46]. Kinetic stability of the emulsions can be considered to be true for all the emulsions formed in the thermal recovery operations due to the presence of a large amount of interfacially active compounds in the heavy oil [64]. Although the temperature is a destabilizing factor for emulsions by reducing the bulk viscosity, this effect seems to be somewhat neutralized by the presence of natural emulsifiers in the heavy oil reservoirs.

Natural Emulsifiers: Natural emulsifiers in heavy oil reservoirs consist of fine solid particles (such as clay, silt, and corrosion products) and surface-active compounds (such as asphaltenes and naphthenic acids) that contribute to the SAGD emulsion stability [4,65]. Most of the natural emulsifiers exist in the heavy fraction of the crude that is made of asphaltenes, resins, and oil-soluble organic acids and bases. **Table 2.3** shows Saturate, Aromatic, Resin, and Asphaltene fractions (SARA analysis) of Athabasca and Cold Lake bitumens in Canada. This table is showing a considerable amount of asphaltenes and resins in the bitumen, which could potentially form micelles and act as the emulsifiers in SAGD conditions.

Table 2.3: SARA analysis of Cold Lake and Athabasca bitumens in Canada (After [66])

	Athabasca	**Cold Lake**
API Gravity	8.05	10.71
Viscosity at 24 °C (Pa.s)	323	65
Saturates (%wt)	17.27	20.74
Aromatics (%wt)	39.70	39.2
Resins (%wt)	25.75	24.81
Asphaltenes (%wt)	17.28	15.25

Asphaltenes are complex polyaromatic molecules that contain aromatic sheets with alkyl and alicyclic side chains and heteroatoms (Nitrogen, Oxygen, sulfur, and trace metals like vanadium and nickel) [67]. The molecular weight of asphaltenes ranges from 500 to over 10,000.

Asphaltenes stabilize the "W/O" emulsions either in the colloidal state (through the formation of rigid films around the droplet) or in a precipitated and aggregated form (through steric hindrance). This fraction of heavy oil can change the wettability of the solids, form rigid films around the droplets after forming micelles with resins, and contains heteroatoms that are surface-active materials and adsorb on water droplets [68]. In experiments that replicated SAGD and Expanding Solvent-SAGD (ES-SAGD) operations, it was found that asphaltenes of produced W/O emulsion have a lower zeta potential value in SAGD operations compared to the ES-SAGD operation, indicating lower stability and a higher tendency for precipitation [35]. Kokal and Al-Dokhi showed that crudes with a higher tendency in asphaltene precipitation are more likely to form a stable emulsion [15]. **Figure 2.6** illustrates the stability mechanisms provided by the asphaltenes.

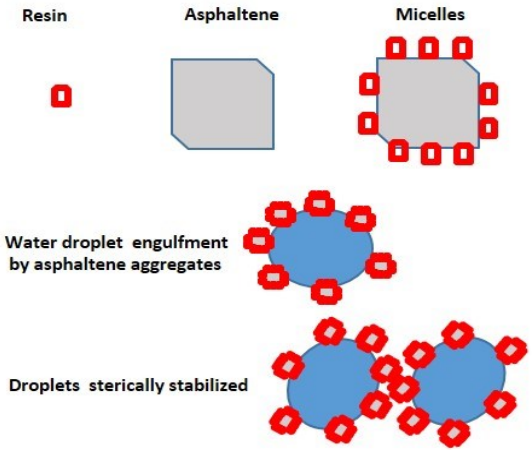

Figure 2.6: Stability of "W/O" emulsions through steric hindrance and film rigidity provided by asphaltene-resin micelles

Effects of Reservoir Clays: SAGD emulsion can also be stabilized by fine solid particles that have a significant presence in the form of silt, clay, shale particles, and corrosion products in the reservoir and near the wellbore region [4]. However, the size of these solid particles is very important, so to act as a stabilizing factor. Particle sizes have to be much smaller than the water droplets to form a viscoelastic rigid film around the water droplets [1].

Wettability Effect: The wettability of the particles is extremely important for the solid particles to act as an emulsifier [69]. The wettability of the particles determines the placement of the solid particles in the system such that if the particles are oil-wet or water-wet, particles will be placed in the oil or water phase, respectively. Therefore, the neutral-wetting condition favors the potential of solid particles forming a film around the droplets, as schematically shown in **Figure 2.7**.

Moreover, fine solid particles may contribute to the stability of the emulsion through an electrical charge repulsion. This is the case only if the particles are electrically charged. Contact angle, particle size, solids concentration, and interparticular interaction all influence the role of the solid particles as an emulsifier [69]. If the conditions permit emulsion stability by fine solid particles, the resulting stabilized emulsion is referred to as Pickering emulsion [70].

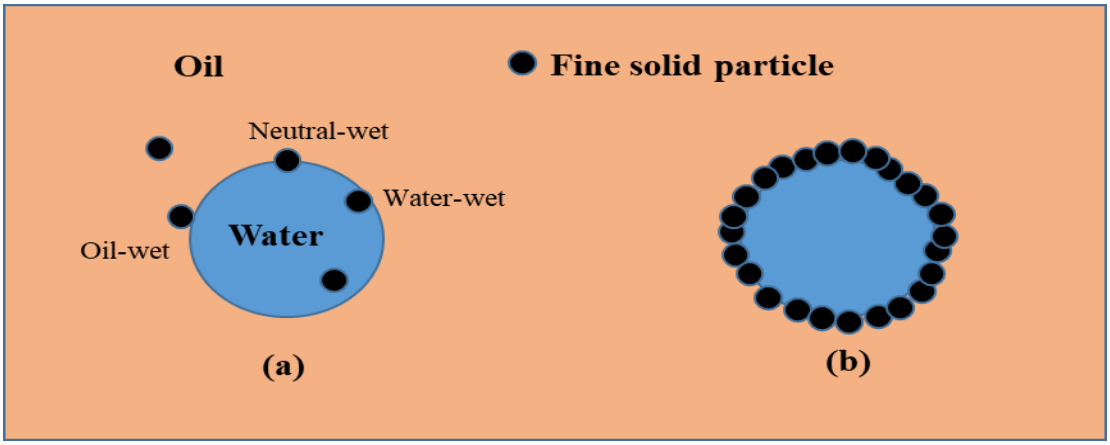

Figure 2.7: Effect of contact angle on the stabilizing role of the solid particles. (a) Neutral wetting conditions (ɵ=90°) favors the possibility of fine particles acting as emulsion stabilizers (b) Pickering emulsion structure

Effect of Phase Inversion: Phase inversion is another phenomenon that might have a slight chance of occurrence in SAGD operations as a result of an increase in the emulsified water cut. Phase inversion is one of the emulsion instability mechanisms, and emulsion properties alter drastically after this phenomenon. As a rule of thumb, if the volume fraction of a phase in an emulsion is so much larger than the other phase, it will eventually form the continuous phase [1]. The inversion point is also influenced by the presence of emulsifiers and their solubility tendency in each phase. In the literature, it is indicated that the emulsified water cut can reach up to 76% in the early stages of SAGD operations [27]. Hence, the chances of a phase inversion occurrence appear to exist to some extent for a short period of time and probably for some production intervals.

Water and oil density difference is minimal in SAGD operations (heavy oils have high densities), which makes the phase separation more difficult. This adds to the stability of the emulsion [33]. Numerous other factors contribute to the stability of the emulsion, including the shear rate, bulk viscosity, interfacial viscosity, and phase composition among others [4].

Effect of High Temperature: The propensity of emulsification has been reported to be more severe in thermal recovery [46]. The physical phenomena involved were described in the SAGD emulsification subsection. Not only higher temperature facilitates the emulsification, but it also destabilizes the emulsion because of the reduction in the viscosity of the system. In general, more viscous emulsions are more stable [52].

pH Effect: There have been reports of a strong influence of pH on emulsion stability in the literature [58]. Whether the interfacial film is formed by asphaltenes, resins, or fine solids, the effect of pH can be different such that asphaltene-based films are strongest in acidic conditions, resin-based films in base conditions, and solids can become oil-wet by the presence of asphaltene. This process is further supported by the acidic medium. Moreover, it was found that brine composition has an interactive effect with pH such that crude/brine systems have an optimum pH range for which the interfacial films show instability [4].

2.6.2 SAGD Emulsion Droplet Size Distribution

Droplet Size Distribution (DSD) of the emulsion has a direct effect on other emulsion properties such as viscosity and stability. However, emulsion stability is not necessarily a function of the dispersed phase size [1]. Yet, more stability can be attained for smaller droplets in some emulsions. Emulsions with homogeneous and narrow DSD's toward smaller size typically possess higher viscosities, and an increase in viscosity contributes to the stability of the emulsions as well [52].

Generally, the droplet size of in-situ oilfield emulsification is at the macroscopic scale. Hence, the emulsions are categorized as macro-emulsions (>0.1 μm) [1,4]. Typically, a mean size range of 0.1 μm to 10 μm has been reported for the oilfield emulsions [46]. **Figure 2.8** displays where the SAGD emulsions stand within the classifications of emulsions regarding the droplet size range.

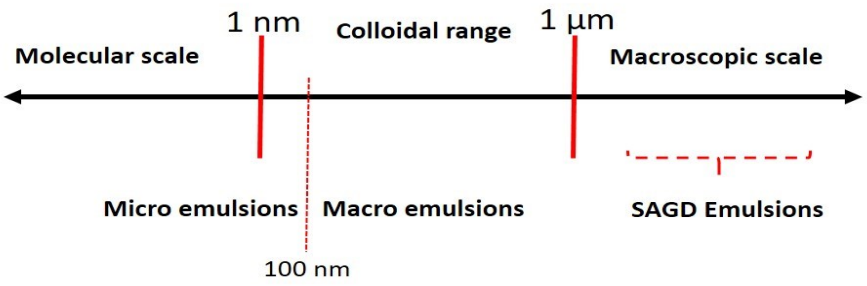

Figure 2.8: SAGD emulsions classification based on the dispersed phase size

Sasaki et al. (2002) conducted experiments in which they attempted to replicate the conventional SAGD operation using a 2-D scaled reservoir model [28]. A high-resolution optical fiberscope was used in the experiments to capture the micro-phenomena visually. The measured droplet sizes were compared with the same for produced fluids samples, and the results matched reasonably. It was reported that the average diameter of the water droplets changes with time. Further, much larger average diameters were observed after the steam breakthrough. These results support the theory that was previously presented by Chung and Butler [25] and Jamaluddin and Butler [28] that linked the emulsification mechanism to the steam chamber growth. The average diameter of the water droplets changed from approximately 10 µm to 15 µm, and the droplet size was measured at approximately 30 µm after steam breakthrough.

Kumasaka et al. (2016) used a micro-reactor and a steam generator to mimic the High pressure-High temperature (HP-HT) SAGD emulsification conditions [31]. They ended up with a "W/O" emulsion with droplet size distribution ranging from 2 µm to 15 µm with a mean diameter of a bit over 10 µm. Droplet size distribution in their experiment appears to be more uniform than the results shown by Sasaki et al.. This is most likely a result of the difference in emulsification mechanisms. The effect of porous media was completely ignored in the micro-reactor method of emulsification. However, the flow through the porous medium can have contrasting effects. The effects are flow shearing, which promotes emulsification and at the same time, may cause droplets breaking. They also compared their measured droplet size with the emulsion produced in Hangingstone, Canada. However, it is not clear where the sampling point of the emulsion is as it can drastically change the emulsion characteristics altogether. The droplet sizes of the Hangingstone field samples are comparable to the same for emulsions produced due to extreme pressure drops across choke valves, as investigated by Noik et al. [29] and Dalmazzone et al. [55].

The droplets formed in the SAGD process are not consistent in size. Micron-sizes as small as 1 µm to as large as 60 µm have been reported in the literature. However, the initial size of water droplets has to be tiny in the beginning. Later on, the droplet size likely increases as a result of coalescence. Visual capturing of the droplet formation in SAGD lab models suggests that the mean size of the droplets is probably between 10 µm- 15 µm based on the different results presented in the literature [28-31].

Another important parameter is the dispersed phase droplet size distribution (DSD), which varies case by case and appears to be a dynamic property. This means that the DSD alters with time, as a function of steam chamber growth and motion of the droplets in the porous media. Currently

available data from the SAGD experiments show that the DSD in SAGD operations follows a rather multimodal distribution with multiple peaks of type "S" in Galtung's classification [71].

2.6.3 SAGD Emulsion Viscosity

At first glance, higher viscosities of SAGD "W/O" emulsions tend to reduce the cumulative production according to Tandrain and Lindrain analytical equations developed for SAGD production [13]. However, more complicated mechanisms are involved as will be explained later in this Section.

While dilute emulsion might exhibit Newtonian behavior, macromolecular fluids, and concentrated emulsions are typically considered as non-Newtonian pseudoplastic (shear thinning) fluids [1]. In other words, the apparent viscosity of the emulsions decreases at higher shear rates.

In general, the viscosity of the emulsions is influenced by the continuous and dispersed phase viscosities, the volume fraction of the dispersed phase, mean droplets size, DSD, shear rate exerted on emulsions, temperature, and presence of emulsifiers [1-4]. Not many emulsion-specific correlations have been developed. Most of the correlations in the literature are defined for the suspensions with assumptions that might not be valid in the case of emulsion. Such correlations have been developed for the cases of constant temperature and variable temperature conditions. **Table 2.4** shows some of the most important correlations.

Table 2.4: Viscosity models presented for dispersed fluid systems

Viscosity models of constant temperature			
Model	**Correlation**	**Variables**	**Assumptions/Hypothesis**
Einstein [72,73]	$\mu_r = 1 + 2.5\,\emptyset$ $\mu_r = \frac{\mu}{\mu_c}$	μ_r: Relative viscosity μ: Dispersed system viscosity μ_c: Continuous phase viscosity $\emptyset$: volume fraction of the dispersed phase	Derived for suspension of non-deformable spherical particles at very low concentrations
Taylor [74]	$\mu_r = 1 + [2.5\left(\frac{(k+0.4)}{(k+1)}\right)]\,\emptyset$ $k = \frac{\mu_D}{\mu_c}$	μ_D: Dispersed phase viscosity	Derived for a small concentration of spherical droplets Often used to describe the SAGD emulsion rheological behavior in numerical modelling
Roscoe [75] and	$\mu_r = \frac{1}{(1 - \emptyset)^{2.5}}$	$\emptyset$: volume fraction of the dispersed phase	Developed for a higher concentration of the dispersed phase

Brinkman [76]			
Richardson [77]	$\ln(\mu_r) = k\,\emptyset$	k: A constant which depends on the system	An exponential increase in relative viscosity is expected with a higher dispersed phase volume fraction
Broughton and Squires [78]	$\ln(\mu_r) = k_1\,\emptyset + k_2$	$k_1\ and\ k_2$: Constants that depend on the system	A modification of Richardson equation
Eilers [79]	$\mu_r = [1 + \left(\frac{1.25\emptyset}{1 - a_E\emptyset}\right)]^2$	a_E: Empirical constant (range: 1.28-1.30)	Obtained based on the experiments on the bitumen emulsions
Mooney [80]	$\ln(\mu_r) = \frac{2.5\emptyset}{1 - k\emptyset}$	k: A constant which depends on the system	Derived for concentrated suspensions Very popular in the emulsion literature
Krieger and Dougherty [81]	$\mu_r = \frac{1}{(1 - \emptyset/\emptyset_m)^{[\mu]\emptyset_m}}$	$[\mu]$: Intrinsic viscosity $\emptyset_m$: Maximum packing concentration	Derived based on functional analysis, similar to Mooney's approach
Hatschek [82]	$\mu_r = \frac{1}{(1 - \emptyset^{1/3})}$		Developed for the concentrated emulsions
Sibree [83,84]	$\mu_r = \frac{1}{[1 - \left(h\emptyset^{\frac{1}{3}}\right)]}$	h: A hydration factor that depends on the emulsion system	A modification of Hatschek equation
Pal and Rhodes [85]	$\mu_r = [1 + \left(\frac{(\emptyset/\emptyset_o)}{1.187 - (\emptyset/\emptyset_o)}\right)]^{2.49}$	$\emptyset_o$: Dispersed phase concentration at which relative viscosity is 100	The empirical correlation obtained for mono-dispersed emulsions with similar phase densities and low IFT
Viscosity models of variable temperature			
Ronningsen [86]	$\ln(\mu_r) = a1 + a2T + a3V + a4T\emptyset$	ai: Shear rate-dependent coefficients T: Temperature	Empirical correlation derived from the experimental results

ASTM standard [87]	$\ln(\ln(z)) = A - B\ln(T)$ $z = v + 0.7 + f(v)$ $\ln(f(v)) = -1.47 - 1.84v - 0.51v^2$	v: kinematic viscosity Z: Viscosity function T: Absolute temperature A & B: Characteristics of each product	Defined for crude oil and its fractions
Farah et al. [88]	$\ln(\ln(\emptyset + 0.7)) = k1 + k2\emptyset + k3\ln(T) + k4\emptyset\ln(T)$	Ki: experimental coefficients	-An extension of the ASTM correlation obtained to include the dispersed phase volume fraction for W/O emulsion -Proposed correlation coefficients must be determined for 2 points (temperature above/below wax appearance temperature)

Phase inversion can occur at very high emulsion qualities (water cuts), which leads to a complete change in rheological behavior. SAGD emulsions are "W/O" emulsions with higher viscosities compared with the continuous phase (oil) viscosity. This behavior in "W/O" emulsions has been observed in many studies, while "O/W" emulsions have been reported to manifest lower viscosities than the oil phase [1-4]. Chances of phase inversion at high water cuts in SAGD operation are not high as the maximum emulsified water content reported in the literature is 76%, and this is the case only for the early production stages and strongly oil-wet systems [27].

Accuracy of SAGD Emulsion Viscosity Models: Temperature decreases the bulk viscosity of the fluids. This parameter has a significant effect on emulsion behavior as it facilitates emulsification and destabilizes the emulsion by reducing the emulsion viscosity. The typical SAGD temperature is about 200 °C (and above). At this temperature, bitumen viscosity is approximately 10 cP for Athabasca oil sands [89]. However, the viscosity of the produced fluid deviates from this magnitude as the water volume fraction increases in the emulsion [90]. Not much research work can be found in the literature in which the viscosity of the emulsion is measured for the actual bitumen-emulsions. Bennion et al. (1993) measured the viscosity of the emulsions at different water cuts for a field oil sample using an HP-HT micro-reactor [46]. Also, Chung and Butler (1988) measured the viscosity of the bituminous emulsions in their scaled reservoir model experiments [25].

Chung and butler's viscosity measurements were carried out for temperatures up to 90 °C. We extrapolated the viscosity value at 200 °C to find the viscosity at SAGD conditions. Power function trend lines were plotted to extrapolate the viscosity values at the desired temperature. Next, we

analyzed different viscosity models presented in the literature (**Table** 2.2) to see which model best describes the emulsion rheological behavior. The most popular method that has been used for numerical modelling of SAGD emulsion in the literature appears to be Taylor's model. **Figures 2.9** and **2.10** show the models plotted against the measured viscosity points in Bennion et al. and Chung and Butler experiments, respectively. **Table 2.5** shows the analysis of the statistical results for different viscosity models.

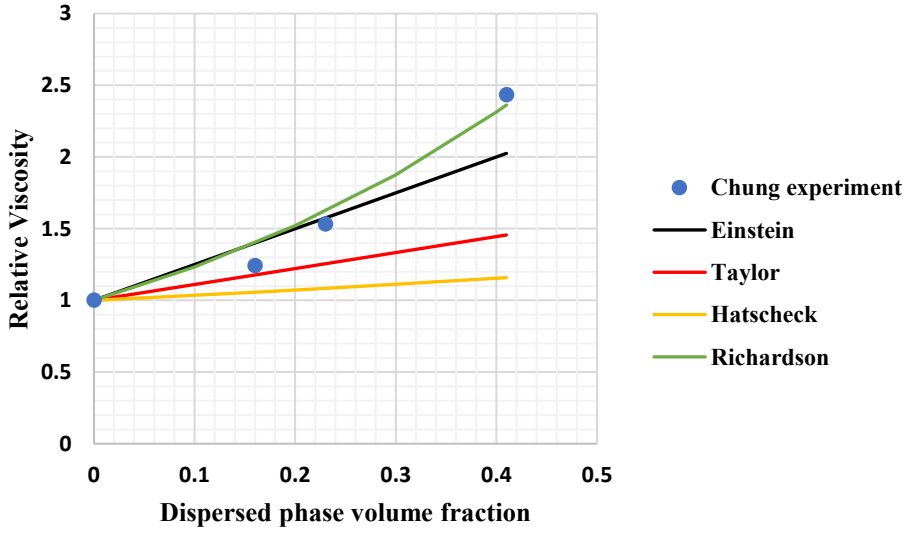

Figure 2.9: Relative viscosity of different models against the experimental data at 200°C

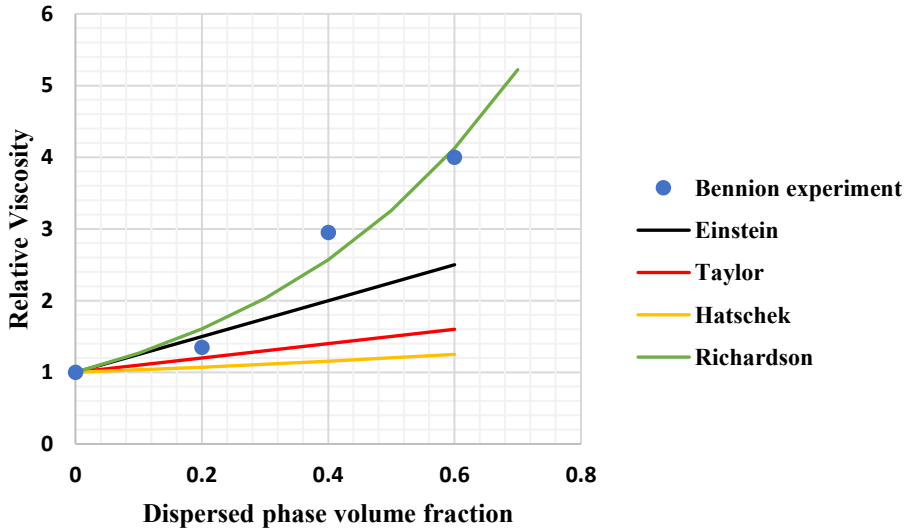

Figure 2.10: Relative viscosity of different models against the experimental data at 200°C

Table 2.5: Statistical analysis of the viscosity models performance for each experimental data set

Experiments	Sum of squared errors (SSE)			
	Einstein	Taylor	Hatscheck	Richardson
Chung experiments	0.193	1.033	1.858	0.037
Bennion experiments	3.173	8.179	10.859	0.223

The reason **Figure 2.9** and **2.10** are plotted separately is the difference in emulsion preparation (emulsification) procedures in the experiments. Further, none of the two papers mention the DSD of the dispersed phase within the emulsion. According to **Figures 2.9** and **2.10**, while models such as Taylor and Einstein predict the emulsion viscosity with acceptable accuracy in lower concentrations, they are unable to give reliable results at higher concentrations of the dispersed phase.

Taylor model has been the method of choice in numerical and analytical modelling of SAGD emulsion flow. However, implementation of this model in the simulator results in a false representation of the emulsion viscosity at higher EWORs (and equivalent dispersed phase volume fractions). This is especially the case since SAGD EWOR values are relatively high as shown in Section 3.1. Richardson model seems to be the most accurate emulsion viscosity model for the SAGD emulsions (This applies to modified Richardson models such as Broughton and Squires model that contains two calibration coefficients). However, the problem with Richardson model is the calibration coefficient in the correlation. Experimental results (In-situ emulsion DSD, emulsion viscosity at different water cuts) are not always available to be used for calibration purposes. Other popular models such as Mooney's correlation were examined, and it was observed that this model predicts the viscosity of SAGD emulsion well only at very high concentration and performs poorly at low concentrations of the dispersed fluid. DSD and viscosity might vary case by case as the oil composition and formation properties affect the emulsion properties. Therefore, the authors suggest the following workflow to determine the field sample emulsion viscosity as shown in **Figure 2.11**.

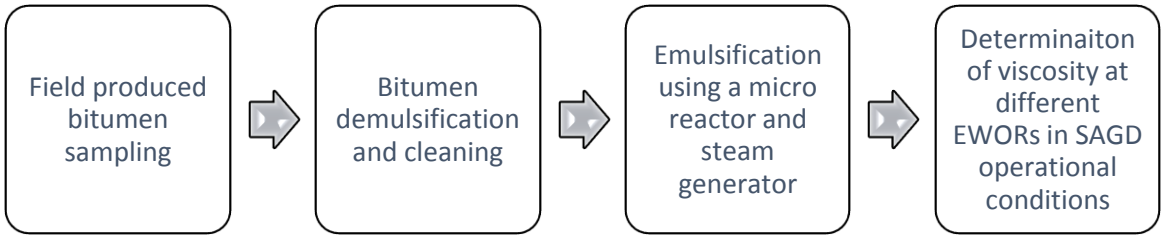

Figure 2.11: Procedure of field emulsion viscosity determination

2.6.4 SAGD Emulsion Flow Modelling

The effect of temperature on different reservoir properties has been investigated by many studies [91-93]. It has been found that temperature could potentially decrease the interfacial forces and

increase the water-wetness and relative permeability of the oil with time [13,61,62]. Relative permeability curves change with temperature in steamflooding operations, such that relative permeability of oil increases and the residual oil is reduced consequently. Additionally, it was observed that steamflooding conditions tend to lower the relative permeability to water. Butler (1991) discussed that such effects are partially due to the formation of emulsions under steaming conditions. He explained that small droplets of water dilute the residual oil drops. Other researchers also speak of the convective heat transfer under SAGD emulsion flow [59,94]. Water relative permeability could be reduced as some of the water might be tied up with the slow-moving oil phase [13].

Adding to the complexity, emulsion droplets may cause emulsion blockage, and larger droplets can potentially clog the pore throats [90]. These droplets are also prone to breaking up as they pass through these pore throats [95]. A reduction in the permeability in some experiments and more catastrophic results such as complete well failure were reported as a result of emulsion blockage [90].

Developed models for SAGD production rates have been reported to deviate from the field production rates [63]. One of the reasons behind the deviation is linked to the emulsion flow in the reservoir [96]. The lag traceable in the Sasaki et al. experiment was linked to the emulsion flow, particularly in the early stages of the production, in which emulsification was more severe in the experiment [96]. **Table 2.6** shows the attempts on the modelling of the SAGD production considering the emulsion flow.

Table 2.6: Presented models considering SAGD emulsions

Model	Remarks
Azom and Sirinvasan [59]	- Coupled an emulsion mechanistic model with SAGD numerical simulation - Emulsion viscosity modeled using Taylor's correlation which is not valid for a high concentration of dispersed phase - Deviation from the experiment production trend
Kumasaka et al. [31]	- Numerical simulation - A viscosity model was developed after experiments on heavy oil - Used hypothetical pseudo-reactions for emulsification which is not supported by sufficient evidence
Ezeuko et al. [63]	- Numerical simulation - Defined hypothetical pseudo-reactions for emulsification

	- Emulsion viscosity modeled using Taylor's correlation which is not valid for a high concentration of dispersed phase
Mojarad and Dehghanpour [97]	- An analytical model of emulsion flow at the edge of the steam chamber - Emulsion viscosity modeled using Taylor's correlation which is not valid for a high concentration of dispersed phase - Assumptions were made based on the experimental work of Noik et al. [30]. One of the assumptions is that all the water is emulsified in the oil phase. In Noik et al. experiments, emulsification was carried out by a flow loop system and a flow restriction. They witnessed full emulsification of water in cases of high threshold energy. That study is meant for emulsification in flow lines, not in-situ reservoir emulsification. Numerous studies using scaled reservoir models illustrate a dynamic range for different wetting systems which depends on the SAGD production stage and steam chamber growth. EWOR can reach as low as 0.19 as shown in some experiments [26] which makes the premise in this study invalid.

In the models introduced in **Table 2.6**, the emulsion was simplified in the form of a single-phase fluid with an effective viscosity, different from the single-phase oil viscosity. However, this approach is associated with some serious shortcomings that make the assumption invalid. Firstly, not all the droplets will remain as the dispersed phase fraction, and most likely, a significant fraction of the droplets will form a continuous water phase. Moreover, emulsion droplets may be trapped in the pore throats if the size of the droplets is in the same order of magnitude as the pore throats. The latter has shown to have a dependency on the flow rate and capillary number [98-100].

Another viable option of looking into the emulsion flow in porous media would be treating the emulsion as a multiphase flow with apparent relative permeability defined for both dispersed water and continuous oil phases. Experiments show the apparent relative permeability is affected by the flow rate, capillary number, and water/oil ratio [101]. Studies indicate that due to the emulsification in porous media, apparent relative permeability of the oil decreases, while at the

same time increases at higher capillary numbers [101]. In steamflooding operations, a higher relative permeability of the oil can be partially credited to the effect of temperature in reducing the viscosity of the fluid such that the capillary number increases as a result of a magnified flow rate.

2.7 Summary

This paper reviewed emulsification and emulsion flow in thermal EOR methods with a focus on SAGD. The paper critically reviewed physical properties and other aspects of SAGD emulsion including the emulsion type, dispersed phase volume fraction, free fluid phase volume fraction, emulsion stability, emulsion viscosity, emulsion droplets size and DSD, emulsification mechanisms, and the relevant thermodynamical concepts, the effect of the reservoir wetting system on the emulsification, interactive effect of the parameters, methods of emulsion characterization, reservoir engineering aspects of emulsion flow and the resulting physical phenomena. Moreover, various SAGD viscosity models and flaws with the current analytical and numerical models were reviewed. Different emulsification mechanisms were reviewed based on experimental and field evidence. Finally, the gaps in the research were identified. **Table 2.7** shows a summary of the results concluded from this review study.

Table 2.7: A summary of the SAGD reservoir emulsion

Parameter	Remarks
Emulsion type	- W/O emulsion, some reports on complex emulsions
Produced fluid volume fraction	- W/O emulsion + Free water phase - High free water values reported in the literature, increasing up to 90 % in the late SAGD production stages
The emulsified water volume fraction	- It depends significantly on the wettability of the system and other factors including steam quality, reservoir, and operating conditions, and geometrical effects of the steam chamber. It often decreases in the late SAGD production stages due to the steam chamber development. Various values in the range of 0.76 to 0.19 EWOR has been reported in the literature under relevant SAGD conditions.
Droplets mean size and DSD	- A wide range of sizes from 1μm-60μm reported. However, the mean size of 10 μm to 15 μm was measured for the size of the droplets. DSD often has multi peaks and follows a multimodal size distribution.
Rheology	- The viscosity of the emulsions increases significantly with the emulsion quality. - Phase inversion possibility is minimal and may exist only at the early stages of SAGD production when EWOR is somewhat higher. This phenomenon results in a drastic drop in the emulsion viscosity. This has not been captured yet in the experiments. - Richardson correlation seems to be the best one that describes the SAGD emulsion viscosity. This applies to modified

	versions of the Richardson equation such as Broughton and Squires correlation.
Stability	- SAGD emulsions are generally categorized as kinetically stable emulsions due to the presence of natural emulsifiers and the shearing provided by the flow through the pores. - Asphaltenes, resins, and fine solids contribute to the stability of SAGD emulsions. It appears that asphaltenes have the main role in the stability of the emulsion. - pH, Brine composition, DSD, pressure, and temperature may also have effects on the emulsion stability.
Emulsification	- SAGD emulsification is a result of steam condensation at the bitumen-steam interface and engulfment of the small droplets by the mobilized oil phase. - Direct condensation of the steam when the steam chamber is rising is associated with higher water emulsification within the continuous mobile oil phase. EWOR decreases as the stable condensate films are formed at the late stages of SAGD production (lateral expansion of the steam chamber).
Emulsion flow modelling	- Most of the analytical, mechanistic, and numerical models employed Taylors' model to describe the emulsion viscosity which does not appear to be valid for high concentrations of the dispersed phase in SAGD. Additionally, the kinematic reaction of the condensation and emulsification needs to be investigated. - Emulsion flow may facilitate convective heat transfer and reduce the residual oil saturation. On the other hand, emulsion blockage by the dispersed phase droplets can reduce the permeability of the reservoir. - It seems that emulsion flow has complex effects on production. However, it may be concluded from the experiments and studies that W/O emulsion in early SAGD production stages reduces the production due to high viscosity resulted from high EWOR. However, in the late stage of production emulsion viscosity is reduced owing to the lower EWOR. Convective heat transfer by the emulsion results in dilution of the residual oil which leads to an increase in production.

Future work

There are several gaps in the literature regarding the characterization of SAGD emulsion flow. Some specific areas that require further research include rheological modelling of SAGD "W/O" emulsion incorporating the DSD and dispersed phase volume fraction effects; understanding the convective heat transfer mechanisms of emulsions; assessment of fines mobilization and sand production under emulsion flow; potential SAGD emulsion blockage and mechanisms; reaction

kinetics of steam condensation; thermodynamics of water droplets emulsification; quantification of emulsion effect on relative permeability and residual saturation of reservoir fluids; and assessment of sand control screens facing emulsion flow, among others.

References

[1] Schramm, L.L., 1992. Fundamentals and applications in the petroleum Industry. *Adv. Chem*, *231*, pp.3-24.

[2] Leal-Calderon, F., Schmitt, V. and Bibette, J., 2007. *Emulsion science: basic principles*. Springer Science & Business Media.

[3] Sjoblom, J., 2001. *Encyclopedic handbook of emulsion technology*. CRC press.

[4] Kokal, S.L., 2005. Crude oil emulsions: A state-of-the-art review. *SPE Production & facilities*, *20*(01), pp.5-13.

[5] Manning, F.S. and Thompson, R.E., 1995. *Oilfield processing of petroleum: Crude oil* (Vol. 2). Pennwell books.

[6] Aziz, H.M.A., Darwish, S.F. and Abdeen, F.M., 2002, January. Downhole emulsion problem, the causes and remedy, Ras Budran Field. In *SPE Asia Pacific Oil and Gas Conference and Exhibition*. Society of Petroleum Engineers.

[7] Butler, R.M., McNab, G.S. and Lo, H.Y., 1981. Theoretical studies on the gravity drainage of heavy oil during in-situ steam heating. *The Canadian journal of chemical engineering*, *59*(4), pp.455-460.

[8] Butler, R.M. and Stephens, D.J., 1981. The gravity drainage of steam-heated heavy oil to parallel horizontal wells. *Journal of Canadian Petroleum Technology*, *20*(02).

[9] Butler, R.M., Stephens, D.J. and Weiss, M., 1980, October. The vertical growth of steam chambers in the in-situ thermal recovery of heavy oils. In *Proc. 30 th Can. Chem. Eng. Conf*(Vol. 4, pp. 1152-1160).

[10] Butler, R.M., 1985. A new approach to the modelling of steam-assisted gravity drainage. *Journal of Canadian Petroleum Technology*, *24*(03), pp.42-51.

[11] Das, S.K. and Butler, R.M., 1998. Mechanism of the vapor extraction process for heavy oil and bitumen. *Journal of Petroleum Science and Engineering*, *21*(1-2), pp.43-59.

[12] Butler, R.M. and Mokrys, I.J., 1998. Closed-loop extraction method for the recovery of heavy oils and bitumens underlain by aquifers: the VAPEX process. *Journal of Canadian Petroleum Technology*, *37*(04).

[13] Butler, R.M., 1991. *Thermal recovery of oil and bitumen* (Vol. 46). Englewood Cliffs, NJ: Prentice Hall.

[14] Emulsion, I.U.P.A.C., 1997. Compendium of Chemical Terminology, (the "Gold Book"). Compiled by AD McNaught and A. Wilkinson.

[15] Kokal, S.L. and Al-Dokhi, M., 2007, January. Case studies of emulsion behavior at reservoir conditions. In *SPE Middle East Oil and Gas Show and Conference*. Society of Petroleum Engineers.

[16] Kokal, S., Al-Yousif, A., Meeranpillai, N.S. and Al-Awaisi, M., 2001, January. Very thick crude emulsions: A field case study of a unique crude production problem. In *SPE annual technical conference and exhibition*. Society of Petroleum Engineers.

[17] Ebnesajjad, S., 2011, Handbook of Adhesives and Surface Preparation. William Andrew Publishing.

[18] Bancroft, W.D., 1913. The theory of emulsification, V. *The Journal of Physical Chemistry*, *17*(6), pp.501-519.

[19] McClements, D.J., 2015. *Food emulsions: principles, practices, and techniques*. CRC press.

[20] Fingas, M. and Fieldhouse, B., 2003. Studies of the formation process of water-in-oil emulsions. *Marine pollution bulletin*, *47*(9-12), pp.369-396.

[21] Fingas, M.F., Fieldhouse, B., Lambert, P., Wang, Z., Noonan, J., Lane, J. and Mullin, J.V., 2002. Water-in-oil emulsions formed at sea, in test tanks, and in the laboratory. *Environment Canada Manuscript Report EE-170, Ottawa, Ont*.

[22] Fingas, M. and Fieldhouse, B., 2004. Formation of water-in-oil emulsions and application to oil spill modelling. *Journal of hazardous materials*, *107*(1-2), pp.37-50.

[23] Tadros, T.F., 2013. Emulsion formation, stability, and rheology. *Emulsion formation and stability*, *1*, pp.1-75.

[24] Spasic, A.M., 2018. *Rheology of Emulsions: Electrohydrodynamics Principles* (Vol. 22). Academic Press.

[25] Chung, K.H. and Butler, R.M., 1988. Geometrical effect of steam injection on the formation of emulsions nn the steam-assisted gravity drainage process. *Journal of Canadian Petroleum Technology*, *27*(01).

[26] Sasaki, K., Akibayashi, S., Yazawa, N., Doan, Q. and Ali, S.M., 1999, January. Experimental Modelling of the SAGD Process 3/4 Enhancing SAGD Performance with Periodic Stimulation of the Horizontal Producer. In *SPE Annual Technical Conference and Exhibition*. Society of Petroleum Engineers.

[27] Jamaluddin, A.K.M. and Butler, R.M., 1988. Factors Affecting the Formation of Water-in-Oil Emulsions During Thermal Recovery. *AOSTRA J. Research*, *4*(2), pp.109-116.

[28] Sasaki, K., Satoshi, A., Yazawa, N. and Kaneko, F., 2002, January. Microscopic visualization with high resolution optical-fiber scope at steam chamber interface on initial stage of SAGD process. In *SPE/DOE Improved Oil Recovery Symposium*. Society of Petroleum Engineers.

[29] Noik, C., Dalmazzone, C.S., Goulay, C. and Glenat, P., 2005, January. Characterisation and emulsion behaviour of Athabasca extra heavy oil produced by SAGD. In *SPE International Thermal Operations and Heavy Oil Symposium*. Society of Petroleum Engineers.

[30] Mohammadzadeh, O. and Chatzis, I., 2010. Pore-level investigation of heavy oil recovery using steam assisted gravity drainage (SAGD). *Oil & Gas Science and Technology–Revue d'IFP Energies nouvelles*, *65*(6), pp.839-857.

[31] Kumasaka, J., Sasaki, K., Sugai, Y., Alade, O.S. and Nakano, M., 2016. Measurement of Viscosity Alteration for Emulsion and Numerical Simulation on Bitumen Production by SAGD Considering In-situ Emulsification. *Journal of Earth Science and Engineering*, *6*, pp.10-17.

[32] Bosch, R., Axcell, E., Little, V., Cleary, R., Wang, S., Gabel, R. and Moreland, B., 2004. A novel approach for resolving reverse emulsions in SAGD production systems. *The Canadian Journal of Chemical Engineering*, *82*(4), pp.836-839.

[33] Balsamo, V., Nguyen, D. and Phan, J., 2014. Non-conventional techniques to characterize complex SAGD emulsions and dilution effects on emulsion stabilization. *Journal of Petroleum Science and Engineering*, *122*, pp.331-345.

[34] Nguyen, D., Phan, J. and Balsamo, V., 2013, June. Effect of diluents on interfacial properties and SAGD emulsion stability: I. Interfacial rheology. In *SPE Heavy Oil Conference-Canada*. Society of Petroleum Engineers.

[35] Kar, T., Williamson, M. and Hascakir, B., 2014, September. The role of asphaltenes in emulsion formation for steam assisted gravity drainage (SAGD) and expanding solvent-SAGD (ES-SAGD). In *SPE Heavy and Extra Heavy Oil Conference: Latin America*. Society of Petroleum Engineers.

[36] Yang, Y., Siqueira, F.D., Vaz, A.S., You, Z. and Bedrikovetsky, P., 2016. Slow migration of detached fine particles over rock surface in porous media. *Journal of Natural Gas Science and Engineering*, *34*, pp.1159-1173.

[37] Khilar, K.C. and Fogler, H.S., 1984. The existence of a critical salt concentration for particle release. *Journal of colloid and interface science*, *101*(1), pp.214-224.

[38] Haftani, M., Wang, C., Montero Pallares, J.D., Mahmoudi, M., Fattahpour, V. and Nouri, A., 2019, April. An Investigation into the Effect of Brine Salinity on Fines Migration in SAGD Operations. In *SPE Western Regional Meeting*. Society of Petroleum Engineers.

[39] Mahmoudi, M., Fattahpour, V., Velayati, A., Roostaei, M., Kyanpour, M., Alkouh, A., Sutton, C., Fermaniuk, B. and Nouri, A., 2018, December. Risk Assessment in Sand Control Selection: Introducing a Traffic Light System in Stand-Alone Screen Selection. In *SPE International Heavy Oil Conference and Exhibition*. Society of Petroleum Engineers.

[40] Mohamed, A.I., Sultan, A.S., Hussein, I.A. and Al-Muntasheri, G.A., 2017. Influence of surfactant structure on the stability of water-in-oil emulsions under high-temperature high-salinity conditions. *Journal of Chemistry*, *2017*.

[41] Dean, E.W. and Stark, D.D., 1920. A Convenient Method for the Determination of Water in Petroleum and Other Organic Emulsions. *Industrial & Engineering Chemistry*, *12*(5), pp.486-490.

[42] Hahn, A.U. and Mittal, K.L., 1979. Mechanism of demulsification of oil-in-water emulsion in the centrifuge. *Colloid and Polymer Science*, *257*(9), pp.959-967.

[43] ASTM D4007, 2011. Standard Test Method for Water and Sediment in Crude Oil by the Centrifuge Method (Laboratory Procedure).

[44] Scholz, E., 2012. *Karl Fischer titration: determination of water*. Springer Science & Business Media.

[45] Mason, S.L., May, K. and Hartland, S., 1995. Drop size and concentration profile determination in petroleum emulsion separation. *Colloids and Surfaces A: Physicochemical and engineering aspects*, *96*(1-2), pp.85-92.

[46] Bennion, D.B., Chan, M.Y.S., Sarioglu, G., Courtnage, D., Wansleeben, J. and Hirata, T., 1993, January. The in-situ formation of bitumen-water-stable emulsions in porous media during thermal stimulation. In *SPE International Thermal Operations Symposium*. Society of Petroleum Engineers.

[47] Olalekan, A.S., Sasaki, K., Sugai, Y., , Ademodi, B., Kumasaka, J., and Ueda, R., 2017. Effect of Emulsification Process Conditions on the Properties of Water-in-Bitumen Emulsion, Journal of the Japanese Association for Petroleum Technology, 82(01), pp.73-84

[48] Mcclements, D.J., 2007. Critical review of techniques and methodologies for characterization of emulsion stability. *Critical reviews in food science and nutrition*, *47*(7), pp.611-649.

[49] Riddick, T.M., 1968. *Control of colloid stability through zeta potential* (p. 51). Wynnewood, PA: Livingston.

[50] Driscoll, D.F., Etzler, F., Barber, T.A., Nehne, J., Niemann, W. and Bistrian, B.R., 2001. Physicochemical assessments of parenteral lipid emulsions: light obscuration versus laser diffraction. *International journal of pharmaceutics*, *219*(1-2), pp.21-37.

[51] Kippax, P., 2005. Appraisal of the laser diffraction particle-sizing. *Pharmaceutical Technology*, *3*, pp.88-89.

[52] Pal, R., 1996. Effect of droplet size on the rheology of emulsions. *AIChE Journal*, *42*(11), pp.3181-3190.

[53] Oldroyd, J.G., 1955. The effect of interfacial stabilizing films on the elastic and viscous properties of emulsions. *Proceedings of the Royal Society of London. Series A. Mathematical and Physical Sciences*, *232*(1191), pp.567-577.

[54] Yarranton, H.W., Sztukowski, D.M. and Urrutia, P., 2007. Effect of interfacial rheology on model emulsion coalescence: I. Interfacial rheology. *Journal of colloid and interface science*, *310*(1), pp.246-252.

[55] Dalmazzone, C., Noik, C., Glenat, P. and Dang, H.M., 2010. Development of a methodology for the optimization of dehydration of extraheavy-oil emulsions. *SPE Journal*, *15*(03), pp.726-736.

[56] Kim, M., Abedini, A., Lele, P., Guerrero, A. and Sinton, D., 2017. Microfluidic pore-scale comparison of alcohol-and alkaline-based SAGD processes. *Journal of Petroleum Science and Engineering*, *154*, pp.139-149.

[57] Qi, Z., Abedini, A., Lele, P., Mosavat, N., Guerrero, A. and Sinton, D., 2017. Pore-scale analysis of condensing solvent bitumen extraction. Fuel, 193, pp.284-293.

[58] Strassner, J.E., 1968. Effect of pH on interfacial films and stability of crude oil-water emulsions. *Journal of Petroleum Technology*, *20*(03), pp.303-312.

[59] Azom, P.N. and Srinivasan, S., 2009, January. Mechanistic modeling of emulsion formation and heat transfer during the steam-assisted gravity drainage (SAGD) process. In *SPE Annual Technical Conference and Exhibition*. Society of Petroleum Engineers.

[60] McDonald, J.E., 1962. Homogeneous nucleation of vapor condensation. I. Thermodynamic aspects. *American Journal of Physics*, *30*(12), pp.870-877.

[61] Poston, S.W., Ysrael, S., Hossain, A.K.M.S. and Montgomery III, E.F., 1970. The effect of temperature on irreducible water saturation and relative permeability of unconsolidated sands. *Society of Petroleum Engineers Journal*, *10*(02), pp.171-180.

[62] Sinnokrot, A.A., Ramey Jr, H.J. and Marsden Jr, S.S., 1971. Effect of temperature level upon capillary pressure curves. *Society of Petroleum Engineers Journal*, *11*(01), pp.13-22.

[63] Ezeuko, C.C., Wang, J.Y.J. and Gates, I.D., 2012, January. Investigation of Emulsion Flow in SAGD and ES-SAGD. In *SPE Heavy Oil Conference Canada*. Society of Petroleum Engineers.

[64] Rodionova, G., Pettersen, B., Kelesoğlu, S. and Sjöblom, J., 2014. Preparation and characterization of reference fluid mimicking behavior of North Sea heavy crude oil. *Fuel*, *135*, pp.308-314.

[65] Alboudwarej, H., Muhammad, M., Shahraki, A.K., Dubey, S., Vreenegoor, L. and Saleh, J.M., 2007. Rheology of heavy-oil emulsions. *SPE Production & Operations*, *22*(03), pp.285-293.

[66] Peramanu, S., Pruden, B.B. and Rahimi, P., 1999. Molecular weight and specific gravity distributions for Athabasca and Cold Lake bitumens and their saturate, aromatic, resin, and asphaltene fractions. *Industrial & engineering chemistry research*, *38*(8), pp.3121-3130.

[67] Groenzin, H. and Mullins, O.C., 1999. Asphaltene molecular size and structure. *The Journal of Physical Chemistry A*, *103*(50), pp.11237-11245.

[68] Yan, J., Plancher, H. and Morrow, N.R., 1997. Wettability changes induced by adsorption of asphaltenes. *SPE Production & Facilities*, *12*(04), pp.259-266.

[69] Binks, B.P. and Clint, J.H., 2002. Solid wettability from surface energy components: relevance to Pickering emulsions. *Langmuir*, *18*(4), pp.1270-1273.

[70] Pickering, S.U., 1907. Cxcvi.—emulsions. *Journal of the Chemical Society, Transactions*, *91*, pp.2001-2021.

[71] Galtung, J., 1967. *Theory and methods of social research*. Universitetsforlaget.

[72] Einstein, A., 1906. Calculation of the viscosity-coefficient of a liquid in which a large number of small spheres are suspended in irregular distribution. *Ann. Phys. Leipzig*, *19*, pp.286-306.

[73] Einstein, A., 1956. *Investigations on the Theory of the Brownian Movement*. Courier Corporation.

[74] Taylor, G.I., 1932. The viscosity of a fluid containing small drops of another fluid. *Proceedings of the Royal Society of London. Series A, Containing Papers of a Mathematical and Physical Character*, *138*(834), pp.41-48.

[75] Roscoe, R., 1952. The viscosity of suspensions of rigid spheres. *British journal of applied physics*, *3*(8), p.267.

[76] Brinkman, H.C., 1952. The viscosity of concentrated suspensions and solutions. *The Journal of Chemical Physics*, *20*(4), pp.571-571.

[77] Richardson, E.G., 1933. Kolloid-Z. 65, 32.

[78] BROUGHTON, J., AND SQUIRES, L., 1938. *J. Phys. Chem*, *42*, p.252.

[79] Eilers, H., 1943. Kolloid-Z., 97, 313.

[80] Mooney, M., 1951. The viscosity of a concentrated suspension of spherical particles. *Journal of colloid science*, *6*(2), pp.162-170.

[81] Krieger, I.M. and Dougherty, T.J., 1959. A mechanism for non-Newtonian flow in suspensions of rigid spheres. *Transactions of the Society of Rheology*, *3*(1), pp.137-152.

[82] Hatschek, E., 1911. Kolloid-Z., 8, 34.

[83] Sibree, J.O., 1930. The viscosity of emulsions.—Part I. *Transactions of the Faraday Society*, *26*, pp.26-36.

[84] Sibree, J.O., 1931. The viscosity of emulsions. Part II. *Transactions of the Faraday Society*, *27*, pp.161-176.

[85] Pal, R. and Rhodes, E., 1989. Viscosity/concentration relationships for emulsions. *Journal of Rheology*, *33*(7), pp.1021-1045.

[86] Ronningsen, H.P., 1995, January. Correlations for predicting viscosity of W/O-emulsions based on North Sea crude oils. In *SPE International Symposium on Oilfield Chemistry*. Society of Petroleum Engineers.

[87] ASTM, C., 2012. Standard test method for compressive strength of cylindrical concrete specimens. *ASTM C39/C39M-12*.

[88] Farah, M.A., Oliveira, R.C., Caldas, J.N. and Rajagopal, K., 2005. Viscosity of water-in-oil emulsions: Variation with temperature and water volume fraction. *Journal of Petroleum Science and Engineering*, *48*(3-4), pp.169-184.

[89] Gates, I.D. and Chakrabarty, N., 2006, January. Design of the steam and solvent injection strategy in expanding-solvent steam-assisted gravity drainage. In *Canadian international petroleum conference*. Petroleum Society of Canada.

[90] Goodarzi, F. and Zendehboudi, S., 2019. A comprehensive review on emulsions and emulsion stability in chemical and energy industries. *The Canadian Journal of Chemical Engineering*, *97*(1), pp.281-309.

[91] Hjelmeland, O.S. and Larrondo, L.E., 1986. Experimental investigation of the effects of temperature, pressure, and crude oil composition on interfacial properties. *SPE Reservoir Engineering*, *1*(04), pp.321-328.

[92] Sanyal, S.K., Marsden Jr, S.S. and Ramey Jr, H.J., 1974, January. Effect of temperature on petrophysical properties of reservoir rocks. In *SPE California regional meeting*. Society of Petroleum Engineers.

[93] Shariatpanahi, S.F., Strand, S. and Austad, T., 2011. Initial wetting properties of carbonate oil reservoirs: effect of the temperature and presence of sulfate in formation water. *Energy & fuels*, *25*(7), pp.3021-3028.

[94] Irani, M. and Ghannadi, S., 2013. Understanding the heat-transfer mechanism in the steam-assisted gravity-drainage (SAGD) process and comparing the conduction and convection flux in bitumen reservoirs. *SPE Journal*, *18*(01), pp.134-145.

[95] Vladisavljević, G.T., Surh, J. and McClements, J.D., 2006. Effect of emulsifier type on droplet disruption in repeated Shirasu porous glass membrane homogenization. *Langmuir*, *22*(10), pp.4526-4533.

[96] Sasaki, K., Akibayashi, S., Yazawa, N., Doan, Q. and Ali, S.M., 1999, January. Experimental Modelling of the SAGD Process 3/4 Enhancing SAGD Performance with Periodic Stimulation of the Horizontal Producer. In *SPE Annual Technical Conference and Exhibition*. Society of Petroleum Engineers.

[97] Mojarad, M. and Dehghanpour, H., 2016. Analytical modeling of emulsion flow at the edge of a steam chamber during a steam-assisted-gravity-drainage process. *SPE Journal*, *21*(02), pp.353-363.

[98] Romero, M.I., 2009, January. Flow of emulsions in porous media. In *SPE Annual Technical Conference and Exhibition*. Society of Petroleum Engineers.

[99] Gómora-Figueroa, A.P., Camacho-Velázquez, R.G., Guadarrama-Cetina, J. and Guerrero-Sarabia, T.I., 2018. Oil emulsions in naturally fractured Porous Media. *Petroleum*.

[100] Raghavan, R. and Marsden Jr, S.S., 1971. Theoretical aspects of emulsification in porous media. *Society of Petroleum Engineers Journal*, *11*(02), pp.153-161.

[101] Cuthiell, D., Green, K., Chow, R., Kissel, G. and McCarthy, C., 1995, January. The in situ formation of heavy oil emulsions. In *SPE International Heavy Oil Symposium*. Society of Petroleum Engineers.

Chapter 3: Physical Features' Characterization of the Water-in-mineral oil Macro Emulsion Stabilized by A Non-ionic Surfactant

This paper was published in the Journal of Dispersion Science and Technology.

Velayati, A. and Nouri, A., 2020. Physical features' characterization of the water-in-mineral oil macro emulsion stabilized by a nonionic surfactant. Journal of Dispersion Science and Technology, pp.1-16.

3.1 Preface

Water-in-oil (w/o) emulsions are widely used in the food and pharmaceutical industries, among others. Moreover, the most common type of emulsion produced and handled in the oil industry processes is the w/o emulsion. This study investigates the features of a water-in-mineral oil macro-emulsion formulated with mineral oil as the continuous phase and Span 83 as the non-ionic surfactant. Emulsions are prepared at room temperature according to the hydrophilic-lipophilic difference (HLD) theory and were tested for the mean droplet size and droplet size distribution, viscosity, and kinetic stability. An empirical correlation was introduced that estimates the viscosity of the water-in-mineral oil macro-emulsions and captures the non-Newtonian behavior at larger water fractions. The effect of electrolyte and internal phase concentration was specifically assessed on the emulsion flocculation and the stability of the system. Stability tests show a threshold electrolyte concentration exists after which droplets coalesce upon collision and flocculation. Salting out is most likely the responsible mechanism of phase separation in the emulsions with higher electrolyte concentrations. The results imply that sedimentation is accountable for the formation of different layers in emulsion with time. The sedimentation rate was intensified for emulsion with smaller water content (64% variation in 3 days between 10% emulsion and 40% emulsion) and concentrated emulsions were found to be more stable. Also, the size of the droplets was influenced by the NaCl concentration, surfactant concentration, and phase ratio.

3.2 Introduction

An emulsion is a dispersion system of immiscible liquids in which one phase is dispersed in a continuous phase. In water-in-oil (w/o) emulsion, water is the dispersed phase and oil is the primary phase. Emulsions are part of a broader dispersion mixture system referred to as colloids. However, in emulsions, both the internal and external phases are liquids [1-3].

Emulsions are often categorized based on the type of the continuous phase, stability, and droplet size [1-4]. While the oil-in-water (o/w) emulsions have been the center of the attention of many research works, w/o emulsions are not investigated as much, probably due to the issues with stability [5]. This is the case despite the importance and application of this type of emulsion in the food industry, pharmaceuticals, and particularly the petroleum industry.

The most common type of emulsion produced in the oil industry is the w/o emulsion [4,6]. A few pieces of research attempted to mimic the bulk viscosity of in-situ reservoir emulsion using the model fluids [7,8]. This is useful in the characterization of the flow inside the tubular and flow lines. For instance, Rodionoval et al. (2014) used a reference fluid that replicated the heavy crude emulsion in terms of viscosity and droplet size to perform a pipeline flow analysis [7]. However, the lack of a comprehensive familiarity with the model emulsion formulations and their physical features is evident in similar studies. This is especially the case regarding the stability analysis of the system.

Opawale and Burgess (1997) investigated the interfacial properties of lipophilic non-ionic surfactants of the sorbitan ester family in water-in-mineral oil emulsions and obtained valuable results in terms of the interfacial elasticity, critical micelle concentration (CMC) values, and effect of salt on the system [9]. There are other studies in the literature in which Span 83 was used to stabilize the crude emulsions and investigated the role of Span 83 along with other surfactants in

the assessment of the rheology and stability of w/o and multiple emulsions [10-12]. However, the effect of internal phase concentration, bulk viscosity of the emulsion, and the detailed discussion on the stability was out of their research scope.

The effect of electrolyte and phase ratio on the physical properties of the emulsion is still an area of debate. Some research works report on the stabilizing effect of the electrolyte whereas some researchers believe in the destabilizing role of the salt in emulsions [13,14]. The same discussions are ongoing on the effect of electrolyte and phase ratio on the mean droplet diameter of the emulsions [14-16]. It seems that such effects may vary from case to case depending on the environmental factors, and constituent phases.

This research investigates the primary properties (droplet size, kinetic stability, viscosity) of the w/o emulsion prepared using a non-ionic surfactant (Span 83) and non-polar mineral oil. HLD criterion was adopted to assess the emulsion requirements in terms of emulsifier characteristic curvature values. Moreover, the effect of electrolyte and internal phase volume concentrations on the system was examined. A viscosity empirical model is also presented, capturing the non-Newtonian fluid behavior of the emulsions at larger water fractions. The results may be useful in formulating w/o emulsions for use as the model fluids emulating reference in-situ fluids, namely oil reservoir emulsions.

3.3 Methods and materials

This study aims to assess the bulk properties and main features of the water-in-mineral oil emulsions stabilized by a non-ionic surfactant (Span 83). Sorbitan sesquioleate (Span 83) from the Span non-ionic surfactant family is widely used as an emulsifier for the formulation of the creams and ointments for cosmetic use and pharmaceuticals [17]. **Figure 3.1** displays the chemical structure of Span 83, and **Table 3.1** summarizes the properties of this type of surfactant. The low HLB value of Span 83 indicates higher solubility in the oil phase and according to Bancroft's rule, this will facilitate the formation of the w/o emulsion.

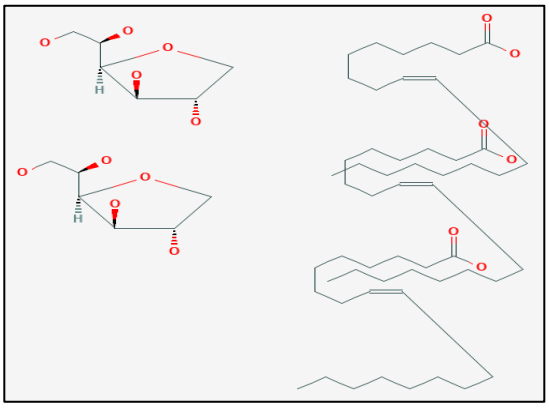

Figure 3.1: 2D depiction Sorbitan sesquioleate (Span 83), 1:2 mixture of dioleate and monooleate [18]

Table 3.1: Sorbitan sesquioleate (Span 83) properties

Feature	Value
HLB	3 [19]
Cc (Measured at 25°C)	4-5 [20]
CMC*	0.024 (%w/v) [9]
Mwt	560
Molecular Area	34.58 $Å^2/molecule$ [9]
IFT @ CMC*	13.18 dyne/cm [9]
Viscosity @ room temp	1500 cP
Density	0.989 g/ml
*CMC was calculated for light mineral oil and water at room temperature	

Mineral oil (0.85 kg/l at 15°C) without surface-active contaminants which contains 96.5 wt% saturate mixtures and 3.5 wt% aromatics, was used in the preparation of the emulsions. The focus is on the overall performance of the emulsifier in terms of stability and bulk features of the emulsion, including the viscosity and the droplet size. The emulsions were prepared at room temperature, and the effect of internal phase concentration and salinity on these properties was investigated.

A rotor/stator homogenizer was used to prepare the emulsions. Optical microscopy was employed to determine the droplet sizes, and a cone and plate viscometer was utilized to measure the viscosity of the samples. Finally, the kinetic stability of the emulsions was monitored by bottle tests and optical microscopy This section of the article describes the theory and processes implemented in the research in more detail. **Figure 3.2** displays the techniques used to determine and evaluate the emulsion samples' properties.

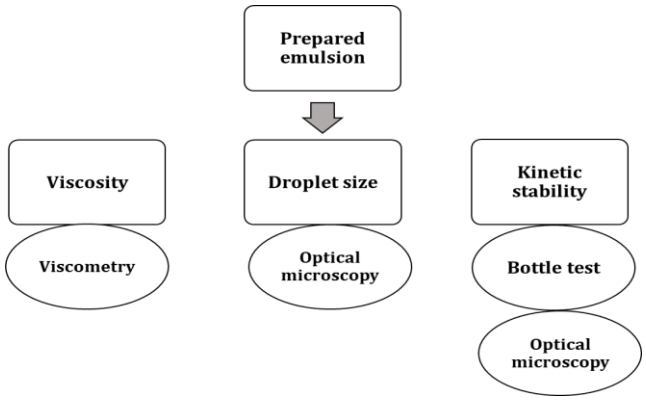

Figure 3.2: Main features of the emulsion samples examined and the methods used for measurements and analysis

Water-in-mineral oil emulsion samples were prepared at room temperature using 5 % w/v Span 83. Different homogenization parameters (rotational speed and mixing time) were applied in the preparation of the samples to correlate the mean droplet size with homogenization operating parameters. In the next phase, all emulsions were made using a consistent set of homogenization conditions, and the samples were examined for viscosity, stability, and mean droplet size.

A range of internal phase volume concentrations (0.1, 0.2, 0.3, 0.4) and salinity (no salt, 3.4E-3 M, 6.8E-2 M, and 5.1E-1 M) were considered as experimental variables to address the effect of electrolyte and dispersed phase concentration on the physical features of the system.

3.3.1 Surfactant selection

It is customary to use different criteria such as critical micelle concentration (CMC), hydrophilic-lipophilic balance (HLB), Bancroft's rule, and phase concentrations for preparation of the desired emulsion system. However, the issue with such criteria is the negligence of the system under which emulsion is formed. For instance, HLB is a measure of the degree to which surfactant is lipophilic or hydrophilic and is determined by calculating the values for different regions of the surfactant molecule [2]. The smaller the HLB value, the more lipophilic (oil soluble) the surfactant. Therefore, HLB only accounts for the affinity of the surfactant molecules to oil/water. Hydrophilic-lipophilic difference (HLD) is a concept which accounts for different conditions in preparing emulsions. The components of the HLD include a surfactant term, oil-specific term, temperature effect, and salinity, as shown in Eq. 1. Therefore, unlike other criteria, HLD is a function of the entire system [21].

$$HLD = Cc - k.EACN - a\Delta T + f(s) \quad (1)$$

where Cc is the characteristic curvature value that represents the surfactant term, k and a are constants, EACN is short for equivalent alkane carbon number and represents the oiliness, ΔT is the temperature difference from 25° Celsius, *f(s)* is the salinity term, and s is salinity in g/100ml. *f(s)* equals *ln(s)* for ionic surfactants and *0.13s* for non-ionic surfactants. Equation 1 reduces to Eq. 2 at room temperature and no salt present in the system:

$$HLD = Cc - k.EACN \quad (2)$$

An HLD value of zero indicates an ideal and balanced system with minimum interfacial tension. This results in the formation of thermodynamically stable micro-emulsions. Positive HLD values lead to the formation of the w/o emulsions and negative values, o/w emulsions [21].

This study aims to assess the water-in-oil emulsion properties. Hence, a positive HLD value is required. The purpose is to create the emulsion at room temperature conditions and explore different electrolyte (NaCl) concentrations. Also, a mineral oil (0.85 kg/l at 15°C) which is pure from the surface-active contaminants and contains 96.5 wt% saturate mixtures and 3.5 wt% aromatics, was utilized in the preparation of the emulsions. EACN of the paraffinic oil is reported 18 at 25°C elsewhere [21].

Three scenarios were defined, and the corresponding Cc values were obtained for each case. The first scenario is a non-saline system with a required Cc > 3.06 at room temperature. In the second scenario, 4000 ppm (6.8E-2 M) salt is present in the aqueous phase with a required Cc > 4 for ionic surfactants. The third scenario is similar to the second one but calculated for the non-ionic surfactants. Cc for the last case was found to be larger than 3.

One can review the Cc values of the different surfactants available in the literature to select the optimum emulsifier for the formation of a w/o emulsion. Based on the required Cc values

determined for the different scenarios, it can be concluded that the non-ionic surfactants with an affinity toward the oil phase are reasonable choices to attain the required emulsion type.

3.3.2 Emulsion preparation and formulations

A classic method was adopted for emulsion preparation [1]. First, the surfactant was added to the oil phase and mixed gently using a magnetic stirrer for one hour. Then, water/salt-water was added to make a 12-ml sample size in all tests. A rotor/stator lab homogenizer with a 12 mm working head diameter and mixing rate range of 1000-28000 rpm was utilized to emulsify the liquids at room temperature of 22 °C. A range of shear rates was applied (1000 rpm and 3000 rpm) to find the correlation between the droplet size and the shear rate and duration of mixing.

Several criteria may be used to determine the surfactant's required concentration in the emulsion, among which CMC is of great significance. Opawale and Burgess (1997) performed the interfacial tension measurements in different concentrations of Span 83 in mineral oil to find the CMC value and molecular area of the surfactant [9]. These parameters are presented in **Table 3.1**. A sensitivity analysis was performed in this study to set the minimum required surfactant for a condensed monolayer coverage of the droplets' interfacial area using the molecular area of Span 83. Sensitivity analysis investigated the effect of the internal phase concentration and the droplet diameter on the required amount of surfactant. **Figure 3.3** displays the results and indicates a higher concentration of the surfactant is necessary when the droplets are smaller (due to the increased interfacial area), and water is present in the emulsion in larger fractions.

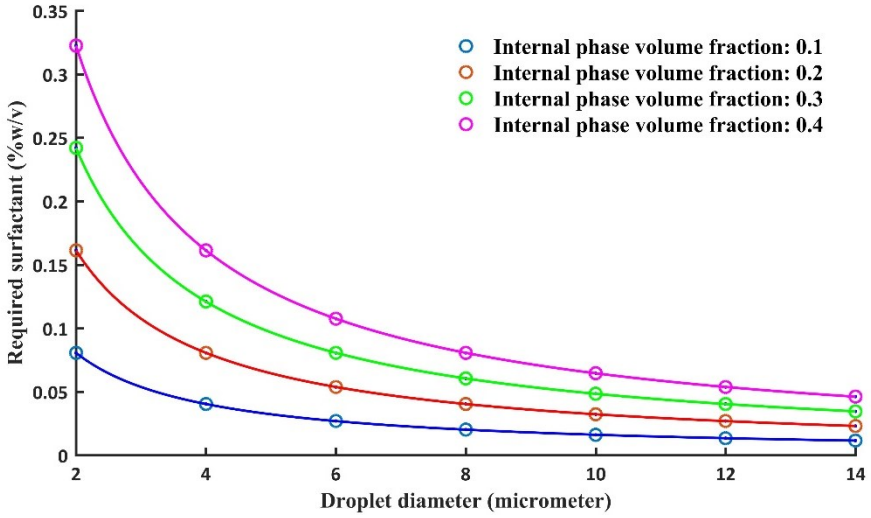

Figure 3.3: required Span 83 dosages for different volume fractions of the water and droplet diameters

Although the calculations indicate an insignificant amount of emulsifier is needed for the emulsions, 5 % w/v (v is the volume of the emulsion) concentration of the surfactant was used in all recipes to overcome the uncertainties associated with droplet size distribution. Moreover, different NaCl salt concentrations (no salt, 3.4E-3 M, 6.8E-2 M, 5.1E-1 M) scenarios were embedded in the test plan. **Table 3.2** displays the testing matrix for each physical feature assessed in this study. Each dependent variable (parameters) is investigated independently with pre-defined testing plans to achieve certain objectives.

A preliminary study was done on the effect of homogenization parameters on the mean droplet size of the 10% emulsion. The objective was to determine an appropriate means of reporting the representative sizes of the droplets throughout the experiments and select a fixed set of homogenization settings to advance the tests. Mean droplet diameters reported are the mean values of 5 samples at this phase of the research.

Alteration in mean droplet diameter is initially measured for two levels of surfactant concentrations (1.5 %w/v and 5 %w/v) and two levels of water content (0.1 and 0.4). In this step, emulsions were prepared without NaCl in the water phase. In the next stage, a 5% surfactant concentration that yields higher stability was selected to look into the effect of salinity on the droplet sizes. Values reported for each test run are the mean value of 3 samples.

Viscosity was measured for different water phase ratios (0.1,0.2,0.3,0.4) to analyze the effect of the dispersed phase on the bulk viscosity of the emulsion. The effect of salt on the viscosity was omitted at this stage of the research. Each viscosity value presented in this study is the average of 2 sample measurements.

As for the kinetic stability analysis, change in the appearance of the emulsion was monitored visually in the bottle test for 4 water fractions (0.1,0.2,0.3,0.4), and 4 salinity levels (0, 3.4E-3, 6.8E-2, 5.1E-1). Analysis of the sedimentation was carried out by micrography and bottle tests. Quantitative assessment of water phase separation was performed for two water fractions (0.1 and 0.4) and all salinity levels and each phase separation value reported is the average of test results on 3 samples.

Table 3.2: Testing plan for assessment of the physical features

Parameter	Fixed variables		Experimental variables		
Mean droplet diameter	Temperature	22°C	Water fraction(s)	Salinity (M)	Surfactant dose (% w/v)
	Pressure	1 atm	0.1, 0.4	0, 6.8E-2	1.5, 5
	Mixing rate	1000 rpm			
	Mixing time	1 min			
Viscosity	**Fixed variables**		Water fraction(s)		
	Temperature	22°C	0.1, 0.2, 0.3, 0.4		
	Pressure	1 atm			
	Span 83 concentration	5 % w/v			
	Mixing rate	1000 rpm			
	Mixing time	1 min			
Kinetic stability	**Fixed variables**		Water fraction(s)	Salinity (M)	
	Temperature	22°C	0.1, 0.2, 0.3, 0.4	0, 3.4E-3, 6.8E-2, 5.1E-1	
	Pressure	1 atm			
	Span 83 concentration	5 % w/v			
	Mixing rate	1000 rpm			
	Mixing time	1 min			

3.3.3 Droplet size measurement and analysis

Several techniques are commonly used to determine the droplet size and droplet size distribution of the emulsion, such as optical microscopy, laser diffraction, Near-Infrared spectroscopy, and scanning electron microscopy [22]. Each method comes with merits and drawbacks; however, microscopic techniques are favored as they provide visual means to identify the size of the droplets in emulsion [1].

The droplet size distribution reported in the optical microscopy technique is susceptible to the sampling methods. Results obtained in this technique may vary from one sample to another, and many samples must be analyzed to attain a reliable report of the size distribution. In this study, five samples were collected from each emulsion, and the samples were taken from the fresh emulsion to mitigate some of the potential errors linked to this technique.

This study employs an optical microscopy method for the characterization of the droplet sizes in an emulsion. A compound microscope (1000x, Omano OM-139) with a camera was used to capture images from the emulsion samples in a range of magnifications: 40x, 100x, and 400x. The

microscope uses the Kohler illumination method which generates an even illumination of the sample and ensures the source of illumination is not visible in the image. Images were then processed using ImageJ 1.x (Java-based open-source image processing software first developed in the US) to obtain the droplet diameter values. Representative sizes and the droplet size distributions were generated, assuming the sphericity of the droplet shapes in the emulsion.

Selecting the characteristic/representative size is an essential step in the analysis of the droplet sizes. The size may be presented as one or more numbers in representative diameters such as D10 (arithmetic mean diameter), D32 (Sauter diameter), D43 (De Broukere, or Herdan diameter), or volume-based distributions, and relative span for the distribution width. Each representative size may yield a different value, and the selection of the appropriate representative size depends solely on the purpose of the study. In this research, all the relevant representative sizes and the size differences for various samples were determined. Equation 3 shows the general form of the representative sizes and Eq. 4 is used for calculating the relative span as a measure of the particle size distribution width [23]:

$$\overline{D}_{pq}^{(p-q)} = \frac{\sum_i D_i^p}{\sum_i D_i^q} \tag{3}$$

$$Relative\ Span = \frac{D_v0.9 - D_v0.1}{D_v0.5} \tag{4}$$

where $\overline{D}$ is the averaged representative size, p and q are integers ranging from 1 to 4, D_i is the diameter of the ith drop, $D_v0.5$ is the volume mean diameter, D_vx is the drop diameter such that x fraction of the total liquid volume consists of drops of smaller diameter. D_Nx is similar to the D_vx except that it is based on the total number of droplets. It is more informative to express more than one representative size to understand the width of the distribution as well as the mean size.

3.3.4 Viscosity measurement

Emulsions exhibit different viscosity profiles compared to their constituent phases. Water-in-oil emulsions typically show higher viscosity than the continuous oil phase. The difference in viscosity is strongly affected by the internal phase concentration. Moreover, emulsions are generally non-Newtonian shear-thinning fluids [1]. Other factors that may contribute to the emulsion viscosity consist of droplet size, the viscosity of the constituent phases, temperature, and pressure, among other factors [1-4,22].

Various viscometers and techniques have been utilized to measure the viscosity of emulsions. Such includes pressure differential measurements inside a capillary tube based on Poiseuille's law, plumbing type viscosity sensors, and rotational viscometers [1]. In this study, a cone and plate geometry viscometer (Brookfield LVT-CP40) was used for the measurements. The advantage of this type of viscometer is its ability to take the measurements for small sample volumes (0.5 ml).

Cone and plate geometry is the fixation of a conical vertex perpendicular to a flat plate. The cone is in point contact with the flat plate and determination of viscosity is made possible by rotation of the cone at a constant speed and measurement of the torque over the conical surface. The mathematical relationships for this specific type of viscometer are as follows [24]:

$$\tau = \frac{T}{\frac{2}{3}\pi r^3} \quad (5)$$

$$\gamma = \frac{\omega}{Sin\,\theta} \quad (6)$$

$$\mu = \frac{Shear\ stress \times 100}{Shear\ rate} \quad (7)$$

where T is the % full-scale torque (dyne-cm), r is the cone radius (cm), ω is the cone speed (rad/sec), θ is the cone angle (degrees), τ is shear stress (dyne/cm^2), γ is the shear rate (1/sec), and μ is viscosity (cP or mPa.s).

3.3.5 Stability characterization of the emulsions

Generally, emulsions are thermodynamically unstable fluids, except for micro-emulsions [6]. However, they show some level of kinetic stability. The primary instability mechanisms in emulsions comprise flocculation, coalescence, creaming, sedimentation, and Ostwald ripening [1-4,6]. Emulsions might be stable in terms of some instability mechanisms but unstable to another. For instance, emulsions may be prone to flocculation, but the droplets may not necessarily coalesce.

An ultimate indication of instability of emulsions is the separation of the phases. This phenomenon can be monitored by basic bottle tests. In this experiment, emulsion samples (12 ml) are poured into graduated cylinders of 14 ml capacity, and the water phase separation is recorded with time (3 days). Also, the appearance of the emulsion samples with time is visually monitored for a one-month storage time. Samples are kept on a flat and level surface, and an ambient temperature of 22°C, and atmospheric pressure throughout the experiments. This study primarily employs this approach to screen the kinetic stability in emulsion samples. Besides, an optical microscopy technique was used for the analysis of the droplet interactions.

3.4 Results and discussions

In this section, the effect of homogenization parameters on the size of the droplets is displayed initially. Then the results of the stability tests, viscosity measurements, and mean droplet diameter analysis are presented for the fixed homogenization parameters of 1000 rpm and 1 minute mixing time to investigate the effect of phase ratio, salinity, and surfactant concentration on the properties of the emulsion.

3.4.1 Analysis of homogenization parameters

Droplet size analysis of the emulsion samples was performed using the optical microscopy method. As discussed before, micrography results are sensitive to the sampling. This may lead to an erroneous report of the representative sizes, and reliable results can only be achieved when many images and samples are processed. The issue with this approach is that attempts to collect so many samples, processing the images, and interpretation of the results can be extremely time-consuming.

The size analysis of one of the emulsion recipes is discussed here to illustrate the differences in results when dealing with different samples. The emulsion is composed of 0.1 water fraction, 5%

w/v Span 83, and was prepared by applying 1000 rpm rotational speed for 2 minutes. Two samples were taken from the emulsion while fresh and their representative sizes were obtained after image processing. **Figure 3.4** displays the number-based distribution and volumetric-distributions of the two emulsion samples. **Table 3.3** contains the representative size for the two samples.

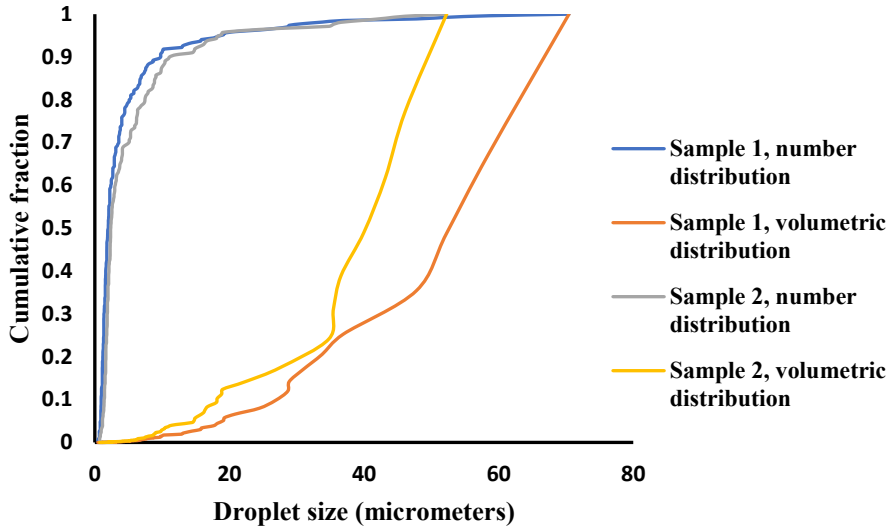

Figure 3.4: Number-based vs. volumetric distribution for two samples collected from one emulsion recipe

Table 3.3: Representative sizes of the two samples from one emulsion recipe

Representative size (µm)	Sample 1	Sample 2
D10	4.75	5.57
D20	9.77	9.74
D21	20.11	17.01
D32	41.54	31.52
D31	28.90	23.16
D30	15.83	14.40
D43	52.57	39.27

The size distributions shown in **Figure 3.4** indicate two differences between the presented sizes: a difference between the number and volumetric distribution, and variation of size distributions between the two samples of the same recipe. The difference in the number and volumetric distributions is related to the very concept of such distribution representations. Volumetric distributions indicate a larger portion of the sample is occupied by the droplets with larger diameters, whereas number distributions consider an equivalent weight for each droplet present in the emulsion.

Another noteworthy observation is the difference of distributions between the two samples that is much more significant for the volumetric distributions. This is due to the spatial distribution of droplets and the limited microscope field of view. If larger droplets are detectable in one image

capture from a sample, volumetric distribution is shifted considerably. However, this is not as significant in the number distributions, again due to the equivalent weight given to each droplet. Therefore, this study employs a mean droplet diameter as a number-based size representation to minimize the inaccuracies associated with the size analysis performed by micrography.

Emulsion samples with a water phase concentration of 0.1 were prepared for a range of homogenizer rotational speed (1000 rpm and 3000 rpm) and a range of mixing time (1-10 minutes). The objective was to find the correlation between the mean droplet size and the homogenization parameters. **Figure 3.5** shows the relationship between these parameters using a specific homogenizer geometry and sample size. Results may differ for other settings used for the preparation of the emulsions. This figure shows that as the rotational speed increases, the size of the droplets decreases. Also, longer mixing time generally has the same influence on droplet sizes. However, there seems to be a critical time after which the decrease in the size of the droplets is insignificant. Such a trend aligns with the reports on the droplet size alteration of the emulsions with homogenization settings [25].

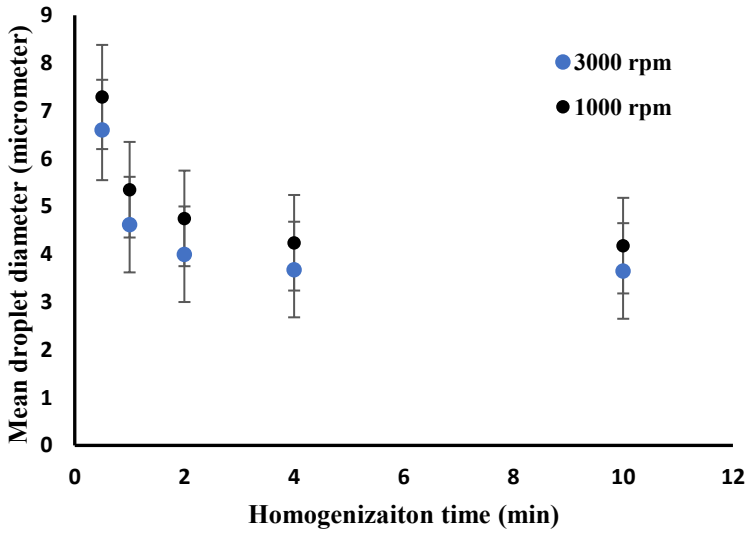

Figure 3.5: Change in the mean droplet size with rotational speed and mixing time

Fixed homogenization parameters of 1000 rpm and 1 min of mixing time were selected to resume the study on the emulsion samples. This selection was made to ensure the diameter of the droplets falls into the size category of macro emulsions. The mean droplet diameter is larger than the rest of the mixing times tested that are higher than 1 minute, but not too large to jeopardize the stability of the emulsions by creating significantly larger droplets.

The emulsion is a macro-emulsion with a mean droplet diameter of 5.35 micrometers and a volumetric distribution width (relative span) of 0.75. The number-based frequency of the distribution shows the distribution is skewed positively (right-skewed) with the mass of distribution on the left. **Figure 3.6** displays the number and volumetric distributions of the droplets in the emulsion.

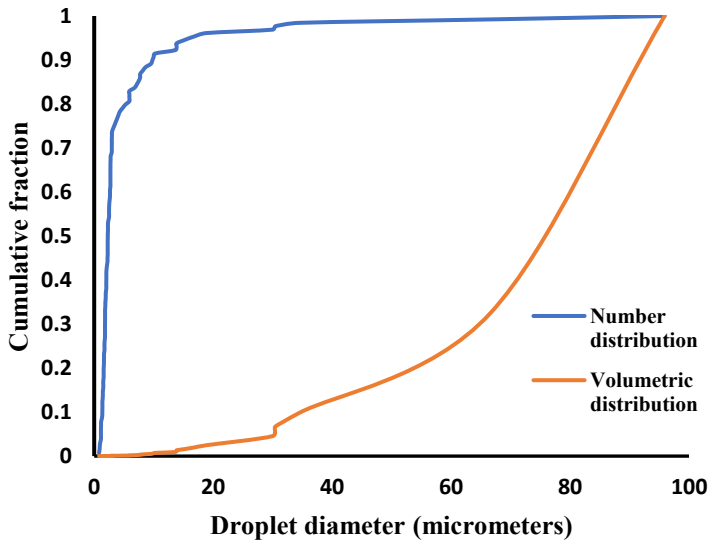

Figure 3.6: Number and volumetric cumulative distributions of the emulsion prepared under 1000 rpm in 1 min

Also, it was found that the addition of NaCl and increasing the water phase ratio influence the size of the droplets. A detailed discussion on this phenomenon is included in the kinetic stability analysis section and droplet size analysis sections.

3.4.2 The viscosity of the emulsions

A w/o emulsion generally shows higher viscosity than the constituent oil phase [7]. In other words, the relative viscosity ($\frac{\mu_{emulsion}}{\mu_{continuous\ phase}}$) for this type of emulsion is often larger than 1. However, other factors, such as the droplet size, viscosity of the constituent phases, temperature, and volume fraction of the dispersed phase, may also affect the viscosity of the emulsions [22]. Several viscosity models have been introduced for the suspensions, such as Einstein's, Taylor's, and Richardson's models [26,27,28]. However, not many emulsion-specific models exist in the literature.

This study introduces an empirical viscosity model for the water-in-oil emulsions prepared by the Span 83 non-ionic surfactant at room temperature (Fixed temperature). Moreover, the accuracy of some of the viscosity models available in the literature was examined for this type of emulsion and compared with the presented correlation.

Base mineral oil, mineral oil and surfactant, and emulsions at different water concentrations were tested for viscosity. Emulsions were prepared at 1000 rpm mixing rate and 1 min mixing time and were tested while fresh. Viscosity was measured for a range of shear rates to assess the Newtonian/non-Newtonian viscosity profiles of the fluids. **Table** A1 in the appendix section contains a summary of the results, device error, and viscometer full-scale measurable range per shear rate, and **Figure 3.7** displays the viscosity values calculated for a range of shear rates for different fluid samples. It was not possible to measure the viscosity of the 40% emulsion (water content) at 90 1/sec shear rate due to the limitation imposed by the cone-plate type viscometer used in the experiments.

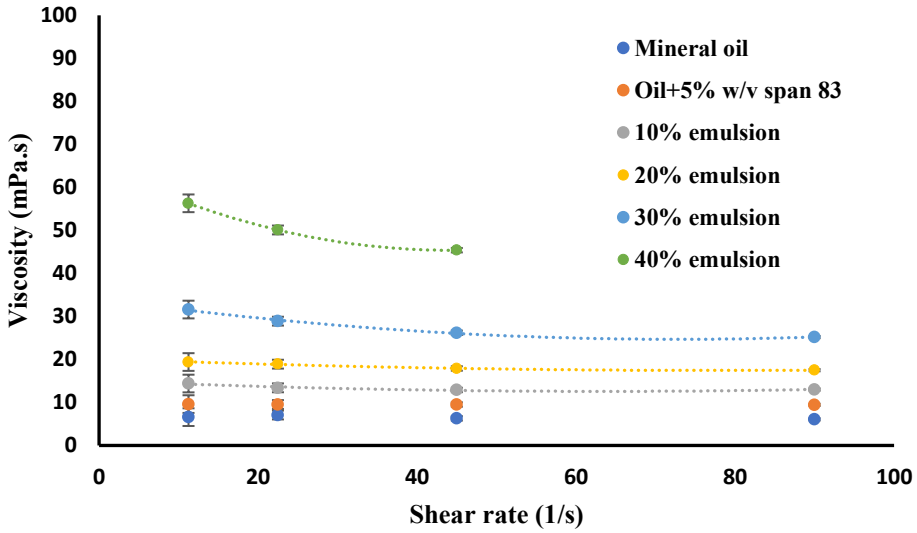

Figure 3.7: Viscosity of the sample fluids at different shear rates.

According to the results presented in **Figure 3.7**, emulsions display a higher viscosity compared to the continuous oil phase, which is the typical behavior of the w/o emulsions. This is evident from the difference between the viscosity values of the emulsions compared to the mineral oil containing surfactant, proving that the increment in viscosity is mainly due to the water content of the emulsion. The larger the amount of water fraction, the higher the viscosity of the emulsions. This is due to the droplets crowding or structural viscosity which indicates non-Newtonian behavior and elevated viscosity in emulsions in comparison to the constituent phases [29]. As will be shown in section 3.4, the increase in viscosity at higher water content cannot be correlated to the droplet size in this case because the mean droplet diameter was increased at higher water fractions in the emulsion.

Results presented in **Figure 3.7** indicate that the dilute emulsions behave like Newtonian fluids. In other words, viscosity is almost constant with the increasing shear rate. This viscosity profile is observed in emulsions up to 20% water volume concentrations in this study. 30% emulsion shows a noticeable higher viscosity at lower shear rates (20% higher viscosity at 11.25 1/s shear rate compared with 45 1/s shear rate), and the situation is more intense for 40% emulsion (24% higher viscosity for the same shear rates). This feature is most observed in the non-Newtonian Shear-thinning (Pseudo-plastic) fluids.

Researchers have introduced several viscosity models for colloids and suspensions, but not many have been presented for the emulsions. Nevertheless, some of these models are widely used to describe the emulsion viscosity behavior including Einstein's, Taylor's, Richardson's, Mooney's, and polynomial equations [1,30-33]. However, none of these models incorporate the shear rate in the correlations. At the same time, the results presented in this study and many studies on the w/o crude emulsions strongly suggest that w/o emulsions may exhibit non-Newtonian behavior at higher water fractions [4,34]. This study suggests a polynomial in two variables form can show promising performance for estimation of viscosity values and capturing the non-Newtonian behavior of the emulsions. Unlike the previously presented polynomial form viscosity models, this

model incorporates shear rate in addition to the dispersed phase concentration and includes the interactive terms between the two parameters. Equation 8 shows the general form of the correlation. The degree of the independent variables in the polynomial can be determined by curve fitting with the experimental viscosity measurements, and the insignificant terms may be removed from the equation.

$$\mu_{rel} = P_{n0}\emptyset^n + P_{0n}\gamma^n + \cdots + P_{20}\emptyset^2 + P_{02}\gamma^2 + P_{11}\emptyset\gamma + P_{10}\emptyset + P_{01}\gamma + P_{00} \quad (8)$$

where μ_{rel} is the relative viscosity, P_{ii} is a coefficient that its value depends on the system, $\emptyset$ is the dispersed phase volume fraction, and γ is the shear rate.

The performance of the proposed empirical correlation was compared with the conventional viscosity models presented in the literature, and the results are presented in **Table 3.4**. Coefficients of the correlations that contain calibration parameters such as Richardson's were found by fitting the models with the experimental results. Viscosity values of the models that show excellent performance along with the values from the correlation introduced in this study are illustrated in **Figure 3.8**. Moreover, **Figure 3.9** shows the results for two sets of viscosity measurements at two additional internal phase fractions of 0.25 and 0.38 for validation of the empirical correlation. The highest deviation from the measurements is occurring at the very lowest shear rate of 11.25 1/sec for 38% emulsion. However, device error is significant at this very low shear rate. Otherwise, a good agreement between the experimental results and model prediction is observed.

Table 3.4: The viscosity models performance for the water in mineral oil viscosity at room temperature

Model	Equation form	Coefficients	Sum of square errors (SSE)	Remarks
Einstein's [26]	$\mu_r = 1 + 2.5\,\emptyset$	N/A	138.34	Poor performance at higher concentrations of water
Taylor's [27]	$\mu_r = 1 + [2.5\left(\frac{(k+0.4)}{(k+1)}\right)]\,\emptyset$ $k = \frac{\mu_D}{\mu_c}$	N/A	169.74	Poor performance at higher concentrations of water
Richardson's [28]	$\ln(\mu_r) = k\,\emptyset$	5.08	3.16	Overall good performance
Mooney [30]	$\ln(\mu_r) = \frac{2.5\emptyset}{1 - k\emptyset}$	1.297	10.56	The least error was observed at the highest dispersed phase concentration
Polynomial [31-33]	$\mu_r = 1 + k\,\emptyset + k_2\emptyset^2 + k_3\emptyset^3 + \cdots$	k: 6.35 k_3: 63.70 k_2: 0.00	3.13	Overall good performance
This study	$\mu_{rel} = P_{00} + P_{10}\emptyset + P_{01}\gamma + P_{20}\emptyset^2 + P_{11}\emptyset\gamma + P_{30}\emptyset^3 + P_{21}\emptyset^2\gamma$	p00: 1 p10: 6.96 p01: 0.004 p20: -2.62 p11: 0.03 p30: 84 p21: -0.34	0.67	Captures the non-Newtonian effect at higher water fractions

Results presented in **Table 3.4** show that Einstein's, Taylor's, and Mooney's viscosity models fail to predict the macro water-in-mineral oil emulsions accurately. However, Einstein's and Taylor's correlations are less erroneous for dilute emulsions. Mooney's correlation shows promising performance only at the highest internal phase fraction of 0.4 with an average variation of -0.2 cP. On the other hand, Richardson's and polynomial models are superior in terms of following the viscosity jump trend at higher water concentrations.

Richardson's and polynomial correlations have almost overlaid on one another in **Figure 3.8**. Also, the magnitude of the residual sum of squares (SSE) is approximately the same for the two models. These findings imply there is no unique solution to predict the viscosity of an emulsion. While both empirical correlations are excellent in pursuing the viscosity increment with larger water fractions in the emulsion, they fail to capture the non-Newtonian behavior of the emulsions. In other words, the straight horizontal lines in **Figure 3.8** imply that such correlations are unable to predict the lower viscosities at higher shear rates.

The correlation presented in this study is derived by curve fitting of a polynomial equation with the experimental results and solving for coefficients using a linear least-squares method. It seems that a higher-order independent variable in the polynomial adds unnecessary and redundant complexity to the correlation without significantly affecting the accuracy of the model. The solution is non-unique, and accuracy is prone to variations if the bounds for coefficients change. This equation incorporates internal phase volume fraction, shear rate, and the interaction between the two parameters. A sensitivity analysis on the correlation with the same structure but without the shear rate terms resulted in a magnified SSE of 7.97. Additionally, **Figure 3.8** confirms that the presented model deviates from a straight horizontal line at higher water concentrations and predicts the lower viscosities obtained at higher shear rates. This capability of the viscosity model is essential to capturing the non-Newtonian behavior of the emulsions at large dispersed phase concentrations.

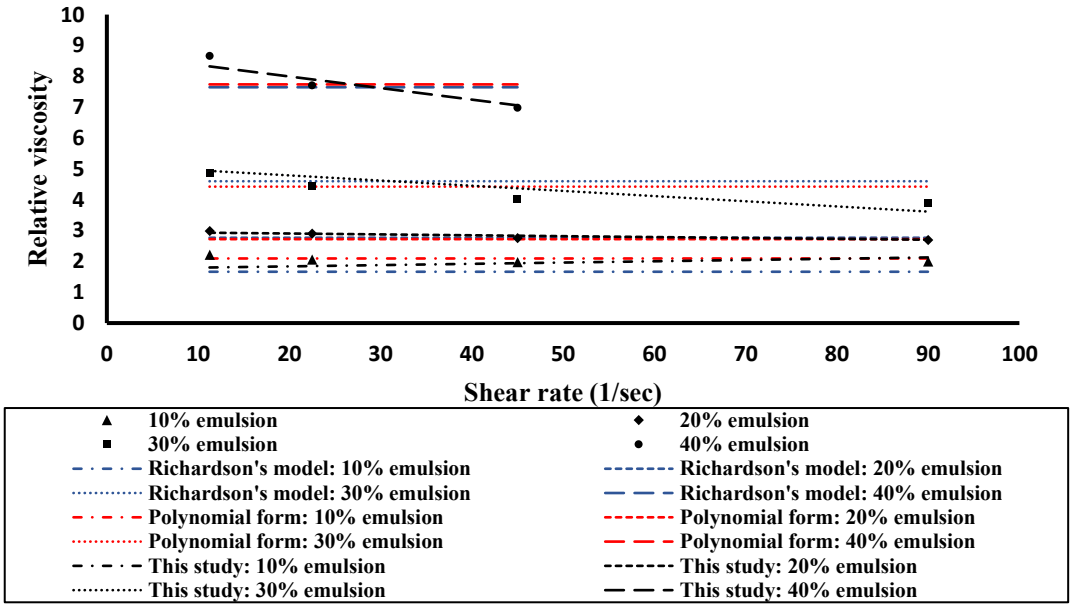

Figure 3.8: Performance comparison of the viscosity models for water-in-mineral oil emulsion

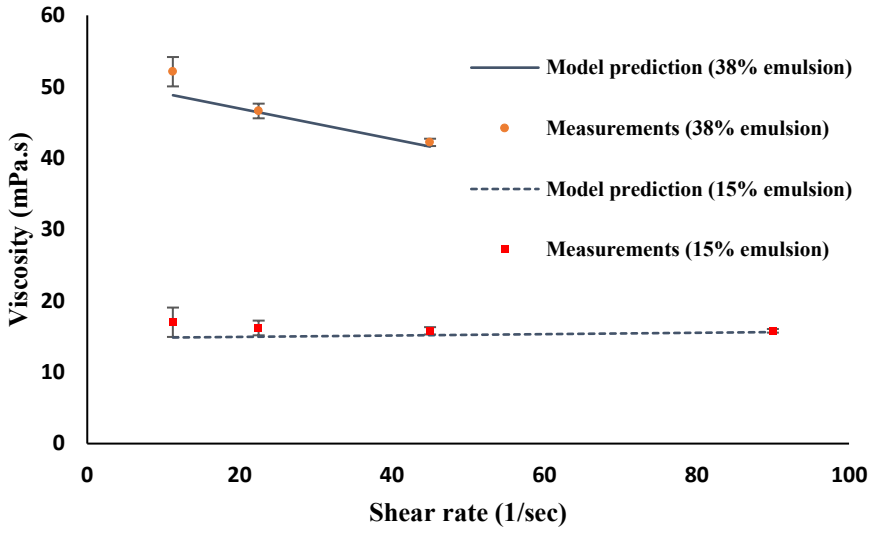

Figure 3.9: Validation of the empirical correlation with experimental results

It is important to recall that studies suggest that the viscosity of the emulsions increases if the size of the droplets is heavily reduced to very small diameters [1,22]. The emulsions prepared in this study are macro-emulsions with sizes ranging from smaller than 1 µm to larger than 70 µm with most of the droplets smaller than 20 µm (80% in case of 0.1 water fraction). Therefore, the values of relative viscosities may change if the size of the droplets shifts toward very small values significantly. Further testing is required to assess the viscosity profiles for such uniform micro-sized emulsions. However, the findings in this study confirm that the viscosity increase in the concentrated emulsions cannot be attributed to the size of the droplets as the mean droplet diameter increases at higher water content (see section 3.4).

3.4.3 Kinetic stability analysis

One of the most important features of an emulsion is stability, which is the resistance of the emulsion against alterations in its physical properties over time. Most emulsions are thermodynamically unstable, and the phases are in an equilibrium state when they are completely separated. This study investigates the stability of the water-in-mineral oil macro emulsions stabilized by a non-ionic surfactant (Span 83). Non-ionic surfactants stabilize the emulsions through steric hindrance [35].

Water-in-oil emulsions were prepared in different NaCl salinities, water types (DI water and tap water), and internal phase volume fractions to assess the effect of such parameters on the stability of the emulsions. The stability of the samples was characterized by the bottle test, which screens the phase separations over time and optical microscopy to observe the instability mechanisms visually. Micrography was performed for fresh emulsion samples. All emulsions were prepared by 1000 rpm mixing rate and 1 min mixing time at ambient temperature and pressure. **Table 3.5** shows the recipes and the summary of the stability results for different samples. The measured pH of all fresh emulsion samples was between 7.5-8.

Table 3.5: Summary of the stability tests

Recipe number	Formulation	Stability				Remarks
		Week1	Week2	Week3	Week4	
1	10 % DI water + 5 % w/v Span 83	Separated oil, creamy emulsion, and emulsion (3 layers)	Separated oil, creamy emulsion, and emulsion (3 layers)	Separated oil, creamy emulsion, and emulsion (3 layers)	Separated oil, creamy emulsion, and emulsion (3 layers)	Flocculation in the system
2	10 % tap water + 5 % w/v Span 83	Separated oil, creamy emulsion, and emulsion (3 layers)	Separated oil, creamy emulsion, and emulsion (3 layers)	Separated oil, creamy emulsion, and emulsion (3 layers)	Separated oil, creamy emulsion, and emulsion (3 layers)	Flocculation in the system (more severe than recipe 1)
3	10 % DI water + 5 % w/v Span 83 + 6.8E-2 M NaCl	Separated oil, water phase separation, creamy emulsion (4 layers)	Separated oil, water phase separation, creamy emulsion (4 layers)	Separated oil, water phase separation, creamy emulsion (4 layers)	Separated oil, water phase separation, creamy emulsion (4 layers)	Flocculation in the system which led to coalescence
4	10 % DI water + 5 % w/v Span 83 + 5.1E-1 M NaCl	The emulsion phase turned into an extended serum phase shortly, water separation, a thin creamy layer (3 layers)	Separated oil, water separation, a thin creamy layer (3 layers)	Separated oil, water separation, a thin creamy layer (3 layers)	Separated oil, water separation, a thin creamy layer (3 layers)	Flocculation in the system. Most of the droplet collisions immediately led to coalescence. Rapid sedimentation
5	20 % DI water + 5 % w/v Span 83	Separated oil, creamy emulsion, and emulsion (3 layers)	Separated oil, creamy emulsion, and emulsion (3 layers)	Separated oil, creamy emulsion, and emulsion (3 layers)	Separated oil, creamy emulsion, and emulsion (3 layers)	Flocculation in the system
6	30 % DI water + 5 % w/v Span 83	Separated oil, creamy emulsion, and emulsion (3 layers)	Separated oil, creamy emulsion, and emulsion (3 layers)	Separated oil, creamy emulsion, and emulsion (3 layers)	Separated oil, creamy emulsion,and emulsion (3 layers)	Flocculation in the system
7	40 % DI water + 5 % w/v Span 83	Separated oil, creamy emulsion, and emulsion (3 layers)	Separated oil, creamy emulsion, and emulsion (3 layers)	Separated oil, creamy emulsion, and emulsion (3 layers)	Separated oil, creamy emulsion, and emulsion (3 layers)	Flocculation in the system
8	40 % DI water + 5 % w/v Span 83 + 6.8E-2 M NaCl	Separated oil, water phase, creamy emulsion, and emulsion (4 layers)	Separated oil, water phase, creamy emulsion, and emulsion (4 layers)	Separated oil, water phase, creamy emulsion, and emulsion (4 layers)	Separated oil, water phase, creamy emulsion, and emulsion (4 layers)	Flocculation in the system
9	40 % DI water + 5 % w/v Span 83 + 5.1E-1 M NaCl	Emulsion, water separation, separated oil (3 layers)	Emulsion, water separation, separated oil (3 layers)	Emulsion, water separation, separated oil (3 layers)	Emulsion, water separation, separated oil (3 layers)	Flocculation in the system. Rapid sedimentation

According to the results presented in **Table 3.5**, all emulsion recipes suffer from the flocculation of droplets in the system. It is more difficult to stabilize the water-in-oil emulsions because the electric double layer is very thin in this type of emulsion compared with the oil-in-water emulsion [1,35]. As a result, repulsive forces are weaker, and droplets may coagulate as the Van der Waals forces are the dominant intermolecular forces in such conditions. Flocculation of the droplets was found to be reversible and did not lead to the fusion of the droplets in emulsions with no or very small salt concentration (Recipes 1,2,5,6,7).

Emulsion samples that contain larger NaCl concentrations experienced coalescence upon collision and flocculation of the droplets. Coalescence of the droplets speeds up the phase separation, and this was the case for Recipes 3,4,8, and 9 with 6.8E-2 M and 5.1E-1 M NaCl. However, tap water (recipe 2), which contains less than 3.4E-3 M salt in its composition did not show any signs of coalescence and phase separation. **Figure 3.10** displays the microscopic images of the emulsions with no NaCl, 6.8E-2 M, and 5.1E-1 M salt concentration in 10% emulsion samples. The signs of coalescence and shape deformation due to the fusion of the droplets are apparent in the images as the electrolyte concentration increases. Besides, it appears that DI water emulsion shows less flocculation compared with the cases that salt is added to the aqueous phase. This is probably due to the lower Van der Waals attraction forces (London dispersion forces) between the molecules because of fewer electrolytes present in the system. Moreover, the literature confirms that the rate of flocculation is higher for emulsions with larger droplets [2.3]. Section 3.4.4 of this study discusses how the presence of the electrolyte leads to the enlargement of emulsion droplets. Hence, salt can indirectly increase the rate of flocculation among droplets here by magnifying the size of the droplets. It is important to note that the results could be different depending on when and how the electrolyte is added in the process of emulsion preparation and further testing (such as zeta potential measurements) is required to better understand the underlying mechanisms which may influence the intermolecular forces and subsequent interaction between the droplets.

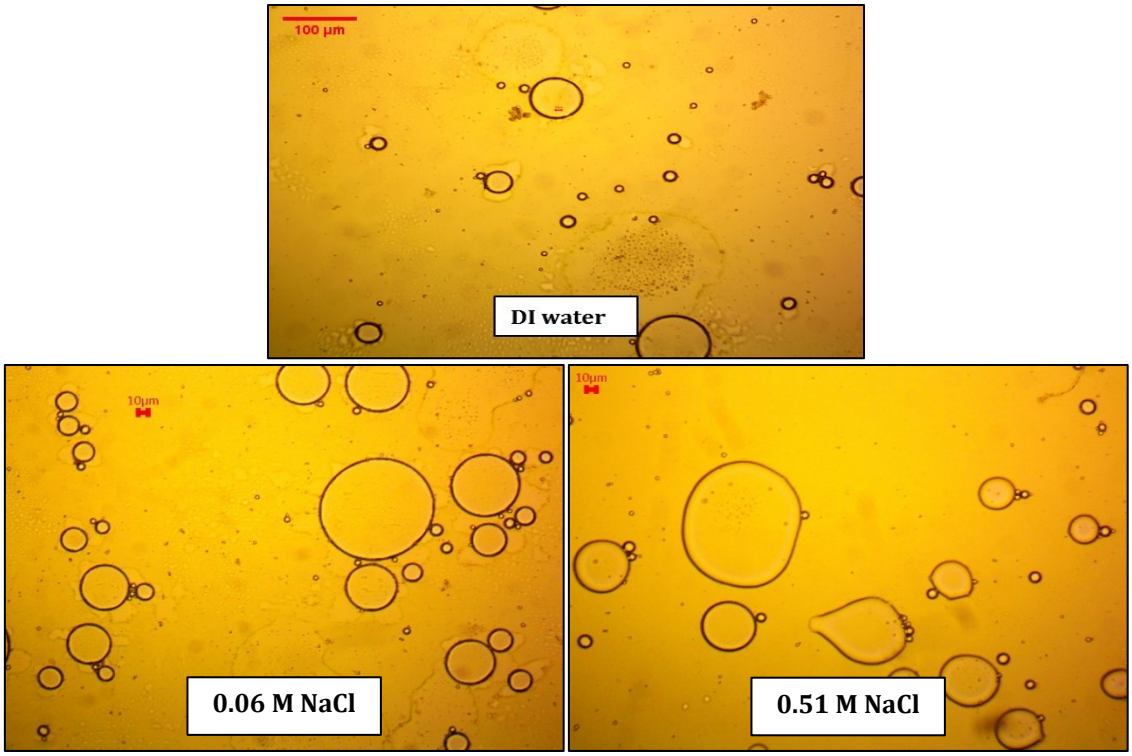

Figure 3.10: Micrography of the emulsions containing different concentrations of NaCl in the aqueous phase.

Electrolyte generally destabilizes the emulsions in two ways. It may either decrease the CMC of the surfactant by reducing the repulsions between the charged heads of the surfactant molecules or change the solubility of the solvent depending on the concentration of the electrolyte [36,37]. The latter is a phenomenon that is referred to as "salting in/out." The first mechanism is unlikely to occur here as the surfactants are non-ionic.

Figure 3.11 shows the emulsion sample bottle tests of Recipes 3,4,8, and 9 which contain NaCl in their composition. The observation that no phase separation occurs for tap water emulsion but takes place for the emulsion with 6.8E-2 M and 5.1E-1 M NaCl in the aqueous phase supports the hypothesis that there must be a threshold value of NaCl concentration where the solubility tendency of the water alters. Moreover, the literature supports that "salting in" usually occurs at very low salt concentrations [38]. Surfactant molecules are partitioned towards the oil phase upon the "salting out" phenomenon that leads to the instability of the emulsions to coalescence. The relatively transparent phase and very thin creamy layer in the 10% emulsion prepared with 5.1E-1 M NaCl shown in **Figure 3.11** (recipe 4) indicates the surfactants are mostly away from the interface and positioned in the oil phase, which is an implication of salting out.

Figure 3.11 also shows that 40% (recipe 9) emulsion with 0.51 M NaCl exhibits a much faster rate of sedimentation compared with the other samples with lower salt concentrations which led to the separation of the mineral oil from the emulsion. This is due to the elevated density of the dispersed phase because of added NaCl to the water which in turn intensifies the sedimentation rate of the droplets.

A comparison of the stability test results in this study for emulsions with different phase ratios implies that the kinetic stability of the emulsion is sensitive to water content. **Figure 3.12** displays the water separation in a 3-days storage period. According to this figure, 40% emulsion is much more stable in the whole electrolyte concentration range tested than the 10% emulsion. In dilute emulsion (10% emulsion), increasing the NaCl concentration resulted in significant magnification in water separation. However, this was not the case in the concentrated emulsion (40% emulsion).

There is a strong interaction between the phase ratio, electrolyte concentration, and the stability of the emulsion. Statistical significance of the results verified this interaction effect. In the two-way ANOVA test where the 3-days water separation percentage was defined as the dependent variable and a function of water content and NaCl concentration as the independent variables, a very small p-value (<0.05) confirmed the interaction between these variables. As the water content increases in the emulsion, the viscosity magnifies. It is well documented in the literature that the viscosity of the emulsion affects the stability of the emulsion because it slows down the rate of approach among droplets [4,15].

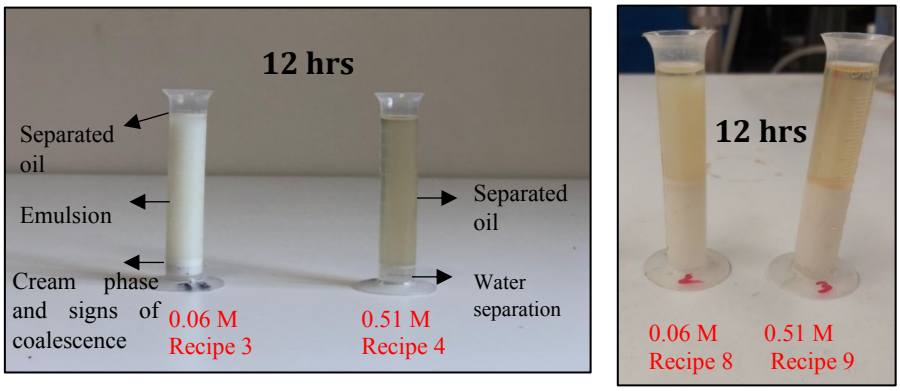

Figure 3.11: Effect of electrolyte on the stability of the 10% emulsion (left) and 40% emulsion (right)

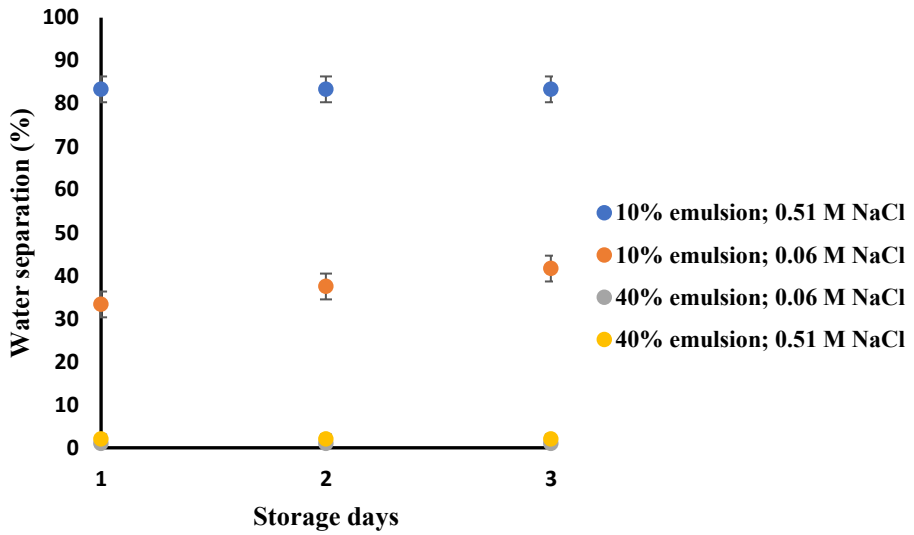

Figure 3.12: Water phase separation for different emulsion qualities and electrolyte concentrations

Another observation from the micrography was the structure and shape of the flocs. Although Van der Waals forces are known to increase in magnitude with a higher radius of the droplets, the flocs in the emulsions consisted of droplets of various sizes. Microscopic images show that the flocs consist of a large droplet and several smaller droplets. Smaller droplets diffuse faster in the medium and attach to the large droplets upon collision. While the motion of larger droplets is governed by gravitational forces (sedimentation), diffusive forces influence the movement of the very small droplets in the system.

Figure 3.13 illustrates the formation of different layers in emulsions with time. Sedimentation of the droplets is a mechanism of instability in the w/o emulsions. This is especially the case when the continuous phase is mineral oil with a difference in density (0.85 g/ml to 1 g/ml) with the water phase. Sedimentation of the water droplets is responsible for the formation of the serum and separated oil phases and different layers observed in the samples. Stokes law explains that larger droplets tend to sediment faster [1,6]. It appears that droplets are more frequent and larger in the creamy emulsion layer (thick milky phase) observed in this study, and fewer and smaller droplets remain in the more transparent phase (dilute emulsion layer). This may partially explain the difference in the volume of the layers with time for emulsions at different water concentrations. Besides, emulsions with smaller droplets are generally more transparent, and the encountering frequency of droplets increases in concentrated emulsions [1-4].

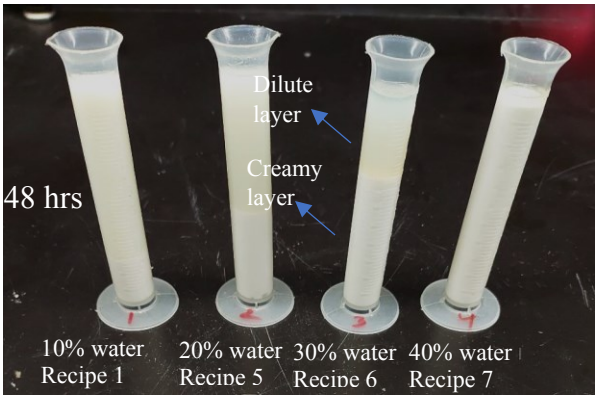

Figure 3.13: Formations of different layers in emulsions with time

The difference in the level of this thick creamy phase can also be related to the overall stability of the emulsions. The results presented verify that the emulsion with a higher water phase ratio is more stable. Thus, the droplets are less likely to coalesce and the sedimentation rate appears to be slower in concentrated emulsions. An experiment was designed to examine this hypothesis. Emulsions in different water contents were prepared and the change in the levels of the creamy layer which contains most of the water droplets was tracked for 3 days. The decline in the volume of this layer with time in emulsions is an implication of the sedimentation rate in the emulsion samples. **Figure 3.13** and **Figure 3.14** show the sedimentation of this creamy layer and it can be concluded that the rate of deposition declines in emulsions with higher water content. This is the case even though the mean droplet size is larger in the emulsions with a larger water fraction. It seems that the effect of phase ratio is more dominant by providing more stability in emulsions. Therefore, dilute emulsions despite having smaller droplets sediment faster. A similar phenomenon has been observed by Souza et al. (2015) in a study on settling velocities in w/o emulsion with the Brazilian crude diluted with mineral oil. They witnessed that sedimentation was governed by the emulsion water content where higher settling velocities were recorded for dilute emulsion despite having smaller droplet sizes [39].

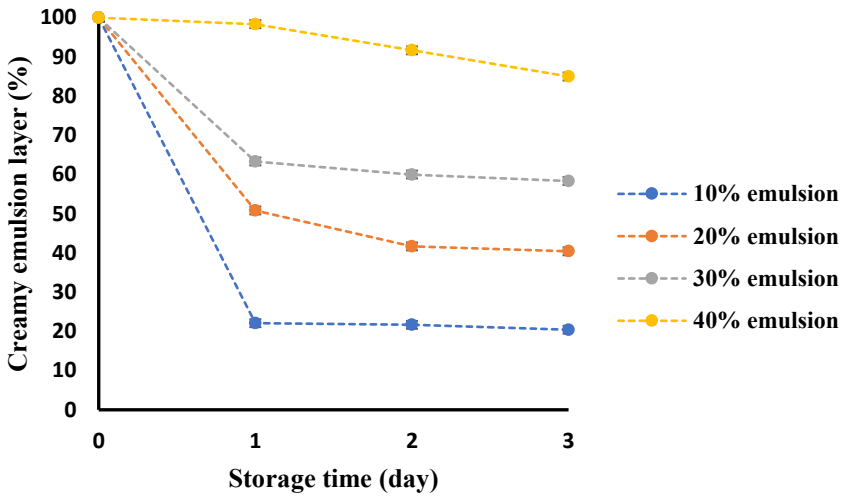

Figure 3.14: Creamy emulsion layer volumetric content with time (Implication of sedimentation)

Moreover, surfactant micelles may migrate to the bottom due to the density difference with the continuous phase. **Figure 3.15** displays the microscopic images of the sample creamy emulsion layer. Optical microscopy images from the bottom part of the emulsion sample where the creamy layer exists support the discussions presented. Larger droplets and accumulated surfactant micelles are detectable in the image.

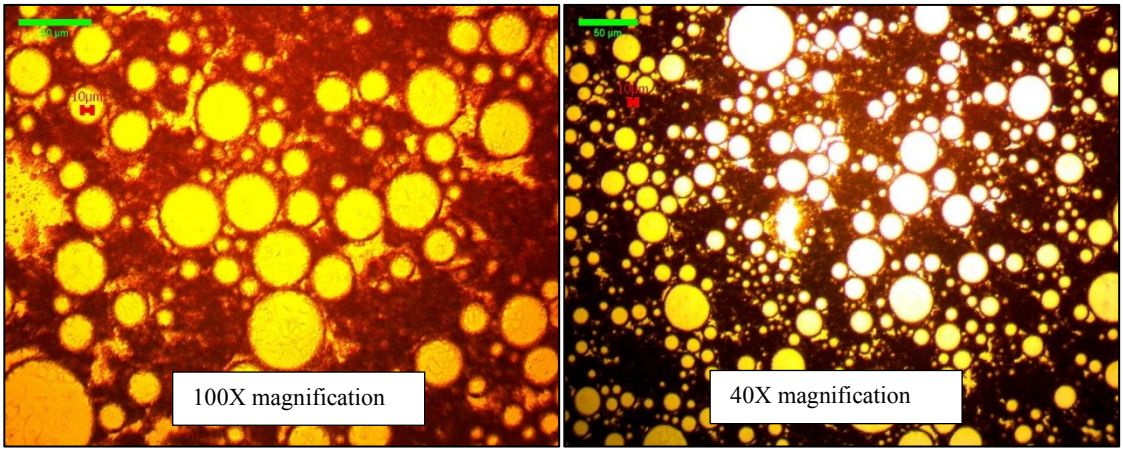

Figure 3.15: Deposition of the surfactant micelles and larger droplets to the bottom of the emulsion (recipe 6)

To summarize, emulsions are prone to reversible flocculation due to the thin EDL in w/o emulsions and prevalence of Van der Waals attractive forces over the repulsive forces in short molecular distances. However, flocculation leads to the coalescence of the droplets only if the system exceeds a threshold electrolyte concentration. Salting out appears to be the responsible mechanism of emulsions instability to coalescence. Moreover, different layers form in the emulsion over time due to the sedimentation of the water droplets and migrations of the surfactant micelles to the

bottom. As the number of larger droplets increases with higher water fraction in the emulsions, the level of these layers changes consequently. The sedimentation rate is governed by the water phase ratio in emulsions and higher water content yields slower sedimentation. Finally, emulsions with higher water content were found to be tighter than the dilute emulsion because of the elevated viscosity in the concentrated emulsion which promotes stability.

3.4.4 Droplet size analysis

It is well documented that the size of the droplets affects the stability and viscosity of emulsions [1-4]. Generally, if the droplets are widely narrowed down toward smaller sizes, emulsions tend to be more stable and viscous [1]. Several factors influence the size of the droplets including the viscosity of the continuous and dispersed phases, surfactant concentration, phase ratio, salinity, pressure, and temperature, among others. This study investigates the alteration in droplet size as a function of Span 83 dosage, water content, and salinity at a fixed ambient temperature of 22 °C and atmospheric pressure in fresh emulsions. Emulsions are prepared by constant homogenization parameters of 1000 rpm and 1 min mixing time.

A two-level factorial experimental design was adopted to assess the effect of Span 83 concentration and phase ratio on the size of the droplets. **Figure 3.16** illustrates the change in the mean droplet diameter with these parameters. It was observed that the mean droplet diameter decreases in higher surfactant concentration. A larger amount of emulsifier in the system results in better coverage of the new droplets formed during homogenization. Moreover, the rate of covering is faster in this case compared to the emulsions prepared with lower surfactant concentration [15]. Thus, the fusion and coalescence of the droplets are mitigated following a smaller interfacial tension caused by the employment of more surfactant in the system.

According to the results displayed in **Figure 3.16**, the phase ratio also plays an important role along with the concentration of the surfactant. Overall, as the water content increases the mean droplet size magnifies as well, however, the difference is smaller when a larger surfactant dosage is utilized in the preparation of the emulsion (112% variation in 0.1 water content to 63% variation in 0.4 water content). Additionally, the change in droplet diameter in 0.4 water content with the surfactant concentration is more significant (38% decrease in size in 0.4 water content and 19% reduction in 0.1 water content) as the frequency of forming droplets is much more in concentrated emulsions which requires a large dosage of surfactant for good surface coverage.

The increase in droplet size in the concentrated emulsion may also be justified by the relatively higher frequency of water droplets forming during homogenization and larger dispersed phase surface area assuming constant droplet diameter when water droplets are forming by the fixed mechanical energy of the homogenizer. This means the higher surface area of the droplets in concentrated emulsions requires much more surfactant for film coverage, lack of which results in coalescence and forming larger droplets during and after homogenization. Larger surfactant concentration in the system lowers the interfacial tension through better coverage of the forming droplets during homogenization which in turn reduces the size of the droplets. Statistical analysis of the results approves the hypothesis made. Two-way ANOVA analysis resulted in a very small P-value (<0.05) which confirms the interaction effect between the mean droplet diameter, water content, and surfactant concentration.

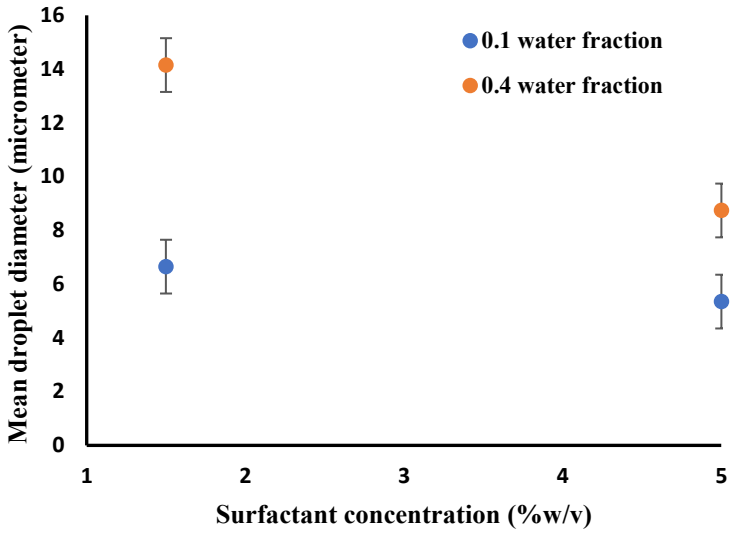

Figure 3.16: Effect of surfactant concentration and phase ratio on the mean droplet diameter

In the previous section, the micrography of the emulsion samples implied that increasing salt concentration would result in the coalescence of the droplets. **Table 3.5** shows this happens rapidly in emulsions prepared with 0.51 M NaCl, however, this instability phenomenon takes more time in emulsion samples with 6.8E-2 M NaCl in the aqueous phase. Hence, the latter concentration of salt was selected as the upper level in a 2-level factorial experimental design to study the effect of salinity and phase ratio on fresh emulsion samples. Emulsions were prepared with fixed 1000 rpm and 1 min mixing time homogenization parameters at the ambient temperature (22 °C) and atmospheric pressure and 5 %w/v Span 83 dosage.

Figure 3.17 illustrates a strong interaction that exists between the salinity, phase ratio, and the corresponding mean droplet diameter. In the dilute emulsion (0.1 water content) mean droplet size increased with salinity. The salting-out mechanism as discussed in the previous section leads to partitioning of the surfactant molecules in the oil phase which results in the formation of larger droplets upon collision of the droplets during homogenization. However, this effect is minimized in concentrated emulsions where the interaction between the droplets and surfactants is much more significant. The effect of phase ratio becomes dominant in concentrated emulsions and the addition of NaCl will not lead to coalescence of the droplets upon collision. Results of 3-days stability tests approve this statement, as shown by **Figure 3.18** where concentrated emulsion exhibits resistance to phase separation at higher NaCl concentrations. It should be noted that higher NaCl concentration (0.51 M) results in the formation of larger droplets as observed in the micrography for both dilute and concentrated emulsions.

Statistical analysis of the results shows that the interaction effect between the salinity, phase ratio, and mean droplet diameter is significant (P-value<0.05 in the two-way ANOVA test). P-value was found to be 0.02 in the two-tail t-test for emulsion with 0.1 water fraction. Thus, the null hypothesis (equal means between the samples) was rejected and the alternative hypothesis that the higher concentration of NaCl increases the mean droplet diameter in emulsions is statistically significant. However, a P-value of 0.16 in the two-tail t-test was obtained which means the difference in the

size of the droplets as a function of NaCl concentration in the emulsion with 0.4 water content is statistically insignificant. Thus, one may conclude that the salinity does not change the size of the droplets in the concentrated emulsion.

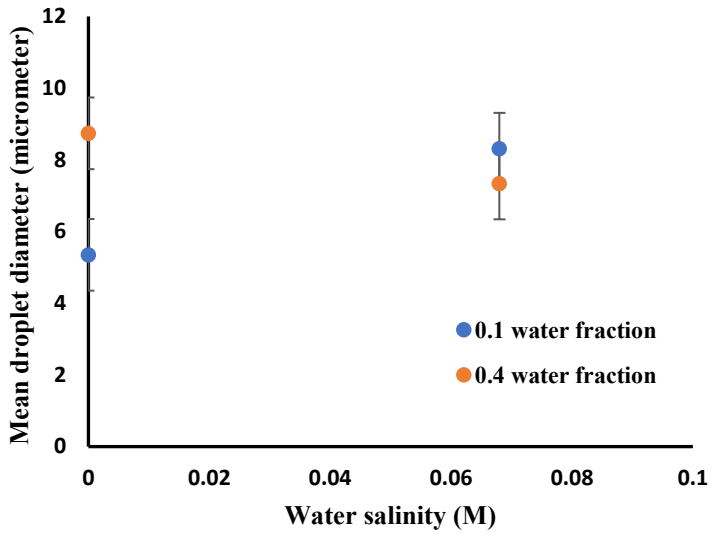

Figure 3.17: Effect of NaCl and phase ratio on the mean droplet diameter

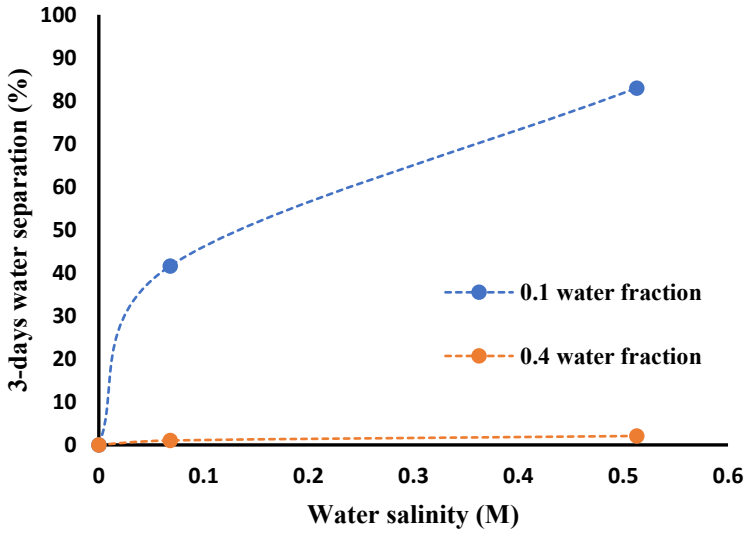

Figure 3.18: Effect of water content and salinity on water separation in emulsion samples

Conclusions

This study characterized the bulk properties of the water-in-mineral oil macro-emulsions in terms of viscosity, droplet size and droplet size distribution, and kinetic stability. HLD theory was employed to select the non-ionic surfactant (Span 83). A relationship between the mean droplet size and the homogenization parameters was developed. It was found that the most consistent results for droplet size characterization using optical microscopy are obtained when the number-based representative sizes are reported. This study also presented a novel viscosity empirical model for w/o emulsions, which incorporates the internal phase volume fraction, shear rate, and

interactive terms. Therefore, the model captures the non-Newtonian behavior of the w/o emulsions at higher water fractions. Moreover, the emulsions were tested for kinetic stability using the bottle tests and optical microscopy methods. It was observed that the emulsions were subject to reversible flocculation that resulted in the coalescence of the droplets if the system contains a larger than a threshold value of NaCl concentration. Salting out is most likely the responsible mechanism of the coalescence. Concentrated emulsions were found to be tighter with slower sedimentation rates and much less water phase separation. Finally, the size of the droplets tends to decrease with higher surfactant concentration. Mean droplet diameter is also affected by the phase ratio and electrolyte concentration.

Nomenclature

ppm: Parts per million

rpm: Rounds per minute

M: Molarity (mol/lit)

D10: Mean droplet diameter (micrometer)

D32: Sauter diameter (micrometer)

D43: De Broukere diameter (micrometer)

DI water: Deionized water

$\emptyset$: Internal phase volume fraction

K: Dispersed to continuous phase ratio

μ_D: Dispersed phase viscosity (mPa.s)

μ_c: Continuous phase viscosity (mPa.s)

μ_{rel}: Relative viscosity

References

[1] Schramm, L.L., 1992. Fundamentals and applications in the petroleum Industry. *Adv. Chem*, *231*, pp.3-24.

[2] Leal-Calderon, F., Schmitt, V. and Bibette, J., 2007. *Emulsion science: basic principles*. Springer Science & Business Media.

[3] Sjoblom, J., 2001. *Encyclopedic handbook of emulsion technology*. CRC press.

[4] Kokal, S.L., 2005. Crude oil emulsions: A state-of-the-art review. *SPE Production & facilities*, *20*(01), pp.5-13.

[5] Colucci, G., Santamaria-Echart, A., Silva, S.C., Fernandes, I.P., Sipoli, C.C. and Barreiro, M.F., 2020. Development of Water-in-Oil Emulsions as Delivery Vehicles and Testing with a Natural Antimicrobial Extract. *Molecules*, *25*(9), p.2105.

[6] Manning, F.S. and Thompson, R.E., 1995. *Oilfield processing of petroleum: Crude oil* (Vol. 2). Pennwell books.

[7] Rodionova, G., Pettersen, B., Kelesoğlu, S. and Sjöblom, J., 2014. Preparation and characterization of reference fluid mimicking behavior of North Sea heavy crude oil. *Fuel*, *135*, pp.308-314.

[8] Balsamo, M., Erto, A. and Lancia, A., 2017. Chemical demulsification of model water-in-oil emulsions with low water content by means of ionic liquids. *Brazilian Journal of Chemical Engineering*, *34*(1), pp.273-282.

[9] Opawale, F.O. and Burgess, D.J., 1998. Influence of interfacial properties of lipophilic surfactants on water-in-oil emulsion stability. *Journal of colloid and interface science*, *197*(1), pp.142-150.

[10] Santini, E., Liggieri, L., Sacca, L., Clausse, D. and Ravera, F., 2007. Interfacial rheology of Span 80 adsorbed layers at paraffin oil–water interface and correlation with the corresponding emulsion properties. *Colloids and Surfaces A: Physicochemical and Engineering Aspects*, *309*(1-3), pp.270-279.

[11] Jiao, J. and Burgess, D.J., 2003. Rheology and stability of water-in-oil-in-water multiple emulsions containing Span 83 and Tween 80. *Aaps Pharmsci*, *5*(1), pp.62-73.

[12] Akbari, S., Nour, A.H., Jamari, S.S. and Fayaz, F., 2006. Rheology and stability mechanism of water-in-crude oil emulsions stabilized by span 83. *ARPN Journal of Engineering and Applied Sciences*, *11*(4).

[13] Pawlik, A., Cox, P.W. and Norton, I.T., 2010. Food grade duplex emulsions designed and stabilised with different osmotic pressures. *Journal of colloid and interface science*, *352*(1), pp.59-67.

[14] Zhu, Q., Pan, Y., Jia, X., Li, J., Zhang, M. and Yin, L., 2019. Review on the stability mechanism and application of water-in-oil emulsions encapsulating various additives. *Comprehensive Reviews in Food Science and Food Safety*, *18*(6), pp.1660-1675.

[15] Cardoso-Ugarte, G.A., Ramírez-Corona, N., López-Malo, A., Palou, E., San Martín-González, M.F. and Jiménez-Munguía, M.T., 2018. Modeling phase separation and droplet size of

W/O emulsions with oregano essential oil as a function of its formulation and homogenization conditions. *Journal of Dispersion Science and Technology*, *39*(7), pp.1065-1073.

[16] Henríquez, C.J.M., 2009. W/O Emulsions: formulation, characterization and destabilization. *Technischen Universität Cottbus zur Erlangung, Caracas*.

[17] Abdurahman, N.H. and Mahmood, W.K., 2012. Stability of water-incrude oil emulsions: effect of cocamide diethanolamine (DEA) and Span 83. *International Journal of Physical Sciences*, *7*(41), pp.5585-5597.

[18] National Center for Biotechnology Information. PubChem Database. Source=Sigma-Aldrich, SID=329824531, https://pubchem.ncbi.nlm.nih.gov/substance/329824531 (accessed on May 25, 2020)

[19] Sorbitan sesquioleate. SID S3386 [online]. Sigma-aldrich: St. Louis, MO, USA. Source: https://www.sigmaaldrich.com/catalog/product/sigma/s3386?lang=en&region=CA (accessed May 18, 2020)

[20] Effective surfactant selection & Formulation of (micro-)emulsions via HLD-NAC. Vlsi presentation. Source: https://www.in-cosmetics.com/__novadocuments/366543?v=636332029055230000 (accessed May 18, 2020)

[21] Abbott, S., 2016. Surfactant science: principles and practice. *Update*, *1*, pp.2-26.

[22] Velayati, A. and Nouri, A., 2020. Emulsification and emulsion flow in thermal recovery operations with a focus on SAGD operations: A critical review. *Fuel*, *267*, p.117141.

[23] Standard, A.S.T.M., 1981. E799-81,". *Practice for Determining Data Criteria and Processing for Liquid Drop Size Analysis*.

[24] *Operating Instructions. Manual No*. M/85-150-P700. Middleboro, MA: Brookfield Engineering Laboratories, Inc. Source: http://www.viscometers org/PDF/Manuals/laboratory/DIAL (accessed May 25, 2020].

[25] Maa, Y.F. and Hsu, C., 1996. Liquid-liquid emulsification by rotor/stator homogenization. *Journal of Controlled Release*, *38*(2-3), pp.219-228.

[26] Einstein, A., 1956. *Investigations on the Theory of the Brownian Movement*. Courier Corporation.

[27] Taylor, G.I., 1932. The viscosity of a fluid containing small drops of another fluid. *Proceedings of the Royal Society of London. Series A, Containing Papers of a Mathematical and Physical Character*, *138*(834), pp.41-48.

[28] Richardson, E.G., 1938. Kolloid-Z. 65, 32 (1933).

[29] Nasery, S., Hoseinpour, S., Phung, L.T.K. and Bahadori, A., 2016. Prediction of the viscosity of water-in-oil emulsions. *Petroleum Science and Technology*, *34*(24), pp.1972-1977.

[30] Mooney, M., 1951. The viscosity of a concentrated suspension of spherical particles. *Journal of colloid science*, *6*(2), pp.162-170.

[31] Thomas, D.G., 1965. A note on the viscosity of Newtonian suspensions of uniform spherical particles. *J. Colloid Sci.*, *20*, pp.267-277.

[32] Guth, E. and Simha, R., 1971. Kolloid Z., 74, 266 (1936)

[33] Saitô, N., 1950. Concentration dependence of the viscosity of high polymer solutions. I. *Journal of the Physical Society of Japan*, *5*(1), pp.4-8.

[34] Dan, D. and Jing, G., 2006. Apparent viscosity prediction of non-Newtonian water-in-crude oil emulsions. *Journal of Petroleum Science and Engineering*, *53*(1-2), pp.113-122.

[35] Tadros, T.F., 2013. Emulsion formation, stability, and rheology. *Emulsion formation and stability*, *1*, pp.1-75.

[36] Nikolovski, B.G., Ilić, J.D. and Sovilj, M.N., 2016. How to formulate a stable and monodisperse water-in-oil nanoemulsion containing pumpkin seed oil: the use of multiobjective optimization. *Brazilian Journal of Chemical Engineering*, *33*(4), pp.919-931.

[37] Aronson, M.P. and Petko, M.F., 1993. Highly concentrated water-in-oil emulsions: Influence of electrolyte on their properties and stability. *Journal of colloid and interface science*, *159*(1), pp.134-149.

[38] Garrett, R. and Grisham, C., 2010. Biochemistry. Brooks Cole Cengage Learning, Boston USA.

[39] Souza, W.J., Santos, K.M.C., Cruz, A.A., Franceschi, E., Dariva, C., Santos, A.F. and Santana, C.C., 2015. Effect of water content, temperature and average droplet size on the settling velocity of water-in-oil emulsions. *Brazilian Journal of Chemical Engineering*, *32*(2), pp.455-464.

Appendix 3.A: Viscosity measurements

Table 3.A1 - Summary of the viscosity test results

Fluid	Shear rate (1/sec)	Shear stress (dyne/cm2)	Viscosity (mPa.s)	Device Error (mPa.s)	Full-scale range (mPa.s)
Mineral oil	11.25	0.74	6.58	2.05	205.60
	22.50	1.59	7.08	1.02	102.80
	45	2.83	6.30	0.51	51.40
	90	5.45	6.06	0.25	25.70
Oil+5% w/v Span 83	11.25	1.08	9.62	2.05	205.60
	22.50	2.14	9.52	1.02	102.80
	45	4.28	9.52	0.51	51.40
	90	8.49	9.44	0.25	25.70
10%* emulsion with 5% w/v Span 83	11.25	1.62	14.40	2.05	205.60
	22.50	3.01	13.40	1.02	102.80
	45	5.80	12.90	0.51	51.40
	90	11.70	13	0.25	25.70
20% emulsion with 5% w/v Span 83	11.25	2.18	19.40	2.05	205.60
	22.50	4.25	18.90	1.02	102.80
	45	8.05	17.90	0.51	51.40
	90	15.75	17.50	0.25	25.70
30% emulsion with 5% w/v Span 83	11.25	3.55	31.60	2.05	205.60
	22.50	6.50	28.90	1.02	102.80
	45	11.79	26.20	0.51	51.40
	90	22.68	25.20	0.25	25.70
40% emulsion with 5% w/v Span 83	11.25	6.33	56.30	2.05	205.60
	22.50	11.27	50.10	1.02	102.80
	45	20.43	45.40	0.51	51.40

* % emulsion refers to the internal phase volume concentration of the emulsion

Chapter 4: Role of Asphaltene in Stability of Water-in-oil Model Emulsions: The Effects of Oil Composition and Size of the Aggregates and Droplets

This paper was published in ACS Journal of Energy & Fuels.

Velayati, A. and Nouri, A., 2021. Role of Asphaltene in Stability of Water-in-Oil Model Emulsions: The Effects of Oil Composition and Size of the Aggregates and Droplets. Energy & Fuels, 35(7), pp.5941-5954.

4.1 Preface

Water-in-oil (W/O) emulsions are the most common type of emulsions handled in petroleum processes. It is thought that the field emulsions are primarily stabilized by asphaltene-resin micelles and several research works have studied the stability mechanisms of asphaltene in crude emulsions. However, there is still plenty of research gaps and unanswered question in this area due to the complexity of the problem and difficulty of access and crude emulsions processing. These challenges can be addressed by investigating the effect of asphaltene on the model emulsions' kinetic stability. This study introduces a model W/O emulsion prepared by a new stabilizer (Gilsonite) that contains asphaltenes and resins in combination with a non-ionic surfactant (Span 83). The colloidal characterization of the asphaltene aggregates in the mineral oil and oil blend of Toluene and mineral oil was carried out. The size of the asphaltene aggregates in the mineral oil was found to increase with the added Gilsonite concentration because of asphaltene precipitation and the process of smaller aggregates clumping together, forming flocs. Gilsonite was also found to precipitate and stabilize the W/O emulsions with the mineral oil as the external phase where the asphaltene precipitation was most severe. The emulsions' least kinetic stability was measured when Toluene was added in the oil blend (50% volume fraction), where 100% water phase separation was observed with 0.25% Gilsonite concentration. However, the dilute Emulsion (10% water content in the emulsion) samples with 25% Toluene revealed higher stability in terms of water phase separation than the case with 12.5% Toluene with 20.83% less water separation in a 3-day storage period. This observation contradicts the expected outcome in a thermodynamic perspective where the W/O emulsion stability is thought to be merely dependent on the asphaltene precipitation. The dilute emulsion with 12.5% Toluene contained asphaltene aggregates larger than the emulsion droplets, which cannot contribute to the stability process. The ratio of mean aggregate size to the mean droplet size was 133% larger for the dilute emulsion with a smaller fraction of Toluene in the oil blend for this case. Therefore, the aggregates' size to droplet size misalignment resulted in less stability for this emulsion than the emulsion with higher aromaticity of the oil blend despite the very high precipitation rate. This paper presents observations of the effects of the asphaltene precipitation rate, size of the aggregates, and size distribution of the emulsion droplets on the model W/O emulsions' stability. The significance of the results is in revealing the importance of Integrating the thermodynamical and colloidal viewpoints to describe the role of asphaltene in stabilizing emulsions. This approach leads to the conclusion that besides the asphaltene precipitation, the aggregates' size distribution in relation to the size of the emulsion droplets is a critical factor in stabilizing the emulsions. Results presented in this study reveal important aspects of asphaltene precipitation and aggregation behavior for different oil compositions which can be of significance in solvent injection operations. Moreover, the findings of this research can be used in introducing model emulsions replicating oil reservoir in-situ emulsion features, synthesis of demulsifiers for the emulsions stabilized with asphaltene-resin micelles, and other industrial applications. Additionally, Gilsonite was introduced as a new additive that can be used to study the role of asphaltene in stabilizing model emulsions.

4.2 Introduction

Emulsions are part of a broader mixture system known as the colloids. An emulsion is a dispersed system of immiscible liquids with water as the internal phase and oil as the external phase in a Water-in-oil (W/O) emulsion [1-3]. Oil-in-Water (O/W) emulsions have been investigated

broadly. In contrast, W/O emulsions are not characterized comparably, which is likely due to the issues with the stability of this type of emulsion [4]. This is the case despite the importance of W/O emulsions, particularly in the petroleum industry.

Gilsonite (Asphaltum) is a naturally occurring form of asphalt (bitumen), which is soluble in aromatics [5]. This solid hydrocarbon mineral is widely used in many products in various industries, including oil well cements and drilling fluids, printing inks and paints, and asphalt modifiers, among others [5]. Literature indicates Gilsonite is an effective fluid-loss control agent in the water-based drilling muds and an excellent shale stabilizer in the oil-based drilling muds [6,7]. Moreover, several patents claim Gilsonite can be used as an asphalt modifier and emulsion pavement sealer [8-10]. To the authors' knowledge, Gilsonite has never been used in model W/O emulsions. This is the first study suggesting the use of this type of mineral to study the role of asphaltenes in stabilizing the W/O emulsions.

Asphaltene is the heaviest and a polarizable fraction of crude oil with a complex structure [11]. Studies show that the asphaltenes precipitate into solids and deposit either due to the change in the field conditions (change in pressure and temperature) or the oil composition [12-14]. Many problems have been linked to the precipitation of asphaltenes in both upstream and downstream facilities of the oil industry [15]. Moreover, the formation of crude emulsions is thought to be mainly a result of natural emulsifiers, such as asphaltenes in the oil reservoir [16-19].

Kokal and Al-Dokhi demonstrated that crudes with a higher tendency of asphaltene precipitation are more likely to form kinetically stable emulsions [20]. Several other research works emphasize the crucial role of asphaltene in stabilizing crude emulsions and present the hypothesis that asphaltenes could also adsorb on the reservoir minerals and contribute to the stability of emulsions [21-23]. Generally, asphaltene precipitation is described by two modelling approaches [11]. One is the thermodynamic model that assumes asphaltene as a part of the non-ideal mixture, which precipitates when solubility values fall below specific values. The other approach is the colloidal model that considers asphaltene as colloidal particles surrounded by adsorbed resins. In this modelling approach, precipitation is assumed to be non-reversible. However, asphaltene precipitation's reversibility is still an area of debate and controversy [11].

Overall, the consensus is that the crude blend's increased aromaticity lowers the emulsion stability, and the kinetic stability is often explained through a thermodynamical lens [23-25]. The colloidal modelling approach states that the asphaltenes and resins form aggregates, and the aggregates clump together, establishing micelles. These micelles cover the droplets' interfacial area and stabilize the emulsions by steric hindrance primarily [26]. Previous studies demonstrate asphaltene materials as hydrophilic functional groups could potentially produce aggregates at the oil-water interface and form viscoelastic interfacial films around the water droplets [27-29]. However, the mechanism and influencing factors are still not fully understood. There is a substantial gap in the literature regarding the identification of the factors that impact the stability of the emulsions by asphaltenes. This study incorporates both approaches and attempts to describe W/O emulsions' stability by the effect of asphaltene precipitation and the colloidal characterization of the aggregates in terms of the relative size of the aggregates to emulsion droplets.

A model W/O emulsion was prepared with Gilsonite, which contains asphaltene in large fractions at ambient temperature and pressure. Initially, asphaltene's colloidal behavior was investigated in the mineral oil and oil mixtures (mineral oil and Toluene). Moreover, the thermodynamical viewpoint was accounted for in terms of asphaltene precipitation rate, which is a function of the asphaltene solubility in oil. Finally, the model emulsions' stability in terms of water phase separation was evaluated in dilute and concentrated emulsions for different oil compositions. The results clarify some crucial effects of the oil composition, size of the aggregates, and size distribution of the water droplets in the stability of W/O emulsions by asphaltene.

A better understanding of emulsion stability with asphaltene-resin micelles is essential to handle field emulsions produced in the petroleum industry and this work attempts to clarify some aspects of mechanisms through which the emulsions are stabilized. The significance of this study is adopting an integrated colloidal-thermodynamics approach in the analysis of the kinetic stability results. The findings presented in this study are useful in better understanding the asphaltene precipitation behavior in the solvents utilized in the enhanced oil recovery, producing model emulsions to characterize the flow behavior of the oil field in-situ emulsions, and designing demulsifiers. Moreover, Gilsonite is introduced as a new stabilizing agent for the W/O emulsions which mimics the asphaltene features.

4.3 Materials and Methods

Mineral oil and Toluene were used in different fractions to prepare the model emulsions and investigate the asphaltenes' colloidal behavior in oil. This study's mineral oil contains 96.5 wt% saturate mixtures and 3.5 wt% aromatics with a specific gravity of 0.85 at 15 °C and Toluene's specific gravity is 0.86 with a dynamic viscosity of 0.59 mPa.s at 20°C. Toluene is an aromatic hydrocarbon composed of a benzene ring which is linked to a methyl group.

A blend of the surfactants, including Gilsonite and Span 83, was used in the experiments. Sorbitan sesquioleate (Span 83) from the Span non-ionic surfactant family is widely used as an emulsifier to formulate creams and ointments for cosmetic use and pharmaceuticals [30-32]. Span 83 has a low hydrophilic-lipophilic balance (HLB) value that is indicative of higher solubility of the surfactant in the oil phase. According to Bancroft's rule, this facilitates the formation of the W/O emulsion. **Figure 4.1** illustrates the chemical structure of Span 83 with a 2:3 attachment ratio of sorbitan (dehydrated sorbitol molecule) with the unsaturated oleic acid. **Table 4.1** summarizes the properties of this non-ionic surfactant. Utah Gilsonite 200 mesh powder was used as the naturally occurring solid hydrocarbon, which is a rich source of asphaltenes. Elemental analysis and Saturate, Aromatic, Resin, and Asphaltene (SARA) fractions of the Gilsonite are shown in **Table 4.2**. Deionized water (DI water) was used in the preparation of the emulsion samples. 1 ppm Total dissolved solids (TDS) was measured for the DI water using a Conductivity/TDS meter. pH of all emulsion samples was between 7.5-8.

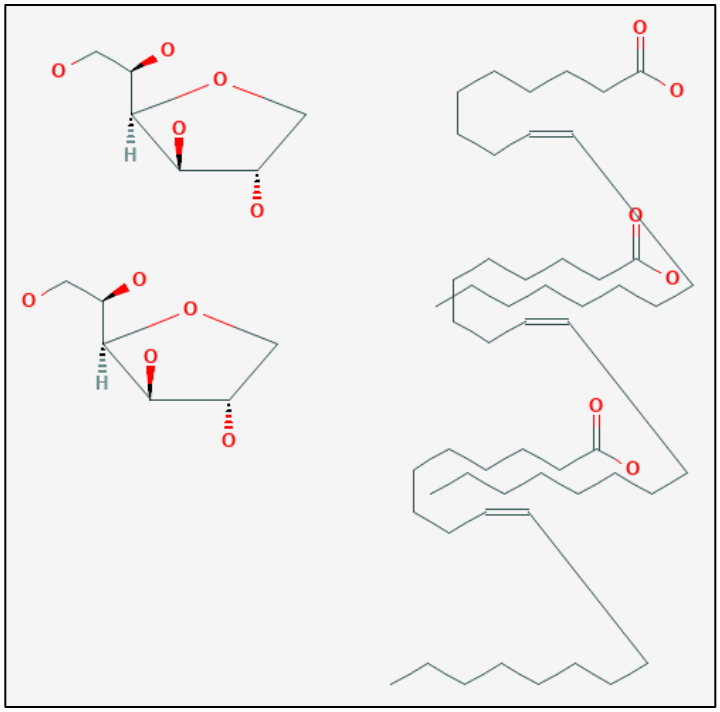

Figure 4.1: 2D depiction Sorbitan sesquioleate (Span 83) [33]

Table 4.1: Sorbitan sesquioleate (Span 83) properties

Property	Value
HLB	3 [34]
Cc	4-5 [35]
CMC*	0.024 (%wt/v) [30]
Mwt	560
IFT @ CMC*	13.18 dyne/cm [30]
Viscosity @ room temp	1500 mPa.s
Density	0.989 g/ml
*CMC was determined for light mineral oil and water	

Table 4.2: Properties of Gilsonite

Property	Value	Components	Value [5]
Carbon, wt%	85-86	Saturates, wt%	1.6
Hydrogen, wt%	8.5-10	Aromatics, wt%	0
Nitrogen, wt%	2.25-3.29	Resins, wt%	18.7
Sulfur, wt%	0.22-0.53%	Asphaltenes, wt%	79.7
Oxygen, wt%	1.5%	Colloidal instability index, CII	4.34

A magnetic stirrer was used for the initial mixing of the surfactants and the oil phase. A lab rotor/stator homogenizer with a 12 mm working head diameter and shearing rate capacity of 1,000-

28,000 rpm was employed to prepare the emulsions at an ambient temperature of 22 °C and atmospheric pressure. A cone and plate viscometer was used to measure the viscosity, and bottle tests were carried out to monitor the phase separation in the sample emulsions. 12-ml emulsion samples were poured into 14 ml graduated cylinders, and the containers were placed and kept on a flat surface for the specified storage time. The water phase separation was tracked and reported for three days.

This study employs the optical microscopy technique to determine the size distribution of the asphaltene aggregates and the emulsion droplets. For this purpose, a compound microscope (1,000X magnification, Omano OM-139) equipped with a high-resolution 10 MP camera was used to capture the samples' images. The Kohler illumination method in the microscope provides even illumination of the sample and ensures the illumination source is not visible in the micrography.

The captured images were processed using ImageJ opensource software. The images were adjusted using enhancing contrast techniques, and the backgrounds were removed. The aggregates and droplets were recognized using the binary method, and the holes were filled. Minimum Feret diameter and area occupied by the aggregates were extracted, and length (diameter) and area were obtained for the droplets in emulsion samples. In-house codes in Matlab were developed to find the representative sizes of the aggregates/droplets. **Figure 4.2** displays the workflow of the particle size analysis adopted and **Figure 4.3** shows the sequence of the work on a sample oil with asphaltene aggregates.

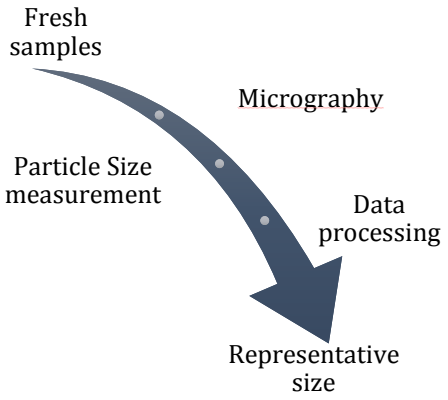

Figure 4.2: Workflow of image processing

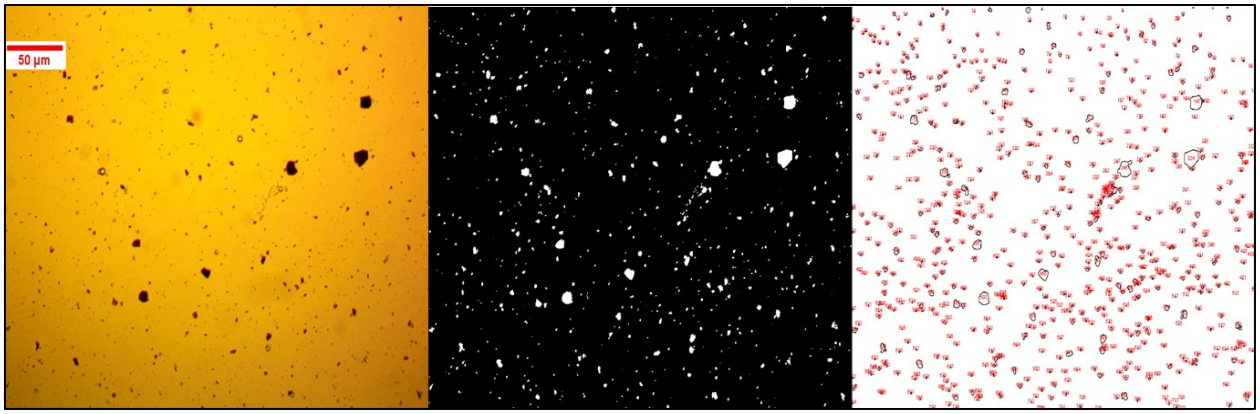

Figure 4.3: Sequence of image processing using ImageJ on the oil samples containing asphaltene: Micrography (Left), Particle detection (Middle), Particle outlines (Right)

Using the obtained data from ImageJ software such as min Feret diameter, length, and area, the representative sizes were calculated. Such includes the Equivalent Projected Circle (EQPC) diameter, maximum Feret diameter, maximum EQPC, and representative diameters. The size of the aggregates and droplets can be presented in several ways, namely D10 (arithmetic mean diameter), D32 (Sauter diameter), D43 (De Broukere, or Herdan diameter), number-based distribution, and volumetric-based distributions [1-4]. These representative sizes yield different values, and each one describes a specific aspect of the size of particles in the system. **Equation** 1 shows the general form of the representative sizes equation [36]:

$$\overline{D}_{pq}^{(p-q)} = \frac{\sum_i D_i^p}{\sum_i D_i^q} \tag{1}$$

where $\overline{D}$ is the averaged representative size, p and q are integers ranging from 1 to 4, and D_i is the ith drop's diameter. It is informative to express particle size analysis with more than one representative size to understand the distribution as well as the mean size.

The characterization of the asphaltenes' size and precipitation was performed in mineral oil and the oil mixture containing mineral oil and Toluene in the first stage of the research. Gilsonite in different concentrations was added to the oil to prepare a 12-ml sample. The sample was first stirred gently using a magnetic stirrer then mixed at 1,000 rpm for 1 min by a lab homogenizer. Fresh samples were analyzed using optical microscopy, and the size of the aggregates was determined using particle detection and image processing techniques. **Table 4.3** demonstrates the testing matrix for this testing phase. Moreover, asphaltene deposition was determined by the SARA method proposed by Gaestel et al. [37]. **Equation** 2 is used to analyze the asphaltene deposition potential by the Colloidal Instability Index (CII) [37].

$$CII = \frac{W_{saturates} + W_{asphaltenes}}{W_{resins} + W_{aromatics}} \tag{2}$$

where W is the mass fraction of the crude fractions (saturates, asphaltenes, resins, aromatics), and CII is the colloidal instability index. If CII is higher than 0.9, asphaltene deposition will likely take place in bitumen.

Table 4.3: Colloidal characterization of asphaltene in oil testing plan

	Objectives	Gilsonite concentration (%wt/v oil)	Type of oil
Colloidal characterization of asphaltene aggregates in oil	-Number of aggregates (implication of precipitation)	0.1,0.5,1,10	Mineral oil
	-Size of the aggregates	0.1, 1	Mineral oil + Toluene (Toluene Volume fraction: 0.125,0.25,0.5)

The second phase of the research involved preparing emulsions using two surfactants (Gilsonite and Span 83) only after evaluating the base emulsion with Span 83 and testing the possibility of formulating W/O emulsions using Gilsonite. A classical approach was adopted for the preparation of the emulsions [1]. Firstly, the surfactant(s) were mixed with the oil (oil mixture) using the magnetic stirrer. Then water (and NaCl solution) was added to prepare 12-ml emulsion samples by homogenizing the fluid mixtures at 1,000 rpm for 1 min. Fresh emulsion samples were used for micrography. Emulsion samples were poured into the 14-ml graduated cylinders, and the phase separation was monitored for three days in the bottle tests. The objective was to compare the kinetic stability in emulsions with different oil compositions and Gilsonite concentrations to investigate Gilsonite's role (asphaltene/resin micelles) in stabilizing the emulsion samples. **Table 4.4** shows the testing plan for this phase of the research.

Table 4.4: Testing plan for the model emulsion and base emulsion

	Objectives	Water fraction	Span 83 (%wt/v)	Type of oil	NaCl (M)
Base emulsion characterization	-Kinetic stability analysis -Size of the droplets	0.1,0.2,0.3,0.4	5	Mineral oil	0, 0.51M
		Water fraction	**Type of oil**	**Gilsonite concentration (%wt/v)**	**NaCl (M)**
Model emulsion with Gilsonite and 5 % wt/v Span 83	-Kinetic stability analysis -Size of the droplets	0.1	Mineral oil	0.25,1	0.51M
		0.1	Mineral oil + Toluene (Volume fraction: 0.125,0.25,0.5)	0.25,1	0.51M
		0.4	Mineral oil + Toluene (Volume fraction: 0.125,0.25)	1	0.51M

4.3.1 Surfactant(s) Selection

Several criteria are commonly used for the selection of suitable surfactants to formulate emulsions. Such includes the surfactant Critical Micelle Concentration (CMC) and Hydrophilic Lipophilic Balance (HLB), among others [1-3]. The issue with such criteria is that they only account for the surfactant-related properties and neglect other important aspects of emulsification such as the

temperature, salinity, and oil composition and properties. Hydrophilic Lipophilic Deviation (HLD) concept attempts to address this issue by accounting for other conditions in the emulsification process [38].

This work adopts the HLD concept to select suitable surfactants and assess the Gilsonite performance as the emulsifier. HLD has several components, including a surfactant-specific term, oil-specific term, temperature, and salinity. HLD is a function of the entire system under which the emulsion is prepared. **Equation** 3 shows the HLD components and equation [38]:

$$HLD = Cc - k.EACN - a\Delta T + f(s) \quad (3)$$

where Cc is the characteristic curvature value that represents the surfactant solubility, EACN stands for equivalent alkane carbon number and describes the oiliness, k and a are constants, ΔT is the temperature difference from 25° Celsius, *f(s)* is the salinity term where s is the salinity in g/100ml. *f(s)* equates *ln(s)* for ionic surfactants and *0.13s* for non-ionic surfactants.

HLD value of zero indicates an ideal and balanced system in which the interfacial tension is minimum. Negative HLD values suggest an O/W emulsion will take shape while positive HLD values indicate the formation of W/O emulsion [38]. In this study, emulsions were prepared at room temperature and ambient pressure, and EACN of Paraffinic mineral oil is reported 18 at room temperature of 25°C elsewhere [38]. Therefore, a Cc larger than 3.06 is required in a non-saline system to formulate a W/O emulsion. Span family of non-ionic surfactants such as Span 83 (Cc: 4-5 measured at room temperature of 25°C) can meet this requirement. However, asphaltene alone as the surfactant with a low Cc value (Cc:0.8-2.3 [39]) cannot stabilize a W/O emulsion when mineral oil is present in the system. Though, a blend of the surfactants can lead to W/O emulsions' formation if the mixture Cc value exceeds 3.06. Cc of a blend of surfactants can be determined by **Equation** 4 in which x is the molar weight of the surfactant i [39]:

$$Cc = \Sigma\, x_i.Cc_i \quad (4)$$

4.4 Results and Discussions

4.4.1 Colloidal Behavior and Precipitation of Asphaltene in Oil

Colloidal instability index (CII) is 4.34 for Gilsonite, indicating very unstable conditions for the asphaltenes. When Gilsonite is added to mineral oil, mainly composed of saturates, CII will only increase, signifying the deposition severity of the asphaltenes in the mineral oil. A visual assessment of this deposition was performed by adding 1% wt/v Gilsonite to the mineral oil, and severe deposition of asphaltene was observed in the sample after only 5 minutes. **Figure 4.4** displays the asphaltene deposits on the bottom surface of the beaker.

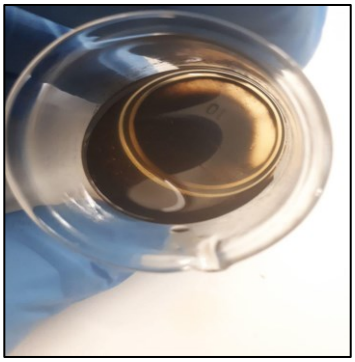

Figure 4.4: Asphaltene deposition in the mineral oil

The size of the aggregates in the mineral oil was determined for four levels of Gilsonite concentration according to the testing plan presented in **Table 4.3**. Experimental values are the average of three samples. **Figure 4.5** displays the variation in the representative sizes with Gilsonite concentration in mineral oil, and **Figure 4.6** shows both number-based and volumetric-based size distributions. Minimum Feret diameter was used to calculate the representative sizes following a comparison study, which showed minimum Feret diameter and EQPC are fairly similar in the description of the aggregate sizes, especially for the aggregate sizes larger than 2 micrometers, with the maximum 10% variability for the aggregates smaller than 0.5 micrometers.

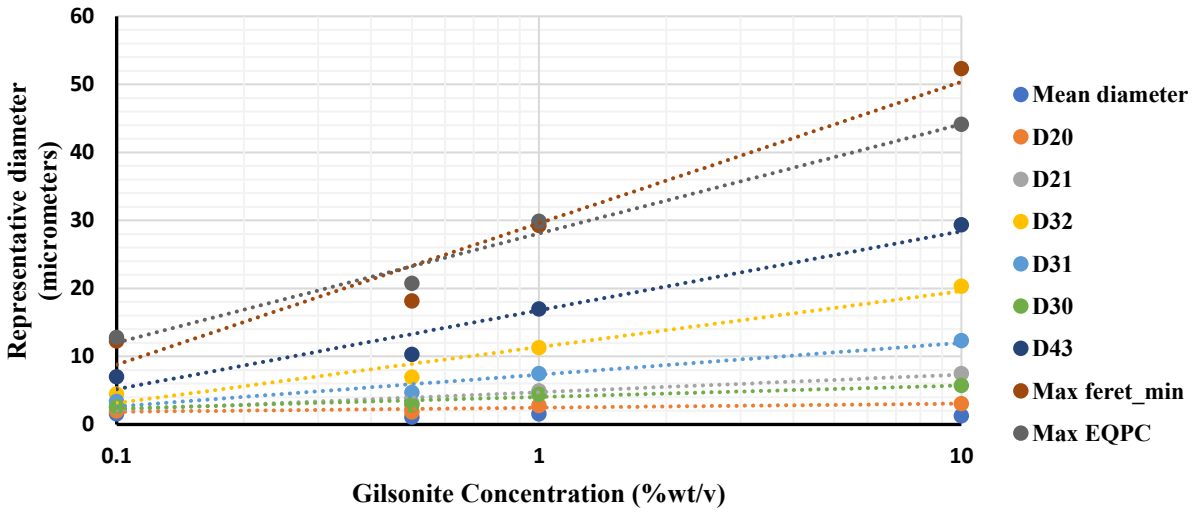

Figure 4.5: Representative sizes of the asphaltene aggregates for different concentrations of Gilsonite in mineral oil

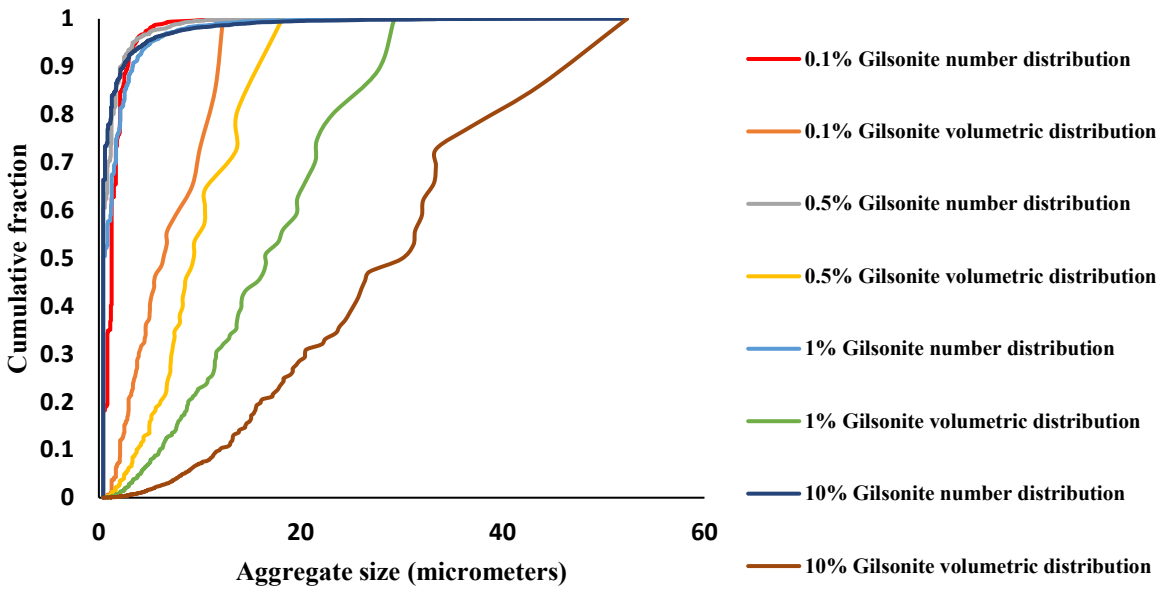

Figure 4.6: Number and volumetric-based size distribution of the asphaltene aggregates for different concentrations of the Gilsonite in mineral oil

According to the results presented in **Figure 4.5** and **Figure 4.6**, number-based representative sizes such as the arithmetic mean diameter of the aggregates and number-based size distribution do not exhibit meaningful differences with Gilsonite concentration. However, area and volumetric representative sizes and volumetric size distribution of the aggregates increase with the added Gilsonite dosage in the mineral oil. This implies a higher fraction of the sample's actual volume is occupied by larger aggregates, while the frequency fraction of the aggregates does not change substantially. The following equation form can describe the mathematical trend of increase in aerial and volumetric representative sizes:

$$Dpq = p_1 \ln(C) + p_2 \quad (7)$$

where Dpq is the representative size in micrometers, C is the concentration of the Gilsonite (~asphaltene) in the oil phase (%wt/v), and $P_{1,2}$ are calibration constants that are functions of the aggregate size.

Literature supports these results and indicates the aggregates' size increases with higher asphaltene concentration in the system [26]. **Figure 4.7** displays the micrographs of the mineral oil samples containing different Gilsonite concentrations that explicitly show that the maximum size and number of the aggregates increase with more asphaltene in the mineral oil. However, the fraction of smaller-sized aggregates increases simultaneously, suggesting only small differences in the frequency-based cumulative fraction of the aggregate size distribution are expected. This fraction corresponds to the new size range forming due to a higher concentration of the asphaltene in the mineral oil. Added Gilssonite concentration corresponds to an increase in the precipitation level in the mineral oil due to insolubility of asphaltene in saturates which in turn results in clumping of the asphaltene aggregates and formation of larger flocs [40].

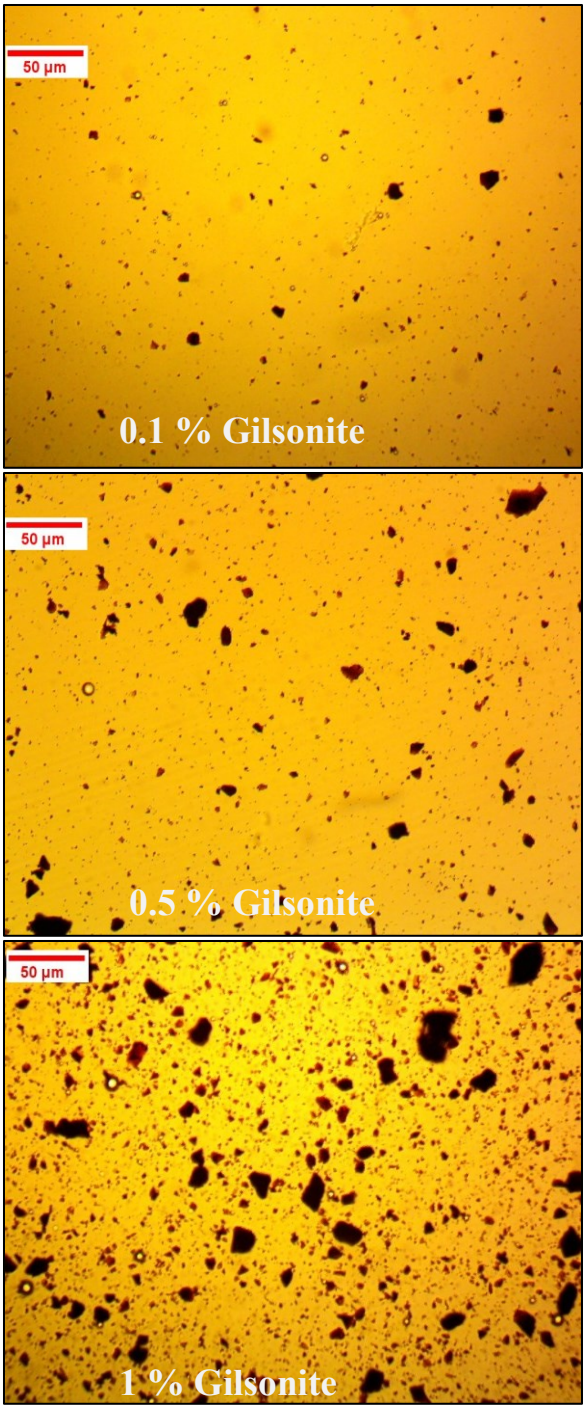

Figure 4.7: Micrography of the mineral oil with different concentrations of Gilsonite

In the next phase, Gilsonite was added in two concentrations to the blended oil containing mineral oil and three volumetric fractions of Toluene. This was done under the testing matrix shown in **Table 4.3** to perform a full factorial experimental design. The number of aggregates and changes in the aggregates' size were determined for each oil blend sample. The total number of aggregates detected by microscopy is a measure of asphaltene solubility or precipitation rate. A lower number of aggregates counted corresponds to less asphaltene precipitation in the oil sample. The

hypothesis is that less precipitation is expected when the fraction of Toluene increases in the oil blend because of the high asphaltene solubility in the aromatics.

Figure 4.8 shows the number of aggregates detected in the micrography of oil blend samples in a Gilsonite concentration range. The largest number of detected asphaltene aggregates is observed in the mineral oil with Gilsonite's highest concentration. As expected, adding Toluene to the oil blend resulted in a decrease in the number of detected precipitates due to asphaltene's solubility in the aromatics. However, the rate of change in the number of precipitates is sharper when the concentration of asphaltene is higher in the oil blend up to a point where the fraction of Toluene is high enough that overcomes the effect of asphaltene concentration in the oil blend (50% Toluene in the oil blend). At that critical point, the precipitation intensity is very small and independent from the concentration of asphaltene in the system (for the range of asphaltene concentration examined here).

Figure 4.9 displays the change in the aggregates' size for the oil blends with 1 %wt/v Gilsonite. Again, the trend shows that the aggregates' mean size does not change, indicating an equal decrease in the size of all the aggregates. This interpretation can be verified by the witnessed decreasing trend of Sauter diameter and De Broukere diameter with a larger fraction of Toluene in the oil blend. These representative diameters suggest that the aggregates' volume is decreasing. For the mean aggregate size to remain somewhat constant, such a decrease should apply to all aggregates in the oil sample.

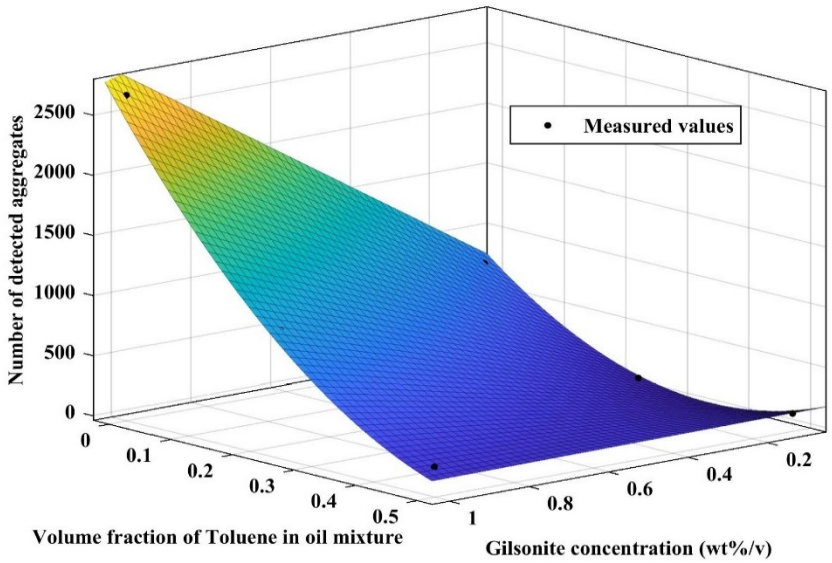

Figure 4.8: Number of asphaltene aggregates detected in the micrograph for a range of Gilsonite concentration and Toluene fraction in the oil blend

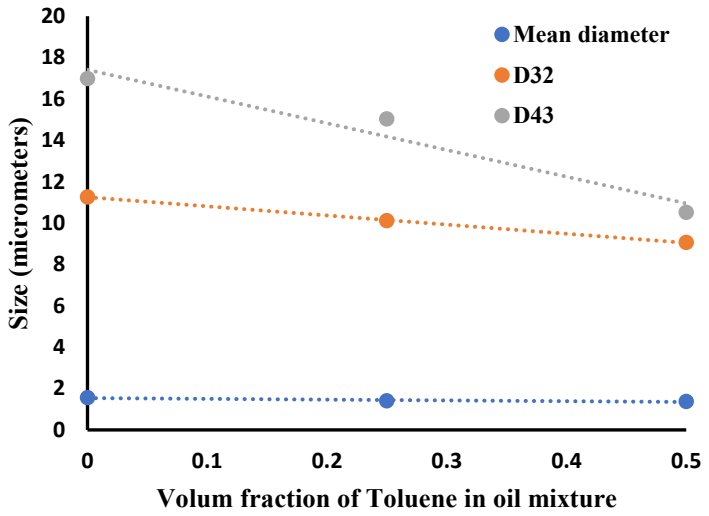

Figure 4.9: Change in the size of the aggregates with the addition of Toluene in different fraction to the oil blend containing mineral oil and Toluene

To summarize, the precipitation severity is the highest in the mineral oil with greater concentrations of Gilsonite. Adding Toluene to the oil causes more solubility of the asphaltenes and less precipitation. Precipitation severity is a function of oil composition and concentration of asphaltene. When the volume fraction of Toluene is large enough, the effect of oil composition dominates the asphaltene concentration parameter. In other words, the solubility of asphaltene in the fluid mixture increases. Larger aggregates form when more Gilsonite is added to the system, and smaller flocs form when Toluene fraction increases in the blended oil. Asphaltene precipitates clump together, forming larger particles (flocs). These larger asphaltene flocs tend to deposit and adsorb on the surfaces [19].

4.4.2 Base W/O Emulsion

A base W/O emulsion composed of 5 %wt/v Span 83 was prepared at ambient temperature and pressure. The emulsion samples were prepared with 1000 rpm and 1 min mixing time homogenization settings. The effects of phase ratio and salinity on the kinetic stability and droplet size of the emulsion samples were investigated.

Figure 4.10 illustrates the effect of salinity (NaCl) and phase ratio on emulsions' mean droplet diameter. The data points are the average of three experimental values for each case. A statistically significant interaction between salinity, water content, and the mean droplet size is visible in **Figure 4.10**. The mean droplet diameter is magnified with salinity in 10% emulsion, whereas the change in the droplet diameter with water salinity is statistically insignificant in the 40% emulsion.

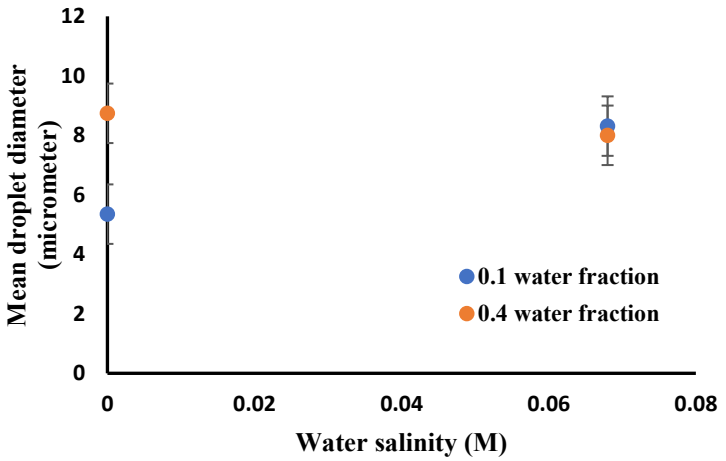

Figure 4.10: Effect of NaCl and phase ratio on the mean droplet diameter (Reproduced with permission from[41])

The increase in the droplet size for the dilute emulsion is most likely a result of the salting-out phenomenon, which leads to partitioning of the surfactant towards the oil phase and misorientation of the surfactant molecules. Salting-out is the reduction in the solubility of the aqueous phase when high concentrations of electrolyte in the water phase leads to the more frequent interactions between the solvent molecules and salt ions, leaving fewer solvent molecules available for interaction with the solute molecules (in this case surfactant molecules) [41].

The viscosity of the W/O emulsion increases in higher water content, which in turn reduces the rate of approach among the droplets. This can prevent the coalescence between the water droplets in the emulsion, causing further stability and preventing the emulsion droplets' enlargement. Kinetic stability results and the viscosity values demonstrated in **Figure 4.11** validates this hypothesis by showing that the concentrated emulsions are tighter than the dilute emulsion. Additionally, larger water droplets in the concentrated emulsions have a smaller interfacial area which requires a reduced amount of surfactant concentration for interfacial film coverage. This factor would also positively affect the kinetic stability of emulsions as observed in the case of concentrated emulsion which resists droplets coalescence in the presence of an electrolyte.

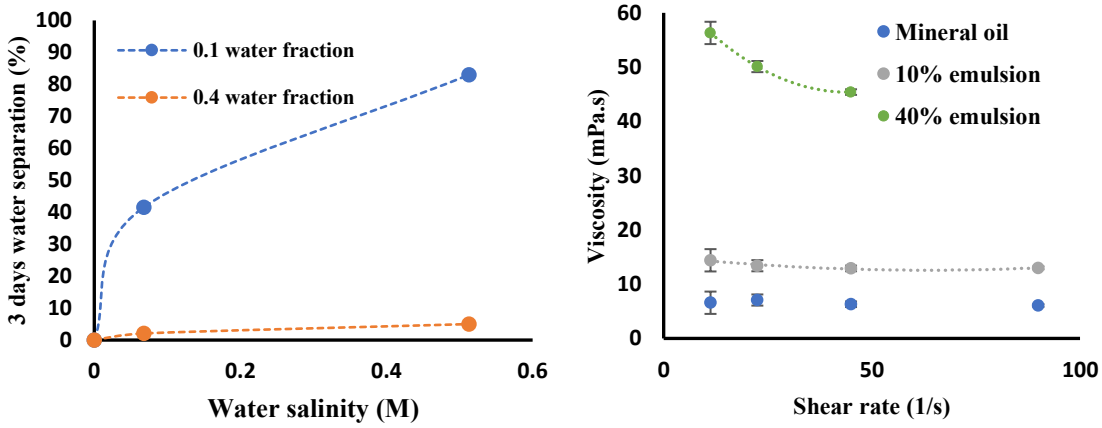

Figure 4.11: Left: Effect of water content and salinity on water separation in emulsion samples; Right: Change in the viscosity of emulsion with the phase ratio (Reproduced with permission from[41])

Statistical analysis of the results verifies the strong interaction between the mean droplet diameter, salinity, and phase ratio. P-value is smaller than 0.05 in the two-way ANOVA test that indicates the interaction effect is statistically significant. P-Value is 0.02 in the two-tail t-test in 10% emulsion between the mean droplet diameter for different salinity levels indicating a significant change in the mean droplet diameter with added salt concentration. However, a P-value of 0.16 in the two-tail t-test means the difference in the mean droplet diameter of the droplets with different levels of NaCl concentration in the 40% emulsion is statistically insignificant. In other words, the phase ratio's effect is dominant in the 40% emulsion, overriding the effect of salt in the system.

Finally, the mean droplet diameter increased with larger water content in the emulsions prepared without NaCl in the water phase. The difference is statistically significant and is caused by the elevation of viscosity in the 40% emulsion that requires higher mixing energy to form smaller droplets.

4.4.3 Model Emulsions

As discussed in Section 2.1, negative HLD values for the emulsions prepared at room temperature, with mineral oil as the continuous phase and Gilsonite as the stabilizer, indicate unlikeliness of forming the W/O emulsion. This was examined by preparing the emulsions in different Gilsonite concentrations (0.1 %wt/v and 1%wt/v). Emulsions exhibited immediate water separation after homogenization, which supports the premise presented. Therefore, a blend of surfactants was used to prepare model emulsion samples that yield a higher Cc value, guaranteeing the formation of W/O emulsion.

5% Span 83 was mixed with different dosages of Gilsonite, and the kinetic stability of the emulsion samples was put to the test. Moreover, the effect of oil composition on the stability of emulsions was assessed. **Figure 4.12** displays the emulsion sample prepared with Gilsonite only and the emulsion sample prepared with a blend of surfactants. Water phase separation is apparent in the bottom part of the samples prepared with Gilsonite in **Figure 4.12**. In contrast, the emulsions with a blend of surfactants show stability in terms of water phase separation upon preparation.

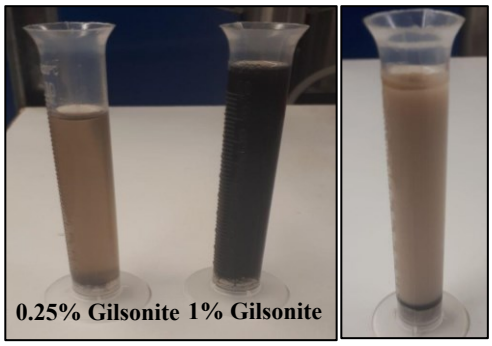

Figure 4.12: Left: Emulsions prepared with Gilsonite; Right: emulsion prepared with a blend of surfactants (0.25% Gilsonite and 5% Span 83)

Figure 4.11 implies that the base emulsion (5% Span 83) is stable during the three-day storage time when no electrolyte is present in the system. Water phase separation occurs when NaCl is added to the water and is magnified with a higher electrolyte concentration. To examine the kinetic

stability of the emulsion samples prepared with Gilsonite and Span 83 surfactant blend, the salt's highest concentration in the water phase (0.51 M) from the previous round of experiments on the base emulsion was selected. The dilute emulsion shows intense water separation in this salinity level, as shown in **Figure 4.11**.

Model Emulsion with Mineral Oil

Bottle tests were performed for the 10% emulsions samples according to the testing matrix presented in **Table 4.4**. Samples were examined in the short term (2 hours) and longer storage time (3-days), and the separation of water from the emulsion with time was monitored. These experiments were initially carried out for the emulsions prepared with mineral oil, with results presented in **Figure 4.13**.

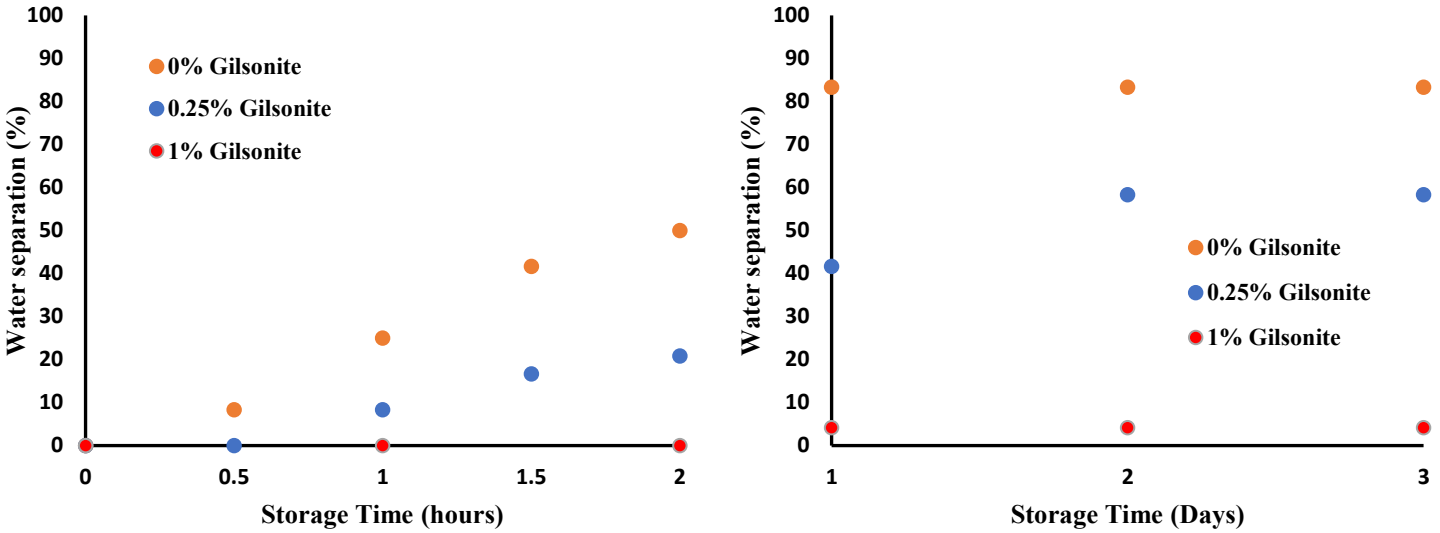

Figure 4.13: Water phase separation in model emulsions with mineral oil as the primary phase

According to the results depicted in **Figure 4.13**, emulsions with no Gilsonite (5% Span 83) demonstrated the highest water phase separation. The kinetic stability increased with the addition of Gilsonite to the emulsion and was improved for higher concentrations of Gilsonite. It can be concluded that the Gilsonite contributes to the kinetic stability of emulsions. Asphaltene aggregates cover the droplets' interfacial area during homogenization, establishing rigid films around them and stabilizing the emulsion through steric hindrance. **Figure 4.14** shows the micrography of the samples with/without Gilsonite and 0.51 M water salinity.

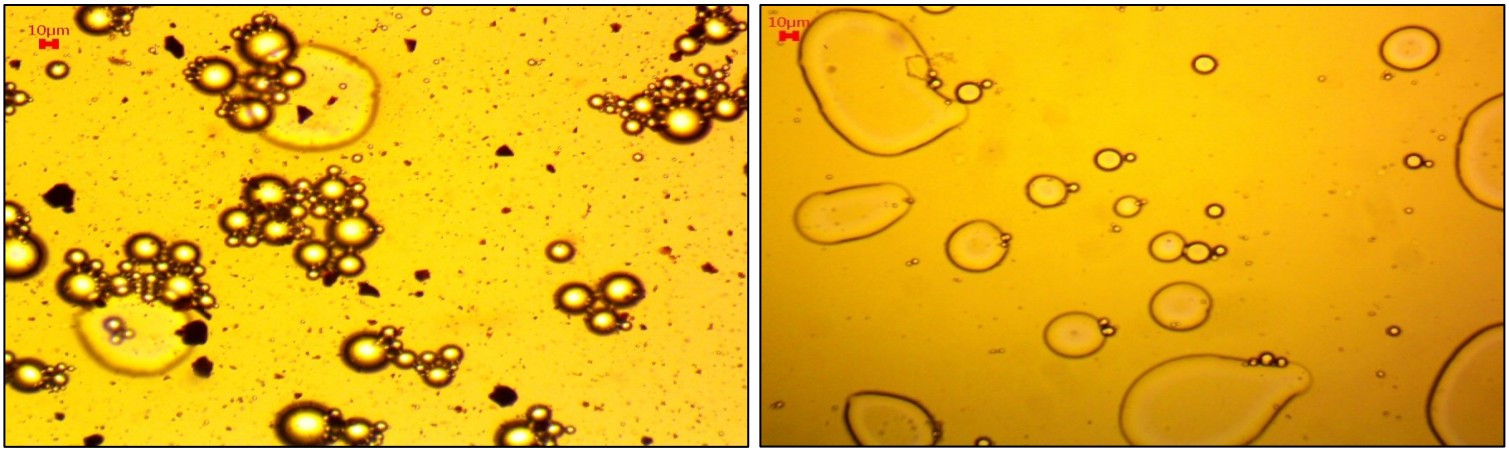

Figure 4.14: Micrgraphs of emulsion samples: 0% Gilsonite and 5% Span 83 (Right) and 0.25% Gilsonite and 5% Span 83 (Left) in emulsions prepared with 0.51 M NaCl

Micrographs show that emulsion without Gilsonite (5% Span 83) displays signs of droplet deformation and coalescence upon collision immediately after preparation. These are recognized mechanisms of instability in emulsions. Salting-out is responsible for the partitioning of the surfactant toward the oil phase and weak coverage of the surfactant molecules' interfacial films. On the other hand, emulsions with a blend of Gilsonite and Span 83 were more stable.

Although flocculation is detected in the emulsion samples because of the strong Van der Waals forces caused by electrolytes' presence in the system, droplets resist coalescence. This is due to the formation of rigid interfacial films with asphaltene aggregates contributing to this phenomenon. Micrographs exhibit the difference in the appearance of the interfacial films of base emulsion and model emulsion with Gilsonite. The droplets are protected by thicker and darker surfactant(s)-covered films. This is in agreement with the results in previous studies where the formation of rigid and viscoelastic interfacial films by asphaltene aggregates is reported [27-29,40]. Nano and micro aggregates cover the droplets during homogenization and prevent the coalescence of the droplets upon flocculation. However, larger asphaltene aggregates are mostly dispersed in the oil phase and are unlikely to stabilize the emulsion. Further notes on the importance of the aggregates' size in stabilizing emulsions are included in section 3.3.2.

Finally, a sensitivity analysis was performed on the effect of Gilsonite concentration on the droplets' size and viscosity of the emulsion. **Figure 4.15** illustrates the change in the mean droplet diameter of the 10% emulsion samples with 5% Span 83 and a range of Gilsonite concentration. The mean droplet diameter increased linearly with the addition of Gilsonite in the emulsion. This is presumably due to the elevated viscosity of the emulsion due to added Gilsonite, which is a well-known viscosifying agent [6].

The effect of Gilsonite on the emulsion's viscosity was characterized for 10% emulsion with 0.1 %wt/v Gilsonite and 5 %wt/v Span 83 and compared to the base emulsion. It should be noted that the attachment of asphaltene aggregates on the cone results in erroneous readings of viscosity. It is generally challenging to measure the viscosity of fluids containing asphaltene, regardless of the type of the viscometer [42]. This is especially the case when higher concentrations of Gilsonite are

added to the fluid. Thus, the emulsion's viscosity was tested only for 0.1 %wt/v Gilsonite, and the results are displayed in **Figure 4.16**.

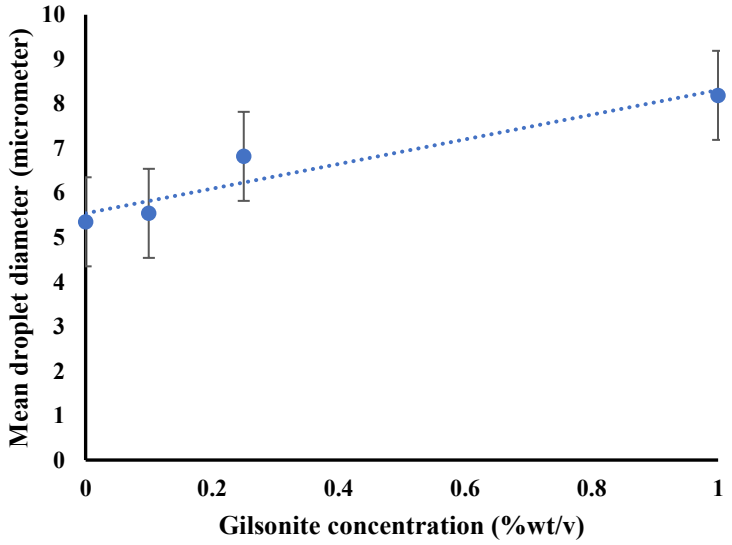

Figure 4.15: Change in the droplet size with Gilsonite concentration

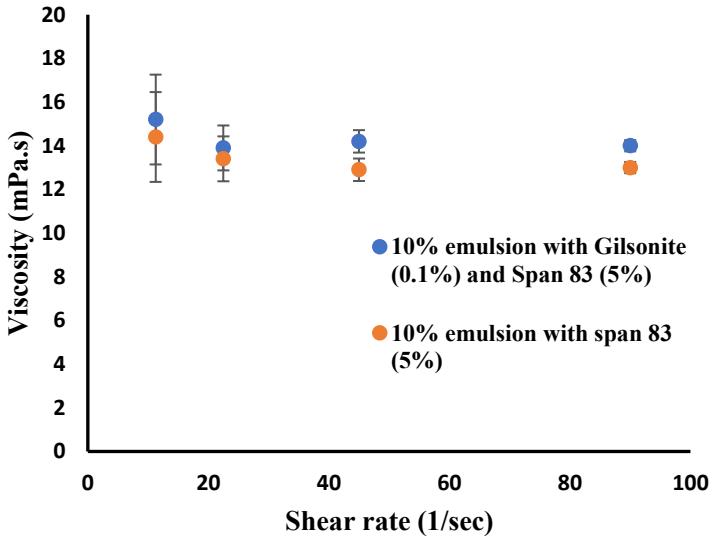

Figure 4.16: Viscosity of the 10% emulsion with and without Gilsonite

Results presented in **Figure 4.16** prove the viscosifying effect of Gilsonite in the fluid mixture. The elevated viscosity influences the size of the droplets and stability of the emulsions, as shown in **Figure 4.13** and **Figure 4.15**. The emulsion's higher viscosity is thought to be a stabilizing factor by reducing the rate of approach among droplets [43]. Therefore, Gilsonite enhances emulsions' stability by increasing the viscosity and steric hindrance provided by small asphaltene aggregates covering the droplets' interfacial film.

Model Emulsion with the Oil Blend

The testing matrix shown in **Table 4.4** was followed with 2 levels of Gilsonite concentration and 3 levels of Toluene to mineral oil volumetric ratios to investigate the effects of oil composition and asphaltene concentration on the kinetic stability of the model emulsions. **Figure 4.17** displays the 3D plot of 3-day water separation in 10% emulsions. **Figure 4.18** displays the short term (2 hours) and a longer storage time (3 days) water phase separation of the model emulsions in different oil blends and 0.25 %wt/v Gilsonite. **Figure 4.19** demonstrates similar test results for model emulsions with 1% wt/v Gilsonite.

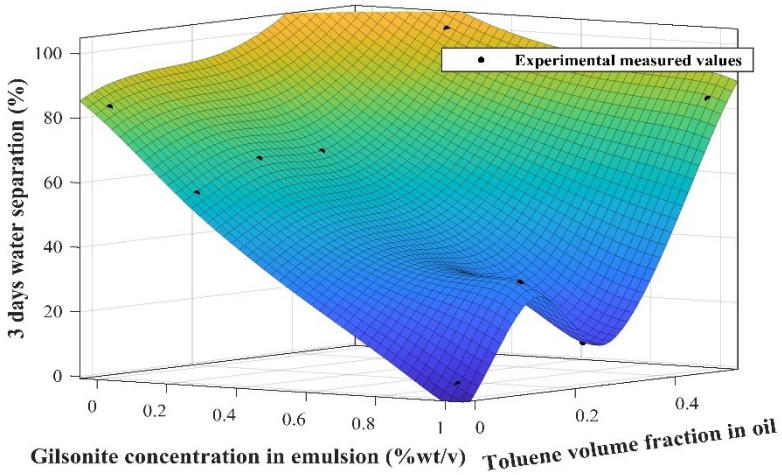

Figure 4.17: Water phase separation (3 days storage time) for the blends of oil and a range of Gilsonite concentration

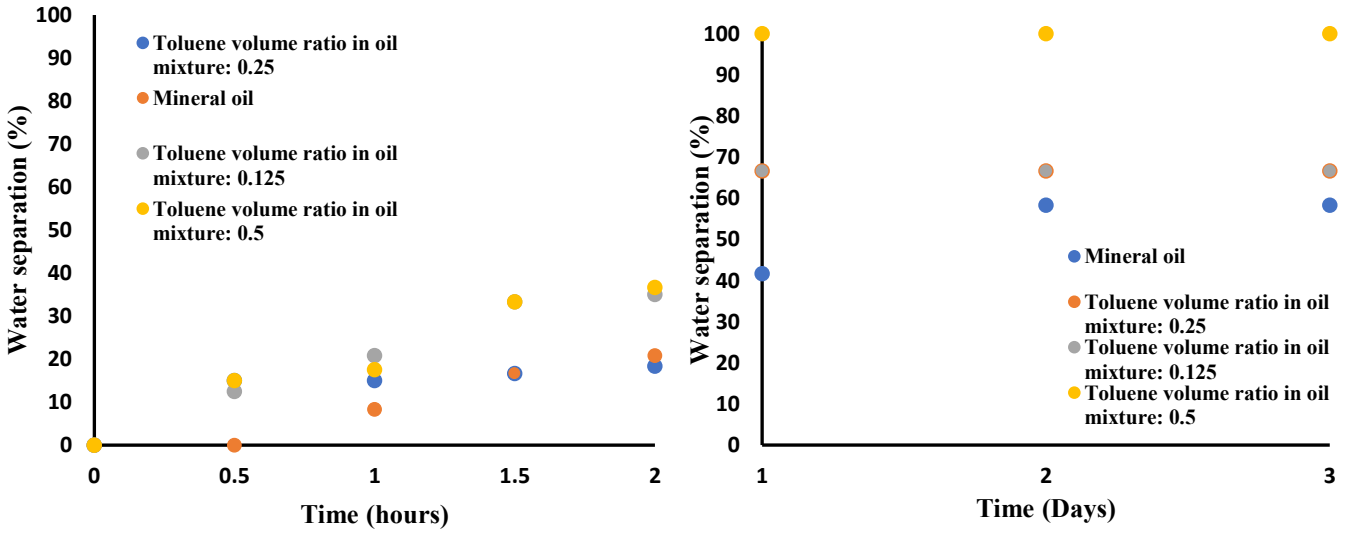

Figure 4.18: Water separation in emulsions with different oil blends and 0.25 %wt/v Gilsonite

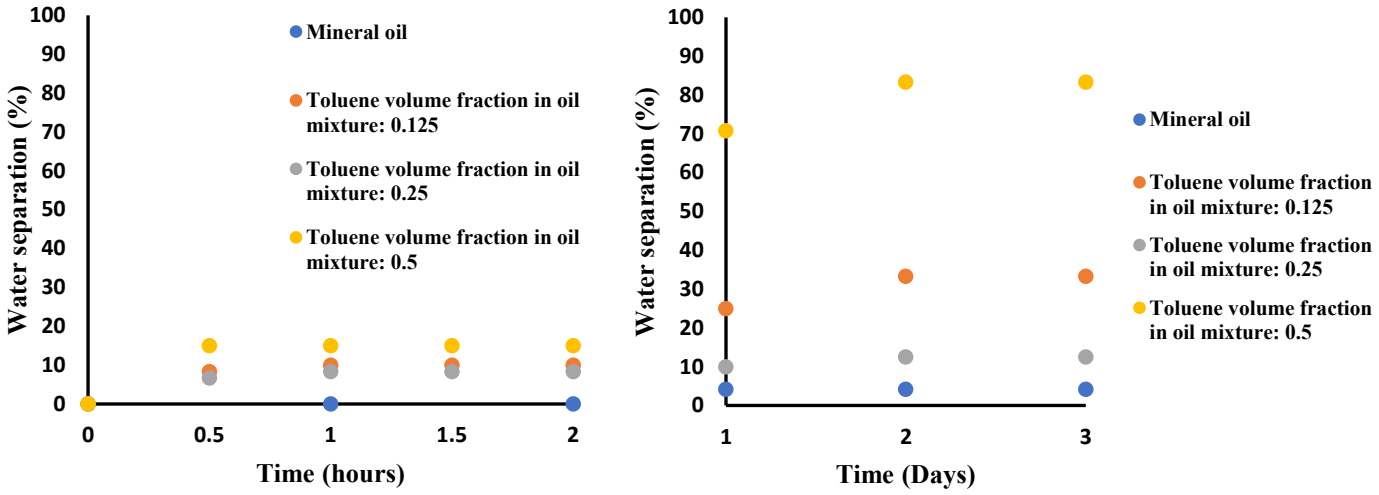

Figure 4.19: Water separation in emulsions with different oil blends and 1% wt/v Gilsonite

As expected, emulsions prepared with mineral oil exhibit the least water phase separation, representing the most stable emulsions. Literature similarly reports the higher stability of the emulsions when precipitation increases [26]. The highest level of precipitation was observed in mineral oil, as shown in **Figure 4.8**. The least stable emulsion was the one prepared with 50% Toluene in the oil mixture. In a high fraction of Toluene in the oil blend, the intensity of precipitation is minimized, as shown in **Figure 4.8**, due to the high solubility of asphaltene in aromatics. Hence, asphaltene precipitation has a crucial role in promoting the stability of emulsions.

Figure 4.17 shows that emulsions' stability in 12.5% and 25% Toluene in oil mixture was quite similar in emulsions with 0.25% wt/v Gilsonite. **Figure 4.19** indicates that emulsion with 25% Toluene in oil mixture is even more stable than the emulsion with 12.5% Toluene and 1% Gilsonite, which contradicts the common assumption that higher precipitation always parallels the formation of a more stable emulsion [23-25]. **Figure 4.8** shows that the higher the Toluene, the less the asphaltene precipitation, and the expectation was to witness higher emulsion stability with lower Toluene in the oil mixture. The experimental results of the stability tests refute this hypothesis.

A colloidal approach was adopted to investigate the role of asphaltene aggregates in stabilizing emulsions. In this perspective, asphaltene aggregates are considered colloidal particles. They are treated as solid particles that cover the droplets' interfacial area and prevent the coalescence of the droplets through steric hindrance. For this to be true, the size of the solid particles must be smaller than the droplets to contribute to emulsion stability, as is the case for a Pickering emulsion [44].

In this approach, both the aggregate and emulsion droplet sizes are equally important. Moreover, the intensity of precipitation and the number of aggregates are of the utmost importance for emulsions stability. The reason the least stable emulsion has the highest fraction of Toluene and the least concentration of Gilsonite, as depicted in **Figure 4.17**, can be associated with less precipitation in such conditions. **Figure 4.8** shows the number of aggregates detected in the oil blends is considerably high for both 12.5% and 25% Toluene especially when Gilsonite

concentration is high (1% wt/v). Besides, there is no significant difference in the number of aggregates between 12.5% and 25% Toluene when Gilsonite concentration is 0.25%. This means that many aggregates can contribute to the droplets' stability in the case of 1% Gilsonite, even for 25% Toluene in oil mixture. Also, the number of aggregates that potentially cover the droplet interfacial area for 25% Toluene is fairly close to the 12.5% Toluene when 0.25% Gilsonite is present in the system. The latter can describe equal stability observed in 12.5% and 25% Toluene emulsion samples with 0.25% Gilsonite. However, the number of aggregates analysis (asphaltene precipitation intensity) cannot justify emulsion's superior stability with 25% Toluene compared to 12.5% Toluene when Gilsonite concentration is 1% wt/v.

Figure 4.9 displays the size of the asphaltene aggregates decrease with the addition of Toluene to the oil blend. In emulsion with 1% wt/v Gilsonite, the mean aggregate size to mean droplet size ratio of the emulsion with 25% Toluene in oil mixture is 0.06 while this value is 0.14 for the 12.5 % Toluene, showing 133% variation between the two emulsions. The smaller this value, the better the potential for the asphaltene aggregates to cover the droplets. Such conditions favor the stability of emulsions with 25% Toluene compared to the 12.5% Toluene.

The mean size of the aggregates/droplets may not be the optimum representative size to describe emulsions' stability. Volumetric-based representative sizes describe the physics more accurately by depicting the sample's actual volume occupied by the particles of a specific size. Therefore, the particle size distributions (aggregates and emulsion droplets) are illustrated in **Figure 4.20** to understand better where the aggregates and droplets' size lie concerning one another.

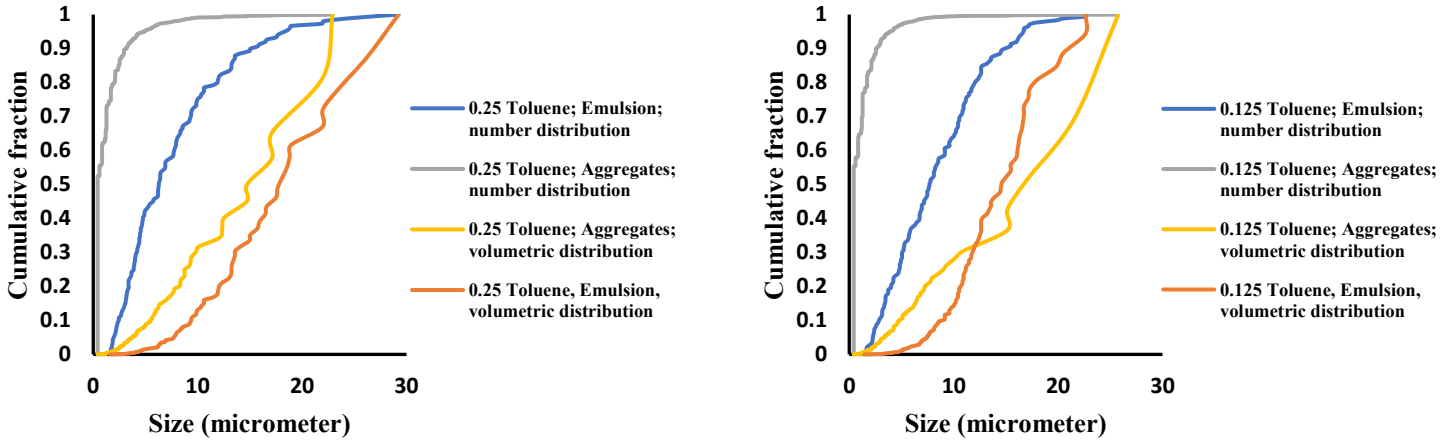

Figure 4.20: Aggregate and droplet size distribution in 10% emulsions with 1% Gilsonite and Left) 25% Toluene; Right) 12.5% Toluene

The particle size distributions shown in **Figure 4.20** indicate the aggregates in emulsion with 25% Toluene are generally sorted in a fashion that the smaller asphaltene aggregates could potentially cover all droplets. However, this is not the case for 12.5% Toluene where a significant portion of aggregates is larger than the droplets, which cannot take part in stabilizing the emulsions. This is reflected in the stability experiments and justifies the improved kinetic stability of the 10% emulsion with 1% wt/v Gilsonite and 25% Toluene compared to the 12.5% Toluene.

Finally, the stability of the emulsion can also be influenced by interfacial tension [2]. However, the kinetic stability of W/O emulsions prepared with non-ionic surfactants and even with

asphaltene is thought to be mainly driven by the steric hindrance and through mechanical stability provided by the surfactants [19]. For completeness, the surface tension of different liquid mixtures was calculated in capillary rise experiments and the contact angle was determined using optical microscopy. Contact angle values obtained in surface tension experiments (liquid-air-capillary tube systems) exhibit no significant difference for the mineral oil+Span and mineral oil+Span+Gilsonite. This was also the case for the surface tension of these two liquids.

IFT between the mineral oil containing Span 83 and water at CMC is reported 13.18 dynes/cm elsewhere [30]. There was an insignificant change in the contact angle of the mineral oil containing Gilsonite and Span 83 compared to the mineral oil+Span 83 and one may conclude the change in interfacial tension is not considerable. However, this requires further examination and measurement of interfacial tension for the system that includes both liquids for a more realistic assessment. **Figure 4.21** and **Figure 4.22** illustrate the contact angles and measured surface tension for different fluids.

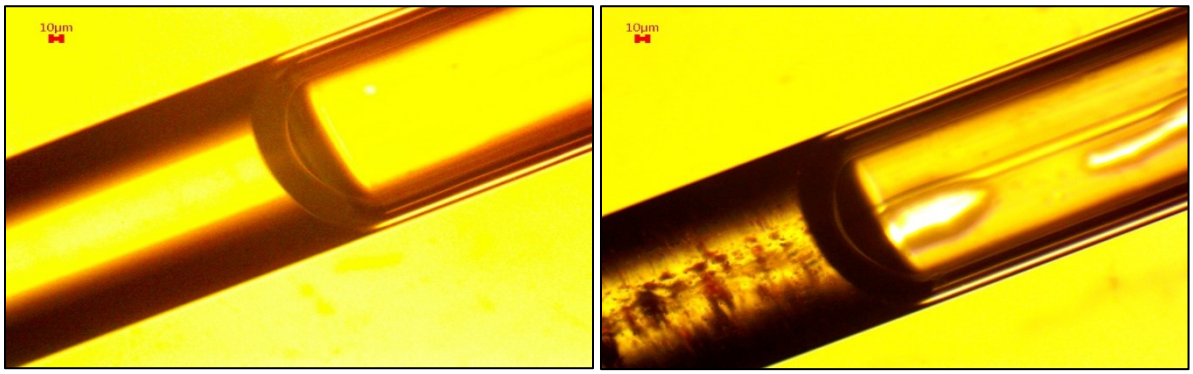

Figure 4.21: Contact angle between mineral oil+Span 83-air (Left) and mineral oil+Span 83+Gilsonite-air (Right) showing the same value of approximately 30°.

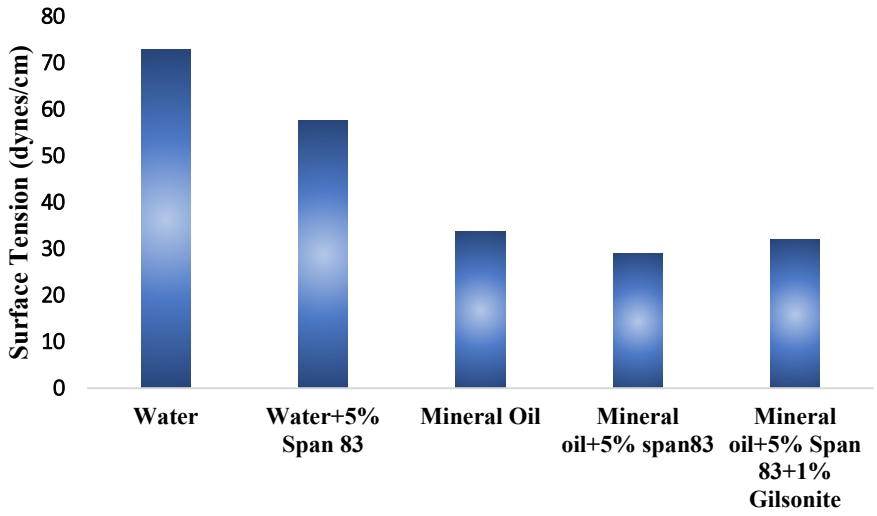

Figure 4.22: Measured surface tension for different liquids

The Effect of Phase Ratio

This trend was reversed for the 40% emulsion with 1% wt/v Gilsonite. The experiments show significantly higher water separation in emulsion with 25% Toluene than 12.5% Toluene in the oil blend when the water content was increased to 40%. Moreover, emulsion stability was improved for the 40% emulsion with 12.5% Toluene than the 10% emulsion containing the same amount of Toluene in the oil blend. **Figure 4.23** displays the water separation for emulsions with 2 levels of water content. It should be noted that the concentration of Gilsonite was kept constant (1% wt/v) with reference to the oil phase, and the same is true for the salt in the water phase (0.51 M). **Figure 4.24** illustrates the mean droplet diameter variation with water content and Toluene fraction in the oil blend.

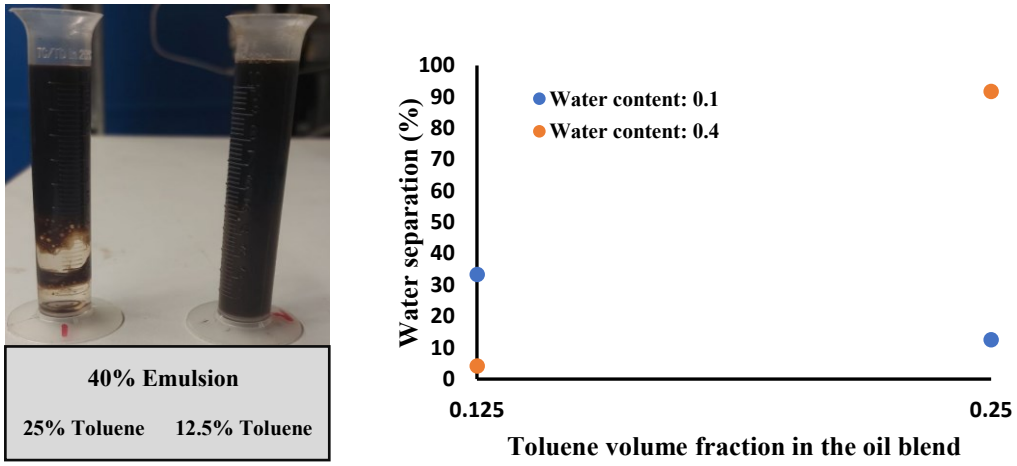

Figure 4.23: Water separation in emulsion with water content and Toluene fraction in the oil blend

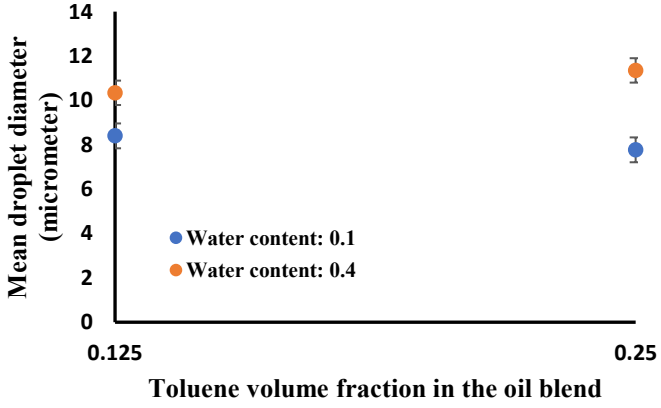

Figure 4.24: Mean droplet diameter variation in emulsions with Toluene fraction in the oil blend

As previously mentioned, two main conditions must be met for the asphaltene to stabilize the emulsions, including the adequate intensity of asphaltene precipitation and smaller aggregate size in relation to the diameter of internal phase droplets. According to **Figure 4.24**, the mean droplet diameter of the emulsion increases in higher water contents due to concentrated emulsions' elevated viscosity. Although the second condition is satisfied still, 40% emulsion with 25% Toluene is extremely unstable compared to 10% emulsion of the same Toluene content in oil.

An increase in the water content of emulsion is associated with more frequency of the number of droplets, as observed in the micrography. This condition amplifies the interfacial area that requires more asphaltene aggregates for interfacial film coverage of the droplets. However, Gilsonite concentration in oil remains unchanged for 40% emulsion with 25% Toluene. The precipitation intensity is insufficient to meet the additional requirement of asphaltene precipitates for the droplets' coverage. Hence, the first condition (intensity of asphaltene precipitation) is not satisfied, resulting in a large water separation.

Asphaltene precipitation is high enough for promoting the stability of the 40% emulsion with 12.5% Toluene. The higher stability of the 40% emulsion than 10% emulsion with similar Toluene content in the oil blend can be explained in two ways. Firstly, the droplets' size is larger in 40% emulsion, and the ratio of mean aggregate size to the mean emulsion droplet diameter is even smaller than 10% emulsion (0.11 in 40% emulsion and 0.14 in 10% emulsion). Additionally, the stability of an emulsion can be augmented by higher viscosity, which reduces the rate of approach among droplets. It was shown in **Figure 4.11** that the base emulsions with higher water content exhibit higher viscosity. It can be concluded that a combination of higher viscosity and smaller aggregate to droplet size ratio provides the means of higher kinetic stability in 40% emulsions with 12.5% Toluene compared to the 10% emulsion of the same oil blend.

To summarize, testing results affirm that increasing the Gilsonite concentration (asphaltene concentration) enhances emulsion stability in all the oil blend samples examined. However, the effect is much more significant in mineral oil, resulting in the most stable emulsions. The least stable emulsions are the ones prepared with very high fractions of Toluene. Nonetheless, the addition of Toluene to the oil blend (mineral oil and Toluene) does not necessarily end in the formation of less stable emulsions.

Incorporating both colloidal and thermodynamical views of asphaltene precipitation indicates high precipitation accompanied by a smaller size of the asphaltene aggregates than the emulsion droplets' size yields higher kinetic stability emulsions. In the case of 10% emulsions with 25% Toluene in oil blend, more resistance to the water separation was recorded because these conditions were met. However, this was not the case for emulsion with 12.5% Toluene due to the significant portion of the asphaltene aggregates larger than the droplets.

The higher water phase ratio increased the emulsion droplets' size, emulsion viscosity, and the frequency of droplets. The lack of high asphaltene precipitation destabilized the 40% emulsion with 25% Toluene. In contrast, the combination of small aggregate to droplet size ratio, the elevated viscosity, and high asphaltene precipitation resulted in excellent stability in 40% emulsion with 12.5% Toluene. These results affirm that both conditions of asphaltene precipitation and smaller aggregates than the droplets must be satisfied to achieve stable emulsions.

The findings of this study have important implications for a better understanding of the crude oil emulsion features. Solvents (n-alkanes) used in the petroleum industry for in-situ upgrading of bitumen could lead to the intense precipitation of asphaltenes and the formation of tight W/O emulsions [45]. Although bitumen upgrading is desirable, the formation of tight emulsions could be costly and requires energy-expensive demulsification processes. It might be beneficial to re-

formulate solvents so that less stable emulsions are produced while sufficient precipitation of asphaltenes from the heavy crudes guarantees an improved recovery.

Conclusions

This paper introduced Gilsonite, mainly composed of asphaltenes, as a surfactant, and investigated the role of Gilsonite in stabilizing W/O model emulsion. Moreover, the effect of Gilsonite concentration and oil composition on the asphaltene precipitation was examined. It was found that the most severe precipitation occurs in the mineral oil with higher concentrations of Gilsonite. The addition of Toluene (aromatics) in the oil blend decreased the precipitation intensity. Also, the size of the asphaltene aggregates decreased by the addition of Toluene to the oil blend. Results indicate that most kinetically stable emulsions are prepared with mineral oil and more asphaltene in the system. Asphaltene precipitates/aggregates stabilize the emulsions through steric hindrance and form rigid interfacial layers around the droplets. The least stable emulsion contains a large fraction of Toluene (50%) in the oil blend. The 10% emulsion containing 25% Toluene in the oil blend exhibited higher stability than the emulsion with 12.5% Toluene. It was observed that the high asphaltene precipitation supported by the smaller aggregates compared to the droplet size causes this improvement in kinetic stability. These results contradict the consensus (thermodynamical models) that simply increasing the aromaticity minimizes the emulsion stability. Integrating colloidal and thermodynamical perspectives of the asphaltene precipitation can explain the results presented. Finally, increasing the water content in emulsion resulted in a change in the droplets' size and the frequency of droplets that require more asphaltene precipitation for stability. Therefore, the 40% emulsion with 12.5% Toluene was more stable than the emulsion with 25% Toluene, mainly due to the higher asphaltene precipitation.

Nomenclature

Cc: Characteristic curvature
CII: Colloidal instability index
CMC: Critical micelle concentration
D10: Mean droplet diameter (micrometer)
D32: Sauter diameter (micrometer)
D43: De Broukere diameter (micrometer)
EACN: Equivalent alkane carbon number
HLB: Hydrophilic lipophilic balance
HLD: Hydrophilic lipophilic deviation
M: Molarity (mol/lit)
ppm: Parts per million
rpm: Rounds per minute
T: Temperature (°C)
W: mass fraction (%)

References

[1] Schramm, L.L., 1992. Fundamentals and applications in the petroleum Industry. Adv. Chem, 231, pp.3-24.

[2] Leal-Calderon, F., Schmitt, V. and Bibette, J., 2007. Emulsion science: basic principles. Springer Science & Business Media.

[3] Sjoblom, J., 2001. Encyclopedic handbook of emulsion technology. CRC press.

[4] Colucci, G., Santamaria-Echart, A., Silva, S.C., Fernandes, I.P., Sipoli, C.C. and Barreiro, M.F., 2020. Development of Water-in-Oil Emulsions as Delivery Vehicles and Testing with a Natural Antimicrobial Extract. Molecules, 25(9), p.2105.

[5] Nciri, N., Song, S., Kim, N. and Cho, N., 2014. Chemical characterization of gilsonite bitumen. Journal of Petroleum & Environmental Biotechnology, 5(5), p.1.

[6] Slagle, K.A. and Carter, L.G., 1959, January. Gilsonite-a unique additive for oil-well cements. In Drilling and Production Practice Conference. American Petroleum Institute.

[7] Pakdaman, E., Osfouri, S., Azin, R., Niknam, K. and Roohi, A., 2020. Synthesis and characterization of hydrophilic Gilsonite fine particles for improving water-based drilling mud properties. Journal of Dispersion Science and Technology, 41(11), pp.1633-1642.

[8] Burris, M.V., Burris Michael V, 1986. Gilsonite-asphalt emulsion composition. U.S. Patent 4,621,108.

[9] Burris, M.V., Burris Michael V, 1978. Asphalt emulsion paving composition. U.S. Patent 4,094,696.

[10] Gabel, R., Vale, G., Bauch, E., Nair, C. and Meyers, A., Ecolab USA Inc., 2020. ASPHALT EMULSION COMPOSITION AND METHOD OF TREATING A PAVEMENT SURFACE. U.S. Patent Application 16/806,416.

[11] Yuan, B. and Wood, D.A. eds., 2018. Formation damage during improved oil recovery: Fundamentals and applications. Gulf Professional Publishing. pp.243-273

[12] De Boer, R.B., Leerlooyer, K., Eigner, M.R.P. and Van Bergen, A.R.D., 1995. Screening of crude oils for asphalt precipitation: theory, practice, and the selection of inhibitors. SPE Production & Facilities, 10(01), pp.55-61.

[13] Leontaritis, K.J. and Mansoori, G.A., 1988. Asphaltene deposition: a survey of field experiences and research approaches. Journal of Petroleum Science and Engineering, 1(3), pp.229-239.

[14] Kokal, S.L. and Sayegh, S.G., 1995, January. Asphaltenes: The cholesterol of petroleum. In Middle East oil show. Society of Petroleum Engineers.

[15] Mohammed, I., Mahmoud, M., Al Shehri, D., El-Husseiny, A. and Alade, O., 2020. Asphaltene precipitation and deposition: A critical review. Journal of Petroleum Science and Engineering, p.107956.

[16] Velayati, A. and Nouri, A., 2020. Emulsification and emulsion flow in thermal recovery operations with a focus on SAGD operations: A critical review. Fuel, 267, p.117141.

[17] Sztukowski, D.M., Jafari, M., Alboudwarej, H. and Yarranton, H.W., 2003. Asphaltene self-association and water-in-hydrocarbon emulsions. Journal of colloid and interface science, 265(1), pp.179-186.

[18] Spiecker, P.M., Gawrys, K.L., Trail, C.B. and Kilpatrick, P.K., 2003. Effects of petroleum resins on asphaltene aggregation and water-in-oil emulsion formation. Colloids and surfaces A: Physicochemical and engineering aspects, 220(1-3), pp.9-27.

[19] Ali, M.F. and Alqam, M.H., 2000. The role of asphaltenes, resins and other solids in the stabilization of water in oil emulsions and its effects on oil production in Saudi oil fields. Fuel, 79(11), pp.1309-1316.

[20] Kokal, S.L. and Al-Dokhi, M., 2007, January. Case studies of emulsion behavior at reservoir conditions. In SPE Middle East Oil and Gas Show and Conference. Society of Petroleum Engineers.

[21] Kokal, S.L., 2005. Crude oil emulsions: A state-of-the-art review. SPE Production & facilities, 20(01), pp.5-13.

[22] Ali, M.F. and Alqam, M.H., 2000. The role of asphaltenes, resins and other solids in the stabilization of water in oil emulsions and its effects on oil production in Saudi oil fields. Fuel, 79(11), pp.1309-1316.

[23] McLean, J.D. and Kilpatrick, P.K., 1997. Effects of asphaltene solvency on stability of water-in-crude-oil emulsions. Journal of Colloid and Interface Science, 189(2), pp.242-253.

[24] Daryasafar, A., Masoudi, M., Kord, S. and Madani, M., 2020. Evaluation of different thermodynamic models in predicting asphaltene precipitation: A comparative study. Fluid Phase Equilibria, p.112557.

[25] Shoushtari, A.B., Asadolahpour, S.R. and Madani, M., 2020. Thermodynamic investigation of asphaltene precipitation and deposition profile in wellbore: A case study. Journal of Molecular Liquids, p.114468.

[26] Hemmati-Sarapardeh, A., Ameli, F., Ahmadi, M., Dabir, B., Mohammadi, A.H. and Esfahanizadeh, L., 2020. Effect of asphaltene structure on its aggregation behavior in toluene-normal alkane mixtures. Journal of Molecular Structure, p.128605.

[27] Rahimi, A., Safari, M., Honarvar, B., Chabook, H. and Gholami, R., 2020. On time dependency of interfacial tension through low salinity carbonated water injection. Fuel, 280, p.118492.

[28] Honarvar, B., Rahimi, A., Safari, M., Khajehahmadi, S. and Karimi, M., 2020. Smart water effects on a crude oil-brine-carbonate rock (CBR) system: further suggestions on mechanisms and conditions. Journal of Molecular Liquids, 299, p.112173.

[29] Rahimi, A., Honarvar, B. and Safari, M., 2020. The role of salinity and aging time on carbonate reservoir in low salinity seawater and smart seawater flooding. Journal of Petroleum Science and Engineering, 187, p.106739.

[30] Opawale, F.O. and Burgess, D.J., 1998. Influence of interfacial properties of lipophilic surfactants on water-in-oil emulsion stability. Journal of colloid and interface science, 197(1), pp.142-150.

[31] Jiao, J. and Burgess, D.J., 2003. Rheology and stability of water-in-oil-in-water multiple emulsions containing Span 83 and Tween 80. Aaps Pharmsci, 5(1), pp.62-73.

[32] Akbari, S., Nour, A.H., Jamari, S.S. and Fayaz, F., 2006. Rheology and stability mechanism of water-in-crude oil emulsions stabilized by span 83. ARPN Journal of Engineering and Applied Sciences, 11(4). pp. 2230-2235.

[33] National Center for Biotechnology Information. PubChem Database. Source=Sigma-Aldrich, SID=329824531, https://pubchem.ncbi.nlm.nih.gov/substance/329824531. Accessed on May 25, 2020

[34] Sorbitan sesquioleate. SID S3386 [online]. Sigma-aldrich: St. Louis, MO, USA. Source: https://www.sigmaaldrich.com/catalog/product/sigma/s3386?lang=en&region=CA. Accessed 18 May, 2020.

[35] Effective surfactant selection & Formulation of (micro-)emulsions via HLD-NAC. Vlsi presentation. Source: https://www.in-cosmetics.com/__novadocuments/366543?v=636332029055230000. Accessed 18 May, 2020

[36] Standard, A.S.T.M., 1981. E799-81,". Practice for Determining Data Criteria and Processing for Liquid Drop Size Analysis.

[37] Gaestel, C., Smadja, R. and Lamminan, K.A., 1971. Contribution à la connaissance des propriétés des bitumes routiers. Rev. Gentile. Routes et Aérodromes, 466, pp.85-94.

[38] Abbott, S., 2016. Surfactant science: principles and practice. Update, 1, Destech Pubns Inc, pp.2-26.

[39] Kiran, S.K., Acosta, E.J. and Moran, K., 2009. Evaluating the hydrophilic–lipophilic nature of asphaltenic oils and naphthenic amphiphiles using microemulsion models. Journal of colloid and interface science, 336(1), pp.304-313.

[40] Piroozian, A., Hemmati, M., Safari, M., Rahimi, A., Rahmani, O., Aminpour, S.M. and Pour, A.B., 2021. A mechanistic understanding of the water-in-heavy oil emulsion viscosity variation: effect of asphaltene and wax migration. Colloids and Surfaces A: Physicochemical and Engineering Aspects, 608, p.125604.

[41] Velayati, A. and Nouri, A., 2020. Physical features' characterization of the water-in-mineral oil macro emulsion stabilized by a nonionic surfactant. Journal of Dispersion Science and Technology, pp.1-16.

[42] Bennion, D.B., Chan, M.Y.S., Sarioglu, G., Courtnage, D., Wansleeben, J. and Hirata, T., 1993, January. The in-situ formation of bitumen-water-stable emulsions in porous media during thermal stimulation. In SPE International Thermal Operations Symposium. Society of Petroleum Engineers.

[43] Cardoso-Ugarte, G.A., Ramírez-Corona, N., López-Malo, A., Palou, E., San Martín-González, M.F. and Jiménez-Munguía, M.T., 2018. Modeling phase separation and droplet size of W/O emulsions with oregano essential oil as a function of its formulation and homogenization conditions. Journal of Dispersion Science and Technology, 39(7), pp.1065-1073.

[44] Pickering, S.U., 1907. Cxcvi.—emulsions. Journal of the Chemical Society, Transactions, 91, pp.2001-2021.

[45] Haghighat, P. and Maini, B.B., 2008, January. Role of asphaltene precipitation in VAPEX process. In Canadian International Petroleum Conference. Petroleum Society of Canada.

Chapter 5: Formulating a Model Emulsion Replicating SAGD In-situ Emulsion

This paper was submitted to the Journal of Petroleum Science and Engineering for publication.

5.1 Preface

Emulsions are widely produced and handled in the petroleum industry, particularly in the recovery of heavy oil and bitumen by steam flooding EOR techniques. Production of emulsions has been detected from the very early stages of steam-assisted gravity drainage (SAGD) operations, and the literature suggests emulsification occurs in the reservoir. The model fluids employed in the current SAGD sand pack testing, such as sand retention test (SRT) and flow line testing, do not account for emulsions and their properties. This study introduces model emulsions formulated to mimic some essential features of the SAGD in-situ emulsion properties in terms of droplet size, viscosity, kinetic stability, and asphaltene precipitation. Moreover, a workflow is presented which can be used to synthesize model emulsions of any desired properties.

Additionally, the effects of gilsonite, Span 83, oil composition, electrolyte, and water content on the emulsion properties were investigated. It was found that the addition of light n-alkanes with a smaller atomic number in the oil blend results in the formation of emulsions with lower viscosity, weaker kinetic stability, and larger droplet sizes. It was also found that gilsonite which is a rich source of asphaltenes can be used in model emulsions to enhance the emulsions' stability. Molecular dynamic simulation results verified by bottle tests, interfacial tension measurements, and optical microscopy demonstrate that π-π covalent bonding, along with asphaltene-asphaltene and water-asphaltene hydrogen bonding results in face-to-face stacking of asphaltene molecules which in turn leads to the asphaltene aggregation. It was observed that the asphaltene molecules tend to settle at the oil-water interface due to the insolubility of asphaltene in the n-alkane oil and the tendency to associate with water molecules and forming hydrogen bonds. Better kinetic stability was achieved when a blend of non-ionic surfactant was used with gilsonite to prepare emulsions. Moreover, the viscosity of emulsions increased when a larger concentration of gilsonite was used in the emulsion recipes. The electrolyte's presence in the emulsions yielded lower stability. However, a higher dosage of gilsonite dominates the detrimental effect of the NaCl on the emulsion kinetic stability.

5.2 Introduction

An emulsion is a particular type of colloid with both internal and external phases in the liquid state [1]. Emulsions are present or extensively used in various industries, with significant importance in the petroleum industry [2]. There are many disadvantages associated with the production of emulsions as a large amount of energy is spent in a costly treatment to demulsify the produced fluids from the wells [3]. Demulsification is carried out due to the requirements of downstream facilities and crude sales requirements. However, not all forms of emulsions in this industry are detrimental. For instance, oil-in-water emulsions are intentionally prepared to facilitate the flow of the produced fluids in the pipelines due to the lower viscosity of this type of emulsion compared to crude oil viscosity [1].

Butler speculated emulsions should form in the steam-assisted gravity drainage (SAGD) operation that he introduced to recover bitumen from the reservoir [4]. He thought emulsification is one of the potential sources of error between his analytical LINDRAIN and TANDRAIN models and the results obtained from the pilot tests [5-7]. Later, other studies confirmed his hypothesis by showing results from SAGD micromodels [8-10]. Researchers have reported on the formation of water-in-

oil (w/o) emulsion and a free water phase with the emulsion quality varying during the production and depending on the state of the steam chamber [9-11].

Emulsions exhibit different physical properties than their constituent phases, affecting the flow properties significantly [1-3]. Namely, w/o emulsions have higher viscosity compared to the oil phase. Also, the droplets may be restrained in the pore throats. Further, the altered polarity of the emulsion may affect the intermolecular interactions with the solid particles resulting in different productivity issues such as fines mobilization, among other possible micro and macro-scale phenomena [12].

Despite the knowledge of such physical and chemical disparities, emulsions have never been used in the core flooding and sand pack testing to the authors' knowledge. No or very few attempts have been made to introduce model emulsions representing the flow characteristics of the reservoir-produced fluids. For instance, the widely used SAGD sand pack testing known as sand retention testing (SRT) employs mineral oil with a close viscosity to the bitumen viscosity at SAGD typical temperature of 200 °C to mimic the flow features of the producing oil [13].

This research introduces a workflow for the preparation of emulsions that replicate specific selected properties of the field emulsions. A model emulsion is presented with features similar to that of SAGD in-situ emulsions that form inside the reservoir. These are major features in the sense of their effect on the flow behavior of the fluids and the potential impacts on the porous media. The features consist of dynamic viscosity, kinetic stability, emulsion type, droplet sizes, and asphaltene precipitation. This model emulsion can be adjusted for application in expanding-solvent SAGD (ES-SAGD) operations as well.

This study explains the aggregation process of gilsonite asphaltene molecules in the w/o emulsion prepared with n-alkane oil and their contribution to the kinetic stability of emulsions through molecular dynamics simulation, IFT measurements, recording water phase separation, and optical microscopy of sample emulsions. The presented results reveal some important aspects of emulsion stability by asphaltenes and the underlying physical mechanisms.

5.3 SAGD Emulsion Features

Emulsions are characterized by many physical properties such as the type of emulsion, dispersed phase content, bulk viscosity, color and appearance, size of the droplets, interfacial properties, and kinetic stability, among others [14]. This study focuses on replicating those features that have the largest impact on the flow behavior and changes in the porous media. Such includes the dynamic viscosity, asphaltene precipitation, kinetic stability, and size of the droplets.

The producing fluids in SAGD operation have been observed as a free water phase, and w/o emulsion with varying water cut in both phases during the steam chamber growth [9-12]. Based on the field data and micro-model experiments, the free water phase varies from 60% to 90% of all the produced water. In comparison, the emulsified water content in the emulsion phase ranges between 10% to 50% of the emulsion [9-12]. Initial water saturation, steam pressure and temperature, wettability of the formation rock, and state of the steam chamber in the reservoir are reportedly among the most influential parameters on the emulsified water content in the emulsion phase [12].

Micro-model experiments show that the emulsification is most severe in the early stages of the SAGD production, where the steam rise results in a counter-current flow between the steam and the mobilized oil phase [9,10]. Once the steam chamber is developed vertically and laterally, the water fraction in the emulsion phase reduces. For a water-wet system similar to the oil sands in Alberta, the water content in the emulsion phase was found to be 25% after the early stages of the steam chamber growth and for most of the production life of SAGD operation [9].

5.3.1 SAGD Emulsion Viscosity

W/O emulsions generally exhibit higher viscosities than their continuous phase [1-3]. This fact is neglected in the SAGD sand pack testing. Chung and Butler (1988) carried out viscosity measurements for Cold Lake bituminous emulsions, and Bennion et al. (1993) made similar measurements for Athabasca bituminous emulsions at different water cuts and a range of temperatures [10,15]. At SAGD typical temperature of 200°C, the relative viscosity of emulsion ($\frac{\mu_{emulsion}}{\mu_{oil}}$) was 1.5 for Cold Lake bitumen and 1.92 for Athabasca bitumen for the emulsified water content of 25% in the emulsion.

Steam-assisted gravity drainage (SAGD) is the preferred method of recovery in the Athabasca region, while cyclic steam stimulation (CSS) is more efficient in production from Cold lake bitumen [16]. Therefore, the research in this paper selected the viscosity value from Athabasca bituminous emulsions as the target viscosity, which is approximately 15 mPa.s at 25% emulsified water content. This value is obtained from Richardson's dispersion viscosity model, which works better for concentrated emulsions than linear viscosity models such as Einstein's or Taylor's [17-19].

Figure 5.1 displays the performance of viscosity models in estimating the viscosity of Athabasca bituminous emulsion as measured by Bennion et al. [15]. The viscosity Sum of absolute error is the smallest for Richardson's model (3.45 mPa.s) and largest for Taylors' (10.90 mPa.s) due to the poor performance of the linear models in high water cuts. However, Einstein's estimation could be reasonable for the target water content of 25%. Therefore, one may select a viscosity window of 13 mPa.s to 15 mPa.s for 25% water in the emulsion phase at 200°C for Athabasca bitumen as SAGD field target values.

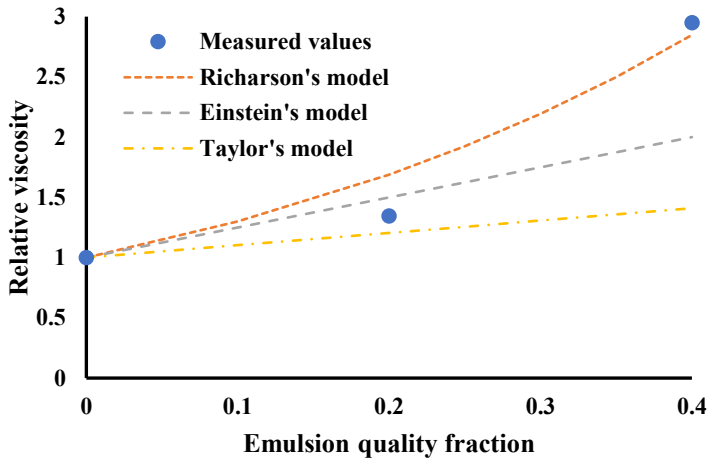

Figure 5.1: Viscosity values of Athabasca bituminous emulsion at 200°C and performance of models in capturing the measured values in Bennion's experiments [15]

5.3.2 SAGD Emulsion Droplet Size and Kinetic Stability

SAGD emulsions are considered kinetically stable primarily due to the contribution of asphaltene and resin micelles to the strengthening of the droplets' interfacial films [12,14]. Kinetic stability of the SAGD emulsions has been confirmed visually in the micro-model experiments and by assessment of the produced fluid emulsions [11,20]. Moreover, the mean droplet size in various reports in SAGD operations is mainly between 10 µm -15 µm with a range of droplets from 1 µm to 70 µm [8-12]. With an estimated average pore throat size of 50 micrometers for the McMurray formation oil sands in Alberta [21], most of the SAGD emulsion droplets should be able to pass through the pores. Nevertheless, there remains a possibility for some larger droplets plugging smaller pores in the pore network.

5.3.3 Asphaltene Precipitation in SAGD Operations

Saturates Aromatics Resins Asphaltenes (SARA) analysis of Athabasca bitumen and Cold Lake bitumen samples shows 17.28 wt% and 15.25 wt% asphaltene content in these crudes, respectively [12]. Previous studies demonstrate that emulsion stability is enhanced when asphaltene precipitates and covers the interfacial film of the droplets [22,23]. Additionally, the production data support the stabilizing role of asphaltene by demonstrating the higher emulsification in the heavy crudes, which contain a larger asphaltene concentration compared to the light crudes [1-3].

There are two primary factors responsible for the precipitation of asphaltene: the changes in the field conditions and the other concerning an alteration in the oil composition [24]. Changes in the pressure and temperature could lead to asphaltene precipitation. Studies show asphaltene precipitation is most severe in the proximity of the oil bubble-point pressure [24,25]. This phenomenon is described by the concept of asphaltene precipitation envelope (APE), a pressure-temperature region under which asphaltene precipitation occurs. Moreover, changes in the oil composition may alter the initial equilibrium state and result in asphaltene precipitation [24].

The pressure and temperature variation in SAGD operations may cause asphaltene precipitation. Moreover, the ES-SAGD recovery method in which an n-alkane solvent is co-injected with steam for bitumen in-situ upgrading alters the oil composition and may result in asphaltene precipitation.

Asphaltene-resin micelles cover the interfacial area of the droplets and stabilize the emulsion, possibly through steric hindrance [12,24,25]. This phenomenon was accounted for in the preparation of the model emulsion here.

In summary, SAGD bituminous emulsions are of w/o type, macro emulsions with a mean droplet size between 10 μm to 15 μm, kinetically stable with a typical water content (phase ratio) of 25% for most of the production life that exhibits an approximate emulsion relative viscosity of 1.66 to 1.92 (13-15 mPa.s) at this water cut and temperature of 200°C. Moreover, there is the potential for asphaltene precipitation in both SAGD and ES-SAGD operations. Model emulsion introduced here should replicate these properties at room temperature and atmospheric pressure conditions.

5.4 Materials and Methods

Deionized water with a total dissolved solids (TDS) value smaller than 1 ppm was used in the recipes for the internal phase of the emulsion. In selecting oil for the emulsion primary phase, the viscosity of the reservoir oil at SAGD conditions, transparency of the oil phase for experimental assessment purposes, and safety risks were taken into consideration. The mineral oil used in formulations is transparent, contains 96.5 wt% saturate mixtures, and 3.5 wt% aromatics with a specific gravity of 0.85 at 15°C and a measured dynamic viscosity of 6.5 mPa.s at room temperature of 22°C. Hexane was added to the base mineral oil to reduce the viscosity of the oil blend and decrease the emulsion viscosity consequently. Hexane has a dynamic viscosity of 0.3 mPa.s and a density of 0.66 g/ml at room temperature of 25°C.

Sorbitan sesquioleate (Span 83) is a non-ionic surfactant from the Span surfactant family with higher solubility in the oil phase, which facilitates the formation of the w/o emulsion according to Bancroft's rule [26,27]. This surfactant was used as the primary stabilizer of the synthetic emulsions accompanied by gilsonite. Gilsonite is a naturally occurring hydrocarbon that is mainly composed of asphaltene [28]. This additive was utilized to formulate model emulsions to mimic the asphaltene colloidal role in the stability of the field emulsions. The properties of Span 83 and gilsonite are presented in **Table 5.1**.

Table 5.1: Span 83 and gilsonite properties

Span 83			
Feature	**Value**		
HLB	3 [29]		
Cc	4-5 [30]		
CMC*	0.024 (%wt/v) [27]		
Mwt	560		
Viscosity @ room temp	1500 mPa.s		
Density	0.989 g/ml		
*CMC was determined for a mineral oil-water system			
Gilsonite			
Property	**Value**	**Components**	**Value [28]**
Carbon, wt%	85-86	Saturates, wt%	1.6
Hydrogen, wt%	8.5-10	Aromatics, wt%	0
Nitrogen, wt%	2.25-3.29	Resins, wt%	18.7
Sulfur, wt%	0.22-0.53%	Asphaltenes, wt%	79.7
Oxygen, wt%	1.5%	Colloidal instability index, CII	4.34

Emulsion preparation

A classic approach was implemented in the preparation of emulsions [1]. Initially, surfactants with more solubility in the oil phase were added to the oil blend and were stirred gently using a magnetic stirrer for one hour. In the next stage, water was added to the oil phase to form a 12 ml sample size in a 14 ml capacity beaker. The emulsification was carried out by a lab rotor/stator homogenizer of 12-mm working head size. All samples were prepared by 1000 rpm mixing rate and 1-minute mixing time at room temperature and atmospheric pressure using the emulsifying machine. The measured pH of all emulsion samples was between 7.5-8.

Surfactant(s) Selection

Several criteria exist for the selection of suitable surfactant(s) to stabilize emulsions, including critical micelle concentration (CMC), Hydrophilic Lipophilic Balance (HLB) values, and Bancroft's rule. However, these criteria are based on the surfactant features and neglect the other conditions which may affect the emulsification process, such as temperature, salinity, and oil properties. Hydrophilic lipophilic deviation (HLD) theory, on the other hand, considers all these other factors and is a function of the entire system [31]. Equation 1 displays the HLD terms [31]:

$$HLD = Cc - k.EACN - a\Delta T + f(s) \quad (1)$$

where Cc is the characteristic curvature value that describes the surfactant solubility and, in that sense, similar to the HLB concept. EACN is equivalent alkane carbon number and represents the oiliness, k and a are constants, ΔT is the temperature difference from 25° Celsius, *f(s)* is the salinity term where s is the salt concentration (g/100ml). *f(s)* equals to *ln(s)* and *0.13s* for ionic and non-ionic surfactants, respectively.

Zero HLD value corresponds to a balanced system with minimum interfacial tension. Positive and negative HLD values suggest the formation of w/o and o/w emulsions, respectively. This study employs this criterion for surfactant selection, considering the conditions at which the emulsion is prepared. As mentioned, the mineral oil used in the study is mainly composed of saturates with an EACN value of 18 at 25°C [31]. Additionally, the emulsions are prepared at room temperature and considering the small values of a coefficient, the temperature term is negligible. Therefore, the Cc value must be larger than 3.06 for the preparation of the w/o emulsion. It is recommended to choose a surfactant with a Cc value close to the required value for enhanced stability of the emulsion, and Span 83 satisfies this condition.

The cc value of asphaltene has been reported 0.8-2.3 at 25°C elsewhere [32], which means asphaltene alone cannot stabilize the w/o emulsion under the existing emulsification conditions. This was examined in an experiment, and immediate separation of the water phase was observed after homogenization, confirming the hypothesis. However, a combination of surfactants can yield improved emulsions' stability, as reported in the literature [1-3]. Cc for a mix of surfactants can be calculated by Equation 2 in which x is the molar fraction of the surfactant i [32]. For a mixture of surfactants with the highest mass fraction of gilsonite in this study (20 wt%) blended with Span 83, Cc is 3.87 at room temperature, which implies the formation of w/o emulsion. Therefore, a mixture of Span 83 and gilsonite should result in the formation of a stable w/o emulsion.

$$Cc = \Sigma\, x_i . Cc_i \tag{2}$$

5.4.1 Emulsion Features Characterization

The selected features of the emulsions to be monitored consist of dynamic viscosity, size of the droplets, asphaltene precipitation, and kinetic stability. The model emulsion should replicate these properties of the SAGD field emulsion. The workflow in **Figure 5.2** was developed to follow certain stages to adjust the model emulsions properties. According to this flowchart, the first step is starting with a base recipe. HLD criterion was used to select the suitable additives to prepare the target w/o emulsion at room temperature and atmospheric pressure conditions. The type of oil was selected based on the viscosity value proximity to the target emulsion viscosity, transparency, and safety concerns. Hence, the base recipe contains DI water, mineral oil, Span 83, and gilsonite.

In the next step, the effect of the homogenizer shearing rate and mixing time on the droplets' size was investigated. Detailed results of this analysis are published in a previous publication [26]. The mixing rate of 1000 rpm and 1 minute mixing time was selected based on the results obtained from a parametric study. The next phase involves screening tests to investigate the effect of surfactant(s) concentration in the base emulsion on emulsion's physical features (kinetic stability, droplet size, asphaltene precipitation, and dynamic viscosity). The outcome of such screening analysis is finding the range of values achievable using the current surfactant(s) and additives. Moreover, the minimum and maximum concentrations employed in the final experimental design for each additive can be approximated at this stage. If a desirable feature from the target emulsion is not achievable with the base recipe, additives may be added to expand the feasible solution for one or more emulsion properties. Alternatively, changing the homogenization setting can shift the attainable feature range of values.

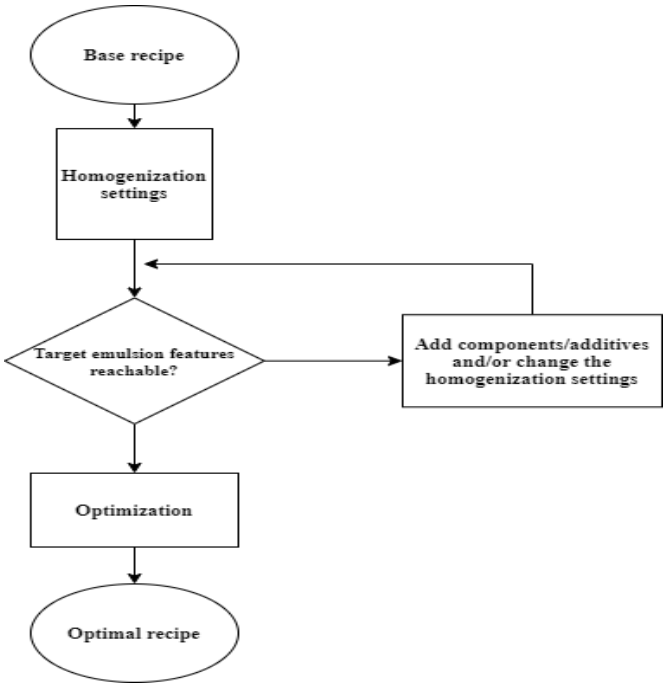

Figure 5.2: Workflow followed to optimize and prepare the model emulsion

Finally, an experimental design with all the selected materials is used to develop functions for the target features. The optimal recipe with properties similar to that of target emulsion features can be reached using the developed correlations as objective functions in multi-objective multivariable optimization. This process results in replication of the target emulsion properties with a model emulsion.

The emulsion target features selected in this study are the dynamic viscosity, kinetic stability, asphaltene precipitation, and size of the droplets. A cone and plate type viscometer was used for measurement of the absolute viscosity. The kinetic stability of the emulsions was examined via bottle tests, optical microscopy, and interfacial tension measurements. The sizes of the droplets and asphaltene precipitation were determined and monitored by optical microscopy.

Emulsion kinetic stability characterization

The stability of emulsions is the resistance to change in the physical properties of emulsions with time [1]. The primary instability mechanisms in emulsions include flocculation, coalescence, Ostwald ripening, creaming, and sedimentation [1-3]. W/O emulsions are more difficult to stabilize due to the thin electrical double layer (EDL) in this type of emulsion [26]. This study adopts several techniques to evaluate the kinetic stability in emulsions, including bottle tests, micrography, and interfacial tension measurements.

Water phase separation is the ultimate indicator of instability of emulsions and is carefully monitored in the experiments. Water droplets (internal phase) flocculate due to attractive forces, which may lead to coalescence. Water droplets form connected films, and the phase gradually separates from the oil. This is because the system tends to go back to its former and lower energy state after emulsification that elevates the system's energy level.

In the bottle test, 12 ml emulsion samples were poured into 14 ml graduated cylinders. Samples were then put on a flat surface for 3 days, and the water phase separation was recorded for this pre-determined storage time. Equation 3 displays the water separation index used here to monitor the water phase separation in emulsions quantitatively:

$$WSI\ (\%) = \frac{Separated\ water\ (ml)}{Initial\ water\ in\ emulsion\ (ml)} \times 100 \quad (3)$$

As described before, enlargement in the size of the droplets occurs with time because of flocculation and coalescence of the droplets. This behavior was tracked by micrography and recording the size of the droplets immediately after emulsification and the second time after 3 days. Finally, interfacial tension measurements were performed for different emulsion systems to analyze surfactant(s) performance in stabilizing the emulsions. For this purpose, the capillary tube method proposed by Rashidnia et al. (1992) was employed [33]. This technique is based on the capillary rise of both liquids in the capillary tube. Firstly, the capillary tube is dipped into liquid 1 (upper liquid), and the surface tension with air is calculated for this system. Then, the tube is dipped into liquid 2 (lower liquid), and a liquid-liquid surface forms inside the tube. **Figure 5.3** shows the schematic of this method, and Equation 4 is used to calculate the interfacial tension between two immiscible liquids [33].

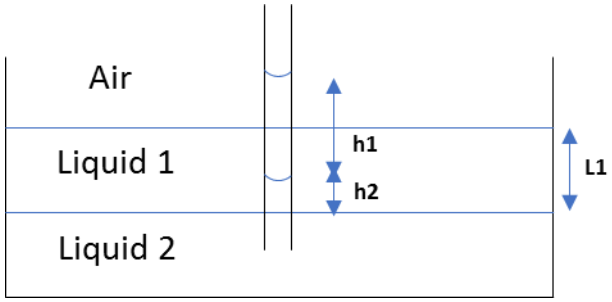

Figure 5.3: Interfacial tension measurement using a capillary tube

$$\sigma_{12} = -\sigma_{1a}\frac{cos\theta_{1a}}{cos\theta_{12}} + \frac{gr}{2cos\theta_{12}}(\rho_1 h_1 + \rho_2 h_2 - \rho_1 L_1) \quad (4)$$

where σ is interfacial tension, θ is contact angle, g is the gravitational acceleration, ρ is liquid density, and r is capillary tube radius. 1 and 2 refer to liquids 1 and 2, and "a" denotes air. **Figure 5.3** illustrates these parameters schematically.

Emulsion viscosity measurement

This study employs a cone and plate geometry viscometer (Brookfield LVT-CP40) to measure the dynamic viscosity of emulsion samples. This type of viscometer requires small sample volumes (0.5 ml) for the measurements. The determination of viscosity is carried out by measuring the torque imposed by the cone's rotation with a fixed speed over the conical surface, which is in point contact with the flat plate [26].

Emulsion droplet size characterization

There are various methods for determining the size of the droplets, among which optical microscopy is very popular due to the visualization of the system and droplets [1-3]. A compound microscope with 1000x magnification capacity, equipped with Kohler illumination technology,

and a 10 MP camera were utilized for capturing images from the emulsion samples. Images were captured immediately upon emulsion preparation and after three days of storage period. Image processing was performed by ImageJ open-source software, where the diameter of the droplets, minimum Feret diameter, and equivalent projected circle (EQPC) of the asphaltene aggregates were obtained.

Representative sizes such as arithmetic mean diameter, Sauter diameter, and De Broukere diameter are often used to describe the characteristic size of a system containing particles of different sizes. The selection of the fitting representative size depends on the purpose of the study and the technique used to characterize the particle sizes. In a previous publication, we have shown that the number-based distribution characterization is reproducible. In contrast, the volumetric distribution is subject to the sampling and microscope's field of view in the micrography of the emulsion samples [26].

5.4.2 Experimental Design and Optimization

The study uses comparative and screening experimental designs for the initial assessment of the emulsion components and their effects on the physical features of the emulsions. The same designs were employed to examine the features of the base recipe and the effect of added components on the systems. After making the final decision on selecting the emulsion components, response surface methodology was used for its advantages in hitting the targets and optimizing a response [34]. In response surface designs (RSM), the model includes the main effects along with the interactions and even quadratic effects.

Box Behnken design is one of the response surface methods with merits over alternative techniques when three factors are presents. The number of experimental runs is fewer in this type of design for 3 factors. However, this advantage vanishes for four factors or more. The levels for each factor are coded such that +1 corresponds to the highest level, -1 refers to the lowest level, and 0 is the mid-point. Therefore, three levels are required for Box Behnken Design [34]. **Table 5.2** shows the experimental runs in the Box-Behnken design for three factors and the coded levels.

Table 5.2: Box-Behnken design for 3 factors

Recipe number	Replicates	X1	X2	X3
1	1	-1	-1	0
2	1	+1	-1	0
3	1	-1	+1	0
4	1	+1	+1	0
5	1	-1	0	-1
6	1	+1	0	-1
7	1	-1	0	+1
8	1	+1	0	+1
9	1	0	-1	-1
10	1	0	+1	-1
11	1	0	-1	+1
12	1	0	+1	+1
13	3	0	0	0
Total Experimental Runs: 15				

After conducting the experimental design tests, correlations were developed for certain features of the emulsions. These correlations were used as objective functions for the optimization part of the research where the goals (SAGD emulsion features) must be achieved. Hence, a multi-objective multivariable optimization problem must be solved to find the optimal recipe that mimics certain features of the SAGD field emulsion. For this purpose, the Golden-section search algorithm was used to find the extreme point for pre-determined intervals of the additive concentrations. An element of slackness was introduced into the problem to reach the goals more flexibly when the goals cannot be rigidly met. The overall form of the optimization problem statement is as follows:

$$\begin{aligned} &\text{Min } \gamma \\ &\gamma \epsilon R \\ &\text{Such that: } Fi(x) - \omega_i \gamma \leq F_i^*, \; i = 1,2,\ldots,m \end{aligned} \tag{6}$$

where F(x) is the set of objective functions, F^* is the set of goals, γ is the slack variable, and ω is the weight. The term $\omega_i \gamma$ introduces an element of slackness into the problem. The problem was solved by the Golden-section search algorithm using MATLAB, a local search method for finding an extremum [36].

5.5 Results and Discussions

5.5.1 Base Emulsion

The initial composition of the base recipe comprises mineral oil, Span 83, and DI water. Emulsion samples prepared were tested for kinetic stability, droplet size, and dynamic viscosity. Emulsion samples containing 5% wt/v Span 83 exhibited 1-month resistance to phase separation. However, the micrography results indicated the formation of flocs which was intensified with the presence of an electrolyte. Moreover, sedimentation was detected in the emulsions due to the density difference between the phases. It was observed that the mean droplet size decreases with added concentration of surfactant (Span 83) for different emulsion qualities. Finally, the emulsion's viscosity increased with the added water content, which is typical behavior of w/o emulsions.

Dilute emulsions show Newtonian behavior, whereas non-Newtonian shear thinning profile was recorded for the concentrated emulsion. A comprehensive analysis of the emulsion features with this recipe is presented in our previous publication [26]. **Table 5.3** summarizes the results obtained from the comparative and screening tests on the base recipe.

Table 5.3: Summary of the results of the emulsion samples stabilized by Span 83

Span 83 concentration (wt%/v)	Water content in emulsion (%)	Mean droplet diameter (micrometer)	3- Days stability	Viscosity (mPa.s)
5	10	5.35	Stable	13
5	40	8.74	Stable	45.4
1.5	10	6.65	Immediate phase separation	10.2
1.5	40	14.15	Phase separation after 3 hours	38

Effect of Hexane

The problem with the base recipe was small mean droplet sizes and high viscosity values compared to the target SAGD emulsion features (estimated for 25% emulsion quality). In the first attempt to address this issue, the concentration of Span 83 was reduced from 5 wt%/v to 1.5 wt%/v. Results presented in **Table 5.3** show that decreasing the surfactant concentration results in larger droplets and lower dynamic viscosity of emulsion for a constant phase ratio. Additionally, bottle test screening demonstrates that reduction of Span 83 concentration could destabilize the emulsions samples and cause water phase separation.

The dynamic viscosity of the base mineral oil used in the base recipe was 6.5 mPa.s. Hexane with a lower viscosity of 0.3 mPa.s was added to the composition of the emulsion to reduce the viscosity of the system. The hypothesis was that a reduction in the viscosity of the continuous phase would result in a decrease in the viscosity of the entire emulsion system and enlargement of the droplets. However, lower viscosity could be detrimental to the stability of the emulsion [12].

A comparative experimental design was adopted to examine the effect of Hexane on the physical features of the emulsion. In this phase, the concentration of Span 83 was fixed at 5% wt/v. The factors were Hexane at two levels of 0 v% and 10 v% in the oil blend and water content at two levels of 10% and 40%. Another experimental run was added to the list of tests to evaluate the effect of electrolyte (NaCl) on the stability of 10% emulsion with 5% wt/v Span 83 and two levels of Hexane of 0% and 10 v%. All emulsion samples were prepared at room temperature and atmospheric pressure with a 1000 rpm mixing rate and 1 minute mixing time. **Figure 5.4** displays the measured viscosity.

According to **Figure 5.4**, adding 10 v% Hexane to the oil blend resulted in a 40.53% and 23.56% reduction in the high shear rate (45 1/s) viscosity of the 10% and 40% emulsions, respectively. This is because of the low viscosity of the Hexane that diminishes the oil mixture viscosity from 6.5 mPa.s to 5.20 mPa.s. The literature suggests lower viscosity of the emulsion may result in enlargement of the droplets due to the less stability seen in, the less viscous emulsions [26]. **Figure**

5.5 shows this is the case here, where an 81.30% increase in mean droplet diameter was recorded for 10% emulsion and 37.30% enlargement for 40% emulsion.

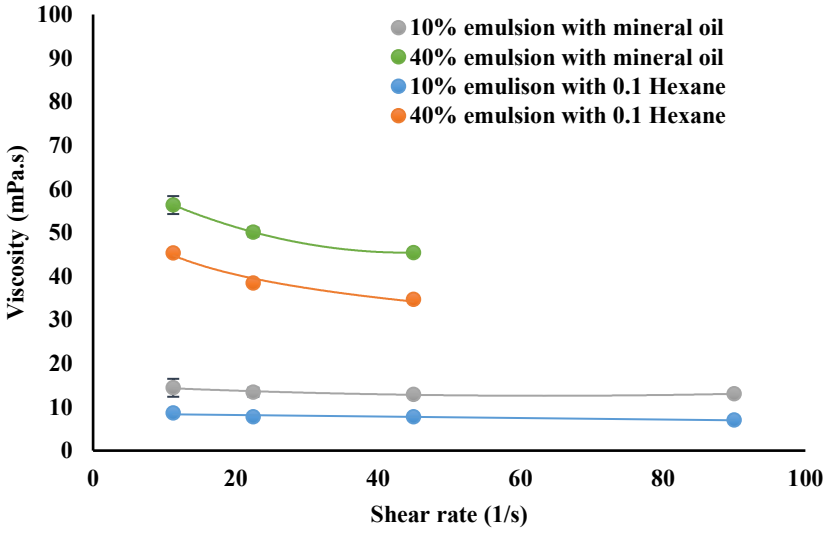

Figure 5.4: Effect of Hexane on the dynamic viscosity of emulsion samples

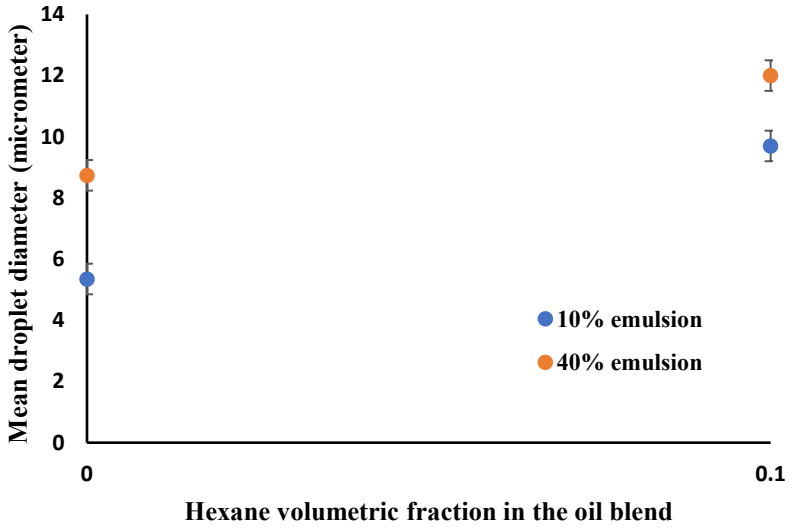

Figure 5.5: Change in the size of the droplets with Hexane in the oil blend

All emulsion samples without NaCl in the water resisted water separation in the 3-days storage period for all levels of Hexane in the oil blend. This implies 5% wt/v Span 83 concentration in the emulsion is sufficient to stabilize the emulsions prepared with DI water for the oil compositions used here. However, **Figure 5.6** shows that the presence of electrolytes leads to water separation that can be attributed to the larger Van der Waals attractive forces between droplets, and misorientation of surfactant molecules at the interface due to the salting-out phenomenon [26]. Emulsion with Hexane in the oil composition demonstrates higher instability, mainly due to the system's lower viscosity. The rate of approach among droplets is faster in less viscous fluids, resulting in coalescence and enlargement in the size of the droplets [36]. The inverse correlation

between the size of the droplets and viscosity has been reported previously for w/o emulsions [17,26,36,37].

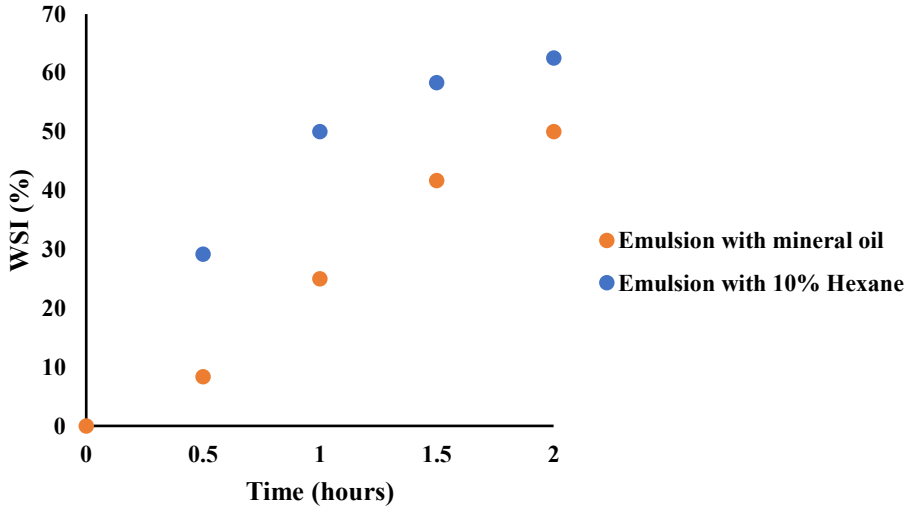

Figure 5.6: Water separation in emulsion samples in the presence of 0.51 M NaCl in the water phase

5.5.2 Characterization of Gilsonite

Gilsonite was added to the emulsion composition to mimic the asphaltene presence in bitumen. Literature indicates that asphaltene precipitation leads to the formation of tight emulsions [22,23,38]. This study utilizes mineral oil for the emulsion continuous phase. Asphaltenes in gilsonite are insoluble in saturates like paraffinic oil and soluble in aromatic compounds like Toluene. This leads to asphaltene precipitation in oil with higher saturates fraction and producing aggregates that clump together and form flocs. Hexane (n-alkane) was added to Toluene in different fractions to determine the onset of asphaltene precipitation for gilsonite in the mineral oil. The samples were examined via optical microscopy to monitor the size of the aggregates in the fluid mixture. The minimum Feret diameter of the aggregates was used in the analysis. **Figure 5.7** illustrates the change in aggregate size with Hexane fraction in Toluene.

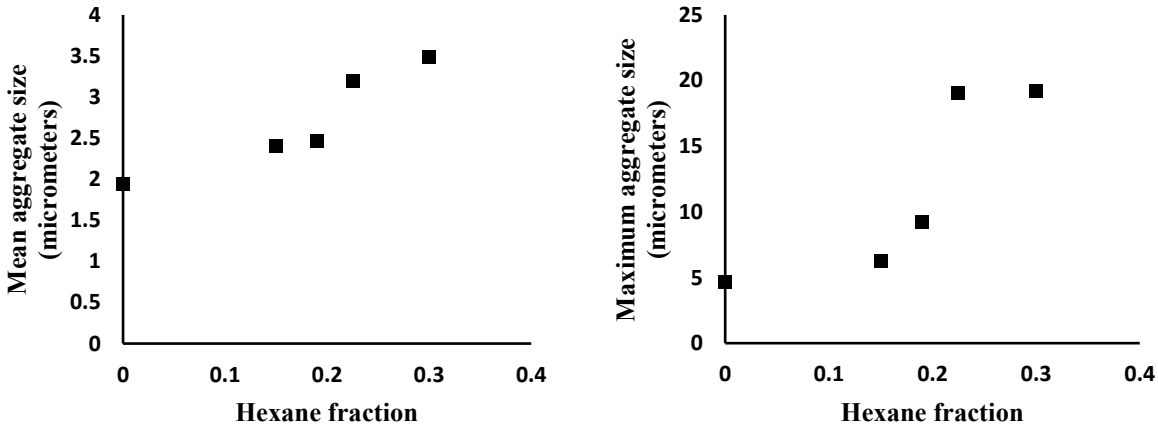

Figure 5.7: Onset of asphaltene precipitation for gilsonite

According to the results shown in **Figure 5.7**, the enlargement in the asphaltene mean aggregate size occurs somewhere between 19 v% and 22.5 v% hexane in the oil blend. A jump in the maximum aggregate size is detectable at 19 v% hexane in oil. It can be concluded that the onset of asphaltene precipitation occurs at 20 v% hexane concentration approximately. This onset of precipitation is due to the change in the oil composition. The results are limited to the atmospheric pressure and room temperature conditions under which the experiments were carried out. It is worth noting that the solvent's impurities (95% Toluene) are likely responsible for the presence of few and very small particles detected at 0% hexane concentration in the oil blend.

Figure 5.8 illustrates the sample micrographs for different hexane fractions in the oil blend. It was observed that the standard deviation increases with more precipitation in the oil blend, which corresponds to a larger scattering of the aggregates in terms of size distribution. **Table A1** in the appendix section contains the measured sizes and the relevant information about the onset of asphaltene precipitation. **Figure 5.7** and **Figure 5.8** show that the aggregates' size increases with elevated saturates fraction in the oil blend, and the rate of precipitation intensifies as well. This was confirmed with a larger number of aggregates detected in micrography for oil blends with a higher fraction of hexane.

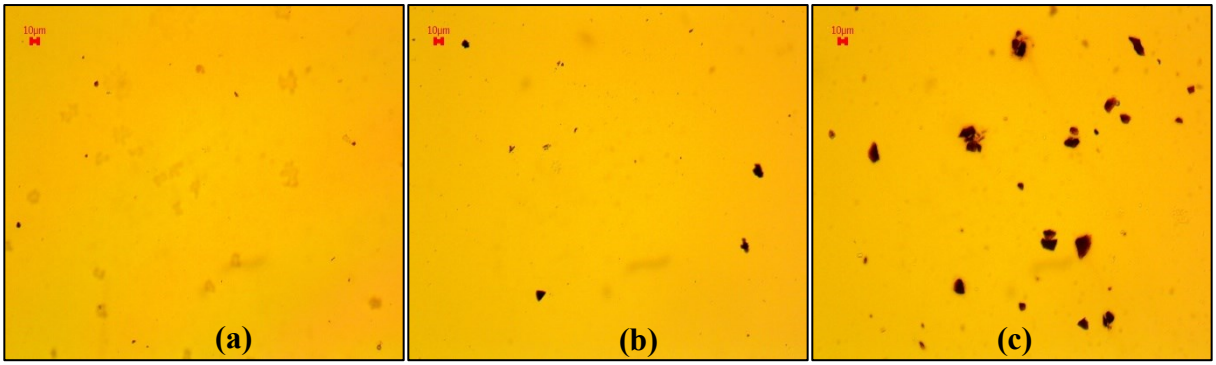

Figure 5.8: Asphaltene precipitation; (a) 0% Hexane (b) 19% Hexane (c) 22.5% Hexane

5.5.3 Effect of Gilsonite on Emulsion Features

Table 5.4 summarizes measured values of the 10% emulsion (water content) samples prepared with mineral oil and stabilized by Span 83 and gilsonite. This blend of surfactants was selected based on the required Cc value to stabilize the w/o emulsion with the components mentioned previously at room temperature. Recipes 1-4 were tested to determine the effect of gilsonite concentration on the target properties of emulsions, namely dynamic viscosity, 3-day water phase separation, and mean droplet size.

Table 5.4: Summary of the gilsonite screening test results

Recipe number	Gilsonite Concentration (% wt/v)	Span 83 Concentration (% wt%/v)	Viscosity (mPa.s)	3-day WSI (%) *	Mean droplet size (micrometer)
1	0	5	13.00	83.33	5.35
2	0.1	5	14.00	75.00	5.54
3	0.25	5	15.65	58.33	6.82
4	1	5	-**	4.16	8.19
*Stability tests were performed for emulsions with 0.51 M NaCl ** The viscosity measurements were not stable at 1% gilsonite concentration					

According to the presented results, the viscosity of the emulsions and size of the droplets magnifies at higher gilsonite dosages. Moreover, the kinetic stability of emulsions increases with added gilsonite concentration. Gilsonite is a well-known viscosifying agent which contains asphaltene in large portions [28,38]. Asphaltene precipitates in the mineral oil due to its insolubility in saturates, and literature suggests higher precipitation results in the formation of tight emulsions [12,22,23]. Asphaltene precipitates form aggregates and flocs that cover the droplets interfacial area and form rigid viscoelastic films, which in turn stabilize the emulsions mainly through steric hindrance [38-40]. This explains the higher stability and resistance to water phase separation in emulsions with larger gilsonite concentrations, as shown in **Table 5.4**. Finally, the larger mean droplet size in emulsions with higher gilsonite dosage is linked to the elevated viscosity of the dispersions. More viscous fluids require higher mixing energy to maintain the size of the droplets [26].

Figure 5.9 displays the micrographs of recipes 1 and 4. Recipe 4 contains gilsonite in the emulsion composition, and asphaltene aggregates are visible in the image. It appears that droplets in emulsions stabilized by the gilsonite/Span 83 surfactant blend have thicker and darker interfacial films, which can be attributed to the asphaltene aggregates covering the droplets. The literature suggests asphaltene aggregates stabilize the emulsions mainly through mechanical means and steric hindrance [38-40]. However, asphaltene is also made of heteroatoms such as Nitrogen, Sulfur, and Oxygen that may contribute to the stability process in emulsions.

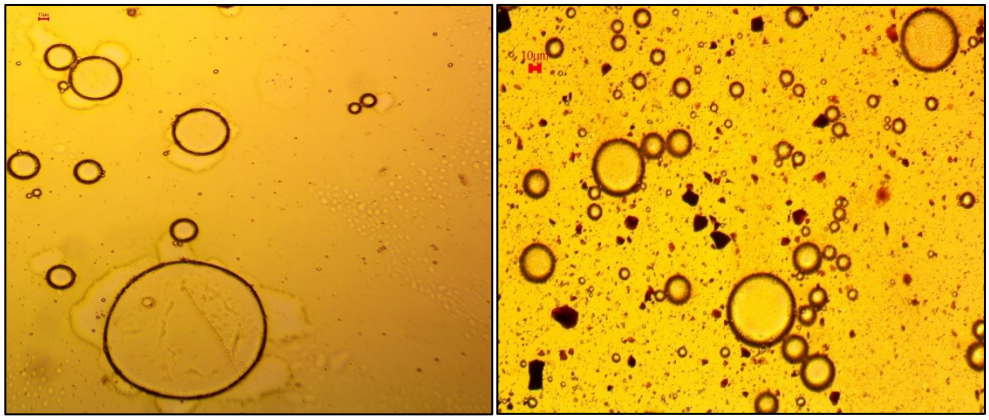

Figure 5.9: Micrographs of emulsions with (Right) and without gilsonite (Left)

Interfacial tension measurements were carried out to analyze further the role of asphaltene in stabilizing emulsions. The methodology explained before was followed to perform the interfacial tension measurements for fluid mixture systems. At first, mineral oil was mixed with 5% wt/v

Span 83 (to make sure Span 83 concentration exceeds CMC value), and the measurement of IFT was carried out between water and the mentioned fluid mixture as the reference point. Then, IFT was measured between water and oil+5% wt/v Span83+1% wt/v gilsonite to compare the two cases and examine the effect of gilsonite.

Figure 5.10 shows the meniscus for the two systems. In both systems, capillary glass is wetted by water as expected due to the high polarity of water and glass and the strong adhesion forces between them. Contact angle decreases from 40 degrees for water-mineral oil+Span 83 system to 28.5 degrees when gilsonite is added to the oil phase. Similarly, IFT decreased from 13.20 dyn/cm for the water-oil+Span 83 system to 9.93 dyn/cm in the water-oil+Span 83+Gilsonite system.

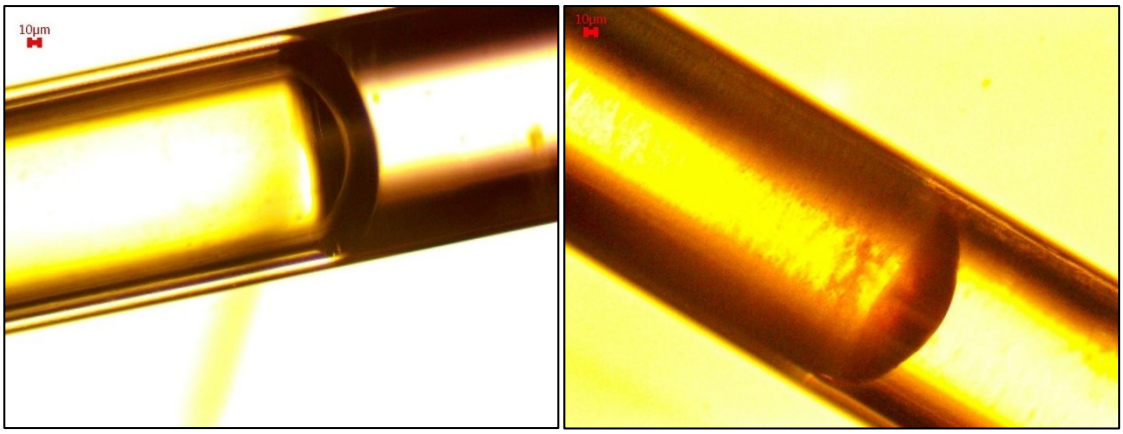

Figure 5.10: Meniscus and contact angle; Left) water-mineral oil+Span 83, Right) water-mineral oil+Span 83+Gilsonite

The IFT reduction for the fluid mixture containing gilsonite can be explained as follows. Gilsonite contains heteroatoms such as Sulfur, Oxygen, and Nitrogen, as previously shown in **Table 5.1**. Literature suggests hydrogen atoms of asphaltene that are bonded to the highly electronegative hetero atoms, namely nitrogen and oxygen, can donate hydrogen bonds [41]. Thus, asphaltene aggregate molecules accumulated at the oil-water interface can potentially form hydrogen bonds with water which results in a decrease in the interfacial tension. Reduced IFT in this process can stabilize emulsion droplets by diminishing interfacial energy of dispersion.

Moreover, asphaltene aggregates establish rigid viscoelastic films around the droplets, which in turn stabilize emulsions sterically [12,22,23]. Higher kinetic stability of emulsions that contain larger concentrations of gilsonite, as shown in **Table 5.4**, can be explained with these observations. Besides, contact angle and capillary rise in IFT measurement were lower for the system containing gilsonite than the system without gilsonite in the oil phase.

In summary, the screening test results show adding gilsonite to the emulsion increases viscosity, droplet size and improves kinetic stability in emulsions. Hexane reduces the viscosity and can be detrimental to the stability of emulsions, while an increase in the size of the droplets may occur. Adding Span 83 non-ionic surfactant increases the viscosity and improves the stability of emulsions but may reduce the size of the droplets in higher concentrations.

5.5.4 Molecular Dynamic Simulation of Asphaltene in Emulsion System

In the previous section, we have shown that the presence of asphaltene in the emulsion system in form of aggregates leads to the reduction in IFT, WSI, and better kinetic stability in emulsions.

Previous studies speculate the stabilizing role of asphaltene in emulsions is primarily through steric hindrance, with some studies pointing out the possibility of hydrogen bonding between water and asphaltene [12,41]. However, such investigations are limited to the aromatic oil blends which dissolve asphaltenes and higher temperatures that are very different from the system studied here [41,42]. To better understand the role of asphaltenes in stabilizing the emulsions prepared in this study and their dynamics, a molecular simulation study was carried out.

Asphaltene molecules are thought to have two main architectures: "Island" (continental) structure with highly condensed aromatic rings and "Archipelago" structure which comprises several smaller aromatic cores that are connected by alkyl bridges [24]. Both structures contain heteroatoms such as N, S, and O in the side chains [24]. Li et al. (2015) investigated the chemistry and structure of gilsonite and found that the "Island" molecular model is the architecture of asphaltene molecules in gilsonite [43]. Further, the elemental analysis, shown in **Table 5.1**, affirms the heteroatoms N, S, and O exist in gilsonite. Thus, an "Island" type structure containing heteroatoms was considered for the asphaltene molecular architecture in the simulation.

Figure 5.11 illustrates the 3D schematic of the model asphaltene. The chemical formula of the model asphaltene is C68 H59 N O3 S. Asphaltene monomers were reported to have a molecular weight in the range of a few hundred to one thousand approximately [44]. This is also true for the molecular weight of asphaltene molecules in gilsonite [43]. The model asphaltene designed here has a molecular weight of 970.26 g/mol. Sulfide, hydroxyl, and amine functional groups were embedded in the molecule design of model asphaltene, as depicted in **Figure 5.11.**

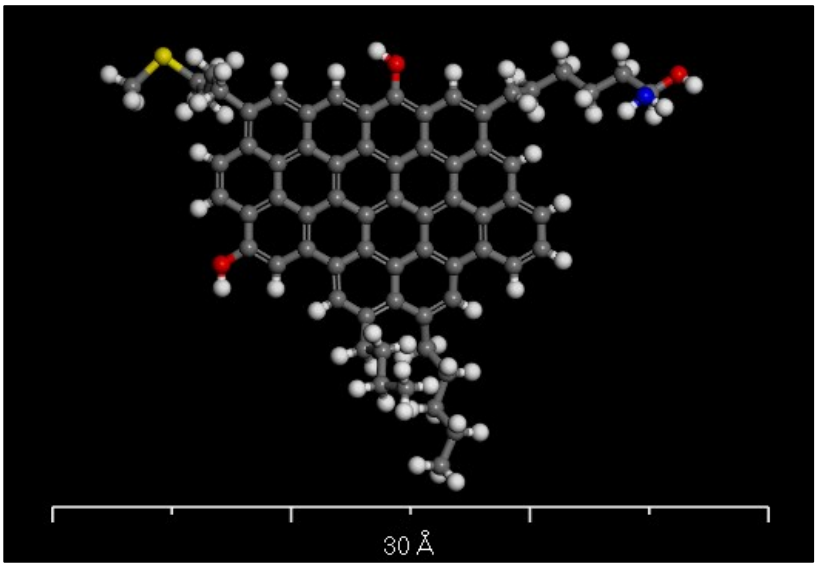

Figure 5.11: 3D depiction of model asphaltene molecule. Red: Oxygen atom; Blue: Nitrogen atom; Yellow: Sulfur atom

Materials Studio software was used to perform the simulation. First, a simulation box in the size of 27×27×27 Angstrom in cartesian coordinates was created which includes asphaltene and hexane molecules with an asphaltene to hexane molecule ratio of 1:12. Then, a simulation box of similar size was created for H_2O (water) molecules and the two layers were incorporated into one system. Therefore, the final system contains two layers extended in the z-direction and separated at the contact surface layer. The layers and finalized simulation box were geometrically optimized using

COMPASS forcefield and Smart algorithm, which is a cascade of the Steepest Descent, Quasi-Newton, and ABNR methods. **Figure 5.12** illustrates the initial state of geometrically optimized molecules, before the start of dynamic simulation.

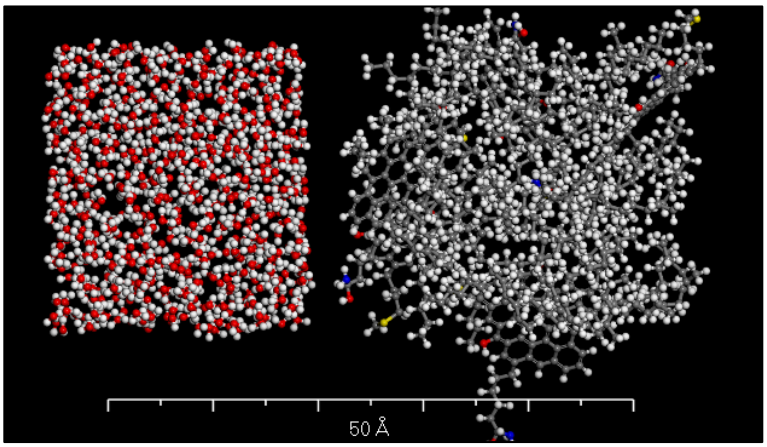

Figure 5.12: Initial state of the geometrically optimized layers; Left layer: water molecules, Right layer: Oil blend containing hexane and asphaltene molecules

The molecular dynamic simulation was performed under NVT ensemble and using COMPASS forcefield. Newton's equation of motion was integrated by the velocity Verlet algorithm. 3D periodic boundary conditions were selected. Total simulation time was set at 0.2 ns (200 ps) which should be long enough for the molecules to go past vibrations and exhibit diffusion/interaction. The Timestep was fixed at 1 fs. Finally, the Nose thermostat model was used to maintain the temperature at 298 K throughout the simulation.

Figure 5.13 displays the orientation of three asphaltene molecules at the end of the simulation. Most of the asphaltene molecules were settled at the proximity of the oil-water interface. Further, face-to-face stacking structure induced by π-π bonding was observed between asphaltene molecules. Hydrogen bonding was detected between asphaltene molecules and asphaltene-water molecules. **Figure 5.14** displays the hydrogen bonds between hydrogen in the asphaltene hydroxyl functional group and water molecules and the bonding between hydrogen in the asphaltene sulfide functional group and water molecules.

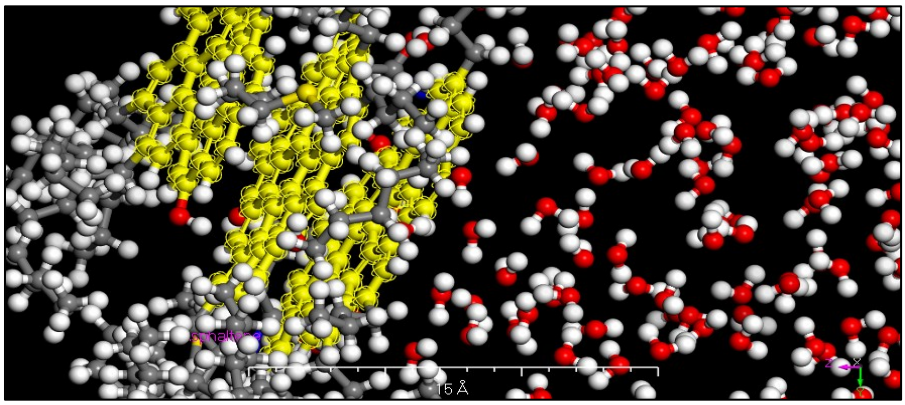

Figure 5.13: Face-to-Face stacking between asphaltene molecules after 0.2 ns. Asphaltene molecules aromatic moieties are colored yellow

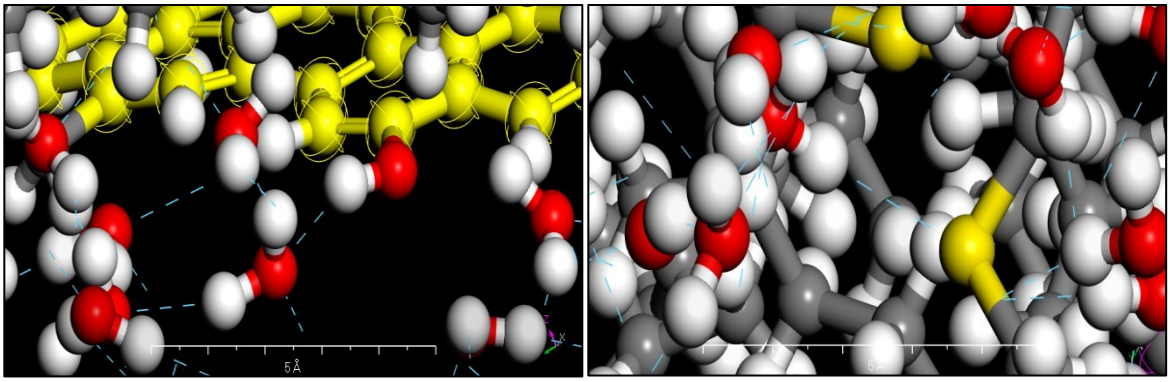

Figure 5.14: Asphaltene-water hydrogen bonding; Lett: hydrogen donor is hydroxyl group, Right: hydrogen donor is sulfide group. Blue dashed lines represent the hydrogen bonds

Figure 5.13 shows the face-to-face stacking morphology in asphaltene molecules visually. Relative concentration profile and radial distribution function are two quantitative indicators of asphaltene aggregation and orientation used in this study. A minimum separation distance of aggregates is typically witnessed in face-to-face stacking of asphaltene molecules, where up to 0.5 nm spacing has been reported in the literature [45]. In contrast, T-shaped and parallel stacking configurations exhibit a higher separation distance of up to 1 nm [44]. The first peak in the radial distribution function depicted in **Figure 5.15**, occurs at approximately 1.40 Angstrom (0.14 nm) which confirms the face-to-face stacking morphology for asphaltene molecules. The probability of finding asphaltene at the distance of 0.14 nm (g(r)) is 254, which implies the high likeliness of aggregation.

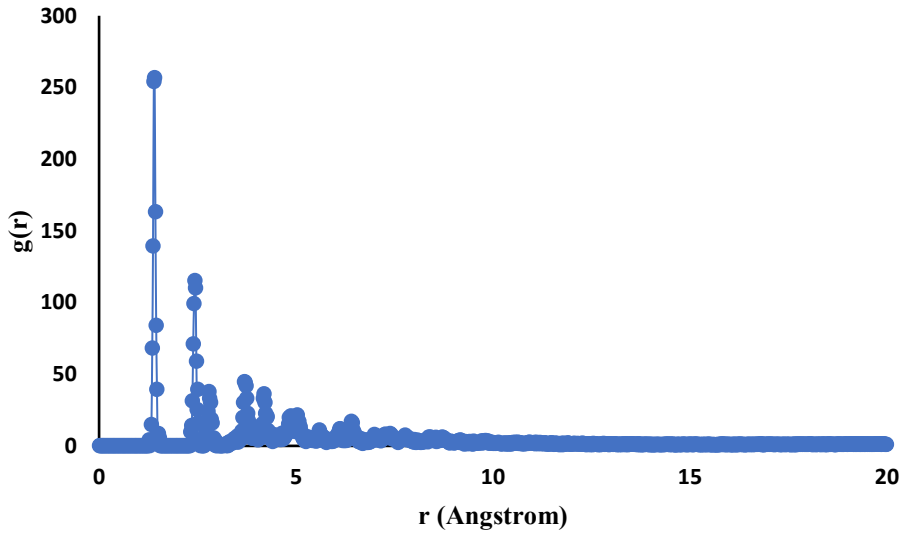

Figure 5.15: Radial distribution function of asphaltene at 0.2 ns

Yaseen and Mansoori (2018) performed MD simulation for different model asphaltenes in o-xylene oil and water systems at high temperature and pressure of 550 K and 200 bar [44]. They demonstrated that asphaltene aggregation occurred primarily as a result of hydrogen bonding between water and asphaltene molecules and discussed asphaltene-asphaltene hydrogen bonding effect is insignificant in the aggregation process. They articulated that at high pressure and

temperature conditions water miscibility increases in the oil phase which in turn triggers aggregation of asphaltene in the system.

In our system, water molecules did not diffuse in the oil phase because of the low-temperature conditions and immiscibility of the two phases. Asphaltene molecules tend to settle at the water-oil interface due to the insolubility of the asphaltene molecules in hexane which contrasts with the results presented by Yaseen and Mansoori, where o-xylene prevented the self-association and interaction between asphaltene molecules. For the same reason, separation distance in RDF (first peak) is 0.24 nm smaller with a much higher probability in our system than theirs (254 to 193 for the first peak), indicating the strong contribution of asphaltene self-association (π-π covalent bonding and asphaltene-asphaltene hydrogen bonding) in the aggregation process. Therefore, it can be concluded that asphaltene-asphaltene self-association in terms of hydrogen bonding, π-π covalent bonding, and hydrogen bonding between asphaltene and water molecules contribute to the aggregation process in the system studied here.

As mentioned earlier, asphaltene molecules did not settle at the oil-water interface in the simulation performed by Yaseen and Mansoori, and the asphaltene aggregation was instigated by the diffusion of water molecules into the oil blend and forming hydrogen bonds with hydrogen from asphaltene molecule functional groups. Although RDF peak values and separation distances are good indications of asphaltene aggregation, the relative concentration profile can describe the motion of asphaltene molecules at different stages of the simulation. **Figure 5.16** illustrates the relative concentration profile at the very beginning of the simulation and after 0.2 ns. Unlike the results presented by Yaseen and Mansoori [44], asphaltene molecules show the tendency to shifting toward the oil-water interface. As discussed before, this phenomenon occurs due to the insolubility of asphaltene in hexane and the presence of heteroatoms in the model asphaltene sidechains which have a propensity to form hydrogen bonds with water molecules. In other words, electrostatic repulsive forces between hexane and asphaltene are responsible for the motion of asphaltene towards the oil-water interface and the hydrogen bonding attractive forces between water molecules and asphaltene maintains the position of the asphaltene aggregates at the oil-water interface.

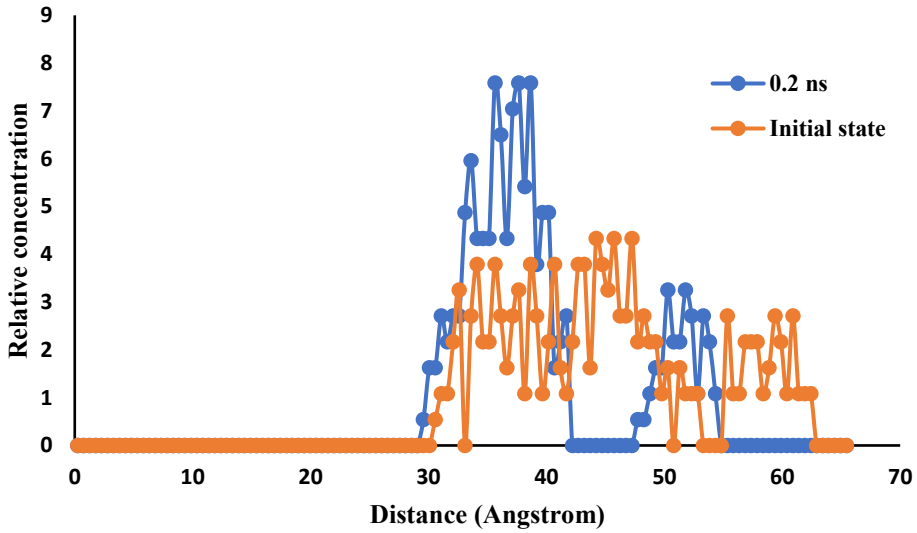

Figure 5.16: Relative concentration profile of asphaltene molecules

The implication of asphaltene aggregation tendency at the oil-water interface is the improved stability of w/o emulsions. This takes place by high precipitation of asphaltene in n-alkane oil, asphaltene aggregation, and positioning at the droplet interface. Hence, emulsions are stabilized through steric hindrance and lower interfacial tension resulted from the hydrogen bonding between asphaltene and water molecules. This is verified in the experiments where the emulsion system containing asphaltene exhibited lower interfacial tension, darker and thicker interfacial films around the droplets were formed with the presence of gilsonite in emulsions as shown in **Figure 5.9**, superior kinetic stability in terms of water phase separation (**Table 5.4**), and partitioning of the asphaltene molecules at the oil-water interface as displayed in **Figure 5.10**.

5.5.5 SAGD Model Emulsion

The final objective is to introduce a model emulsion that replicates certain features of SAGD field emulsions, such as kinetic stability, dynamic viscosity, mean droplet size, and asphaltene precipitation. The workflow presented in **Figure 5.2** was followed to examine the base recipe and include more additives and substances when required. The decision on final components in the model emulsion was made based on the observations in previous sections and target features of SAGD field emulsions.

Components of model emulsion consist of mineral oil, DI water, Span 83, gilsonite, and hexane. Water content is fixed at 25 v%, and the three variables are Span 83 concentration, gilsonite Concentration, and hexane volumetric fraction in the oil blend. The box-Behnken design was followed to develop objective functions. The objective functions can be written in the following form:

$$F_{i(phi)} = f(X1, X2, X3) \quad (7)$$

where X1 is the hexane volumetric fraction in the oil blend with the highest level at 0.15 volume fraction coded as +1, the lowest level at 0.05 volume fraction coded as -1, and mid-point at 0.10 volume fraction. Coded as 0. X2 is Span 83 concentration with the highest level at 5% wt/v, lowest at 1.2% wt/v, and mid-point at 3.1% wt/v. Parameter X3 is gilsonite concentration with 0.3% wt/v,

0.1% wt/v, and 0.2% wt/v for highest, lowest, and mid-point levels, respectively. Subscript i is the emulsion feature of interest which includes mean droplet diameter, dynamic viscosity, and 3-day water separation (WSI %). Subscript phi is the water content and is fixed at 25 v% of emulsion, replicating the most common water fraction in SAGD operations reported in the literature. **Table 5.5** summarizes the results of the emulsion features testing in the Box-Behnken experimental design.

Table 5.5: Summary of the experimental results

Recipe number	X1	X2	X3	Fresh sample mean droplet size (µm)	Standard deviation of Mean droplet size (µm)	3-day aged sample mean droplet size (µm)	3-day WSI (%)	High shear rate dynamic viscosity (mPa.s)
1	-1	-1	0	10.17	0.05	16.86	0	15.8
2	1	-1	0	16.46	3.10	25.10	3.33	10.7
3	-1	1	0	11.50	1.02	15.30	0	20.3
4	1	1	0	13.89	0.68	15.08	0	15.5
5	-1	0	-1	11.59	1.80	15.29	0	18.5
6	1	0	-1	10.38	2.30	15.81	0	13.9
7	-1	0	1	8.23	0.88	16.03	0	19.2
8	1	0	1	17.42	1.51	18.12	0	14.4
9	0	-1	-1	16.00	1.00	25.50	20	15.5
10	0	1	-1	10.99	0.59	20.66	0	20.1
11	0	-1	1	14.19	3.12	19.00	4	15.7
12	0	1	1	14.91	0.52	17.90	0	20.5
13	0	0	0	9.45	1.48	18.94	0	19

Pearson correlation coefficient was used to statistically measure the correlation (linear association) between the emulsion physical features. **Table 5.6** displays the correlation matrix for viscosity, 3-day water separation, mean droplet size for fresh samples, and 3 days aged samples. In this table, stronger correlations are colored red, weaker correlations are colored gray, and moderate correlations are in yellow.

Table 5.6: Correlation matrix of the model emulsion features.

	3-Days WSI	Viscosity	Mean droplet diameter (Fresh samples)	Mean droplet diameter (aged samples)
3-Days WSI	1	-0.26	0.43	0.71
Viscosity	-0.26	1	-0.51	-0.41
Mean droplet diameter (Fresh samples)	0.43	-0.51	1	0.52
Mean droplet diameter (aged samples)	0.71	-0.41	0.52	1

Table 5.7: Correlation coefficients between additives and emulsion features.

	X1	X2	X3
3-Days WSI	0.06	-0.50	-0.29
Viscosity	-0.66	0.64	0.06
Mean droplet diameter (Fresh samples)	0.58	-0.19	0.20
Mean droplet diameter (aged samples)	0.31	-0.51	-0.18

Three-Days WSI is an ultimate indication of emulsion stability. The size of the droplets has a major role in the stability of emulsions, and larger particles are reportedly less stable [1-3]. This is due to the faster motion of the droplets, which leads to flocculation, coalescence, and magnified settling/creaming velocities of the droplets. The results presented in **Table 5.5** and correlation coefficients in **Table 5.6** are in line with these descriptions. There is a strong positive correlation between the mean droplet diameter of the aged emulsion sample with mean droplet diameter of the fresh emulsion. Water separation was much more severe in the emulsions with large droplet sizes, with the sedimentation of coalesced droplets forming a separated water layer at the bottom of the samples.

The results show more viscous samples had smaller droplets and consequently less WSI, which implies higher kinetic stability in the emulsions. This is evident from the moderate negative correlation between the viscosity and WSI and a strong negative correlation between viscosity and the mean droplet diameter of emulsions. This agrees with the published literature indicating the rate of approach among droplets is less frequent in viscous emulsions, thus enhancing emulsion's stability [36,37].

Viscous fluids require higher mixing energy to prevent the formation of larger droplets. **Table 5.7** shows the increase in viscosity is strongly correlated with Span 83 concentration with almost no significant correlation with gilsonite concentration (this is due to the low concentrations of gilsonite selected for the experimental design). It was shown earlier that the increase in Span 83 dosage results in a higher viscosity of emulsions and reduced droplet size. The same observations are verified in this part of the study, affirming the dominance of the Span 83 effect over gilsonite in reducing the size of the droplets in more viscous emulsion samples. Reduced droplets' size in high concentrations of Span 83 can be attributed to superior and faster interfacial film coverage of droplets by surfactant molecules, which improves emulsion stability and prevents enlargement of droplets due to coalescence during homogenization [26].

Correlation coefficients shown in **Table 5.7** indicate hexane and Span 83 highly influence emulsion viscosity, and almost no significant relationship was found between gilsonite concentration and dynamic viscosity of emulsions. However, gilsonite reduces the 3-day mean droplet size in emulsions, resulting in enhanced kinetic stability of emulsions. Moreover, hexane shows a strong positive correlation with the size of the fresh emulsion droplets and a strong negative correlation with viscosity. However, no significant relation was discovered between hexane and water phase separation. Kinetic stability is primarily influenced by gilsonite and Span 83 concentration in the emulsions.

Objective Functions

Objective functions were developed to perform the final optimization and formulate the model emulsion with desired features. Maximum variations in mean droplet size of 9.18 μm for fresh emulsions and 10.02 μm for aged emulsions were recorded in the experiments. This significant variation in the mean droplet size is triggered by the concentration of the additives used, showing the feasible droplet sizes reachable for the range of additive concentrations used here. **Table 5.7** signifies all variables that affect the size of the droplets, with the strongest effect noted for hexane fraction in the oil blend.

Initially, a quadratic polynomial function was selected to find the mean droplet size in fresh emulsions based on the additives' concentrations. However, the smallest model error (MSE) achievable using GRG non-linear solver with the constraints applied was found to be 2.45. This is an implication of the relatively high non-linearity of the problem. Hence, a cubic model was nominated to develop the objective function. The irrelevant terms were excluded from the function using regression analysis, and the final form of the correlation is shown by Equation 5:

$$MDS = B_0 + B_1X1 + B_2X2 + B_{12}X1X2 + B_{13}X1X3 + B_{23}X2X3 + B_{11}X1^2 + B_{123}X1X2X3 + B_{112}X1^2X2 + B_{113}X1^2X3 + B_{133}X3^2X1 + B_{223}X2^2X3 + B_{233}X3^2X2 + B_{111}X1^3 + B_{333}X3^3 \quad (5)$$

where MDS is the fresh emulsion mean droplet diameter (μm), X1 is the hexane volumetric fraction in the oil blend, X2 is Span 83 concentration (% wt/v), and X3 is gilsonite concentration (% wt/v). MSE for this objective function is 7.73E-6 between the model predictions and the measured values, and the coefficients (B) were optimized by a genetic algorithm for the function.

Figure 5.17 shows the viscosity profiles for different recipes in **Table 5.5**, where emulsions show non-Newtonian shear-thinning behavior. In other words, the apparent viscosity of emulsions decreases at higher shear rates. This behavior is due to the presence of gilsonite and Span 83 with large molecule chains, which affect large volumes of fluid as they fall at random under low shear rate but align themselves progressively in the path of increasing shear, showing less resistance.

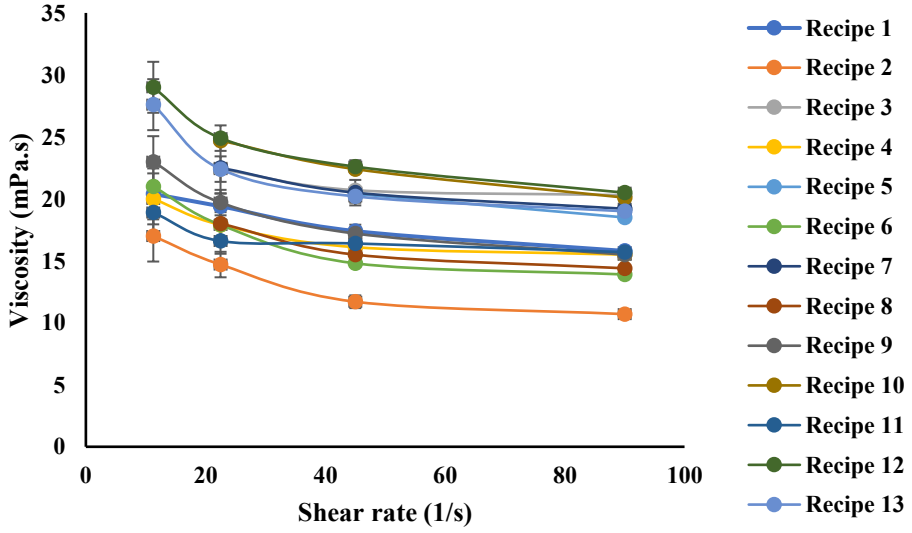

Figure 5.17: Viscosity profiles of emulsions

Figure 5.18 illustrates the shear stress measured for a range of shear rates applied to the emulsions. Flow behavior index (n) in the power-law model is higher than 0.7 and close to 1 for most recipes. This shows that although emulsions are categorized as pseudoplastic shear-thinning fluids (n<1), these fluids behave rather like Newtonian fluids. Since model emulsions are prepared to mimic the SAGD emulsion features in the reservoir, dynamic viscosity measured at a higher shear rate (90 1/s) was selected to generate the viscosity objective function. This selection was made due to the existing flow of fluids toward the producer well at the field conditions, which produces moderate shear rates in the porous media [12].

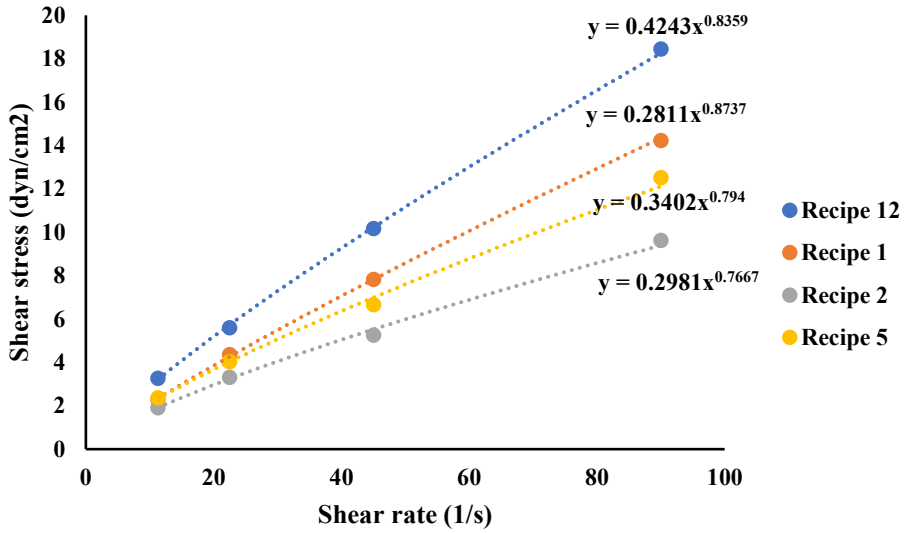

Figure 5.18: Viscosity profiles of emulsions

A quadratic model was sufficient to estimate the dynamic viscosity of emulsions as the function of additives concentrations, yielding an MSE of 0.18 between model predictions and measured values. Equation 6 displays the function developed for dynamic viscosity of emulsion, where Vis is the emulsion viscosity in mPa.s. The quadratic model coefficients were optimized using the genetic algorithm and shown in **Table 5.8** along with MDS (Mean droplet size) function coefficients. These functions were validated with three recipes, where small error values were observed between model predictions and measured values. **Table A2** in the **Appendix** section contains the validation test results.

$$Vis = C_0 + C_1X1 + C_2X2 + C_3X3 + C_{13}X1X3 + C_{23}X2X3 + C_{11}X1^2 + C_{22}X2^2 + C_{33}X3^2 \qquad (6)$$

Table 5.8: Coefficients of mean droplet size and viscosity Objective functions

MDS (Mean droplet size) function														
B0	**B1**	**B2**	**B12**	**B13**	**B23**	**B11**	**B123**	**B112**	**B113**	**B133**	**B223**	**B233**	**B111**	**B333**
-4.79	7.12	2.64	-0.66	-7.67	-28.89	-0.58	-0.07	0.02	0.72	-3.51	3.93	31.95	0.01	183.04

Vis (Dynamic viscosity) function								
C0	**C1**	**C2**	**C3**	**C13**	**C23**	**C11**	**C22**	**C33**
6.93	1.12	3.14	14.96	-0.69	-0.47	-0.07	-0.30	-8.81

Three-Day WSI values presented in **Table 5.5** show most of the recipes exhibit resistance to water phase separation, indicating excellent kinetic stability in emulsions. Water phase separation occurs

only in emulsions that contain the lowest concentration of Span 83 (lower bound concentration "X2 = -1"). This observation can be explained by the strong inverse correlation between X2 (Span 83) and 3-day WSI, as shown in **Table 5.7**. Again, this shows that a blend of surfactants is much more effective in stabilizing the emulsions than the cases shown previously, where base emulsion stabilized only by Span 83 in lower concentrations showed immediate and significant water phase separation.

Figure 5.19 shows the contour plot of 3-Days WSI for Span 83 concentration of 1.2% wt/v, which is the lower bound concentration of X2 and the only dosage for which water phase separation occurs. The piecewise linear interpolation method was used for the estimation of 3-day WSI between the measured data points. According to this figure, emulsions with the lowest fraction of hexane in the oil blend resist water phase separation. This is because of the higher viscosity and smaller droplet size, which enhance the kinetic stability of emulsions.

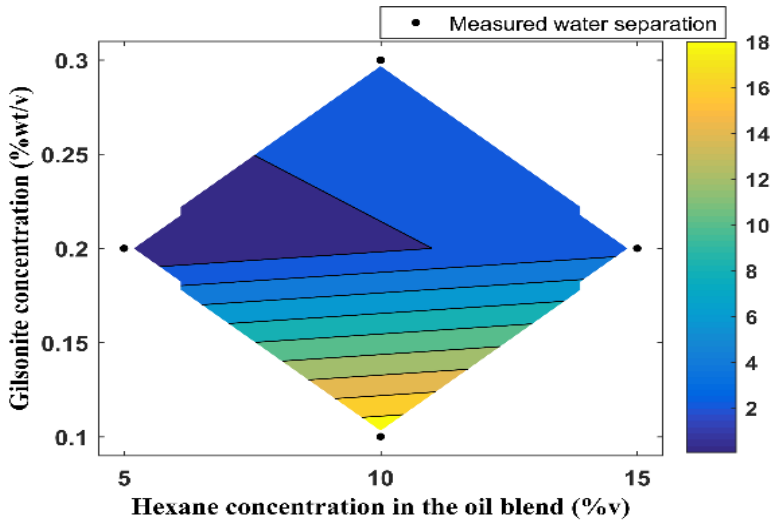

Figure 5.19: 3-Days WSI (%) contour map for emulsion samples containing 1.2% wt/v Span 83

Gilsonite plays an essential role in stabilizing emulsions when the hexane fraction increases in the oil blend. A significant difference in water separation is detectable in emulsions prepared with 10 v% hexane in the oil blend with and without gilsonite. The 16% difference in 3-Days WSI of emulsions with 10 v% hexane can be attributed to the presence of gilsonite in the system, where emulsion with 0.3% wt/v is much more stable than the emulsion with 0.1% wt/v. In combination with Span 83, Gilsonite forms stronger and rigid interfacial films around the droplets, which stabilize the emulsions sterically and prevent coalescence of the droplets. Since most of the recipes show excellent resistance to water phase separation, a decision was made to continue the optimization without an objective function for emulsions' stability. Just a constraint was implemented in the final optimization, dictating the search to continue if the final recipe contains 1.2% wt/v Span 83 and 10 v% hexane in the oil blend.

Optimization and Final Recipe

In the final stage of the research, the objective functions were used to find the optimal concentrations for additives that yield the SAGD emulsion features in terms of mean droplet size,

dynamic viscosity, and kinetic stability. For this purpose, SAGD features were set as goals in the optimization problem with the mean droplet diameter of 13 µm and viscosity of 15 mPa.s. The Golden-section search method was employed to perform the optimization. As previously described, a condition was introduced in the code to continue the search if the final recipe contains 1.2% wt/v Span 83 and 10 v% hexane in the oil blend.

The final recipe resulted from the optimization comprises of 5 v% hexane, 1.2% wt/v Span 83, and 0.1046% wt/v gilsonite, with a dynamic viscosity of 15.06 mPa.s and mean droplet size of 13.06 µm based on the model predictions with a slight deviation from the desired features due to the tradeoffs that had to be made to obtain the goals simultaneously. The model emulsion was prepared with the finalized recipe components and concentrations and examined for the size of the droplets, dynamic viscosity, and kinetic stability.

Figure 5.20 displays the micrograph of the model emulsion. **Figure 5.21** shows the number-based distribution of droplet diameters and histogram for three sample emulsions. **Figure 5.22** illustrates the comparison between the fresh emulsion and aged emulsion in terms of the size of the droplets for one sample. Mean droplet size averaged for the three samples yields a value of 13.54 µm with a sample standard deviation of 1.75. The mean droplet diameter of the emulsion aged for three days is 15.76 µm, indicating a 16.39% enlargement in the mean droplet diameter compared with the fresh emulsion.

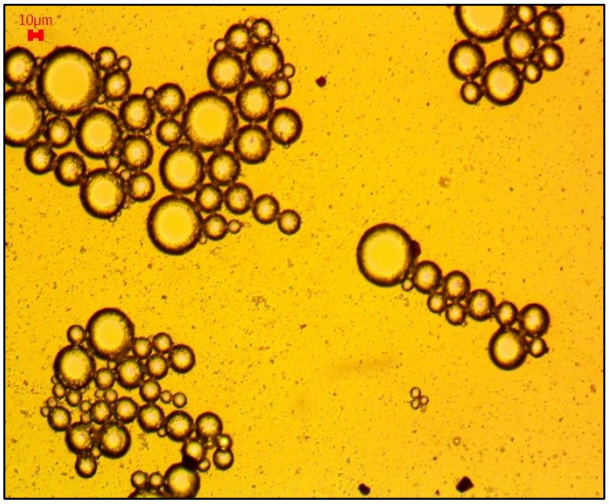

Figure 5.20: Micrograph of the model emulsion

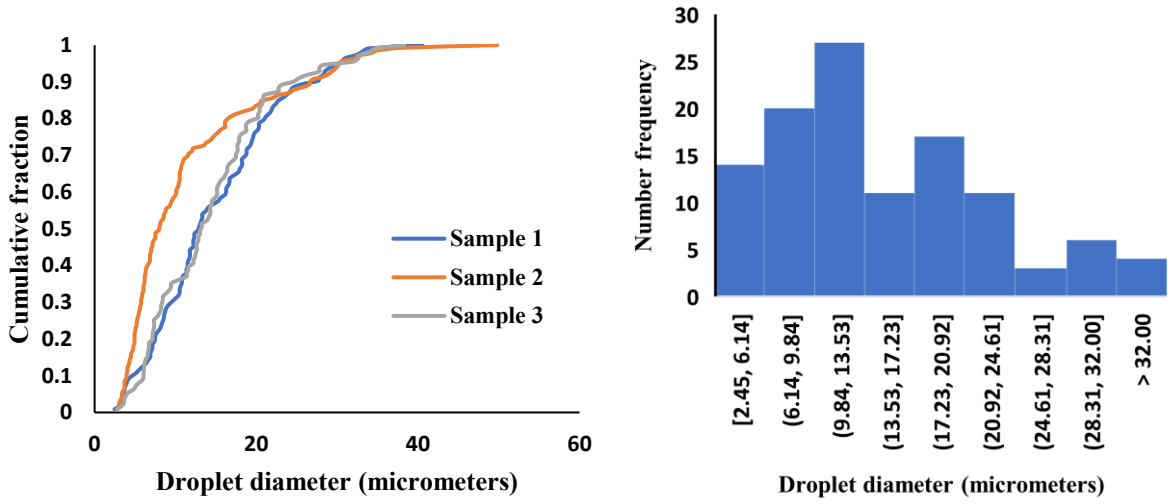

Figure 5.21: Left) Number-based distribution of emulsion droplet diameters for three samples. Right) Histogram of droplet diameters for sample 1

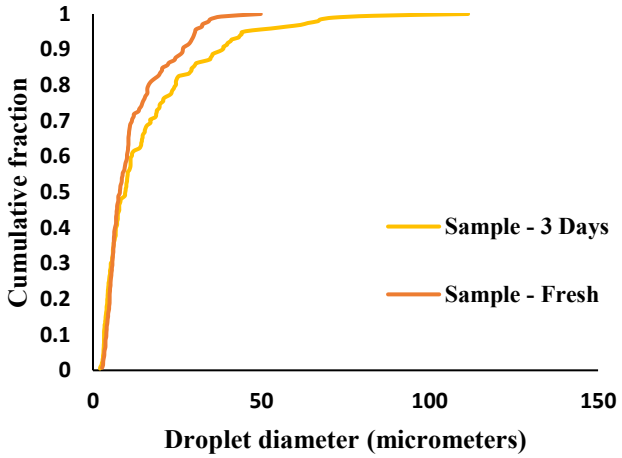

Figure 5.22: Comparison of droplet size between fresh and aged sample emulsion

The mean droplet diameter is 4.15% larger than the target size, indicating a reasonable accuracy considering the standard deviation and variability in droplet size associated with sampling. For all samples shown in **Figure 5.21**, the median is smaller than the mean droplet diameter, which indicates the distribution is positively (Right) skewed. However, median and mean are relatively close for the sample emulsions; for instance, sample 3 has a median of 13.26 µm and a mean of 14.80 µm. Therefore, slight skewness in the sample emulsions implies that most droplets have a smaller size than the mean droplet diameter but close to the mean diameter. The histogram in **Figure 5.21** affirms this and shows that the frequency of the droplets in the 9.84 µm -13.53 µm size range is the highest. This type of distribution is desirable as most of the studies on SAGD in-situ emulsions report most of the droplets fall within the 10 µm -15 µm size range.

Figure 5.20 shows although flocculation is observed in the sample emulsions, which is typical behavior of the w/o emulsion due to the non-polarity of the continuous phase, droplets do not coalesce upon collision and flocculation. The micrograph shows that the emulsion is sterically

stabilized by the blend of non-ionic surfactant and gilsonite, acting as mechanical barriers between the droplets. The enlargement after three days is 16.39% which is small compared to the recipes in **Table 5.5** for which water phase separation transpired. Moreover, the mean droplet diameter after three days is 15.76 μm which is amongst the small values with reference to the size of the emulsion droplet sizes after the three days aging period shown in **Table 5.5**. The result of such behavior should be reflected in the kinetic stability of emulsions.

A bottle test was carried out for the model emulsion, and no phase separation was recorded for this recipe. However, sedimentation brings about the formation of distinguishable layers in emulsions with time. This happens due to the density difference between water and oil phases that leads to establishing a milky layer where most of the water droplets are located and a creamy layer of dilute emulsion phase. **Figure 5.23** displays the fresh emulsion and aged emulsion sample. It was observed that gentle stirring could prevent and reverse the layering in emulsion samples. Finally, the dynamic viscosity of fresh emulsion samples was measured, and the viscosity profile is shown in **Figure 5.24**. Viscosity at the shear rate of 90 1/s was found to be 15.2 mPa.s, 1.33% larger than the target SAGD in-situ emulsion viscosity.

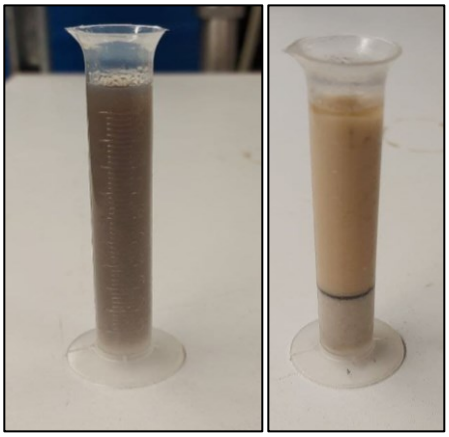

Figure 5.23: Left) Fresh model emulsion; Right) Aged model emulsion.

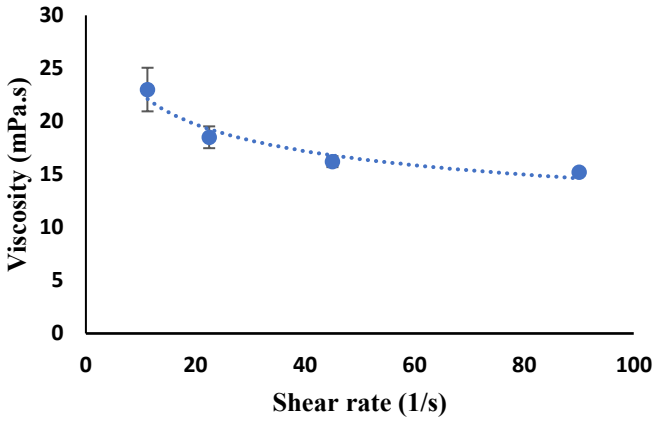

Figure 5.24: Viscosity profile of the model emulsion

To summarize, the measurements show that the model emulsion mimics the bulk properties and features of the SAGD in-situ emulsion in terms of mean droplet size, dynamic viscosity, and kinetic stability. The optimized model emulsion replicates these features with excellent accuracy and has unique features such as asphaltene precipitates in the system. This model fluid is intended for use in sand pack and flowline testing to evaluate the well productivity and productivity issues associated with SAGD and solvent-SAGD operations. It could potentially eliminate the need to use hazardous bituminous emulsions and the difficult process of asphaltene extraction from the bitumen.

Conclusion

This study presents a workflow to produce a model emulsion with features similar to field emulsion properties, focusing on SAGD in-situ emulsion characteristics. To this end, features that affect the emulsion flow were selected and include the type of emulsion, water content, dynamic viscosity, kinetic stability, droplet size, and asphaltene precipitation. HLD criterion was utilized to select surfactants to stabilize the emulsions. The base recipe was tested for the viscosity, droplet size, and stability, where the effect of surfactant(s) concentration on these features was investigated. The screening results show that the blend of Span 83 and gilsonite enhances the stability of the model emulsion, and gilsonite, which is mainly composed of asphaltene, can be used to replicate the asphaltene precipitation in field conditions due to the change in oil composition. Other components such as hexane were selected in the evaluation stage of the research to adjust the emulsion features to establish the feasible solution domain where it is possible to replicate SAGD emulsion features. Objective functions were developed for viscosity and mean droplet diameter as functions of Span 83, gilsonite, and oil composition. The final recipe for model emulsion was determined by optimization, and the model emulsion was shown to replicate the SAGD emulsion features with excellent accuracy. Other significant findings in this study include determining correlations between w/o emulsion features such as stability, fresh emulsion droplet size, aged emulsion droplet size, viscosity, and the effect of hexane concentration, gilsonite concentration, Span 83 concentration on these features. Moreover, it was shown that asphaltene in gilsonite reduces the IFT in the system due to the hydrogen bonding between asphaltenes and water. Also, the results of molecular simulation verified with experiments indicate the asphaltene molecules tend to partition towards the oil-water interface in paraffinic oil, unlike the reported results on

aromatic oil systems. Hydrogen bonds between water and asphaltene molecules maintain the position of the asphaltene aggregates at the oil-water interface. It was found that asphaltene self-association in terms of π-π covalent bonding, asphaltene-asphaltene hydrogen bonding, and water-asphaltene hydrogen bonding, all contribute to the asphaltene aggregation process. Face-to-facing stacking was the dominant morphology of aggregated asphaltenes. Such behavior in the system led to the improved kinetic stability of the emulsions. Finally, the onset of asphaltene precipitation was found at 20 v% hexane in the oil blend at the lab temperature and pressure conditions.

Nomenclature

APE: Asphaltene Precipitation Envelope
Cc: Characteristic Curvature
CMC: Critical Micelle Concentration
CSS: Cyclic Steam Stimulation
DI Water: Deionized Water
EACN: Equivalent Alkane Number
ES-SAGD: Expanding Solvent Steam Assisted Gravity Drainage
HLB: Hydrophilic Lipophilic Balance
HLD: Hydrophilic Lipophilic Deviation
IFT: Interfacial Tension
M: Molarity
ppm: Parts Per Million
rpm: Rounds Per Minute
SAGD: Steam Assisted Gravity Drainage
SARA: Saturates Aromatics Resins Asphaltenes
TDS: Total Dissolved Solids

References

[1] Schramm, L.L., 1992. Fundamentals and applications in the petroleum Industry. *Adv. Chem*, *231*, pp.3-24.
[2] Leal-Calderon, F., Schmitt, V. and Bibette, J., 2007. *Emulsion science: basic principles*. Springer Science & Business Media.
[3] Sjoblom, J. *Encyclopedic Handbook of Emulsion Technology*; CRC Press, 2001.
[4] Butler, R.M., 1991. Thermal recovery of oil and bitumen., Vol. 46, Prentice Hall, Englewood Cliffs, NJ (1991)
[5] Butler, R.M., 1985. A new approach to the modelling of steam-assisted gravity drainage. *Journal of Canadian Petroleum Technology*, *24*(03), pp.42-51.
[6] Butler, R.M. and Stephens, D.J., 1981. The gravity drainage of steam-heated heavy oil to parallel horizontal wells. *Journal of Canadian Petroleum Technology*, *20*(02).
[7] Butler, R.M., McNab, G.S. and Lo, H.Y., 1981. Theoretical studies on the gravity drainage of heavy oil during in-situ steam heating. *The Canadian journal of chemical engineering*, *59*(4), pp.455-460.
[8] Mohammadzadeh, O. and Chatzis, I., 2010. Pore-level investigation of heavy oil recovery using steam assisted gravity drainage (SAGD). *Oil & Gas Science and Technology–Revue d'IFP Energies nouvelles*, *65*(6), pp.839-857.
[9] Jamaluddin, A.K.M. and Butler, R.M., 1988. Factors Affecting the Formation of Water-in-Oil Emulsions During Thermal Recovery. *AOSTRA J. Research*, *4*(2), pp.109-116.

[10] Chung, K.H. and Butler, R.M., 1988. Geometrical effect of steam injection on the formation of emulsions nn the steam-assisted gravity drainage process. *Journal of Canadian Petroleum Technology*, *27*(01).
[11] Sasaki, K., Akibayashi, S., Yazawa, N., Doan, Q.T. and Ali, S.M., 2001. Experimental modeling of the SAGD process-enhancing SAGD performance with periodic stimulation of the horizontal producer. *SPE Journal*, *6*(01), pp.89-97.
[12] Velayati, A. and Nouri, A., 2020. Emulsification and emulsion flow in thermal recovery operations with a focus on SAGD operations: A critical review. *Fuel*, *267*, p.117141.
[13] Wang, C., Pang, Y., Mahmoudi, M., Haftani, M., Salimi, M., Fattahpour, V. and Nouri, A., 2020. A set of graphical design criteria for slotted liners in steam assisted gravity drainage production wells. *Journal of Petroleum Science and Engineering*, *185*, p.106608.
[14] Kokal, S.L., 2005. Crude oil emulsions: A state-of-the-art review. *SPE Production & facilities*, *20*(01), pp.5-13.
[15] Bennion, D.B., Chan, M.Y.S., Sarioglu, G., Courtnage, D., Wansleeben, J. and Hirata, T., 1993, January. The in-situ formation of bitumen-water-stable emulsions in porous media during thermal stimulation. In *SPE International Thermal Operations Symposium*. Society of Petroleum Engineers.
[16] Speight, J.G., 2015. *Handbook of petroleum product analysis*. John Wiley & Sons.
[17] RICHARDSON, E., 1937. THE PHYSICAL PROPERTIES OF DISPERSE SYSTEMS. *Science Progress (1933-)*, *31*(123), pp.462-475.
[18] Taylor, G.I., 1932. The viscosity of a fluid containing small drops of another fluid. *Proceedings of the Royal Society of London. Series A, Containing Papers of a Mathematical and Physical Character*, *138*(834), pp.41-48.
[19] Einstein, A., 1906. Calculation of the viscosity-coefficient of a liquid in which a large number of small spheres are suspended in irregular distribution. *Ann. Phys. Leipzig*, *19*, pp.286-306.
[20] Kumasaka, J., Sasaki, K., Sugai, Y., Alade, O.S. and Nakano, M., 2016. Measurement of viscosity alteration for emulsion and numerical simulation on bitumen production by SAGD considering in-situ emulsification. *Journal of Earth Science and Engineering*, *6*(1), pp.10-17.
[21] Mahmoudi Eshkaftaki, M., 2017. New sand control design criteria and evaluation testing for steam assisted gravity drainage (SAGD) wellbores.
[22] Kokal, S. L.; Sayegh, S. G. January. Asphaltenes: The cholesterol of petroleum, *Middle East Oil Show*; Society of Petroleum Engineers, 1995
[23] Kokal, S. L.; Al-Dokhi, M. January. Case studies of emulsion behavior at reservoir conditions. *SPE Middle East Oil and Gas Show and Conference*; Society of Petroleum Engineers, 2007
[24] Yuan, B. and Wood, D.A. eds., 2018. *Formation damage during improved oil recovery: Fundamentals and applications*. Gulf Professional, 2018; pp 243– 273
[25] Mohammed, I., Mahmoud, M., Al Shehri, D., El-Husseiny, A. and Alade, O., 2020. Asphaltene precipitation and deposition: A critical review. *Journal of Petroleum Science and Engineering*, p.107956.
[26] Velayati, A. and Nouri, A., 2020. Physical features' characterization of the water-in-mineral oil macro emulsion stabilized by a nonionic surfactant. *Journal of Dispersion Science and Technology*, pp.1-16.
[27] Opawale, F.O. and Burgess, D.J., 1998. Influence of interfacial properties of lipophilic surfactants on water-in-oil emulsion stability. *Journal of colloid and interface science*, *197*(1), pp.142-150.

[28] Nciri, N., Song, S., Kim, N. and Cho, N., 2014. Chemical characterization of gilsonite bitumen. *Journal of Petroleum & Environmental Biotechnology*, *5*(5), p.1.
[29] Sorbitan sesquioleate. SID S3386 [online]; Sigma-Aldrich: St. Louis, MO, USA. Source: https://www.sigmaaldrich.com/catalog/product/sigma/s3386?lang=en&region=CA (acce ssed 18 May, 2020).
[30] Effective surfactant selection & Formulation of (micro-)emulsions via HLD-NAC. Vlsi presentation. Source: https://www.in-cosmetics.com/__novadocuments/366543?v=636332029055230000 (accessed 18 May, 2020).
[31] Abbott, S. *Surfactant Science: Principles and Practice*, Update 1; Destech Pubns Inc, 2016; pp 2– 26.
[32] Kiran, S.K., Acosta, E.J. and Moran, K., 2009. Evaluating the hydrophilic–lipophilic nature of asphaltenic oils and naphthenic amphiphiles using microemulsion models. *Journal of colloid and interface science*, *336*(1), pp.304-313.
[33] Rashidnia, N., Balasubramaniam, R. and Delsignore, D., 1992. Interfacial tension measurement of immiscible liq uids using a capillary tube. *NASA STI/Recon Technical Report N*, *92*, p.21262.
[34] NIST/SEMATECH e-Handbook of Statistical Methods, http://www.itl.nist.gov/div898/handbook/, 26 March, 2021.
[35] Kiefer, J., 1953. Sequential minimax search for a maximum. *Proceedings of the American mathematical society*, *4*(3), pp.502-506.
[36] Cardoso-Ugarte, G.A., Ramírez-Corona, N., López-Malo, A., Palou, E., San Martín-González, M.F. and Jiménez-Munguía, M.T., 2018. Modeling phase separation and droplet size of W/O emulsions with oregano essential oil as a function of its formulation and homogenization conditions. *Journal of Dispersion Science and Technology*, *39*(7), pp.1065-1073.
[37] Bouchemal, K., Briançon, S., Perrier, E. and Fessi, H., 2004. Nano-emulsion formulation using spontaneous emulsification: solvent, oil and surfactant optimisation. *International journal of pharmaceutics*, *280*(1-2), pp.241-251.
[38] Velayati, A. and Nouri, A., 2021. Role of Asphaltene in Stability of Water-in-Oil Model Emulsions: The Effects of Oil Composition and Size of the Aggregates and Droplets. *Energy & Fuels*.
[39] Ali, M.F. and Alqam, M.H., 2000. The role of asphaltenes, resins and other solids in the stabilization of water in oil emulsions and its effects on oil production in Saudi oil fields. *Fuel*, *79*(11), pp.1309-1316.
[40] Piroozian, A., Hemmati, M., Safari, M., Rahimi, A., Rahmani, O., Aminpour, S.M. and Pour, A.B., 2021. A mechanistic understanding of the water-in-heavy oil emulsion viscosity variation: effect of asphaltene and wax migration. *Colloids and Surfaces A: Physicochemical and Engineering Aspects*, *608*, p.125604.
[41] Yaseen, S. and Mansoori, G.A., 2017. Molecular dynamics studies of interaction between asphaltenes and solvents. *Journal of Petroleum Science and Engineering*, *156*, pp.118-124.
[42] Song, X., Shi, P., Zhao, S., Duan, M., Wang, C. and Ma, Y., 2016. Dissipative particle dynamics study on the aggregation behavior of asphaltenes under shear fields. *Industrial & Engineering Chemistry Research*, *55*(33), pp.9077-9086.
[43] Li, K., Vasiliu, M., McAlpin, C.R., Yang, Y., Dixon, D.A., Voorhees, K.J., Batzle, M., Liberatore, M.W. and Herring, A.M., 2015. Further insights into the structure and chemistry of the Gilsonite asphaltene from a combined theoretical and experimental approach. *Fuel*, *157*, pp.16-20.

[44] Yaseen, S. and Mansoori, G.A., 2018. Asphaltene aggregation due to waterflooding (A molecular dynamics study). *Journal of Petroleum Science and Engineering*, *170*, pp.177-183.
[45] Frigerio, F. and Molinari, D., 2011. A multiscale approach to the simulation of asphaltenes. *Computational and Theoretical Chemistry*, *975*(1-3), pp.76-82.

Appendix 5.A

Table 5.A1: Onset of asphaltene precipitation test results

Hexane fraction in the oil blend	Mean aggregate size (micrometer)	Maximum aggregate size (micrometer)	Standard deviation
0	1.94	4.63	1.37
0.15	2.41	6.25	1.67
0.19	2.46	9.22	2.68
0.225	3.2	19.01	3.23
0.3	3.49	19.2	3.85

Table 5.A2: Validation test results

Recipes				Viscosity (mPa.s)		Mean droplet diameter (µm)		Errors
Recipe number	X1 (vol fraction)	X2 (%wt/v)	X3 (%wt/v)	Model prediction	Measured	Model prediction	Measured	Viscosity MSE
1	12	1.5	0.3	14.68	14.85	14.88	14.65	14.88
2	8	3	0.1	18.57	18.35	12.78	12.87	Mean droplet size MSE
3	10	2	0.2	16.84	16.8	11.36	11.22	13.00

Chapter 6: Conclusions and Contributions

6.1 Conclusions and Contributions

A model emulsion was introduced which replicates the features of SAGD reservoir emulsion in terms of the type of emulsions, dynamic viscosity, emulsified water content, kinetic stability, and asphaltene precipitation. The model emulsion can be used in SAGD lab testing practices (SRT, SCT, FCT, and flow line experiments), replacing the current single-phase flow or multi-phase separated flow injection scenarios to evaluate the production and productivity issues more realistically. This could lead to the reduction of costs and hazards associated with the utilization of bitumen in the experiments.

The research was conducted in a stepwise manner, where the effect of various parameters on the emulsion features was investigated. The conclusions and contributions can be summarized as follows:

1. A model emulsion was introduced which replicates SAGD emulsion features at room temperature and pressure conditions.
2. A framework was presented which allows adjusting the emulsion features for any target emulsion.
3. A comprehensive characterization of w/o macro emulsion stabilized by a non-ionic surfactant (Span 83) was carried out.
    a. Higher mixing rate and mixing time in homogenization correspond to the formation of smaller droplets in the emulsion. The change in droplet size is insignificant after a certain mixing time for all shear rates.
    b. Number-based distributions are the preferred method for representing emulsion droplet sizes using optical microscopy. This is the case due to the sensitivity of the optical microscopy technique to the sampling and microscope limited field of view. A number-based distribution such as mean droplet diameter is reproducible for an emulsion sample due to the equal weight of each droplet in the calculation of the representative size.
    c. Increased Span 83 concentration resulted in a reduction of droplet diameter due to the better interfacial film coverage during homogenization and improved stability of emulsions.
    d. The viscosity of emulsion magnifies with water content and emulsions exhibit non-Newtonian shear thinning behavior at higher water fractions in the emulsion. This pseudoplastic behavior is due to the presence of large molecules (Span 83) that fall at random at low shear rates but align themselves parallel to the direction of shear at higher mixing rates, thus showing less resistance to flow at high shear rates.
    e. A correlation was introduced which captures the shear thinning behavior in emulsions. This correlation is a function of shear rate and emulsified water content.
    f. Reversible flocculation was observed in emulsions due to the thin EDL in w/o emulsions. The flocculation was more severe in presence of an electrolyte.
    g. A threshold electrolyte concentration was detected after which coalescence occurs upon droplets collision and flocculation. Salting-out is responsible for the misorientation of the surfactant molecules in high salinity conditions that results in

instability of emulsions through the coalescence of the droplets and water phase separation.

h. The sedimentation rate was found to be faster in dilute emulsions. This is the case because of the lower stability and viscosity of dilute emulsions.
i. Concentrated emulsions display higher kinetic stability even in high salinity conditions. This is due to the higher viscosity of concentrated emulsions and reduced rate of approach among droplets.

4. Reducing the viscosity of the continuous phase by adding hexane to the oil blend resulted in the formation of emulsions with lower viscosity. Emulsions with higher hexane fractions in the primary phase were less stable. For similar reasons, the size of the droplets for emulsion with higher hexane content in the oil phase was larger.
5. Gilsonite was introduced as a new additive that can be used to mimic the asphaltene precipitation behavior in emulsions.
6. The higher gilsonite concentration in the emulsion is associated with the higher dynamic viscosity of emulsions. Gilsonite is a well-known viscosifying agent.
7. The consensus that thermodynamics governs the stability of emulsions by asphaltene was challenged, an integrated colloidal-thermodynamics approach was offered as an alternative.
8. The following conditions can describe the stability of w/o emulsion by asphaltenes through an integrated colloidal-thermodynamics perspective:
    a. Asphaltene precipitation: It was demonstrated that emulsions with higher asphaltene precipitation were more stable.
    b. Aggregation of asphaltene: Precipitated asphaltene molecules form nano and micro aggregates, where the aggregates clump together establishing flocs.
    c. The size of the aggregates and droplets: The relative size of the aggregates to droplets can significantly influence the stability of emulsions. Our experiments show that the smaller aggregates to droplets size ratio correspond to improved kinetic stability of emulsions if all the other conditions are met. This size ratio is strongly influenced by water content, viscosity, oil composition, and so on.

9. The size of the asphaltene aggregates is influenced by oil composition and gilsonite concentration. The higher the concentration of gilsonite, the larger the size of the aggregates. Adding toluene in the oil blend (aromatic compounds) results in the reduction in the number and size of the asphaltene aggregates due to the solubility of asphaltene molecules in aromatic compounds.

10. Asphaltene self-association (π-π covalent bonding), asphaltene-asphaltene hydrogen bonding, and asphaltene-water hydrogen bonding all contribute to the asphaltene aggregation process in a system of n-alkane oil in interface contact with water (emulsion).

11. Face-to-Face stacking of asphaltene aggregation morphology was observed for the emulsion prepared with n-alkane oil. This aggregation morphology is primarily induced by π-π covalent bonding and asphaltene molecules' self-association.

12. Interfacial tension in emulsion decreased due to the hydrogen bonding between water and asphaltene molecules at the oil-water interface.
13. Emulsions with gilsonite in the system were stabilized by steric hindrance and reduced interfacial tension. The resistance to water phase separation was promoted in these emulsions despite the presence of electrolytes in the system.
14. In the emulsions prepared with n-alkane oil, the tendency of the asphaltene aggregates to settle at the oil-water interface was observed in both MD simulation and experiments.

6.2 Future Work

Current SAGD lab testing practices overlook the emulsion flow. The model emulsion can be used in sand pack (SRT, SCT, FCT), core flooding, and flowline testing to characterize the emulsion flow and its effect on production and productivity issues such as sand production, fines migration, formation damage, and pressure drops in flowlines, among others.

The emulsion flow scenario should be embedded in the testing statement of procedure (SOP) to replace the separate multiphase flow injection stages with emulsion and free water phase injection. Moreover, the model emulsion can be used in flow line testing to investigate the pressure drops in emulsion flow and develop models for the fluid flow in pipes.

The current model emulsion is developed at ambient temperature and pressure conditions. In case the sand pack and flowline testing are designed to operate at high pressure and temperature conditions, the model emulsion needs to be re-evaluated and adjusted accordingly for the new operating environments.

The features of the model emulsions prepared in this research are prone to change with a different homogenization setting and beaker (container) size. One may need to use a different technique to prepare model emulsions at a larger scale for the sand pack testing. In this case, the workflow presented in Figure 5.2 must be followed to reach the target properties in emulsions with the recipe introduced in this research. In other words, the required concentration of the additives used in the recipe may be different if another emulsification technique is used or the size of the container and blade assembly are chosen differently than the ones employed in this study.

Acknowledgments

We would like to acknowledge and immensely appreciate the Future Energy Systems (FES) for financial support of the research project “Thermal Well Design and Testing”.

Bibliography

Abbott, S. Surfactant Science: Principles and Practice, Update 1; *Destech Pubns* Inc, 2016; pp 2– 26.

Abdurahman, N.H. and Mahmood, W.K., 2012. Stability of water-incrude oil emulsions: effect of cocamide diethanolamine (DEA) and Span 83. *International Journal of Physical Sciences*, *7*(41), pp.5585-5597.

Akbari, S., Nour, A.H., Jamari, S.S. and Fayaz, F., 2006. Rheology and stability mechanism of water-in-crude oil emulsions stabilized by span 83. *ARPN Journal of Engineering and Applied Sciences*, *11*(4).

Alboudwarej, H., Muhammad, M., Shahraki, A.K., Dubey, S., Vreenegoor, L. and Saleh, J.M., 2007. Rheology of heavy-oil emulsions. *SPE Production & Operations*, *22*(03), pp.285-293.

Ali, M.F. and Alqam, M.H., 2000. The role of asphaltenes, resins and other solids in the stabilization of water in oil emulsions and its effects on oil production in Saudi oil fields. Fuel, 79(11), pp.1309-1316.

Aronson, M.P. and Petko, M.F., 1993. Highly concentrated water-in-oil emulsions: Influence of electrolyte on their properties and stability. *Journal of colloid and interface science*, *159*(1), pp.134-149.

ASTM D4007, 2011. Standard Test Method for Water and Sediment in Crude Oil by the Centrifuge Method (Laboratory Procedure).

ASTM, C., 2012. Standard test method for compressive strength of cylindrical concrete specimens. *ASTM C39/C39M-12*.

Aziz, H.M.A., Darwish, S.F. and Abdeen, F.M., 2002, January. Downhole emulsion problem, the causes and remedy, Ras Budran Field. In *SPE Asia Pacific Oil and Gas Conference and Exhibition*. Society of Petroleum Engineers.

Azom, P.N. and Srinivasan, S., 2009, January. Mechanistic modeling of emulsion formation and heat transfer during the steam-assisted gravity drainage (SAGD) process. In *SPE Annual Technical Conference and Exhibition*. Society of Petroleum Engineers.

Balsamo, M., Erto, A. and Lancia, A., 2017. Chemical demulsification of model water-in-oil emulsions with low water content by means of ionic liquids. *Brazilian Journal of Chemical Engineering*, *34*(1), pp.273-282.

Balsamo, V., Nguyen, D. and Phan, J., 2014. Non-conventional techniques to characterize complex SAGD emulsions and dilution effects on emulsion stabilization. *Journal of Petroleum Science and Engineering*, *122*, pp.331-345.

Bancroft, W.D., 1913. The theory of emulsification, V. *The Journal of Physical Chemistry*, *17*(6), pp.501-519.

Bennion, D.B., Chan, M.Y.S., Sarioglu, G., Courtnage, D., Wansleeben, J. and Hirata, T., 1993, January. The in-situ formation of bitumen-water-stable emulsions in porous media during thermal stimulation. In *SPE International Thermal Operations Symposium*. Society of Petroleum Engineers.

Binks, B.P. and Clint, J.H., 2002. Solid wettability from surface energy components: relevance to Pickering emulsions. *Langmuir*, *18*(4), pp.1270-1273.

Bosch, R., Axcell, E., Little, V., Cleary, R., Wang, S., Gabel, R. and Moreland, B., 2004. A novel approach for resolving reverse emulsions in SAGD production systems. *The Canadian Journal of Chemical Engineering*, *82*(4), pp.836-839.

Bouchemal, K., Briançon, S., Perrier, E. and Fessi, H., 2004. Nano-emulsion formulation using spontaneous emulsification: solvent, oil and surfactant optimisation. *International journal of pharmaceutics*, *280*(1-2), pp.241-251.
Brinkman, H.C., 1952. The viscosity of concentrated suspensions and solutions. *The Journal of Chemical Physics*, *20*(4), pp.571-571.
BROUGHTON, J., AND SQUIRES, L., 1938. *J. Phys. Chem*, *42*, p.252.
Burris, M.V., Burris Michael V, 1978. Asphalt emulsion paving composition. U.S. Patent 4,094,696.
Burris, M.V., Burris Michael V, 1986. Gilsonite-asphalt emulsion composition. U.S. Patent 4,621,108.
Butler, R.M. and Mokrys, I.J., 1998. Closed-loop extraction method for the recovery of heavy oils and bitumens underlain by aquifers: the VAPEX process. *Journal of Canadian Petroleum Technology*, *37*(04).
Butler, R.M. and Stephens, D.J., 1981. The gravity drainage of steam-heated heavy oil to parallel horizontal wells. *Journal of Canadian Petroleum Technology*, *20*(02).
Butler, R.M., 1985. A new approach to the modelling of steam-assisted gravity drainage. *Journal of Canadian Petroleum Technology*, *24*(03), pp.42-51.
Butler, R.M., 1991. *Thermal recovery of oil and bitumen* (Vol. 46). Englewood Cliffs, NJ: Prentice Hall.
Butler, R.M., McNab, G.S. and Lo, H.Y., 1981. Theoretical studies on the gravity drainage of heavy oil during in-situ steam heating. *The Canadian journal of chemical engineering*, *59*(4), pp.455-460.
Butler, R.M., Stephens, D.J. and Weiss, M., 1980, October. The vertical growth of steam chambers in the in-situ thermal recovery of heavy oils. In *Proc. 30 th Can. Chem. Eng. Conf*(Vol. 4, pp. 1152-1160).
Cardoso-Ugarte, G.A., Ramírez-Corona, N., López-Malo, A., Palou, E., San Martín-González, M.F. and Jiménez-Munguía, M.T., 2018. Modeling phase separation and droplet size of W/O emulsions with oregano essential oil as a function of its formulation and homogenization conditions. *Journal of Dispersion Science and Technology*, *39*(7), pp.1065-1073.
Chung, K.H. and Butler, R.M., 1988. Geometrical effect of steam injection on the formation of emulsions nn the steam-assisted gravity drainage process. *Journal of Canadian Petroleum Technology*, *27*(01).
Colucci, G., Santamaria-Echart, A., Silva, S.C., Fernandes, I.P., Sipoli, C.C. and Barreiro, M.F., 2020. Development of Water-in-Oil Emulsions as Delivery Vehicles and Testing with a Natural Antimicrobial Extract. *Molecules*, *25*(9), p.2105.
Cuthiell, D., Green, K., Chow, R., Kissel, G. and McCarthy, C., 1995, January. The in situ formation of heavy oil emulsions. In *SPE International Heavy Oil Symposium*. Society of Petroleum Engineers.
Dalmazzone, C., Noik, C., Glenat, P. and Dang, H.M., 2010. Development of a methodology for the optimization of dehydration of extraheavy-oil emulsions. *SPE Journal*, *15*(03), pp.726-736.
Dan, D. and Jing, G., 2006. Apparent viscosity prediction of non-Newtonian water-in-crude oil emulsions. *Journal of Petroleum Science and Engineering*, *53*(1-2), pp.113-122.
Daryasafar, A., Masoudi, M., Kord, S. and Madani, M., 2020. Evaluation of different thermodynamic models in predicting asphaltene precipitation: A comparative study. Fluid Phase Equilibria, p.112557.

Das, S.K. and Butler, R.M., 1998. Mechanism of the vapor extraction process for heavy oil and bitumen. *Journal of Petroleum Science and Engineering*, *21*(1-2), pp.43-59.
De Boer, R.B., Leerlooyer, K., Eigner, M.R.P. and Van Bergen, A.R.D., 1995. Screening of crude oils for asphalt precipitation: theory, practice, and the selection of inhibitors. SPE Production & Facilities, 10(01), pp.55-61.
Dean, E.W. and Stark, D.D., 1920. A Convenient Method for the Determination of Water in Petroleum and Other Organic Emulsions. *Industrial & Engineering Chemistry*, *12*(5), pp.486-490.
Driscoll, D.F., Etzler, F., Barber, T.A., Nehne, J., Niemann, W. and Bistrian, B.R., 2001. Physicochemical assessments of parenteral lipid emulsions: light obscuration versus laser diffraction. *International journal of pharmaceutics*, *219*(1-2), pp.21-37.
Ebnesajjad, S., 2011, Handbook of Adhesives and Surface Preparation. William Andrew Publishing.
Effective surfactant selection & Formulation of (micro-)emulsions via HLD-NAC. Vlsi presentation. Source: https://www.in-cosmetics.com/__novadocuments/366543?v=636332029055230000 (accessed May 18, 2020)
Eilers, H., 1943. Kolloid-Z., 97, 313.
Einstein, A., 1906. Calculation of the viscosity-coefficient of a liquid in which a large number of small spheres are suspended in irregular distribution. *Ann. Phys. Leipzig*, *19*, pp.286-306.
Einstein, A., 1956. *Investigations on the Theory of the Brownian Movement*. Courier Corporation.
Emulsion, I.U.P.A.C., 1997. Compendium of Chemical Terminology, (the "Gold Book"). Compiled by AD McNaught and A. Wilkinson.
Ezeuko, C.C., Wang, J.Y.J. and Gates, I.D., 2012, January. Investigation of Emulsion Flow in SAGD and ES-SAGD. In *SPE Heavy Oil Conference Canada*. Society of Petroleum Engineers.
Farah, M.A., Oliveira, R.C., Caldas, J.N. and Rajagopal, K., 2005. Viscosity of water-in-oil emulsions: Variation with temperature and water volume fraction. *Journal of Petroleum Science and Engineering*, *48*(3-4), pp.169-184.
Fingas, M. and Fieldhouse, B., 2003. Studies of the formation process of water-in-oil emulsions. *Marine pollution bulletin*, *47*(9-12), pp.369-396.
Fingas, M. and Fieldhouse, B., 2004. Formation of water-in-oil emulsions and application to oil spill modelling. *Journal of hazardous materials*, *107*(1-2), pp.37-50.
Fingas, M.F., Fieldhouse, B., Lambert, P., Wang, Z., Noonan, J., Lane, J. and Mullin, J.V., 2002. Water-in-oil emulsions formed at sea, in test tanks, and in the laboratory. *Environment Canada Manuscript Report EE-170, Ottawa, Ont*.
Frigerio, F. and Molinari, D., 2011. A multiscale approach to the simulation of asphaltenes. *Computational and Theoretical Chemistry*, *975*(1-3), pp.76-82.
Gabel, R., Vale, G., Bauch, E., Nair, C. and Meyers, A., Ecolab USA Inc., 2020. ASPHALT EMULSION COMPOSITION AND METHOD OF TREATING A PAVEMENT SURFACE. U.S. Patent Application 16/806,416.
Gaestel, C., Smadja, R. and Lamminan, K.A., 1971. Contribution à la connaissance des propriétés des bitumes routiers. Rev. Gentile. Routes et Aérodromes, 466, pp.85-94.
Galtung, J., 1967. *Theory and methods of social research*. Universitetsforlaget.
Garrett, R. and Grisham, C., 2010. Biochemistry. Brooks Cole Cengage Learning, Boston USA.
Gates, I.D. and Chakrabarty, N., 2006, January. Design of the steam and solvent injection strategy in expanding-solvent steam-assisted gravity drainage. In *Canadian international petroleum conference*. Petroleum Society of Canada.

Gómora-Figueroa, A.P., Camacho-Velázquez, R.G., Guadarrama-Cetina, J. and Guerrero-Sarabia, T.I., 2018. Oil emulsions in naturally fractured Porous Media. *Petroleum*.
Goodarzi, F. and Zendehboudi, S., 2019. A comprehensive review on emulsions and emulsion stability in chemical and energy industries. *The Canadian Journal of Chemical Engineering*, *97*(1), pp.281-309.
Groenzin, H. and Mullins, O.C., 1999. Asphaltene molecular size and structure. *The Journal of Physical Chemistry A*, *103*(50), pp.11237-11245.
Guth, E. and Simha, R., 1971. Kolloid Z., 74, 266 (1936)
Haftani, M., Wang, C., Montero Pallares, J.D., Mahmoudi, M., Fattahpour, V. and Nouri, A., 2019, April. An Investigation into the Effect of Brine Salinity on Fines Migration in SAGD Operations. In *SPE Western Regional Meeting*. Society of Petroleum Engineers.
Haghighat, P. and Maini, B.B., 2008, January. Role of asphaltene precipitation in VAPEX process. In Canadian International Petroleum Conference. Petroleum Society of Canada.
Hahn, A.U. and Mittal, K.L., 1979. Mechanism of demulsification of oil-in-water emulsion in the centrifuge. *Colloid and Polymer Science*, *257*(9), pp.959-967.
Hatschek, E., 1911. Kolloid-Z., 8, 34.
Hemmati-Sarapardeh, A., Ameli, F., Ahmadi, M., Dabir, B., Mohammadi, A.H. and Esfahanizadeh, L., 2020. Effect of asphaltene structure on its aggregation behavior in toluene-normal alkane mixtures. Journal of Molecular Structure, p.128605.
Henríquez, C.J.M., 2009. W/O Emulsions: formulation, characterization and destabilization. *Technischen Universität Cottbus zur Erlangung, Caracas*.
Hjelmeland, O.S. and Larrondo, L.E., 1986. Experimental investigation of the effects of temperature, pressure, and crude oil composition on interfacial properties. *SPE Reservoir Engineering*, *1*(04), pp.321-328.
Honarvar, B., Rahimi, A., Safari, M., Khajehahmadi, S. and Karimi, M., 2020. Smart water effects on a crude oil-brine-carbonate rock (CBR) system: further suggestions on mechanisms and conditions. Journal of Molecular Liquids, 299, p.112173.
Irani, M. and Ghannadi, S., 2013. Understanding the heat-transfer mechanism in the steam-assisted gravity-drainage (SAGD) process and comparing the conduction and convection flux in bitumen reservoirs. *SPE Journal*, *18*(01), pp.134-145.
Jamaluddin, A.K.M. and Butler, R.M., 1988. Factors Affecting the Formation of Water-in-Oil Emulsions During Thermal Recovery. *AOSTRA J. Research*, *4*(2), pp.109-116.
Jiao, J. and Burgess, D.J., 2003. Rheology and stability of water-in-oil-in-water multiple emulsions containing Span 83 and Tween 80. *Aaps Pharmsci*, *5*(1), pp.62-73.
Kar, T., Williamson, M. and Hascakir, B., 2014, September. The role of asphaltenes in emulsion formation for steam assisted gravity drainage (SAGD) and expanding solvent-SAGD (ES-SAGD). In *SPE Heavy and Extra Heavy Oil Conference: Latin America*. Society of Petroleum Engineers.
Khilar, K.C. and Fogler, H.S., 1984. The existence of a critical salt concentration for particle release. *Journal of colloid and interface science*, *101*(1), pp.214-224.
Kiefer, J., 1953. Sequential minimax search for a maximum. *Proceedings of the American mathematical society*, *4*(3), pp.502-506.
Kim, M., Abedini, A., Lele, P., Guerrero, A. and Sinton, D., 2017. Microfluidic pore-scale comparison of alcohol-and alkaline-based SAGD processes. *Journal of Petroleum Science and Engineering*, *154*, pp.139-149.
Kippax, P., 2005. Appraisal of the laser diffraction particle-sizing. *Pharmaceutical Technology*, *3*, pp.88-89.

Kiran, S.K., Acosta, E.J. and Moran, K., 2009. Evaluating the hydrophilic–lipophilic nature of asphaltenic oils and naphthenic amphiphiles using microemulsion models. Journal of colloid and interface science, 336(1), pp.304-313.
Kokal, S. L.; Al-Dokhi, M. January. Case studies of emulsion behavior at reservoir conditions. *SPE Middle East Oil and Gas Show and Conference*; Society of Petroleum Engineers, 2007
Kokal, S. L.; Sayegh, S. G. January. Asphaltenes: The cholesterol of petroleum, *Middle East Oil Show*; Society of Petroleum Engineers, 1995
Kokal, S., Al-Yousif, A., Meeranpillai, N.S. and Al-Awaisi, M., 2001, January. Very thick crude emulsions: A field case study of a unique crude production problem. In *SPE annual technical conference and exhibition*. Society of Petroleum Engineers.
Kokal, S.L. and Al-Dokhi, M., 2007, January. Case studies of emulsion behavior at reservoir conditions. In *SPE Middle East Oil and Gas Show and Conference*. Society of Petroleum Engineers.
Kokal, S.L. and Sayegh, S.G., 1995, January. Asphaltenes: The cholesterol of petroleum. In Middle East oil show. Society of Petroleum Engineers.
Kokal, S.L., 2005. Crude oil emulsions: A state-of-the-art review. *SPE Production & facilities*, *20*(01), pp.5-13.
Krieger, I.M. and Dougherty, T.J., 1959. A mechanism for non-Newtonian flow in suspensions of rigid spheres. *Transactions of the Society of Rheology*, *3*(1), pp.137-152.
Kumasaka, J., Sasaki, K., Sugai, Y., Alade, O.S. and Nakano, M., 2016. Measurement of Viscosity Alteration for Emulsion and Numerical Simulation on Bitumen Production by SAGD Considering In-situ Emulsification. *Journal of Earth Science and Engineering*, *6*, pp.10-17.
Leal-Calderon, F., Schmitt, V. and Bibette, J., 2007. *Emulsion science: basic principles*. Springer Science & Business Media.
Leontaritis, K.J. and Mansoori, G.A., 1988. Asphaltene deposition: a survey of field experiences and research approaches. Journal of Petroleum Science and Engineering, 1(3), pp.229-239.
Li, K., Vasiliu, M., McAlpin, C.R., Yang, Y., Dixon, D.A., Voorhees, K.J., Batzle, M., Liberatore, M.W. and Herring, A.M., 2015. Further insights into the structure and chemistry of the Gilsonite asphaltene from a combined theoretical and experimental approach. *Fuel*, *157*, pp.16-20.
Maa, Y.F. and Hsu, C., 1996. Liquid-liquid emulsification by rotor/stator homogenization. *Journal of Controlled Release*, *38*(2-3), pp.219-228.
Mahmoudi Eshkaftaki, M., 2017. New sand control design criteria and evaluation testing for steam assisted gravity drainage (SAGD) wellbores.
Mahmoudi, M., Fattahpour, V., Velayati, A., Roostaei, M., Kyanpour, M., Alkouh, A., Sutton, C., Fermaniuk, B. and Nouri, A., 2018, December. Risk Assessment in Sand Control Selection: Introducing a Traffic Light System in Stand-Alone Screen Selection. In *SPE International Heavy Oil Conference and Exhibition*. Society of Petroleum Engineers.
Manning, F.S. and Thompson, R.E., 1995. *Oilfield processing of petroleum: Crude oil* (Vol. 2). Pennwell books.
Mason, S.L., May, K. and Hartland, S., 1995. Drop size and concentration profile determination in petroleum emulsion separation. *Colloids and Surfaces A: Physicochemical and engineering aspects*, *96*(1-2), pp.85-92.
Mcclements, D.J., 2007. Critical review of techniques and methodologies for characterization of emulsion stability. *Critical reviews in food science and nutrition*, *47*(7), pp.611-649.
McClements, D.J., 2015. *Food emulsions: principles, practices, and techniques*. CRC press.

McDonald, J.E., 1962. Homogeneous nucleation of vapor condensation. I. Thermodynamic aspects. *American Journal of Physics*, *30*(12), pp.870-877.
McLean, J.D. and Kilpatrick, P.K., 1997. Effects of asphaltene solvency on stability of water-in-crude-oil emulsions. Journal of Colloid and Interface Science, 189(2), pp.242-253.
Mohamed, A.I., Sultan, A.S., Hussein, I.A. and Al-Muntasheri, G.A., 2017. Influence of surfactant structure on the stability of water-in-oil emulsions under high-temperature high-salinity conditions. *Journal of Chemistry*, *2017*.
Mohammadzadeh, O. and Chatzis, I., 2010. Pore-level investigation of heavy oil recovery using steam assisted gravity drainage (SAGD). *Oil & Gas Science and Technology–Revue d'IFP Energies nouvelles*, *65*(6), pp.839-857.
Mohammed, I., Mahmoud, M., Al Shehri, D., El-Husseiny, A. and Alade, O., 2020. Asphaltene precipitation and deposition: A critical review. Journal of Petroleum Science and Engineering, p.107956.
Mojarad, M. and Dehghanpour, H., 2016. Analytical modeling of emulsion flow at the edge of a steam chamber during a steam-assisted-gravity-drainage process. *SPE Journal*, *21*(02), pp.353-363.
Mooney, M., 1951. The viscosity of a concentrated suspension of spherical particles. *Journal of colloid science*, *6*(2), pp.162-170.
Mooney, M., 1951. The viscosity of a concentrated suspension of spherical particles. *Journal of colloid science*, *6*(2), pp.162-170.
Nasery, S., Hoseinpour, S., Phung, L.T.K. and Bahadori, A., 2016. Prediction of the viscosity of water-in-oil emulsions. *Petroleum Science and Technology*, *34*(24), pp.1972-1977.
National Center for Biotechnology Information. PubChem Database. Source=Sigma-Aldrich, SID=329824531, https://pubchem.ncbi.nlm.nih.gov/substance/329824531 (accessed on May 25, 2020)
Nciri, N., Song, S., Kim, N. and Cho, N., 2014. Chemical characterization of gilsonite bitumen. Journal of Petroleum & Environmental Biotechnology, 5(5), p.1.
Nguyen, D., Phan, J. and Balsamo, V., 2013, June. Effect of diluents on interfacial properties and SAGD emulsion stability: I. Interfacial rheology. In *SPE Heavy Oil Conference-Canada*. Society of Petroleum Engineers.
Nikolovski, B.G., Ilić, J.D. and Sovilj, M.N., 2016. How to formulate a stable and monodisperse water-in-oil nanoemulsion containing pumpkin seed oil: the use of multiobjective optimization. *Brazilian Journal of Chemical Engineering*, *33*(4), pp.919-931.
NIST/SEMATECH e-Handbook of Statistical Methods, http://www.itl.nist.gov/div898/handbook/, 26 March, 2021.
Noik, C., Dalmazzone, C.S., Goulay, C. and Glenat, P., 2005, January. Characterisation and emulsion behaviour of Athabasca extra heavy oil produced by SAGD. In *SPE International Thermal Operations and Heavy Oil Symposium*. Society of Petroleum Engineers.
Olalekan, A.S., Sasaki, K., Sugai, Y., , Ademodi, B., Kumasaka, J., and Ueda, R., 2017. Effect of Emulsification Process Conditions on the Properties of Water-in-Bitumen Emulsion, Journal of the Japanese Association for Petroleum Technology, 82(01), pp.73-84
Oldroyd, J.G., 1955. The effect of interfacial stabilizing films on the elastic and viscous properties of emulsions. *Proceedings of the Royal Society of London. Series A. Mathematical and Physical Sciences*, *232*(1191), pp.567-577.
Opawale, F.O. and Burgess, D.J., 1998. Influence of interfacial properties of lipophilic surfactants on water-in-oil emulsion stability. *Journal of colloid and interface science*, *197*(1), pp.142-150.

Operating Instructions. Manual No. M/85-150-P700. Middleboro, MA: Brookfield Engineering Laboratories, Inc. Source: http://www.viscometers org/PDF/Manuals/laboratory/DIAL (accessed May 25, 2020].
Pakdaman, E., Osfouri, S., Azin, R., Niknam, K. and Roohi, A., 2020. Synthesis and characterization of hydrophilic Gilsonite fine particles for improving water-based drilling mud properties. Journal of Dispersion Science and Technology, 41(11), pp.1633-1642.
Pal, R. and Rhodes, E., 1989. Viscosity/concentration relationships for emulsions. *Journal of Rheology*, *33*(7), pp.1021-1045.
Pal, R., 1996. Effect of droplet size on the rheology of emulsions. *AIChE Journal*, *42*(11), pp.3181-3190.
Pawlik, A., Cox, P.W. and Norton, I.T., 2010. Food grade duplex emulsions designed and stabilised with different osmotic pressures. *Journal of colloid and interface science*, *352*(1), pp.59-67.
Peramanu, S., Pruden, B.B. and Rahimi, P., 1999. Molecular weight and specific gravity distributions for Athabasca and Cold Lake bitumens and their saturate, aromatic, resin, and asphaltene fractions. *Industrial & engineering chemistry research*, *38*(8), pp.3121-3130.
Pickering, S.U., 1907. Cxcvi.—emulsions. *Journal of the Chemical Society, Transactions*, *91*, pp.2001-2021.
Piroozian, A., Hemmati, M., Safari, M., Rahimi, A., Rahmani, O., Aminpour, S.M. and Pour, A.B., 2021. A mechanistic understanding of the water-in-heavy oil emulsion viscosity variation: effect of asphaltene and wax migration. Colloids and Surfaces A: Physicochemical and Engineering Aspects, 608, p.125604.
Poston, S.W., Ysrael, S., Hossain, A.K.M.S. and Montgomery III, E.F., 1970. The effect of temperature on irreducible water saturation and relative permeability of unconsolidated sands. *Society of Petroleum Engineers Journal*, *10*(02), pp.171-180.
Qi, Z., Abedini, A., Lele, P., Mosavat, N., Guerrero, A. and Sinton, D., 2017. Pore-scale analysis of condensing solvent bitumen extraction. Fuel, 193, pp.284-293.
Raghavan, R. and Marsden Jr, S.S., 1971. Theoretical aspects of emulsification in porous media. *Society of Petroleum Engineers Journal*, *11*(02), pp.153-161.
Rahimi, A., Honarvar, B. and Safari, M., 2020. The role of salinity and aging time on carbonate reservoir in low salinity seawater and smart seawater flooding. Journal of Petroleum Science and Engineering, 187, p.106739.
Rahimi, A., Safari, M., Honarvar, B., Chabook, H. and Gholami, R., 2020. On time dependency of interfacial tension through low salinity carbonated water injection. Fuel, 280, p.118492.
Rashidnia, N., Balasubramaniam, R. and Delsignore, D., 1992. Interfacial tension measurement of immiscible liq uids using a capillary tube. *NASA STI/Recon Technical Report N*, *92*, p.21262.
RICHARDSON, E., 1937. THE PHYSICAL PROPERTIES OF DISPERSE SYSTEMS. *Science Progress (1933-)*, *31*(123), pp.462-475.
Richardson, E.G., 1933. Kolloid-Z. 65, 32.
Richardson, E.G., 1938. Kolloid-Z. 65, 32 (1933).
Riddick, T.M., 1968. *Control of colloid stability through zeta potential* (p. 51). Wynnewood, PA: Livingston.
Rodionova, G., Pettersen, B., Kelesoğlu, S. and Sjöblom, J., 2014. Preparation and characterization of reference fluid mimicking behavior of North Sea heavy crude oil. *Fuel*, *135*, pp.308-314.
Romero, M.I., 2009, January. Flow of emulsions in porous media. In *SPE Annual Technical Conference and Exhibition*. Society of Petroleum Engineers.

Ronningsen, H.P., 1995, January. Correlations for predicting viscosity of W/O-emulsions based on North Sea crude oils. In *SPE International Symposium on Oilfield Chemistry*. Society of Petroleum Engineers.
Roscoe, R., 1952. The viscosity of suspensions of rigid spheres. *British journal of applied physics*, *3*(8), p.267.
Saitô, N., 1950. Concentration dependence of the viscosity of high polymer solutions. I. *Journal of the Physical Society of Japan*, *5*(1), pp.4-8.
Santini, E., Liggieri, L., Sacca, L., Clausse, D. and Ravera, F., 2007. Interfacial rheology of Span 80 adsorbed layers at paraffin oil–water interface and correlation with the corresponding emulsion properties. *Colloids and Surfaces A: Physicochemical and Engineering Aspects*, *309*(1-3), pp.270-279.
Sanyal, S.K., Marsden Jr, S.S. and Ramey Jr, H.J., 1974, January. Effect of temperature on petrophysical properties of reservoir rocks. In *SPE California regional meeting*. Society of Petroleum Engineers.
Sasaki, K., Akibayashi, S., Yazawa, N., Doan, Q. and Ali, S.M., 1999, January. Experimental Modelling of the SAGD Process 3/4 Enhancing SAGD Performance with Periodic Stimulation of the Horizontal Producer. In *SPE Annual Technical Conference and Exhibition*. Society of Petroleum Engineers.
Sasaki, K., Satoshi, A., Yazawa, N. and Kaneko, F., 2002, January. Microscopic visualization with high resolution optical-fiber scope at steam chamber interface on initial stage of SAGD process. In *SPE/DOE Improved Oil Recovery Symposium*. Society of Petroleum Engineers.
Scholz, E., 2012. *Karl Fischer titration: determination of water*. Springer Science & Business Media.
Schramm, L.L., 1992. Fundamentals and applications in the petroleum Industry. *Adv. Chem*, *231*, pp.3-24.
Shariatpanahi, S.F., Strand, S. and Austad, T., 2011. Initial wetting properties of carbonate oil reservoirs: effect of the temperature and presence of sulfate in formation water. *Energy & fuels*, *25*(7), pp.3021-3028.
Shoushtari, A.B., Asadolahpour, S.R. and Madani, M., 2020. Thermodynamic investigation of asphaltene precipitation and deposition profile in wellbore: A case study. Journal of Molecular Liquids, p.114468.
Sibree, J.O., 1930. The viscosity of emulsions.—Part I. *Transactions of the Faraday Society*, *26*, pp.26-36.
Sibree, J.O., 1931. The viscosity of emulsions. Part II. *Transactions of the Faraday Society*, *27*, pp.161-176.
Sinnokrot, A.A., Ramey Jr, H.J. and Marsden Jr, S.S., 1971. Effect of temperature level upon capillary pressure curves. *Society of Petroleum Engineers Journal*, *11*(01), pp.13-22.
Sjoblom, J., 2001. *Encyclopedic handbook of emulsion technology*. CRC press.
Slagle, K.A. and Carter, L.G., 1959, January. Gilsonite-a unique additive for oil-well cements. In Drilling and Production Practice Conference. American Petroleum Institute.
Song, X., Shi, P., Zhao, S., Duan, M., Wang, C. and Ma, Y., 2016. Dissipative particle dynamics study on the aggregation behavior of asphaltenes under shear fields. *Industrial & Engineering Chemistry Research*, *55*(33), pp.9077-9086.
Sorbitan sesquioleate. SID S3386 [online]. Sigma-aldrich: St. Louis, MO, USA. Source: https://www.sigmaaldrich.com/catalog/product/sigma/s3386?lang=en&region=CA (accessed May 18, 2020)

Souza, W.J., Santos, K.M.C., Cruz, A.A., Franceschi, E., Dariva, C., Santos, A.F. and Santana, C.C., 2015. Effect of water content, temperature and average droplet size on the settling velocity of water-in-oil emulsions. *Brazilian Journal of Chemical Engineering*, *32*(2), pp.455-464.
Spasic, A.M., 2018. *Rheology of Emulsions: Electrohydrodynamics Principles* (Vol. 22). Academic Press.
Speight, J.G., 2015. *Handbook of petroleum product analysis*. John Wiley & Sons.
Spiecker, P.M., Gawrys, K.L., Trail, C.B. and Kilpatrick, P.K., 2003. Effects of petroleum resins on asphaltene aggregation and water-in-oil emulsion formation. Colloids and surfaces A: Physicochemical and engineering aspects, 220(1-3), pp.9-27.
Standard, A.S.T.M., 1981. E799-81,". *Practice for Determining Data Criteria and Processing for Liquid Drop Size Analysis*.
Strassner, J.E., 1968. Effect of pH on interfacial films and stability of crude oil-water emulsions. *Journal of Petroleum Technology*, *20*(03), pp.303-312.
Sun, H., 1998. COMPASS: an ab initio force-field optimized for condensed-phase applications overview with details on alkane and benzene compounds. The Journal of Physical Chemistry B, 102(38), pp.7338-7364.
Sztukowski, D.M., Jafari, M., Alboudwarej, H. and Yarranton, H.W., 2003. Asphaltene self-association and water-in-hydrocarbon emulsions. Journal of colloid and interface science, 265(1), pp.179-186.
Tadros, T.F., 2013. Emulsion formation, stability, and rheology. *Emulsion formation and stability*, *1*, pp.1-75.
Taylor, G.I., 1932. The viscosity of a fluid containing small drops of another fluid. *Proceedings of the Royal Society of London. Series A, Containing Papers of a Mathematical and Physical Character*, *138*(834), pp.41-48.
Thomas, D.G., 1965. A note on the viscosity of Newtonian suspensions of uniform spherical particles. *J. Colloid Sci.*, *20*, pp.267-277.
Velayati, A. and Nouri, A., 2020. Emulsification and emulsion flow in thermal recovery operations with a focus on SAGD operations: A critical review. *Fuel*, *267*, p.117141.
Velayati, A. and Nouri, A., 2020. Physical features' characterization of the water-in-mineral oil macro emulsion stabilized by a nonionic surfactant. Journal of Dispersion Science and Technology, pp.1-16.
Velayati, A. and Nouri, A., 2021. Role of Asphaltene in Stability of Water-in-Oil Model Emulsions: The Effects of Oil Composition and Size of the Aggregates and Droplets. *Energy & Fuels*.
Vladisavljević, G.T., Surh, J. and McClements, J.D., 2006. Effect of emulsifier type on droplet disruption in repeated Shirasu porous glass membrane homogenization. *Langmuir*, *22*(10), pp.4526-4533.
Wang, C., Pang, Y., Mahmoudi, M., Haftani, M., Salimi, M., Fattahpour, V. and Nouri, A., 2020. A set of graphical design criteria for slotted liners in steam assisted gravity drainage production wells. *Journal of Petroleum Science and Engineering*, *185*, p.106608.
Yan, J., Plancher, H. and Morrow, N.R., 1997. Wettability changes induced by adsorption of asphaltenes. *SPE Production & Facilities*, *12*(04), pp.259-266.
Yang, Y., Siqueira, F.D., Vaz, A.S., You, Z. and Bedrikovetsky, P., 2016. Slow migration of detached fine particles over rock surface in porous media. *Journal of Natural Gas Science and Engineering*, *34*, pp.1159-1173.

Yarranton, H.W., Sztukowski, D.M. and Urrutia, P., 2007. Effect of interfacial rheology on model emulsion coalescence: I. Interfacial rheology. *Journal of colloid and interface science*, *310*(1), pp.246-252.
Yaseen, S. and Mansoori, G.A., 2017. Molecular dynamics studies of interaction between asphaltenes and solvents. *Journal of Petroleum Science and Engineering*, *156*, pp.118-124.
Yaseen, S. and Mansoori, G.A., 2018. Asphaltene aggregation due to waterflooding (A molecular dynamics study). *Journal of Petroleum Science and Engineering*, *170*, pp.177-183.
Yuan, B. and Wood, D.A. eds., 2018. Formation damage during improved oil recovery: Fundamentals and applications. Gulf Professional Publishing. pp.243-273
Zhu, Q., Pan, Y., Jia, X., Li, J., Zhang, M. and Yin, L., 2019. Review on the stability mechanism and application of water-in-oil emulsions encapsulating various additives. *Comprehensive Reviews in Food Science and Food Safety*, *18*(6), pp.1660-1675.

Appendix 6.A

The following workflow can be used as a general guideline for the preparation of model emulsions at a larger scale for sand pack testing:

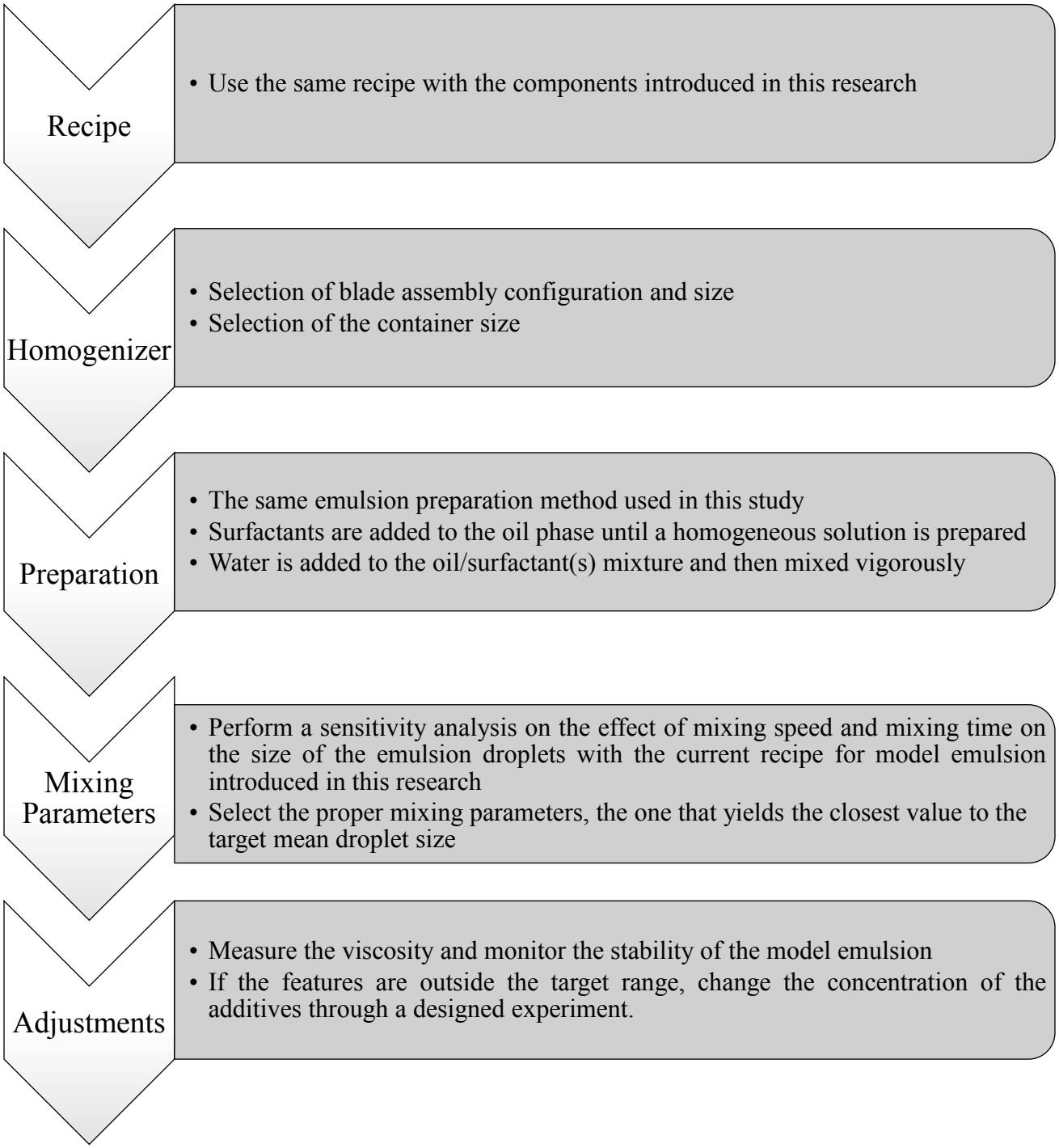

Figure 6.A1: A general guideline for preparation of model emulsions at larger scales

Appendix 6.B

Structural bond lengths of benzene and cyclohexane compounds in Compass forcefield (the forcefield used in this study) are displayed in Table A6.1 and compared with CFF93 forcefield values. More information on structural parameters in the Compass forefield can be found elsewhere (Sun, 1998)

Table 6.B1: Comparison of bond length (in Å) of Alkane and Benzene compounds (After Sun, 1998)

Cyclohexane		
Property	**Compass**	**CFF93**
C-C	1.537	1.543
C-H	1.104	1.114
C-C-C	111	111
C-C-H	110.4	110.5
H-C-H	106.5	106.4
C1-C2-C3-C4	56	56.2
Benzene		
Property	**Compass**	**CFF93**
C-C	1.398	-
C-H	1.099	-
C-C-C	120	-
C-C-H	120	-

Appendix 6.C
Calibrations:

- Calibration of the microscope resolution was performed using a stage micrometer. Table A6.2 shows the pixel to length (micrometer) ratios for different objective plans used in the microscopy of emulsion samples.

Table 6.C1: Resolution of microscopes for different objective plans

Objective plan	Pixel/micrometer
4x	1.24
10x	3.02
40x	12.00

- Verification of interfacial tension measurement accuracy in capillary tube method was carried out by comparing the results obtained for mineral oil+Span 83 and water system, where the measured value in this study was compared with the value of a similar system (under the same environmental conditions but different measurement method) reported in the literature (Opawale & Burgess; 1998). The measured value was 0.02 dyn/cm larger in our study which shows reasonable accuracy of the method adopted.